SAPIENZA
UNIVERSITÀ DI ROMA

Unitarity Triangle Analysis and Recent Theoretical Advancements of ϵ'/ϵ

Facoltà di Scienze Matematiche, Fisiche e Naturali

Corso di Laurea Magistrale in Theoretical Physics

Candidate

Davide Morgante
ID number 1745276

Thesis Advisor

Prof. Guido Martinelli

Co-Advisor

Prof. Marco Nardecchia

Academic Year 2020/2021

Unitarity Triangle Analysis and Recent Theoretical Advancements of ϵ'/ϵ
Master's thesis. Sapienza – University of Rome

This thesis has been typeset by LaTeX and the Sapthesis class.

Version: October 11, 2021

Author's email: morgante.1745276@studenti.uniroma1.it

Dedicated to Evita,
my forever life companion.

Acknowledgments

Contents

Introduction

Flavour physics is an essential tool for testing the Standard Model (SM) in search of New Physics (NP). In this regard, a fundamental quantity to be studied is CP-violation in the Kaon system which is measured by two observables called ϵ_K and ϵ'/ϵ. While the former is well understood both theoretically and experimentally, the latter posed some very hard theoretical problems that made its prediction difficult. Only recently the RBC collaboration gave a reasonable prediction for it and in this thesis we want to explore the effect that this result can have on the analysis of the Unitarity Triangle (UT).

The Standard Model of particle physics is a theory that encapsulates our best understanding of the world of subatomic particles and their interactions. Its results have been thoroughly tested by high energy experiments, up to incredible precision. Despite the numerous successes, however, there are many reasons as to why we may think that the SM is not the complete and definite answer. The first reason that come to mind is that the SM does not provide an explanation for the gravitational force. But there are many others: the lack of an explanation for the masses of the neutrinos, the instability of the Higgs mass due to radiative corrections, the absence of a candidate for dark matter, baryon asymmetry, and so on.

All of these issues, and many others, could find an answer in a more fundamental theory, corresponding to new physics, which manifests itself at higher energies whose effects are highly suppressed at the lower energy scales of the SM. These effects could be probed in high energy experiments at accelerators like the LHC at CERN, or by studying highly energetic events in our universe.

In this regard, the study of flavour physics, due to its highly non-trivial structure, is very sensitive to the effects of higher energy scales and thus offers a very interesting window on the effects of new physics. In particular, weak interactions of quarks, involve elements of the Cabibbo-Kobayashi-Maskawa (CKM) matrix. The accurate determination of the CKM matrix elements, obtained by combining the experimental inputs with theoretical calculations and results coming from lattice simulations, represents one of the strictest tests of the Standard Model.

In the SM the CKM matrix, which describes the quark flavour mixing in weak interactions, is given by a 3×3 unitary matrix

$$V_{CKM} = \begin{pmatrix} V_{ud} & V_{us} & V_{ub} \\ V_{cd} & V_{cs} & V_{cb} \\ V_{td} & V_{ts} & V_{tb} \end{pmatrix}.$$

The CKM matrix can be parametrized by a set of three angles $\theta_{12}, \theta_{23}, \theta_{13}$ and one

complex phase δ. The angle θ_{12} is also known as Cabibbo angle. The complex phase is the parameter that enables CP violation in weak decays.

Experimental measurements of $|V_{ud}|$, $|V_{cb}|$ and $|V_{ub}|$ from K and B meson decays shows that there's an hierarchy in the mixing angles, so that the CKM matrix can be expanded in powers of the sine of Cabibbo angle $\lambda \equiv \sin\theta_{12} \approx 0.22$. First define

$$\lambda \equiv \sin\theta_{12}, \qquad A \equiv \sin\theta_{23}/\lambda^2, \qquad (\rho + i\eta) \equiv \sin\theta_{13}e^{i\delta}/(A\lambda^3),$$

which are known as Wolfenstein parameters. Then, another two quantities are also useful

$$\bar{\rho} = \rho\left(1 - \frac{\lambda^2}{2}\right), \qquad \bar{\eta} = \eta\left(1 - \frac{\lambda^2}{2}\right).$$

The unitarity of the CKM matrix implies triangular relations like

$$V_{ud}V_{us}^* + V_{cd}V_{cs}^* + V_{td}V_{ts}^* = 0$$
$$V_{ud}V_{td}^* + V_{us}V_{ts}^* + V_{ub}V_{tb}^* = 0$$

and many others. One of this unitary triangles is of particular interest and is called The Unitary Triangle (UT) and is given by the unitarity relation

$$V_{ud}V_{ub}^* + V_{cd}V_{cb}^* + V_{td}V_{tb}^* = 0$$

By means of the Wolfenstein parametrization, all the sides of the UT given by the above relation are of $O(\lambda^3)$, so we can normalize all the sides dividing by $V_{td}V_{tb}^*$ giving the normalized UT

$$-\frac{V_{ud}V_{ub}^*}{V_{cd}V_{cb}^*} - \frac{V_{td}V_{tb}^*}{V_{cd}V_{cb}^*} = 1.$$

This relation defines a triangle in the $(\bar{\rho}, \bar{\eta})$ plane. By measuring independently different elements of the CKM matrix, it is possible to test the SM by verifying that these triangular relations are experimentally satisfied.

Many ways have been developed over the years to measure the CKM matrix elements. The relevant processes used today are semileptonic production and decay rates which are, under very broad assumptions about possible physics beyond the SM, dominated by tree level amplitudes with a $W^{\pm}$ boson as an intermediate state. Measurements of semileptonic decays of beauty and strange particles give information on the values of λ and A while the values of $\bar{\rho}, \bar{\eta}$ are constrained mainly by four parameters: $|\epsilon_K|$, $|V_{ub}/V_{cb}|$, Δm_d, Δm_s.
More up-to-date methods have been developed over the years to allow greater precision. In particular, for the $|V_{ud}|$ matrix element, the most exact up to date method makes use of superallowed Fermi transitions, i.e. beta decays connecting two $J^P = 0^+$ nuclides in the same isospin multiplet.

From the theoretical standpoint, the difficulties in the calculation arise from the effects of strong dynamics, which are described in the SM by Quantum Chromodynamics (QCD). At low energy, below $\Lambda_{QCD} \approx 1$ GeV threshold, the strong dynamics in non-perturbative and thus requires lattice QCD methods to be solved. On the contrary, at energies above the Λ_{QCD} threshold, the theory becomes weakly

interacting thanks to asymptotic freedom, and perturbation theory can be used. Under certain conditions, effective theories can be deployed making theoretical calculations readily accessible.

Of particular interest for our analysis are the ϵ_K and ϵ'/ϵ parameters that describe CP-violation in the neutral Kaon system. The first parameter ϵ_K directly relates to the δ phase in the CKM matrix and theoretically can be evaluated using an effective theory

$$
\begin{aligned}
|\epsilon_K| = \frac{G_F^2 M_W^2}{4\sqrt{2}\pi^2 m_k \Delta m_k} A^2 \lambda^6 \sigma \sin\delta \left\langle \bar{K}^0 \middle| \bar{s}\gamma^\mu P_L d \bar{s}\gamma_\mu P_L d \middle| K^0 \right\rangle \\
\times \left[\eta_3 S_0(x_c, x_t) - \eta_1 S_0(x_c) + A^2 \lambda^4 (1 - \sigma\cos\delta)\eta_2 S_0(x_t) \right].
\end{aligned}
\tag{0.1}
$$

What poses the most difficulties, both experimentally and theoretically, is the ϵ'/ϵ observable, where

$$
\epsilon' \approx \frac{i}{\sqrt{2}} e^{i(\delta_2 - \delta_0)} \frac{\text{Im}(A_2 A_0^*)}{|A_0|^2}.
\tag{0.2}
$$

The evaluation of hadronic matrix elements A_0 and A_2 is subject to large uncertainties, that are problematic in particular for ϵ'/ϵ, where important cancellations need to occur so to get the exceedingly small value found in experiments.

For many years, even the experimental situation was unclear: the NA31 Collaboration and the E731 Collaboration gave very different results. The KTeV Collaboration then settled down the situation. From that, we know now the ϵ' parameter, although non zero, is exceedingly small, of the order of 10^{-6}.

From the theoretical standpoint, this very small value comes because of an accidental cancellation among the various contributions to ϵ'. These cancellations are very subtle which meant that the theoretical analysis of ϵ'/ϵ has been subject to various refinements over the years. In fact, at tree level, both the hadronic matrix elements A_0 and A_2 come from the same contribution and have the same phase. This means that, at tree level, $\epsilon' = 0$. One has to compute the various loop corrections to the two amplitudes to get a meaningful result. It was soon found that gluonic penguins, as well as electromagnetic penguins, play a fundamental role and give the first non-trivial contributions to ϵ'. Yet, because of the strong cancellations, and because of the uncertainties in the hadronic matrix elements, an accurate prediction of ϵ'/ϵ was not possible.

Recently, through lattice QCD calculations, a satisfactory result was found [2]

$$
\text{Re}\left(\frac{\epsilon'}{\epsilon}\right) = 21.7(2.6)(6.2)(5.0) \times 10^{-4}
$$

where errors are statistical and systematic respectively and the third error represents omitted isospin breaking effects.

This new and exciting result opens up the possibility for an update of the analysis of the Unitarity Triangle. Through statistical analysis, based on the Bayesian approach, gathering all the experimental, as well as theoretical, results from rare disintegration processes, the UTfit collaboration searches for an accurate fit of the UT triangle shine light on the possibility of new physics beyond the Standard Model. The new and improved analysis could lead to interesting results and give more

accurate constraints on the values of the CKM matrix elements.

The brief outline of this thesis work is as follows: the first five chapters set up the theoretical background for the study of weak decays of light mesons and their oscillations. In particular we will focus on the K meson and the study of the two CP-violating parameters ϵ_K and ϵ'/ϵ. In Chapter 6 we are going to give the basic background on the analysis of the Unitarity Triangle and how we implemented the new result for ϵ'/ϵ. The last chapter, chapter 7, is the main one where we give our original result with the improved state-of-the-art analysis of the Unitarity Triangle including ϵ'/ϵ.

Chapter 1

Electroweak Interactions in the Standard Model
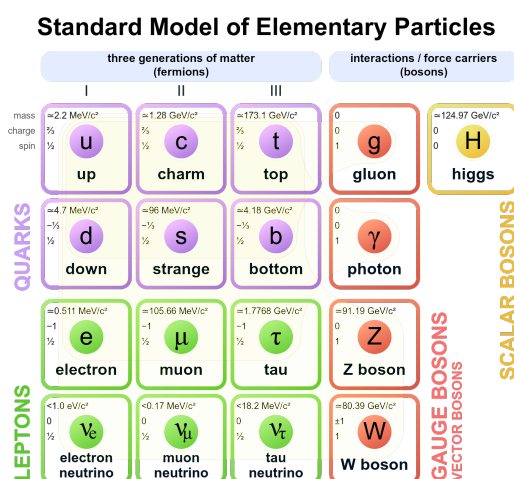
Figure 1.1. The Standard Model of particle physics.

Whenever somebody asks questions like how many particles there are? How do these particles interact with each other? What are the properties of certain particles? Are they fundamental or composite? What makes up a composite particle? How do they decay if they decay? And so on, the answer, as far as we know, can be found in a theory which is called by physicists the Standard Model (SM) of particle physics [78, 126, 142].

Loosely one can think of the SM as a Periodic Table for subatomic particles, but the reality is much more complicated. In some way this statement is not completely incorrect and, just like a Periodic Table, the Standard Model can be summarized in a table like the one in figure (1.1). However, this famous table is deceiving: it does not show all of the subatomic particles and their antiparticle! But for the purpose of the physics, particles and antiparticles are much of the same in their properties and their interactions, so it would be redundant to show them both.

Although this picture is very pretty, some physicists have a more pragmatic way

of presenting what they call the SM, which is as follows: the SM is a non-Abelian Yang-Mills theory whose symmetry group is given by

$$SU(3) \times SU(2) \times U(1). \tag{1.1}$$

Equation eq. (1.1) is what we call the *gauge group of the Standard Model*. Mathematically speaking even this sentence is not very precise since what we know exactly is the Lie algebra of the SM. From the Lie algebra and the properties of the particles, we can infer the precise Lie group of the SM [17], which is somewhat different from the one in equation eq. (1.1) and is given by the following quotient

$$\mathfrak{su}(3) \oplus \mathfrak{su}(2) \oplus \mathfrak{u}(1) \rightsquigarrow \frac{SU(3) \times SU(2) \times U(1)}{\mathbb{Z}_6}. \tag{1.2}$$

Yet, this is beyond the scope of this thesis and we will stick to the mathematically imprecise, physicist way, of equation eq. (1.1) to avoid any confusion.

With this introduction one would be lead to believe that the SM has the possibility to answer all of our questions but, unfortunately (or fortunately, depends on who's the question being asked), this is not the case. Many questions, both theoretical and experimental, cannot be answered by a pure SM analysis, and here is when effective theories come into play. We will discuss effective theories and how they enter the game in the next chapters.

For now let us focus on what actually is the Standard Model. In this chapter we are going to give the basics upon which the Standard Model is built and how particles are described within this theory. In the first part we will focus on the $\mathfrak{su}(2) \oplus \mathfrak{u}(1)$ bit of equation eq. (1.2), the so-called *electroweak* (EW) sector or *Glashow-Weinberg-Salam* (GWS) theory [77, 127, 143], carrying the name of the physicists that theorized it and consequently won the Nobel prize for it in 1979. Then we will show how, within this theory, an incredible thing happens: the particles that make up hadrons, what we call quarks, can mix with one another in a way initially theorized by Nicola *Cabibbo* [42] and then expanded by *Kobayashi* and *Maskawa* [103] (the latter two winning the Nobel prize for it, while the former sadly did not receive it).

1.1 Basics of the Standard Model

For a more in-depth analysis of the contents of these chapters, there are many excellent books. Schwart's [128] and Sredniki's [134] texts are, in my opinion, two of the best and up to date. For a more experimental prospective, Peskin's book [120] is optimal.

In the Standard Model there are three types of particles: the matter constituents called quarks and leptons, which obey the Fermi-Dirac statistic, and the force-carrying particles, that obey the Bose-Einstein. In nature there are four main forces: gravitational, electromagnetic, weak and strong force. The bosons which carry these forces are given in table (1.1). Then the last piece is the Higgs[1] particle. This is again

---

[1]I would like to mention all the other physicists that, in some way, worked on the theory of the Higgs that are, most of the time, going unseen: Englert, Brout, Higgs, Guralnik, Hagen and Kibble.

Table 1.1. Vector and tensor boson carriers in the SM. The Graviton has not yet been discovered, it is just theorized.

Field	Boson	Spin
Grav.	Graviton	2
EM	Photon γ	1
Weak	$W^\pm, Z^0$	1
Strong	Gluon g	1

a boson, a scalar boson, whose interactions does not come from a gauge principle, that through the Higgs mechanism [85, 92, 94, 95, 101], after EW symmetry breaking gives masses to the various particles of the SM. In table (1.2) the main properties of the SM particles are given. With all the experimental properties out of the way, we can concentrate on the theoretical side of things.

The basic SM Lagrangian, before EW symmetry breaking, can be divided into five main pieces

$$\mathcal{L}_{\text{SM}} = \mathcal{L}_{\text{gauge}} + \mathcal{L}_{\text{fermions}} + \mathcal{L}_{\text{Higgs}} + \mathcal{L}_{\text{Yukawa}} + \mathcal{L}_{\text{Theta-vacuum}}, \tag{1.3}$$

where[2][3]

$$\mathcal{L}_{\text{gauge}} = -\frac{1}{2} \operatorname{Tr} G_{\mu\nu} G^{\mu\nu} - \frac{1}{2} \operatorname{Tr} W_{\mu\nu} W^{\mu\nu} - \frac{1}{4} B_{\mu\nu} B^{\mu\nu}$$

$$= -\frac{1}{4} \sum_{\text{a}=1}^{8} G^{\text{a}}_{\mu\nu} G^{\text{a}\mu\nu} - \frac{1}{4} \sum_{a=1}^{3} W^{a}_{\mu\nu} W^{a\mu\nu} - \frac{1}{4} B_{\mu\nu} B^{\mu\nu} \tag{1.4}$$

$$\mathcal{L}_{\text{fermions}} = \sum_{\substack{\text{left} \\ \text{quarks}}} i\bar{Q}^i_L \slashed{D}^{(q)} Q^i_L + \sum_{\substack{\text{up} \\ \text{quarks}}} i\bar{u}^i_R \slashed{D}^{(u)} u^i_R + \sum_{\substack{\text{down} \\ \text{quarks}}} i\bar{d}^i_R \slashed{D}^{(d)} d^i_R$$

$$+ \sum_{\substack{\text{left} \\ \text{leptons}}} i\bar{L}^i \slashed{D}^{(\ell)} L^i + i\bar{e}^i_R \slashed{D}^{(e)} e^i_R \tag{1.5}$$

$$\mathcal{L}_{\text{Higgs}} = \left| D_\mu H \right|^2 + m^2 |H|^2 - \lambda_H |H|^4 \tag{1.6}$$

$$-\mathcal{L}_{\text{Yukawa}} = Y_D^{ij} \left(\bar{Q}^i_L H d^j_R + \bar{d}^j_R H^\dagger Q^i_L \right) + Y_U^{ij} \left(\bar{Q}^i_L \tilde{H} u^j_R + \bar{u}^j_R \tilde{H}^\dagger Q^i_L \right)$$

$$+ Y_\ell \left[\bar{L}_i H e^i_R + \bar{e}^i_R H^\dagger L_i \right] \tag{1.7}$$

$$\mathcal{L}_{\text{Theta-vacuum}} = -\frac{\theta}{16\pi^2} \varepsilon^{\mu\nu\rho\sigma} \operatorname{Tr} G_{\mu\nu} G_{\rho\sigma} = -\frac{\theta}{32\pi^2} \varepsilon^{\mu\nu\rho\sigma} G^{\text{a}}_{\mu\nu} G^{\text{a}}_{\rho\sigma}, \tag{1.8}$$

where we used the convention that italicized indices are the $SU(2)$ indices $a = 1, 2, 3$, the non-italicized ones are for the $SU(3)$ color indices $\text{a} = 1, \cdots, 8$ and the fermion indices are to label the three families of leptons and quarks $i = 1, 2, 3$. Moreover we call *up quarks* the up, charm and top quarks, while the *down quarks* are the remaining down, strange and bottom quarks.

The theta-vacuum term is a consequence of the strong CP problem [106, 119] and

---

[2]From hereafter the Einstein summation convention is used unless stated otherwise. Sometimes the summation will be shown for clarity's sake.

[3]We make use of the Feynman slash notation where $\gamma^\mu a_\mu = \slashed{a}$.

Table 1.2. Properties of the Standard Model Particles as given by the PDG [152].

	Particle	Mass (MeV)	Mean Life (s)	Charge (e)
Leptons	e^-	0.511 ± 10^{-9}	$> 6.6 \times 10^{28}$ yr	
	μ^-	105.7 ± 10^{-6}	2.197 ± 10^{-6}	-1
	τ^-			
	ν_e, ν_μ, ν_τ	$< 2 \times 10^{-6}$	-	0
Quarks[a]	u	$2.2^{+0.5}_{-0.4}$	-	$\frac{2}{3}$
	c	$1.27^{+0.025}_{-0.035} \times 10^3$	-	
	t	$(173.0 \pm 0.4) \times 10^3$	-	
	d	$4.7^{+0.5}_{-0.3}$	-	$-\frac{1}{3}$
	s	95^{+9}_{-3}	-	
	b	$4.18^{+0.04}_{-0.03} \times 10^3$	-	
	Particle	Mass (GeV)	Decay Width (GeV)	Charge
Bosons	γ	$< 1 \times 10^{-24}$	Stable	$< 1 \times 10^{-35}$
	$W^\pm$	80.379 ± 0.012	2.085 ± 0.042	± 1
	Z^0	91.1876 ± 0.0021	2.4952 ± 0.0023	0
	g	0	-	-
	h^0	125.18 ± 0.16	< 0.013	0

[a] The u, d and s quark masses are estimates of so-called "current-quark masses", in a mass-independent subtraction scheme such as $\overline{\text{MS}}$ at a scale $\mu \approx 2$ GeV. The c and b quark masses are the running masses in the $\overline{\text{MS}}$ scheme. The t quark mass comes from direct measurements.

is given just for completion since we won't discuss the nature of this term in this thesis.

We will treat in more details equations eqs. (1.4) to (1.7) in the upcoming sections. For now we just set up our various conventions that we will use throughout the whole thesis.

Starting with the gauge Lagrangian eq. (1.4), the three kinetic terms are written in terms of the field strength associated to each gauge connection of the gauge group.

That is[45]

$$G^{\mathrm{a}}_{\mu\nu} = \partial_{[\mu}G^{\mathrm{a}}_{\nu]} + g_s f^{\mathrm{abc}}G^{\mathrm{b}}_{\mu}G^{\mathrm{c}}_{\nu}, \tag{1.9}$$

$$W^{a}_{\mu\nu} = \partial_{[\mu}W^{a}_{\nu]} + g\epsilon^{abc}W^{b}_{\mu}W^{c}_{\nu}, \tag{1.10}$$

$$B_{\mu\nu} = \partial_{[\mu}B_{\nu]}, \tag{1.11}$$

where G^{a}_{μ} is the $SU(3)$ gauge connection (the gluon field), W^{a}_{μ} is the $SU(2)$ connection and B_{μ} is the $U(1)$ connection. The field W^{a}_{μ} and B_{μ} will later combine, after symmetry breaking, to make up the $W^{\pm}_{\mu}, Z^{0}_{\mu}$ bosons which are the massive vector bosons which mediate the weak interactions and the A_{μ} boson, the photon, which mediates the electromagnetic one. The constants f^{abc} are the structure constants of $SU(3)$ and the Levi-Civita symbol ϵ^{abc} gives the structure constants of $SU(2)$. In this thesis we use the convention where the Lie algebra of the groups [74] is given by the commutators

$$\left[t^{\mathrm{a}}, t^{\mathrm{b}}\right] = if^{\mathrm{abc}}t^{\mathrm{b}} \qquad \left[\tau^{a}, \tau^{b}\right] = i\epsilon^{abc}\tau^{c}, \tag{1.12}$$

where, in the fundamental representation, the eight $SU(3)$ generators t^{a} are given by the Gell-Mann matrices while the three $SU(2)$ generators are given by $\tau^{a} = \sigma^{a}/2$ where σ^{a} are the Pauli matrices and are both normalized as

$$\mathrm{Tr}\, t^{a}t^{b} = \frac{1}{2}\delta^{ab} \tag{1.13}$$

More complicated representations can be found in the literature or constructed using methods like the highest weight method.

The three coupling constants are g_s for the strong interactions, g for the W interactions before symmetry breaking and g' for the B interactions before SB as well.

1.2   Particles and Their Representations

Being the SM a Quantum Filed Theory, every particle belongs to some representation of the underlying symmetry group. In the case of the SM we know that the symmetry group, before symmetry breaking, is the one of equation eq. (1.1). We call the various pieces with the quantum number associated to that specific group. In particular

- $SU(3)_C$ quantum number is called *color*,

- $SU(2)_L$ quantum number is called *isospin*,

- $U(1)_Y$ quantum number is called *weak hypercharge*.

---

[4]We use the notation for the antisymmetrization of the indices where $a_{[\mu}b_{\nu]} = a_{\mu}b_{\nu} - a_{\nu}b_{\mu}$. A similar notation is used for the symmetrization $a_{(\mu}b_{\nu)} = a_{\mu}b_{\nu} + a_{\nu}b_{\mu}$.

[5]More generally the field strength is defined as the curvature tensor induced by the group structure on the spacetime manifold and is therefore given by

$$F_{\mu\nu} = \frac{i}{g_F}\left[D^{(A)}_{\mu}, D^{(A)}_{\nu}\right]$$

where $D^{(A)}_{\mu}$ is the covariant derivative constructed from the gauge connection A.

The symmetry breaking pattern of the SM induced by the non-zero vacuum expectation value (VEV) of the Higgs [64, 93, 86] is given by

$$SU(3)_C \times SU(2)_L \times U(1)_Y \to SU(3)_C \times U(1)_{\text{em}}. \tag{1.14}$$

The remaining symmetry after SB is given by the same color symmetry as before plus the electromagnetic symmetry which gives to all particles a quantum number called *electric charge*.

Given this, we can give all the fields appearing in equations eqs. (1.4) to (1.7) their appropriate quantum numbers and with that it can be easily shown that every component of the Lagrangian is by itself a scalar for the SM symmetry group. All the particles and their representation are given in table (1.3).
From the Yukawa Lagrangian eq. (1.7) there is another field which is the charge-conjugate field of the Higgs. This is given by

$$\tilde{H} = i\sigma^2 H^*, \tag{1.15}$$

where σ^2 is a Pauli matrix and H^* is the complex conjugate of the Higgs field H. This field transforms in the $(1,2)_{-1}$ representation and is needed to make all the possible scalar terms such as $\left(\bar{Q}_L^{\mathrm{a}i}\tilde{H}\right)u_R^{\mathrm{a}j}$ where i,j are flavour indices. In fact under $SU(3)$ this is a scalar since we have the following tensor product

$$\mathbf{\bar{3}} \otimes \mathbf{1} \otimes \mathbf{3} = \mathbf{1} \oplus \mathbf{8} \tag{1.16}$$

and we take the trace. Same goes for the isospin since we have

$$\mathbf{2} \otimes \mathbf{2} \otimes \mathbf{1} = \mathbf{1} \oplus \mathbf{3}, \tag{1.17}$$

and for the hypercharge

$$-\frac{1}{3} - 1 + \frac{4}{3} = 0, \tag{1.18}$$

which come out to be scalars for the entire SM symmetry group.

Table 1.3. Representations of the SM particles before symmetry breaking. The last column refers to the representation under the Lorentz group.

Field	$SU(3)_C$	$SU(2)_L$	$U(1)_Y$	$SO(1,3) \simeq SU(2) \times SU(2)$[a]
Q_L^i	3	2	$1/3$	$(1/2, 0)$
u_R^i	3	1	$4/3$	$(0, 1/2)$
d_R^i	3	1	$-2/3$	$(0, 1/2)$
L^i	1	2	-1	$(1/2, 0)$
e_R^i	1	1	-2	$(0, 1/2)$
G_μ	8	1	1	$(1/2, 1/2)$
W_μ	1	3	0	$(1/2, 1/2)$
B_μ	1	1	0	$(1/2, 1/2)$
H	1	2	1	$(0, 0)$

[a] The isomorphism is at the level of the complexified algebras $\mathfrak{so}(1;3) \hookrightarrow \mathfrak{so}(1;3)_{\mathbb{C}} \simeq \mathfrak{su}(2)_{\mathbb{C}} \oplus \mathfrak{su}(2)_{\mathbb{C}}$ but we label it with the group for simplicity.

After EW symmetry breaking, the relevant quantum numbers become the color and the electric charge. Using the remaining unbroken generator of the $SU(2)_L \times U(1)_Y$ group, we can find the relation between the isospin and hypercharge quantum numbers with the electric charge. This is the well known Gell-Mann–Nishijima formula[6] [71, 117]

$$Q = \tau^3 + \frac{Y}{2}, \tag{1.19}$$

where T_3 is the generator which labels the third component of the isospin and Y is the generator of the hypercharge. Just for a sanity check, one can use formula eq. (1.19) to see if the quantum numbers given in table (1.3) give back the expected electric charge. For example, take the right-handed electron which we expect to have a electric charge of -1 and, using eq. (1.19), find

$$e_R^i \rightarrow Q = 0 + (-1) = -1. \quad \checkmark \tag{1.20}$$

1.3 Electroweak Sector

We now have sufficient knowledge to formulate the GSW theory of weak and electromagnetic interactions among leptons and quarks and to study its properties. Let us first state the starting point and the aim of our study

1. There exist charged and neutral currents.

2. The charged currents contain only couplings between left-handed fermions. This result is given by Fermi theory of weak interactions which, as we'll see, is the low energy limit of the GSW theory.

3. The bosons $W^\pm, Z^0$ mediating the weak interaction must be very massive.

4. Nevertheless we'll begin with massless bosons which then receive masses through the Higgs mechanism. At that point we want to simultaneously include the photon field.

Given this list of properties, we can begin to build up the first part of the SM which accounts for the electroweak sector.

1.3.1 The GWS Lagrangian and symmetry breaking

Let's begin, as we always must, to find the symmetry group of the theory. We know that at least there must be one gauge boson for the photon. Moreover there must be another two vector bosons for the $W^\pm$ fields. With this we need at least the $SU(2)$ symmetry group since it has 3 generators. But it turns out that this group is too small since it only accounts for left-handed interactions but we know that the electromagnetism is perfectly symmetric between left and right-handed fermions. What Glashow proposed was the following minimal group

$$SU(2)_W \otimes U(1)_Y, \tag{1.21}$$

---

[6]Depending on the convention used, there can be a factor of $1/2$ difference in the hypercharge giving $Q = \tau^3 + Y$. We use the convention where the factor $1/2$ is present.

where the reps are defined, as we have seen before, by the isospin symmetry and the hypercharge. Based on this symmetry group, the existence of a fourth gauge boson was theorized since the group has 4 generators. It will turn out that the additional gauge boson is, in fact, the Z^0 which mediates the weak neutral currents.

Since we have that the total symmetry group is the product of two groups, we need two different coupling constants g, g'. The kinetic part of the Lagrangian will be then by the second half of the Lagrangian eq. (1.4)

$$\mathcal{L} = -\frac{1}{4}W_{\mu\nu}^a W^{a\mu\nu} - \frac{1}{4}B_{\mu\nu}B^{\mu\nu}. \tag{1.22}$$

Given the local nature of the interactions, we need to give mass to the bosons. On the other hand, the photon will be given by a linear combination of the symmetry generators which remain unbroken under the action of the Higgs mechanism.

To induce the symmetry breaking, we have a complex isospin doublet with hypercharge 1, the Higgs

$$H = \begin{pmatrix} H^+ \\ H^0 \end{pmatrix}. \tag{1.23}$$

The hypercharge is set by the Gell-Mann Nishijima formula eq. (1.19).

The Lagrangian for the Higgs field is given in equation eq. (1.6). In particular, we have to specify how the covariant derivative of equation eq. (1.6) acts on the Higgs doublet. This is easily done by exploiting the Higgs representation under the gauge group

$$D_\mu = \partial_\mu - ig'\frac{Y}{2}B_\mu - igW_\mu^a\tau^a = \partial_\mu - i\frac{g'}{2}B_\mu - igW_\mu^a\tau^a, \tag{1.24}$$

where the τ^a are the the generators of the fundamental **2** representation of $SU(2)$. The Higgs potential with the opposite mass sign, induces a VEV for H, which can be taken to be real and in the lower component without loss of generality. Thus we choose

$$H = \exp\left(\frac{i}{v}\pi^a\tau^a\right)\begin{pmatrix} 0 \\ \dfrac{h+v}{\sqrt{2}} \end{pmatrix}, \tag{1.25}$$

where $v = \langle 0| H |0\rangle = \mu/\sqrt{\lambda}$. Since we are going to study how the gauge bosons and the fermions gain mass through the Higgs mechanism, we will fix the gauge to the *unitary gauge* where, essentially, we set $\pi^a = 0$. With the VEV fixed it is easy to find that the broken generators, i.e. the ones for which $\tau^a\langle H\rangle \neq 0$ are given by

$$\tau^1 = \frac{1}{2}\begin{pmatrix} 0 & 1 \\ 1 & 0 \end{pmatrix} \qquad \tau^2 = \frac{1}{2}\begin{pmatrix} 0 & -i \\ i & 0 \end{pmatrix} \qquad \tau^3 - \frac{Y}{2} = \begin{pmatrix} 0 & 0 \\ 0 & 1 \end{pmatrix} \tag{1.26}$$

and the unbroken generator is given by

$$\tau^3 + \frac{Y}{2} = \begin{pmatrix} 1 & 0 \\ 0 & 0 \end{pmatrix} \tag{1.27}$$

which is exactly the electric charge as given by the Gell-Mann Nishijima formula! The symmetry breaking pattern is therefore

$$SU(2)_W \otimes U(1)_Y \to U(1)_{\text{em}} \tag{1.28}$$

and we expect, thanks to Goldstone theorem and the Higgs mechanism, three out of four vector bosons to be massive while one remains massless (spoiler: the only vector boson without mass will be the photon!).

Putting the VEV in the kinetic part of the Higgs, making use of gauge freedom and choosing a gauge which "eats" the Goldstone bosons π^a called *unitary gauge*[7], we get

$$
\begin{aligned}
|D_\mu H|^2 &= \\
&= \frac{v^2}{8} \begin{pmatrix} 0 & 1 \end{pmatrix} \begin{pmatrix} g'B_\mu + gW_\mu^3 & g(W_\mu^1 - iW_\mu^2) \\ g(W_\mu^1 + iW_\mu^2) & g'B_\mu - gW_\mu^3 \end{pmatrix} \begin{pmatrix} g'B_\mu + gW_\mu^3 & g(W_\mu^1 - iW_\mu^2) \\ g(W_\mu^1 + iW_\mu^2) & g'B_\mu - gW_\mu^3 \end{pmatrix} \begin{pmatrix} 0 \\ 1 \end{pmatrix} \\
&= g^2 \frac{v^2}{8} \left[\left(W_\mu^1 \right)^2 + \left(W_\mu^2 \right)^2 + \left(\frac{g'}{g} B_\mu - W_\mu^3 \right)^2 \right]
\end{aligned}
$$

(1.29)

The W^1, W^2 terms are degenerate in mass

$$
M_W^2 = \frac{v^2 g^2}{4}
$$

The remaining terms are given by

$$
\frac{v^2 g^2}{4} (W_\mu^3)^2 + \frac{v^2 g'^2}{4} B_\mu^2 - \frac{2gg'v^2}{4} B^\mu W_\mu^3 = \frac{v^2}{4} \begin{pmatrix} B_\mu & W_\mu^3 \end{pmatrix} \begin{pmatrix} g^2 & gg' \\ gg' & g'^2 \end{pmatrix} \begin{pmatrix} B^\mu \\ W_3^\mu \end{pmatrix} \quad (1.30)
$$

it is clear that the initial basis is not the basis given by the mass eigenstates. We can therefore go to the latter by diagonalizing eq. (1.30)

$$
\begin{aligned}
\det \begin{pmatrix} g^2 - m & gg' \\ gg' & g'^2 - m \end{pmatrix} &= (g^2 - m)(g'^2 - m) - (gg')^2 = 0 \\
&= m^2 + (gg')^2 - m(g^2 + g'^2) - (gg') \\
&= m(m - g^2 - g'^2) = 0 \\
m = 0 \quad & m = g^2 + g'^2
\end{aligned}
$$

(1.31)

The two solutions give us what we wanted: a massless mode and a massive one. Looking for the eigenvectors will give us linear combinations of the B_μ and W_μ^3 fields which will turn out to be the massless photon field and the massive Z^0 gauge boson field.

By means of the following reparametrization

$$
\sin \theta_W = \frac{g'}{\sqrt{g^2 + g'^2}}, \qquad \cos \theta_W = \frac{g^2}{\sqrt{g^2 + g'^2}}, \qquad (1.32)
$$

where θ_W is called the *Weinberg angle* [78, 142], one can easily show that rotation based on this angle gives us indeed the linear combination that we need

$$
\begin{pmatrix} Z_\mu^0 \\ A_\mu \end{pmatrix} = \begin{pmatrix} \cos \theta_W & -\sin \theta_W \\ \sin \theta_W & \cos \theta_W \end{pmatrix} \begin{pmatrix} W_\mu^3 \\ B_\mu \end{pmatrix} \implies \begin{cases} Z_\mu^0 = \cos \theta_W W_\mu^3 - \sin \theta_W B_\mu \\ A_\mu = \sin \theta_W W_\mu^3 + \sin \theta_W B_\mu. \end{cases}
$$

(1.33)

---

[7]One needs to be aware of which gauges are at play and the ones to choose for specific calculations.

Now notice the following

$$W_\mu^a \tau^a = \frac{1}{\sqrt{2}} \left(W_\mu^+ \tau^+ + W_\mu^- \tau^- \right) + W_\mu^3 \tau^3, \tag{1.34}$$

where

$$\tau^\pm = \tau^1 \pm i\tau^2. \tag{1.35}$$

Under this definition, the charged gauge fields are given by

$$W_\mu^+ = \frac{1}{\sqrt{2}}(W_\mu^1 + iW_\mu^2) \qquad W_\mu^- = \frac{1}{\sqrt{2}}(W_\mu^1 - iW_\mu^2). \tag{1.36}$$

Therefore what we have in the hand are the following fields

$$\begin{aligned}
W_\mu^\pm &\rightsquigarrow M_W = \frac{vg}{2}, \\
Z_\mu^0 &\rightsquigarrow m_Z = \frac{1}{2\cos\theta_W} gv = \frac{v}{2}\sqrt{g^2 + g'^2} = \frac{M_W}{\cos\theta_W}, \\
A_\mu &\rightsquigarrow m_A = 0.
\end{aligned} \tag{1.37}$$

Already there's an unambiguous prediction: the W bosons should be lighter than the Z boson.
Moreover we find that, at tree level the following result should hold

$$\rho = \frac{M_W^2}{\cos^2\theta_W m_Z^2} = 1 \tag{1.38}$$

This is the result of an hidden symmetry of the Standard Model, the *custodial symmetry*[8].

1.3.2 Gauge Sector

Putting together what we found, we can write down the kinetic term in the Lagrangian for the Z and A bosons after symmetry breaking, in the unitary gauge, as

$$\mathcal{L}_{\rm K} = -\frac{1}{4}F_{\mu\nu}F^{\mu\nu} - \frac{1}{4}Z_{\mu\nu}Z^{\mu\nu} + \frac{1}{2}m_Z^2 Z_\mu Z^\mu, \tag{1.39}$$

where

$$Z_{\mu\nu} = \partial_\mu Z_\nu - \partial_\nu Z_\mu \qquad F_{\mu\nu} = \partial_\mu A_\nu - \partial_\nu A_\mu. \tag{1.40}$$

Since the gauge bosons transform in the adjoint rep, their interactions are given by commutators and in particular, the W_μ^3 part of the photon field gives us the known coupling

$$g[A_\mu, W_\nu^a \tau^a] = g\sin\theta_W W_\mu^3 W_\nu^a \left[\tau^3, \tau^a\right] \implies e = g\sin\theta_W = g'\cos\theta_W \tag{1.41}$$

---

[8]"Turning down" the couplings to the Higgs $g, g' \to 0$ we can see that the Lagrangian eq. (1.6) has a bigger symmetry group which we label as $SU(2)_L \times SU(2)_R$. The symmetry breaking pattern then becomes $SU(2)_L \times SU(2)_R \to SU(2)_V$ which is a bigger symmetry than the one with the couplings so that only at tree level we can see it is effects.

With this in mind, the $W^{\pm}$ combinations will have ± 1 charge in units of e, which is what we want.

Without giving the full calculation, one can find that the full gauge Lagrangian is

$$
\begin{aligned}
\mathcal{L} = & -\frac{1}{4} F_{\mu\nu} F^{\mu\nu} - \frac{1}{4} Z_{\mu\nu} Z^{\mu\nu} - \frac{1}{2} (\partial_\mu W_\nu^+ - \partial_\nu W_\mu^+)(\partial^\mu (W^-)^\nu - \partial^\nu (W^-)^\mu) \\
& + \frac{1}{2} m_Z^2 Z_\mu Z^\mu - M_W^2 W_\mu^+ (W^-)^\mu \\
& + ie \cot\theta_W \left[Z^{\mu\nu} W_\mu^+ W_\nu^- - (\partial_\mu W_\nu^+ - \partial_\nu W_\mu^+) Z^\mu (W^-)^\nu + (\partial_\mu W_\nu^- - \partial_\nu W_\mu^-) Z^\mu (W^+)^\nu \right] \\
& + ie \left[F^{\mu\nu} W_\mu^+ W_\nu^- - (\partial_\mu W_\nu^+ - \partial_\nu W_\mu^+) A^\mu (W^-)^\nu + (\partial_\mu W_\nu^- - \partial_\nu W_\mu^-) A^\mu (W^+)^\nu \right] \\
& + \frac{1}{2} \frac{e^2}{\sin^2\theta_W} \left(W_\mu^+ (W^+)^\mu W_\nu^- (W^-)^\nu - W_\mu^+ (W^-)^\mu W_\nu^+ (W^-)^\nu \right) \\
& + e^2 \left(A^\mu W_\mu^+ A^\nu W_\nu^- - A_\mu A^\mu W_\nu^+ (W^-)^\nu \right) + e^2 \cot\theta_W \left(Z^\mu W_\mu^+ Z^\nu W_\nu^- - Z_\mu Z^\mu W_\nu^+ (W^-)^\nu \right) \\
& + e^2 \cot\theta_W \left(W_\mu^+ W_\nu^- A^\mu Z^\nu + W_\mu^- W_\nu^+ A^\mu Z^\nu - 2 W_\mu^+ (W^-)^\mu A^\nu Z_\nu \right)
\end{aligned}
\tag{1.42}
$$

1.3.3 Higgs Sector

We can now return to the field h, the *Higgs Boson*. This boson remains in the spectrum of the theory even after the choice of the unitary gauge $\pi = 0$ by the Higgs mechanism.

The part of the Lagrangian which gives us the dynamics of the Higgs field is given by the expansion of the covariant derivative after symmetry breaking

$$
\begin{aligned}
\mathcal{L}_{\mathrm{H}} = & \frac{1}{2} (\partial_\mu h)(\partial^\mu h) - \frac{m_h^2}{2} ^2 - g \frac{m_h^2}{4 M_W} h^3 - \frac{g^2 m_h^2}{32 M_W^2} h^4 + \\
& + 2 \frac{h}{v} \left(M_W^2 W_\mu^+ (W^-)^\mu + \frac{1}{2} m_Z^2 Z^\mu Z_\mu \right) + \frac{h^2}{v^2} \left(M_W^2 W_\mu^+ (W^-)^\mu + \frac{1}{2} m_Z^2 Z^\mu Z_\mu \right),
\end{aligned}
\tag{1.43}
$$

where $m_h = \sqrt{2}\,\mu$ and μ is the initial symmetry breaking parameter in the unbroken Higgs doublet Lagrangian and v is the induced VEV.

As we can see from eq. (1.43), the Higgs field interacts with itself in cubic and quartic interactions and with the other gauge bosons, again, with cubic and quartic interactions. As in all the other interaction terms, the strength of the interaction is proportional to the masses.

1.3.4 Lepton Sector

Let's study the interactions between the electroweak gauge bosons and the leptons. As seen in table (1.3) we have classified leptons into left-handed $L^i = (2,1)_{-1}$ and right-handed $e_R^i = (1,1)_{-2}$

$$
L^i = \begin{pmatrix} \nu_e \\ e^- \end{pmatrix}_L, \begin{pmatrix} \nu_\mu \\ \mu^- \end{pmatrix}_L, \begin{pmatrix} \nu_\tau \\ \tau^- \end{pmatrix}_L, \qquad e_R^i = \{e_R, \mu_R, \tau_R\} \qquad i = 1, 2, 3.
\tag{1.44}
$$

We see that the left-handed field shows up as an isospin doublet, whereas the right-handed field as singlet. In equation eq. (1.44) we highlighted the three *generations* left $SU(2)$ doublets and right singlets of leptons. These all transform as a left/right-handed Weyl spinors. From now on we consider only one generation of leptons for simplicity's sake, but the argument can be easily generalized to all three.

The coupling between the leptons and the gauge boson is given by the covariant derivative in the fermion Lagrangian eq. (1.5)

$$\mathcal{L} = i\bar{L}\slashed{D}^{(\ell)}L + i\bar{e}_R\slashed{D}^{(e)}e_R, \tag{1.45}$$

where the covariant derivatives are different between the left-handed part and the right-handed one. All leptons couple to the hypercharge gauge boson as we stated in table (1.3). We denote Y_L the left-handed hypercharge and Y_R the right-handed one. So the expanded Lagrangian will be

$$\mathcal{L} = i\bar{L}\left(\slashed{\partial} - ig\slashed{W}^a\tau^a - i\frac{g'}{2}Y_L\slashed{B}\right)L + i\bar{e}_R\left(\slashed{\partial} - i\frac{g'}{2}Y_R\slashed{B}\right)e_R. \tag{1.46}$$

To be clear, the L or R subscript in the Lagrangian are just for convenience, since they indicate the implicit chirality of the field. But since all leptons are all left- or right-handed Weyl spinors, it would be technically correct to replace

$$\begin{aligned}\bar{L}_R\slashed{\partial}L &\to L^\dagger\bar{\sigma}^\mu\partial_\mu L, \\ \bar{e}_R\slashed{\partial}e_R &\to e_R^\dagger\sigma^\mu\partial_\mu e_R,\end{aligned} \tag{1.47}$$

where $\sigma^\mu = (\mathbb{1}, \sigma^i)$ and $\bar{\sigma}^\mu = (\mathbb{1}, -\sigma^i)$. However, since we'll almost always deal with the fields in the broken phase, where the left- and right-handed spinors combine into Dirac spinors, for simplicity we'll always write everything in the Dirac rep where[9]

$$\begin{aligned}\bar{L}\slashed{\partial}L &= L^\dagger\gamma^0\gamma^\mu\frac{1-\gamma_5}{2}\partial_\mu L, \\ \bar{e}_R\slashed{\partial}e_R &= e\gamma^0\gamma^\mu\frac{1+\gamma_5}{2}\partial_\mu e.\end{aligned} \tag{1.48}$$

As it is clear, there are still no masses for the leptons. To find them we have to build the Yukawa sector of the Lagrangian where the fields interact with the Higgs doublet. This will give mass to the leptons after symmetry breaking.

From the transformation rule of the lepton fields and the Higgs doublet, it is easy to see that the only scalar quantities we can construct are the ones in Lagrangian eq. (1.7)

$$\mathcal{L} = Y\left[\bar{L}_e H e_R + \bar{e}_R H^\dagger L_e\right]. \tag{1.49}$$

After symmetry breaking, this part will give us the mass for the electrons with the following term

$$-m_e\left(\bar{e}_L e_R + \bar{e}_R e_L\right), \qquad m_e = \frac{Y}{\sqrt{2}}v. \tag{1.50}$$

---

[9]Sometimes we will use the notation where the chirality projector are written as

$$P_L = \frac{1-\gamma^5}{2} \qquad P_R = \frac{1+\gamma^5}{2}$$

Again, only after electroweak symmetry breaking, together with the diagonalization of the masses for the gauge bosons, the Lagrangian eq. (1.46) becomes

$$\mathcal{L} = \bar{L}_e \left[g\tau^3 \left(Z_\mu \cos\theta_W + A_\mu \sin\theta_W \right) + \frac{g'}{2} Y_L \left(-Z_\mu \sin\theta_W + A_\mu \cos\theta_W \right) \right] \gamma^\mu L_e +$$

$$+ Y_R \frac{g'}{2} \bar{e}_R \left(-Z_\mu \sin\theta_W + A_\mu \cos\theta_W \right) \gamma^\mu e_R.$$

$$(1.51)$$

The terms proportional to the photon field are

$$A_\mu \left[\bar{L}_e \left(g\tau^3 \sin\theta_W + \frac{g'}{2} Y_L \cos\theta_W \right) L_e + \left(\frac{g'}{2} \cos\theta_W \right) Y_R \left(\bar{e}_R \gamma^\mu e_R \right) \right], \qquad (1.52)$$

and using the fact that $g \sin\theta_W = g' \cos\theta_W = gg'/\sqrt{g^2 + g'^2}$, we get to the expected result for the QED interaction between photons and charged leptons

$$A_\mu g \sin\theta_W \left[\bar{L}_e \gamma^\mu \left(\tau^3 + \frac{Y_L}{2} \right) L_e + \frac{Y_R}{2} \left(\bar{e}_R \gamma^\mu e_R \right) \right]$$

$$= A_\mu g \sin\theta_W \left[-\bar{e}_L \gamma^\mu e_L - \bar{e}_R \gamma^\mu e_R \right]$$

$$= g \sin\theta_W A_\mu J_{\text{em}}^\mu,$$

where we used the unbroken generator in eq. (1.27) and

$$J_{\text{em}}^\mu = Q_e (\bar{e} \gamma^\mu e), \qquad (1.53)$$

with $Q_e = e = g \sin\theta_W$. As expected, the electromagnetic interaction does not differentiate between left and right-handed chirality.

The terms proportional to the Z^0 boson are

$$Z_\mu \left[g \cos\theta_W \bar{L}_e \gamma^\mu \tau^3 L_e - \frac{Y_L}{2} g' \sin\theta_W \bar{L}_e \gamma^\mu L_e - \frac{Y_R}{2} g' \sin\theta_W \bar{e}_R \gamma^\mu e_R \right]$$

$$= Z_\mu \left[(g \cos\theta_W + g' \sin\theta_W) \bar{L}_e \gamma^\mu \tau^3 L_e - g' \sin\theta_W q J_{\text{em}}^\mu \right] \qquad (1.54)$$

$$= Z_\mu \frac{g}{\cos\theta_W} \left(J_3^\mu - q \sin^2\theta_W J_{\text{em}}^\mu \right).$$

Therefore the Z^0 boson not only couples to the EM current but even with an axial current

$$J_3^\mu = \bar{L}_e \gamma^\mu \tau^3 L_e. \qquad (1.55)$$

There remain only the interaction terms between the leptons and the $W^\pm$ bosons. Recalling eq. (1.34) we get, from the Lagrangian eq. (1.46)

$$g W_\mu^a \bar{L}_e \gamma^\mu \tau^a L_e = g \left[\frac{1}{\sqrt{2}} W_\mu^+ \bar{L}_e \gamma^\mu \tau^- L_e + \frac{1}{\sqrt{2}} W_\mu^- \bar{L}_e \gamma^\mu \tau^+ L_e + W_\mu^3 \bar{L}_e \gamma^\mu \tau^3 L_e \right]$$

$$(1.56)$$

and we can directly see that the charged currents are

$$J_\mu^+ = \bar{L}_e \gamma_\mu \tau^+ L_e = \begin{pmatrix} \bar{\nu}_e & \bar{e}^- \end{pmatrix}_L \gamma_\mu \begin{pmatrix} 0 & 1 \\ 0 & 0 \end{pmatrix} \begin{pmatrix} \nu_e \\ e^- \end{pmatrix}_L = \begin{pmatrix} \bar{\nu}_e & \bar{e}^- \end{pmatrix}_L \gamma_\mu \begin{pmatrix} e^- \\ 0 \end{pmatrix}_L$$

$$= \bar{\nu}_{eL} \gamma_\mu e_L^- = \bar{\nu}_e \gamma_\mu \frac{1 - \gamma_5}{2} e^-$$

$$(1.57)$$

and

$$J_\mu^- = (J_\mu^+)^\dagger = \bar{e}\gamma_\mu \frac{1-\gamma_5}{2}\nu_e. \tag{1.58}$$

The axial part for W^3 goes into the photon and Z_0 boson.

The full interaction Lagrangian between the leptons and the gauge boson after electroweak symmetry breaking becomes

$$\mathcal{L} = qeA_\mu J_{\text{em}}^\mu + \frac{g}{\cos\theta_W} Z_\mu \left(J_3^\mu - q\sin\theta_W J_{\text{em}}^\mu\right) + \frac{g}{\sqrt{2}}\left(W_\mu^+ J^{\mu-} + W_\mu^- J^{\mu+}\right). \tag{1.59}$$

1.4 Quark Mixing and CKM

Now that we talked about the electroweak sector

$$SU(2)_L \times U(1)_Y \to U(1)_{\text{em}} \tag{1.60}$$

of the Standard Model, we're ready to add one of the missing part: the quarks. We will not talk about QCD in this section, which is the remaining $SU(3)$ of the full symmetry of the Standard Model, but only how quarks enter in the electroweak theory and how we can give masses to them with the help of the Higgs mechanism. It will turn out that whenever we try to diagonalize the mass spectrum, we'll introduce some kind of mixing between the quarks which will be mediated by the electroweak gauge bosons.

1.4.1 The Quarks

The quarks that enter in the Standard Model and their representations are summarized in table (1.3). To be more specific, quarks come in three flavours, just like leptons, and appear in the theory in their chiral basis

$$Q_L^i = \begin{pmatrix} u \\ d \end{pmatrix}_L, \begin{pmatrix} c \\ s \end{pmatrix}_L, \begin{pmatrix} t \\ b \end{pmatrix}_L$$
$$u_R^i = \{u_R, c_R, t_R\}, \qquad d_R = \{d_R, s_R, b_R\}. \tag{1.61}$$

Their name are: up, down, charm, strange, top and bottom quarks. In the case of the quarks, we now consider all three families since, as we will see, they can mix with themselves, while leptons do not. Whenever using the notation u^i we'll mostly mean the up row of quarks in the SM which are up and have electric charge, in units of e, 2/3, charm and top quarks, the others are the d^is which have electric charge $-1/3$.

Their irrep in the full SM gauge group is

$$Q_L \sim (2,3)_{\frac{1}{3}}, \quad u_R \sim (1,3)_{\frac{4}{3}}, \quad d_R \sim (1,3)_{-\frac{2}{3}}. \tag{1.62}$$

Quarks carry a lot of indices: one index for the isospin charge, one index for the color charge, one family index and a Lorentz index. We'll omit them, as per usual, since the notation would be too cluttered with them. But remember still that to construct invariant quantities all indices must be saturated in such a way to have a singlet for any of the possible symmetries.

1.4.2 Interactions and Lagrangian

In the same way as we did with the leptons, we start from the following Lagrangian given in equation eq. (1.5)[10]

$$
\begin{aligned}
\mathcal{L} = i\bar{Q}_L \left(\slashed{\partial} - ig\slashed{W}^a \tau^a - i\frac{g'}{2} Y_{Q_L} \slashed{B} \right) Q_L \\
+ i\bar{u}_R \left(\slashed{\partial} - i\frac{g'}{2} Y_{u_R} \slashed{B} \right) u_R + i\bar{d}_R \left(\slashed{\partial} - i\frac{g'}{2} Y_{d_R} \slashed{B} \right) d_R.
\end{aligned}
\tag{1.63}
$$

By direct comparison with the leptons, we can easily see that the calculations will be the same and so we give directly the results for the various currents that one expects to find, coupled to the respective gauge bosons.
The full fermion currents will be the following

$$
J_{\text{em}}^\mu = -\bar{e}\gamma^\mu e + \frac{2}{3}\bar{u}^a \gamma^\mu u_a - \frac{1}{3}\bar{d}^a \gamma^\mu d_a
\tag{1.64}
$$

is the EM current coupled to the photon[11],

$$
J_\mu^3 = \bar{\nu}_e \gamma_\mu \frac{1 - \gamma_5}{2} \nu_e - \bar{e}\gamma_\mu \frac{1 - \gamma_5}{2} e + \bar{u}^a \gamma_\mu \frac{1 - \gamma_5}{2} u_a + \bar{d}^a \gamma_\mu \frac{1 - \gamma_5}{2} d_a
\tag{1.65}
$$

is the axial current coupled to the Z^0 boson, and the charged ones

$$
J_\mu^+ = \bar{L}_e \gamma_\mu \tau^+ L_e + \bar{Q}^a \gamma_\mu \tau^+ Q_a,
\tag{1.66}
$$

$$
J_\mu^- = \bar{L}_e \gamma_\mu \tau^- L_e + \bar{Q}^a \gamma_\mu \tau^- Q_a
\tag{1.67}
$$

which are coupled to the charged $W^\pm$ bosons.

1.4.3 Yukawa Sector

From the irreps eq. (1.62) and the Higgs we need to construct all the possible renormalizable scalar quantities. As stated in the previous sections, to do so we'll need however another form of the Higgs field since H^* won't cut it. The field we'll use is the charge conjugate of H defined by equation eq. (1.15).
  Now let's see what kind of scalars we can build up. If we start from $\bar{Q}_L H$ we can easily see that this we'll be

$$
\bar{Q}_L H \sim (\bar{2}, \bar{3})_{-\frac{1}{3}} (2, 1)_1 = (\bar{2} \times 2, \bar{3} \times 1)_{1 - \frac{1}{3}}.
\tag{1.68}
$$

We know that $\bar{2} \times 2$ contains a singlet state. What's missing is the hypercharge singlet since $1 - \frac{1}{3} = 2/3$ and the color singlet. If we search in eq. (1.62) for a suitable quantity, we see that the d_R quark serves our purpose and so a suitable renormalizable operator for our Yukawa sector will be

$$
\bar{Q}_L H d_R + \text{h.c.} = \bar{Q}_R H d_R + \bar{d}_R H^\dagger Q_L,
\tag{1.69}
$$

---

[10]Again the computations are given for only one family of quarks if not else specified. The arguments can be easily extended to three.
  [11]Note the color index $a = 1, 2, 3$ on the quarks which is saturated.

where we added the Hermitian conjugate, as always, to include the reality of the Lagrangian. And this settles down the down part of the Lagrangian. For the up part we'll use the charge conjugate Higgs since, if you try, we cannot construct scalar quantities between up quarks with the normal Higgs doublet.

it is easy to see that the only renormalizable scalar quantity we can construct using u_R is

$$\bar{Q}_L \tilde{H} u_R + \bar{u}_R \tilde{H}^\dagger Q_L \tag{1.70}$$

Therefore, if we now put in all the families and the Yukawa coupling we get the Yukawa sector for quarks

$$\mathcal{L}_{\mathrm{Y}} = Y_U^{ij} \left(\bar{Q}_L^i H d_R^j + \bar{d}_R^j H^\dagger Q_L^i \right) + Y_D^{ij} \left(\bar{Q}_L^i \tilde{H} u_R^j + \bar{u}_R^j \tilde{H}^\dagger Q_L^i \right) \tag{1.71}$$

which is exactly the one which was given without explanation in equation eq. (1.7). Again here we consider all three quark families since in the end quark will mix among themselves. This is not true for leptons since in the SM we are considering there are no right-handed neutrinos, which means that they will always be massless and therefore the mixing matrix can always be "rotated away" and go back to a diagonal matrix. There cannot be any mixing among neutrinos without their right-handed counterpart.

1.4.4 Symmetry Breaking

For example, given the Yukawa sector, we can use symmetry breaking and, by going in the unitary gauge[12], we get for the down quarks

$$\begin{pmatrix} \bar{u}_L & \bar{d}_L \end{pmatrix} \begin{pmatrix} 0 \\ \frac{v+h}{\sqrt{2}} \end{pmatrix} d_R = \bar{d}_L d_R \left(\frac{v+h}{\sqrt{2}} \right). \tag{1.72}$$

Thus the mass for the down quarks is given by a $SU(2)$ symmetry breaking Dirac term and, with several generations of down-like quarks, we expect

$$Y_D^{ij} \frac{v}{\sqrt{2}} \bar{d}_L^i d_R^j \implies M_D^{ij} = \frac{v}{\sqrt{2}} Y_D^{ij} \tag{1.73}$$

For the up quarks is the same but the mass matrix is given in terms of the Yukawa of the up quarks

$$M_U^{ij} = \frac{v}{\sqrt{2}} Y_U^{ij} \tag{1.74}$$

With this, we see that the mass terms in the Lagrangian for the quarks are

$$\mathcal{L} = \bar{d}_L^i M_{ij}^D d_R^j + \bar{d}_R^j M_{ij}^{D\dagger} d_L^i + \bar{u}_L^i M_{ij}^U u_R^j + \bar{u}_R^j M_{ij}^{U\dagger} u_L^i \tag{1.75}$$

Nobody assures us that the mass matrices will be diagonal, but we would like them to be diagonal since we expect the quarks, just like any other particle, to have a definite mass[13]. Since we don't have any constraint on the specific form of the mass matrix we just found, we do not know if it is possible to diagonalize it.

---

[12] Remember that whenever we speak about unitary gauge we're implying that we set the Goldstone boson "to zero", which is a way of saying that the gauge field eats the Goldstone boson gaining a new degree of freedom.

[13] The values of the masses of the quarks are quite difficult to define since they cannot be experimentally measured due to confinement.

1.4.5 On the Diagonalization of Matrices

We now prove that there exist a method through which we can diagonalize any matrix. This process is called *singular value decomposition* and it provides two unitary matrices L, R such that

$$L^\dagger M R = \hat{M}, \tag{1.76}$$

where we'll use the hatted matrix for the diagonal form of M.
From the generic matrix M we can construct two Hermitian matrices

$$MM^\dagger \qquad M^\dagger M \tag{1.77}$$

which in general do not commute. Provided that there is no singular eigenvalue and that the determinant is non-zero, we can easily prove that these matrices have the same eigenvalues. Indeed we gave

$$
\begin{aligned}
P_{MM^\dagger} &= \det\left(MM^\dagger - \lambda\right) = \det\{M\}\det\left(M^\dagger - \lambda M^{-1}\right) \\
&= \det\left(M^\dagger - \lambda M^{-1}\right)\det M = \det\left(M^\dagger M - \lambda\right) = P_{M^\dagger M},
\end{aligned}
\tag{1.78}
$$

and since both matrices have the same characteristic polynomial, they'll have the same eigenvalues. Being both Hermitian, we know that they can be diagonalized thanks to the spectral theorem and so there exist two matrices L and R which diagonalize the matrices to the same diagonal form since they have both the same eigenvalues

$$L(MM^\dagger)L^\dagger = \hat{D} = R(M^\dagger M)R^\dagger \tag{1.79}$$

Starting from this we define the following

$$M' = LMR^\dagger \qquad (M')^\dagger = RM^\dagger L^\dagger, \tag{1.80}$$

from which it is easy to see that

$$M'(M')^\dagger = (M')^\dagger M' = \hat{D}. \tag{1.81}$$

We know that we can always decompose a matrix into two Hermitian matrices as

$$M' = \left(\frac{M' + M'^\dagger}{2}\right) + i\left(\frac{M' - M'^\dagger}{2}\right) = H_1 + iH_2 \tag{1.82}$$

The two matrices we just defined H_1, H_2 are obviously diagonalizable since they hare Hermitian but we would like them to be diagonalizable by the same unitary matrix. From linear algebra, we know that this is possible if the two matrices commute! And it is easy to see that

$$[H_1, H_2] = \frac{1}{4i}\left[M' + M'^\dagger, M' - M'^\dagger\right] = \frac{1}{2i}\left(M'M'^\dagger - M'^\dagger M'\right) = 0 \tag{1.83}$$

Therefore there exists a unitary matrix W such that $W^\dagger M' W = \hat{M}'$ is a complex diagonal matrix and therefore, being complex diagonal we can put it in the form

$$\hat{M}' = \hat{M}\hat{U}_\varphi, \tag{1.84}$$

where $\hat{U}_\varphi = \text{diag}\left(e^{\phi_1}, e^{\phi_2}, \cdots, e^{\phi_N}\right)$ is a matrix of phases. Moreover

$$W^\dagger M' W = \hat{M}\hat{U}_\varphi = W^\dagger L^\dagger M R W \tag{1.85}$$

and therefore if we define

$$\tilde{L} = LW \qquad \tilde{R} = RW\hat{U}_\varphi^{-1} \tag{1.86}$$

we found the matrices that diagonalize M.

1.4.6 The CKM Matrix

Now that we know a way for diagonalizing any matrix, we can use it for the mass matrix for the quarks. Take the up quarks for example

$$\bar{u}_L^i \hat{m}_{ij}^u u_R^j = \bar{u}_L^{i\prime}(U_{u_L}^\dagger)_{ik} M_{kl}^U (U_{u_R})_{kj} u_R^{j\prime}, \tag{1.87}$$

where

$$\hat{m}^u = \begin{pmatrix} m_u & 0 & 0 \\ 0 & m_c & 0 \\ 0 & 0 & m_t \end{pmatrix} \tag{1.88}$$

and the new mass eigenstates are written in terms of the old ones as

$$u_L^i = (U_{u_L})_{ij} u_L^{j\prime} \qquad u_R^i = (U_{u_R})_{ij} u_R^{j\prime}. \tag{1.89}$$

To distinguish the quarks in the two basis, we put a prime on the current basis quarks.

Same thing goes for the down quarks where the diagonal form of the mass matrix will be

$$\hat{m}^d = \begin{pmatrix} m_d & 0 & 0 \\ 0 & m_s & 0 \\ 0 & 0 & m_b \end{pmatrix} \tag{1.90}$$

and the mass eigenstates

$$d_L^i = (U_{d_L})_{ij} d_L^{j\prime} \qquad d_R^i = (U_{d_R})_{ij} d_R^{j\prime}. \tag{1.91}$$

The kinetic terms do not change under this change of basis. In fact it is easy to see that, if we start from the original current base lagrangian

$$
\begin{aligned}
\mathcal{L} =& \begin{pmatrix} \bar{u}_L' & \bar{d}_L' \end{pmatrix}^i \left[i\slashed{\partial} + \gamma_\mu \begin{pmatrix} \frac{g'}{6} B_\mu + \frac{g}{2} W_\mu^3 & \frac{g}{\sqrt{2}} W_\mu^+ \\ -\frac{g}{\sqrt{2}} W_\mu^- & \frac{g'}{6} B_\mu - \frac{g}{2} W_\mu' \end{pmatrix} \right] \begin{pmatrix} u_L' \\ d_L' \end{pmatrix}^i \\
&+ \bar{u}_R^{i\prime} \left(i\slashed{\partial} + g'\frac{2}{3}\slashed{B} \right) u_R^{i\prime} + \bar{d}_R^{i\prime} \left(i\slashed{\partial} - g'\frac{1}{3}\slashed{B} \right) d_R^{i\prime},
\end{aligned} \tag{1.92}
$$

when we do the change of basis the unitarity of the transformation makes the matrices drop out since the hypercharge interactions are generation diagonal

$$i\sum_i \bar{u}_R^i \slashed{D} u_R^i \underset{\text{flavour}}{\equiv} \bar{u}_R \mathbb{1} u_R \rightarrow \bar{u}_R \underbrace{U_{u_R}^\dagger \mathbb{1} U_{u_R}}_{\mathbb{1}} u_R = \bar{u}_R \mathbb{1} u_R \tag{1.93}$$

Moreover the same happens on the B_μ and W_μ^3 terms since these do not mix up and down-type quarks. This in turn makes the interaction with the photon unchanged. The mass term, as we expect, becomes diagonal

$$
\begin{aligned}
\mathcal{L}_{\text{mass}} &= \bar{d}_L^{i'} M_{ij}^D d_R^{j'} + \bar{u}_L^{i'} M_{ij}^U u_R^{j'} + h.c. \\
&= \bar{d}_L^i \left(U_{d_L} M_d U_{d_R}^\dagger \right)_{ij} d_R^j + \bar{u}_L^i \left(U_{u_L} M_u U_{u_R}^\dagger \right)_{ij} u_R^j + h.c. \\
&= \bar{d}_L^i \hat{m}_{ij}^D d_R^j + \bar{u}_L^i \hat{m}_{ij}^U u_R^j + h.c.
\end{aligned}
\tag{1.94}
$$

The interesting bit comes out from the isospin doublet, the left part, where the two components change with different unitary matrices

$$
Q_L^i = \begin{pmatrix} u_L^i \\ d_L^i \end{pmatrix} \rightarrow \begin{pmatrix} U_{u_L}^{ij} u_L^j \\ U_{d_R}^{ij} d_L^j \end{pmatrix},
\tag{1.95}
$$

whenever the interaction mixes the two quark types. This happens with the $W^\pm$ couplings

$$
\frac{g}{\sqrt{2}} W_\mu^+ \bar{u}_L' \gamma^\mu \mathbb{1} d_L' \underset{\text{flavour}}{\equiv} \bar{u}_L' \mathbb{1} d_L' = \bar{u}_L \underbrace{U_{u_L} \mathbb{1} U_{d_L}^\dagger}_{V_{CKM}} d_L,
\tag{1.96}
$$

where a new matrix in flavour space appears since we cannot use unitarity to reduce the $U_{u_L} U_{d_L}^\dagger$ term to the identity. This matrix is known as the *Cabibbo-Kobayashi-Maskawa (CKM) matrix*. The CKM matrix is a complex unitary matrix, and thus has nine real degrees of freedom, or three complex degrees of freedom. If V_{CKM} were real, it would be a $O(3)$ matrix, i.e. with three degrees of freedom. This means that out of the nine parameters of the complex CKM, three are angles and six are phases. However since the quark fields as mass eigenstates have a residual $U^6(1)$ symmetry

$$
d_{L/R}^i = e^{i\alpha_i} d_{L/R}^i, \quad u_{L/R}^i = e^{i\beta_i} u_{L/R}^i.
\tag{1.97}
$$

Thus, we can use this freedom to set some phases to zero. Under these transformations, V_{CKM} generally transforms. However, if the two rotations are the same $\alpha_i = \beta_i$, the matrix remains unchanged. Therefore out of the 6 possible phases we could have set to zero, there remain only 5 possible combinations that effectively change the CKM matrix. Therefore there remain only one free phase in the CKM. The total remaining degrees of freedom are: three angles $\theta_{12}, \theta_{23}, \theta_{13}$, corresponding to rotations in the ij-flavour planes, and a phase δ. The angle θ_{12} is called the *Cabibbo angle θ_C*.

One possible representation of the CKM matrix is the following

$$
V = \begin{pmatrix} V_{ud} & V_{uc} & V_{ub} \\ V_{cd} & V_{cs} & V_{cb} \\ V_{td} & V_{ts} & V_{tb} \end{pmatrix}.
\tag{1.98}
$$

The presence of the phase reflects the CP violation of the weak charged currents. We will see other representations of the CKM matrix in later sections.

For completeness we give here the full interaction Lagrangian between the four gauge bosons γ, Z^0 and $W^\pm$. Starting from the diagonal interactions, which are the

ones between the photon γ

$$
\begin{aligned}
\mathcal{L}_{\text{qA}} = i \sum_k \Bigg(& \bar{u}_L^k \gamma^\mu \Big[\partial_\mu + ie\frac{2}{3}A_\mu\Big] u_L^k + \bar{u}_R^k \gamma^\mu \Big[\partial_\mu + ie\frac{2}{3}A_\mu\Big] u_R^k \\
& + \bar{d}_L^k \gamma^\mu \Big[\partial_\mu - i\frac{e}{3}A_\mu\Big] d_L^k + \bar{d}_R^k \gamma^\mu \Big[\partial_\mu - i\frac{e}{3}A_\mu\Big] d_R^k \Bigg)
\end{aligned}
\tag{1.99}
$$

and the Z^0 boson

$$
\begin{aligned}
\mathcal{L}_{\text{qZ}} = \sum_k \Bigg(& -\bar{u}_L^k \gamma^\mu u_L^k \Big[\frac{eZ_\mu}{\sin 2\theta_W}\Big]\Big[1 - \frac{4}{3}\sin^2\theta_W\Big] + \bar{u}_R^k \gamma^\mu u_R^k \Big[\frac{eZ_\mu}{\sin 2\theta_W}\Big]\frac{4}{3}\sin^2\theta_W \\
& + \bar{d}_L^k \gamma^\mu d_L^k \Big[\frac{eZ_\mu}{\sin 2\theta_W}\Big]\Big[1 - \frac{2}{3}\sin^2\theta_W\Big] - \bar{d}_R^k \gamma^\mu d_R^k \Big[\frac{eZ_\mu}{\sin 2\theta_W}\Big]\frac{2}{3}\sin^2\theta_W \Bigg).
\end{aligned}
\tag{1.100}
$$

The non-diagonal interactions with the $W^\pm$ bosons are given by

$$
\mathcal{L}_{\text{qW}} = -\frac{e}{\sqrt{2}\sin\theta_W} \sum_{ij} \left(V_{CKM}^{ij} \bar{u}_{Li}\gamma^\mu d_{Lj} W_\mu^+ + \left(V_{CKM}^{ij}\right)^\dagger \bar{d}_{Li}\gamma^\mu u_{Lj} W_\mu^- \right).
\tag{1.101}
$$

We note also that in the SM there are no *Flavour Changing Neutral Currents* (FCNC) at tree level. At loop level these are highly suppressed by the GIM mechanism [79].

1.4.7 Wolfenstein Parametrization and Standard Parametrization

The CKM matrix is usually parametrized in some specific way. The purpose of a specific parametrization is to incorporate in some way the unitarity condition of the CKM. A property that is used throughout all parametrization is the so-called *rephasing invariance* which is the possibility of changing the overall phase of any row, or any column, of the CKM matrix, without changing the physics contained in that matrix. Using this invariance, one usually sets V_{ud} and V_{us} to be real and positive[14].

As we discussed in the previous sections, we know that the CKM matrix depends on four parameters: three angles and one phase. This is, of course, independent of the specific parametrization used. One such parametrization, which does not highlight the number of free parameters, is the one given in equation eq. (1.98). There are better parametrizations that make clearer the nature of the CKM matrix. One such parametrization is the *standard parametrization*: the free parameters are three

---

[14]The reason for this choice has to do with a particular parameter that comes into play in the physics of the neutral kaon system.

angles $\theta_{12}, \theta_{13}, \theta_{23}$ and one complex phase δ and the CKM has the form

$$
V = \begin{pmatrix} 1 & 0 & 0 \\ 0 & \cos\theta_{23} & \sin\theta_{23} \\ 0 & -\sin\theta_{23} & \cos\theta_{23} \end{pmatrix}
$$

$$
\times \begin{pmatrix} \cos\theta_{13} & 0 & \sin\theta_{13}e^{i\delta} \\ 0 & 1 & 0 \\ -\sin\theta_{13}e^{i\delta} & 0 & \cos\theta_{13} \end{pmatrix} \begin{pmatrix} \cos\theta_{12} & \sin\theta_{12} & 0 \\ -\sin\theta_{12} & \cos\theta_{12} & 0 \\ 0 & 0 & 1 \end{pmatrix} \tag{1.102}
$$

$$
= \begin{pmatrix} c_{12}c_{13} & s_{12}c_{13} & s_{13}e^{-i\delta} \\ -s_{12}c_{23} - c_{12}s_{23}s_{13}e^{i\delta} & c_{12}c_{23} - s_{12}s_{23}s_{13}e^{i\delta} & s_{23}c_{13} \\ s_{12}s_{23} - c_{12}c_{23}s_{13}e^{i\delta} & -c_{12}s_{23} - s_{12}c_{23}s_{13}e^{i\delta} & c_{23}c_{13} \end{pmatrix},
$$

where we used the notation $s_{ij} = \sin\theta_{ij}$ and $c_{ij} = \cos\theta_{ij}$.

From the physical point of view, this matrix does not give us much more information than the original form of equation eq. (1.98). From this prospective the *Wolfenstein parametrization* is better suited. This parametrization incorporates some experimental informations from the measured moduli of the matrix elements, which we gave in equations eqs. (1.121) to (1.128). This parametrization it is based on the approximation of the various matrix elements in terms of $\lambda = \sin\theta_C \approx 0.22$ and is given, up to third order in λ, by

$$
V = \begin{pmatrix} 1 - \lambda^2/2 & \lambda & A\lambda^3(\rho - i\eta) \\ -\lambda & 1 - \lambda^2/2 & A\lambda^2 \\ A\lambda^3(1 - \rho - i\eta) & A\lambda^2 & 1 \end{pmatrix} + \mathcal{O}(\lambda^4), \tag{1.103}
$$

where, with respect to the standard parametrization, we define [41, 47, 149]

$$
s_{12} = \lambda = \frac{|V_{us}|}{\sqrt{|V_{ud}|^2 + |V_{us}|^2}}, \qquad s_{23} = A\lambda^2 = \lambda \left| \frac{V_{cb}}{V_{us}} \right|,
$$
$$
\tag{1.104}
$$
$$
s_{12}e^{i\delta} = V_{ub}^* = A\lambda^3(\rho + i\eta) = \frac{A\lambda^3(\bar{\rho} + i\bar{\eta})\sqrt{1 - A^2\lambda^4}}{\sqrt{1 - \lambda^2}[1 - A^2\lambda^4](\bar{\rho} + i\bar{\eta})}
$$

which are called, together with λ, *Wolfenstein parameters*. These relations ensure that $\bar{\rho} + i\bar{\eta} = -(V_{ud}V_{ub}^*)/(V_{cd}V_{cb}^*)$ is phase convention independent and that the CKM matrix written in terms of the four parameters $A, \lambda, \bar{\rho}, \bar{\eta}$ is unitary to all orders in λ.

While $\lambda = 0.220658 \pm 0.00044$ and $A = 0.818 \pm 0.012$ [27] are relatively well known, the parameters ρ and η are much more uncertain. The main goal of CP-violation experiments is to over-constrain these parameters and, possibly, to find inconsistencies suggesting the existence of physics beyond the SM. And is precisely what we are going to do in this thesis by introducing the new result on the parameter ϵ'/ϵ, which we will discuss at later time.

1.4.8 Unitarity Triangle

The condition on unitarity poses a strong constrain on the physics of the CKM matrix. In fact, from the unitarity condition $V^\dagger V = \mathbb{1}_{3\times3}$ we can write six equations

for the off-diagonal elements. For example, one such equation is of the form

$$\sum_{i=1}^{3} V_{id} V_{is}^* = 0. \tag{1.105}$$

Every one of these equations define a triangle in the complex plane where each one of the legs of the triangle is one of the elements of the sum. These are called *unitarity triangles*. The Wolfenstein parametrization comes in very handy since from that of equation eq. (1.103) we can see that of the six unitary triangles, only two come with the same power of λ

$$O(\lambda^3): \quad \begin{array}{l} V_{ud} V_{ub}^* + V_{cd} V_{cb}^* + V_{td} V_{tb}^* = 0 \\ V_{td} V_{ud}^* + V_{ts} V_{us}^* + V_{tb} V_{ub}^* = 0. \end{array} \tag{1.106}$$

These two specific triangles are useful for the study of the B-meson decay. The other four triangles contain terms with different powers of λ and so they make up some squeezed triangles.

Above all this unitarity triangle there is *The Unitarity Triangle* (UT). This is given by the first of the relations in equation eq. (1.106) with the sides normalized by $V_{cd} V_{cb}^*$

$$\frac{V_{ud} V_{ub}^*}{V_{cd} V_{cb}^*} + 1 + \frac{V_{td} V_{tb}^*}{V_{cd} V_{cb}^*} = 0. \tag{1.107}$$

We can draw this relation in the complex plane as follows: we start from $(0,0)$ and then we move to $(1,0)$ using the second factor of eq. (1.107), then we take either one of the other two factors and go back to the origin. This process leaves us with the triangle in the complex plane in figure (1.2) alongside the experimental determination of $(\bar{\rho}, \bar{\eta})$
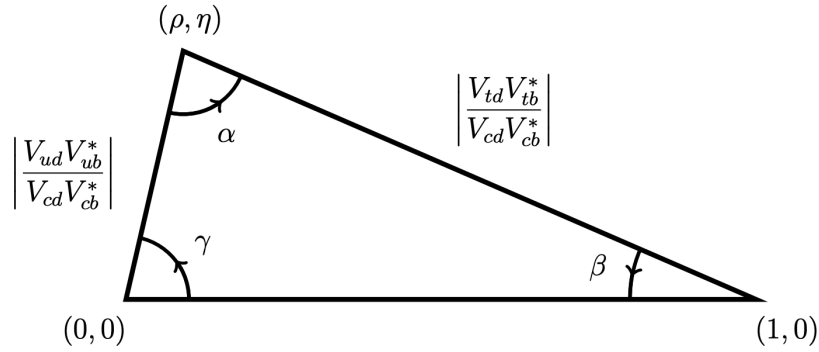
(a) Theoretical Unitarity Triangle.
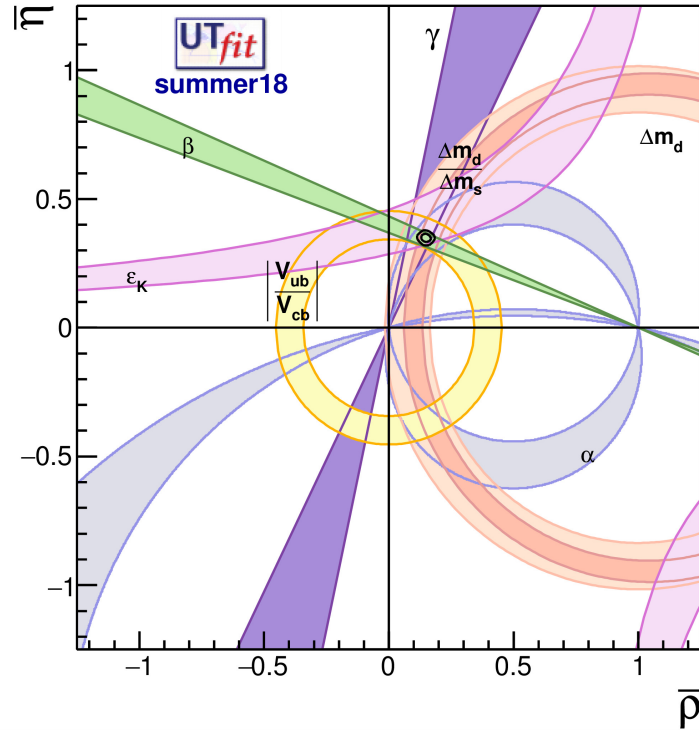
(b) Experimental determination of $(\bar{\rho}, \bar{\eta})$, courtesy of the UTfit collaboration.

Figure 1.2. The Unitarity Triangle

The parameters $\bar{\rho}$ and $\bar{\eta}$ can be expressed in terms of the Wolfenstein parameters ρ and η by means of the following relations

$$\bar{\rho} = \rho\left(1 - \frac{\lambda^2}{2}\right) + \mathcal{O}(\lambda^4) \qquad \bar{\eta} = \eta\left(1 - \frac{\lambda^2}{2}\right) + \mathcal{O}(\lambda^4). \tag{1.108}$$

The angles in the Unitarity Triangle are defined[15] as

$$\alpha \equiv \arg\left[-\frac{V_{td}V_{tb}^*}{V_{cd}V_{cb}^*}\right], \qquad \beta \equiv \arg\left[-\frac{V_{cd}V_{cb}^*}{V_{td}V_{tb}^*}\right],$$
$$\gamma \equiv \arg\left[-\frac{V_{ud}V_{ub}^*}{V_{cd}V_{cb}^*}\right], \qquad \beta_s \equiv \arg\left[-\frac{V_{ts}V_{tb}^*}{V_{cs}V_{cb}^*}\right]. \tag{1.109}$$

---

[15]Note this important feature: the definition of the angles are independent of any additional phase since any added phase to some quark is going to get cancelled by the ratio with the other elements. Equivalently, any CKM triangle can be rotated or scaled in the complex plane without modifying the angles that make them up.

1.5 Just a Taste: Flavour in the Standard Model

1.5.1 Global Symmetries

This peculiarity of the Yukawa interaction sparks an immediate question: what would be the full symmetry group of the SM if there wasn't any Yukawa interaction? To answer this, let us set for now all the Yukawa couplings to zero $Y_\ell, Y_U, Y_D = 0$[16]. Under this assumption, the whole global symmetry group of the SM is huge, in particular

$$G_{\rm SM}(Y = 0) = U(3)^5 = U(3)_{\rm q}^3 \times U(3)_\ell^2 = SU(3)_{\rm q}^3 \times SU(3)_\ell^2 \times U(1)^5, \quad (1.110)$$

where we defined

$$U(3)_{\rm q}^3 = U(3)_{Q_L} \times U(3)_{u_R} \times U(3)_{d_R}, \qquad U(3)_\ell^2 = U(3)_L \times U(3)_e. \quad (1.111)$$

For the second equality of eq. (1.110) the isomorphism[17] $U(3) \simeq SU(3) \times U(1)$ is used, together with the definition

$$U(1)^5 = U(1)_B \times U(1)_L \times U(1)_Y \times U(1)_{\rm PQ} \times U(1)_e. \quad (1.112)$$

Of the residual five charges we identify the first three with the *baryon number*, the *lepton number* and the hypercharge. These are the ones that are not broken by the Yukawa interactions. The remaining two are identified by the *Peccei-Quinn symmetry*. The important thing is that the Lagrangians eqs. (1.5) and (1.6) are invariant under the flavour symmetry group $SU(3)_q^3 \times SU(3)_\ell^2$. The Yukawa interactions break this symmetry, leaving us with the residual global symmetry

$$G_{\rm SM}(Y \neq 0) = U(1)_B \times U(1)_e \times U(1)_\mu \times U(1)_\tau. \quad (1.113)$$

Therefore the SM is not flavour invariant.

1.5.2 Counting the Physical Parameters

The discussion made until here may seem arbitrary but in fact is very useful if we want to count the number of independent parameters in the Yukawa coupling matrices.
Let us start with the Yukawa sector for the quarks: how many independent parameters does $\mathcal{L}_Y^q$ have? Consider a more general theory where the number of flavours is n. The two Yukawa matrices Y_U, Y_D are two 3×3 complex matrices, which means that they both have n^2 real parameters and n^2 imaginary ones. The kinetic part

---

[16]Physically we can think of this as studying the theory at an energy where the Yukawa couplings are negligible.

[17]This isomorphism is not given by the direct product. In fact there is a short exact sequence of Lie groups

$$\mathbf{1} \to SU(n) \to U(n) \xrightarrow{\det} U(1) \to \mathbf{1}$$

and therefore $U(n)$ is given by the semidirect product

$$U(n) \simeq SU(n) \rtimes U(1).$$

of the Lagrangian for the quarks has a global $U(n)^3$ symmetry that enables us to constrain $3n^2$ parameters. But the baryon number is a broken symmetry, which means that we need to remove one constrain from the global symmetry. So in the end we have

$$N_{\text{indep.}} = 2 \times 2n^2 - 3n^2 + 1 = n^2 + 1. \tag{1.114}$$

How many independent parameters are imaginary? To find them consider the limit in which $Y = 0$. In this limit, the Lagrangian is $SO(n)^3$ symmetric which implies that we can remove $3n(n-1)/2$ parameters. Therefore the number of real parameters is just

$$N_{\text{Re}} = 2n^2 - \frac{3n(n-1)}{2} = n + n + \frac{n(n-1)}{2}. \tag{1.115}$$

The division in equation eq. (1.115) is not at random: the first n real parameters are the masses of the n d-type quarks while the other n is the number of the masses for the u-type quarks. The third factor is the number of mixing angles. We can find now the number of complex phases

$$N_{\text{indep.}} = N_{\text{Re}} + \frac{(n-1)(n+1)}{2}. \tag{1.116}$$

Taking the limit of $n \to 3$ we get that the Yukawa matrices Y_D, Y_U, can be expressed in terms of 9 real parameters (three masses for the down quarks, three masses for the up quarks and three mixing angles) and one complex phase. This complex phase is crucial since it cannot be eliminated by any change of basis and, as we will see later, enables the possibility of CP violation in weak decays.

Now we do the same for the Yukawa coupling of the leptons. Here we have only one Yukawa matrix Y_ℓ that has in principle n^2 real parameters and n^2 imaginary ones. In the limit where no Yukawa interaction is present, the kinetic term for the leptons has a global $U(n)^2$ symmetry which constrains $2n^2$ parameters. In analogy with what we have done for the quarks, we can use the residual $SO(n)$ symmetry to eliminate $n(n-1)$ parameters in such a way that the number of real independent parameters becomes

$$N_{\text{Re}} = n^2 - n(n-1) = n. \tag{1.117}$$

These n parameters are exactly the n masses of the charged leptons. Since in the broken phase we still have a residual $U(1)^n$ symmetry (one for every lepton) the total number of parameters becomes

$$N_{\text{indep.}} = 2n^2 - 2n^2 + n = n = N_{\text{Re}}. \tag{1.118}$$

This means that no matter what, in the lepton sector there are *no complex phases*. This means that in the lepton sector there cannot be any CP violation and mixing!

Based on the arguments given in the previous sections, this is exactly what we expected. After symmetry breaking the leptons all got a mass matrix which was diagonal while the quarks didn't. By diagonalizing the quarks mass matrix we introduced the possibility of mixing in the weak sector and, buy the nature of the initial mass matrix, we could not require that the mixing matrix be real. By an analogous computation we found that the number of parameters in the mixing matrix was four: three angles and one complex phase. Plus we had the six masses of

the quarks. The complex CKM matrix is pivotal in the analysis that we will carry in the following sections. By this mean, we can now complete the discussion with an in-depth study of the CKM matrix.

1.6 What's so Special About the CKM Matrix?

1.6.1 Interaction Vertices

Now that we have a complete theory of weak interactions we can start constructing Feynman diagrams and evaluating some measurable quantities. It turns out that whenever we have a flavour changing current we'll need now to insert in the interaction vertex one of the possible elements of the CKM matrix.

Let's take for example the pion decay. At the level of the hadrons, the decay is given by

$$\pi^+ \to \mu^+ \nu_\mu \tag{1.119}$$

which, at the level of the quarks is given at tree-level by the following Feynman diagram
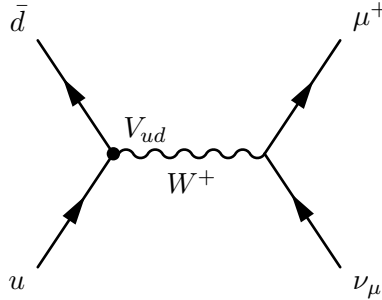
Figure 1.3. Pion decay at tree level mediated by a W^+ boson

The amplitude for such Feynman diagram is given, in the unitary gauge, by

$$\left(\frac{g}{2\sqrt{2}}\right)^2 V_{ud}^* \bar{v}_d \gamma^\mu (1 - \gamma_5) u_u \frac{1}{q^2 - M_W^2} \left(-g_{\mu\nu} + \frac{q_\mu q_\nu}{M_W^2}\right) \bar{u}_\mu \gamma^\nu (1 - \gamma_5) v_\nu, \tag{1.120}$$

where an additional V_{ud} term appears with respect to the naive amplitude and $q = \sqrt{s}$. This factor can greatly suppress some processes for which the CKM matrix element is very small.

1.6.2 How to Measure the CKM Elements

The CKM matrix elements are usually measured from leptonic and semileptonic decays. With the top quarks the processes are a little bit more difficult since it is mass prevents it from forming bound states with other quarks. In that case we use hadron mixing; we won't go into much detail about it. Due to the fact that in the theoretical predictions, only the square of the amplitude for the process appears, it is not possible to measure experimentally the precise value of the CKM matrix elements but rather we can measure either the moduli of them or the difference in phases between two.

Here we give some details on how the CKM moduli are measured experimentally and their values as they appear in the PDG [152]. All of the processes governed by weak decays are proportional to some power of the Fermi constant $G_F = \frac{\sqrt{2}g_2^2}{8M_W^2}$. This is precisely measured from the decay of the muon to the electron.

$|\mathbf{V_{ud}}|$ This matrix element involves only quarks of the first generation and is thus the one which can be best determined. There are basically three ways of measuring it. The first one involves superallowed Fermi transitions, which are beta decays connecting two $J^P = 0^+$ nuclides in the same isospin multiplet. The second one is by using the neutron decay which at tree level is given by the diagram in figure (1.4).
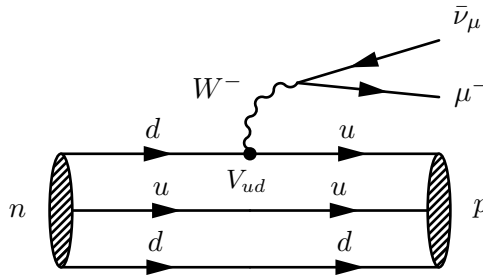
Figure 1.4. Neutron decay at tree level.

The moduli of this matrix element, as given by the PDG [87], comes out to be

$$|V_{ud}| = 0.97370 \pm 0.00014 \tag{1.121}$$

$|\mathbf{V_{us}}|$ This matrix element can be extracted from the analysis of semileptonic decays of the K-meson such as the one in figure (1.5).
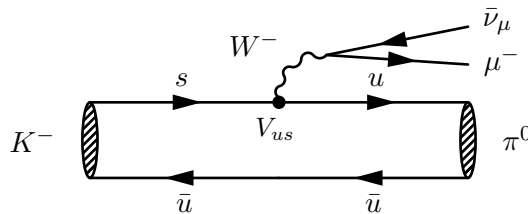
Figure 1.5. $K^- \to \pi^0 \mu^- \bar{\nu}_\mu$ at tree level

This matrix element comes out to be [14]

$$|V_{us}| = 0.2245 \pm 0.0008. \tag{1.122}$$

Another interesting way to measure the value of this matrix element is by hyperon decays [43].

$|\mathbf{V_{ub}}|$ This matrix element can be measured from the semileptonic decay of B meson such as the one in figure (1.6).
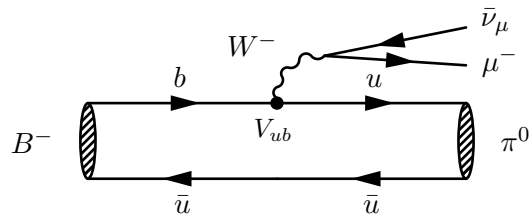
Figure 1.6. $B^- \to \pi^0 \mu^- \bar{\nu}_\mu$ at tree level

From these processes, we find a value for the moduli of this matrix element of [104]

$$|V_{ub}| = 0.00382 \pm 0.00024. \tag{1.123}$$

$|\mathbf{V_{cd}}|$ This matrix element can be measured from the semileptonic decay of charmed particles like the D meson. One such process can be found in figure (1.7).
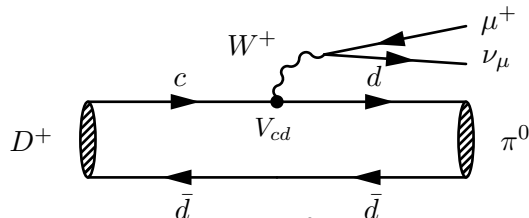
Figure 1.7. $D^+ \to \pi^0 \mu^+ \nu_\mu$ at tree level

The moduli of such matrix element come out to be [99, 75]

$$|V_{cd}| = 0.221 \pm 0.004. \tag{1.124}$$

$|\mathbf{V_{cs}}|$ This matrix element can be found by semileptonic decays of charmed particles like the D meson in which the c quark goes into a s quark. The lightest meson which contains an s quark is the K meson. Such decay is depicted at tree level in figure (1.8)
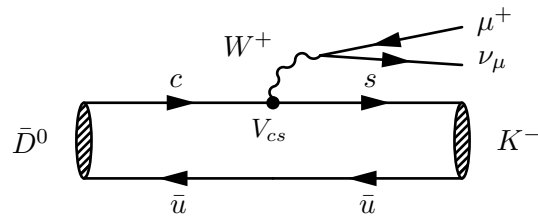
Figure 1.8. $\bar{D}^0 \to K^- \mu^+ \nu_\mu$ at tree level

This matrix element comes out to be [61, 151, 3, 4, 12]

$$|V_{cs}| = 0.978 \pm 0.011. \tag{1.125}$$

$|\mathbf{V_{cb}}|$ This matrix element is determined by the decay $B^0 \to D^{*-} l^+ \nu_l$ like the one in figure (1.9).
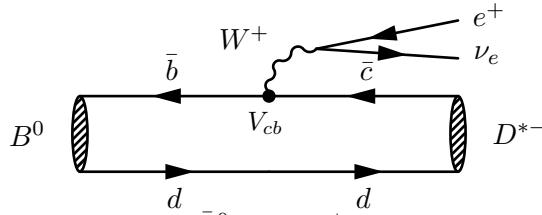
Figure 1.9. $\bar{D}^0 \to K^- \mu^+ \nu_\mu$ at tree level

For these decays, we gathered a lot of measurements that got us a value of [104]

$$|V_{cb}| = 0.041 \pm 0.0014. \tag{1.126}$$

$|\mathbf{V_{td}}|$ These are two of the three matrix elements which involve the top quark.
$|\mathbf{V_{ts}}|$ These matrix elements are measured by neutral meson mixing like $B^0 - \bar{B}^0$ and $B_s - \bar{B}_s$. The diagrams describing these oscillations, which will be of fundamental importance for CP violation in later sections, are so-called *box diagrams.* One such diagram is depicted in figure (1.10).
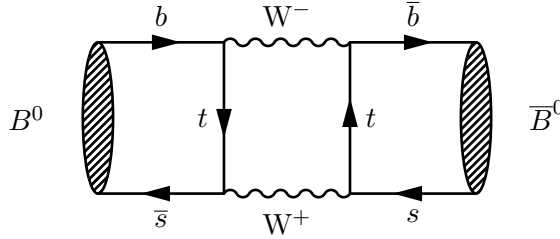
Figure 1.10. Relevant box diagram for the measurement of $|V_{td}|$ and $|V_{ts}|$.

By evaluating these processes on the lattice assuming $V_{tb} = 1$

$$|V_{td}| = 0.0080 \pm 0.0003 \qquad |V_{ts}| = 0.0388 \pm 0.0011. \tag{1.127}$$

$|\mathbf{V_{tb}}|$ This matrix element has been found by the CDF [6] and D0 [1] collaborations by measuring the branching ratio $\text{Br}(t \to Wb)/\text{Br}(t \to Wq)$ assuming three generations of quarks. The value they gave is

$$|V_{tb}| = 1.013 \pm 0.030. \tag{1.128}$$

1.6.3 CP-violation in the SM

We can now briefly discuss how the complex phase in the CKM breaks CP-invariance in the weak charged currents.

First, we need to see how the two discrete symmetries, parity and charge conjugation, act on the relevant fields for our analysis. These fields are bosonic vector fields, for the $W^\pm$, and four-spinors Ψ, for the quarks. Starting from parity, let us define a state of a single particle A with momentum p and other quantum numbers σ as $|A, p, \sigma\rangle$. The parity operator will act on this state as

$$\mathcal{P} |A, p, \sigma\rangle = \eta_A |A, -p, \sigma\rangle \tag{1.129}$$

since, at the classical level, parity just inverts the coordinates. On the antiparticle state the operator will act similarly, but with another rephasing

$$\mathcal{P}\left|\bar{A}, p, \sigma\right\rangle = \eta_{\bar{A}}\left|\bar{A}, -p, \sigma\right\rangle. \tag{1.130}$$

Given the creation operator $a_\sigma^\dagger$ we have

$$\mathcal{P}a_\sigma^\dagger(p)\left|0\right\rangle = a_\sigma^\dagger(-p)\left|0\right\rangle \eta_A \tag{1.131}$$

henceforth

$$\mathcal{P}a_\sigma^\dagger(p)\mathcal{P}^{-1}\mathcal{P}\left|0\right\rangle = \mathcal{P}a_\sigma^\dagger(p)\mathcal{P}^{-1}\left|0\right\rangle = \eta_A a_\sigma^\dagger(-p)\left|0\right\rangle$$
$$\implies \mathcal{P}a_\sigma^\dagger(p)\mathcal{P}^{-1} = \eta_A a_\sigma^\dagger(-p). \tag{1.132}$$

Similarly for the antiparticle. Now let us consider a scalar field $\Phi(x)$ and its expansion in creation and annihilation operators, then

$$\mathcal{P}\Phi(x)\mathcal{P}^{-1} = \int \frac{d^3p}{(2\pi)^3 2E_p}\left[\mathcal{P}a_p\mathcal{P}^{-1}e^{-ipx} + \mathcal{P}b_p^\dagger\mathcal{P}^{-1}e^{ipx}\right]$$
$$= \int \frac{d^3p}{(2\pi)^3 2E_p}\left[\eta_A^* a_{-p}e^{-ipx} + \eta_{\bar{A}}b_{-p}^\dagger e^{ipx}\right] \doteq \eta_\Phi^* \Phi(\mathcal{P}x). \tag{1.133}$$

In order for the equality to hold, we need to have $\eta_A^* = \eta_{\bar{A}} = \eta_\Phi^*$ which implies $\eta_A \eta_A = 1$. What we need to define still is the intrinsic phase η_Φ^*. Doing a similar thing for a spinor field, defining its transformation property under parity as

$$\mathcal{P}\phi(x)\mathcal{P}^{-1} \doteq \eta_A^* \gamma^0 \psi(\mathcal{P}x) \tag{1.134}$$

we get a slightly different result

$$\mathcal{P}\psi(x)\mathcal{P}^{-1} = \int \frac{d^3p}{(2\pi)^3\sqrt{2E_p}}\left[\eta_A^* a_\sigma(-p)u^\sigma(p)e^{-ipx} + \eta_{\bar{A}}b_\sigma^\dagger(-p)v^\sigma(p)e^{ipx}\right]$$
$$= \int \frac{d^3p}{(2\pi)^3\sqrt{2E_p}}\left[\eta_A^* a_\sigma(-p)\gamma^0 u^\sigma(-p)e^{-ipx} - \eta_{\bar{A}}b_\sigma^\dagger(-p)\gamma^0 v^\sigma(-p)e^{ipx}\right]$$
$$\tag{1.135}$$

which implies $\eta_{\bar{A}} = -\eta_{\bar{A}}^*$, which depends only on the choice of $\eta_{\bar{A}}$. For a vector field we get a similar result as for the calar field $\mathcal{P}A^\mu(x)\mathcal{P}^{-1} = -\eta_A^* \mathcal{P}^\mu_{\ \nu} A^\nu(\mathcal{P}x)$.

Next, there is charge conjugation. This can be found by imposing that the following conditions hold: take a spinor field ψ and denote its charge conjugate as $\psi^c = \mathcal{C}\bar{\psi}^T$, then

$$\bar{\psi}^c\psi^c = \bar{\psi}\psi \qquad \bar{\psi}^c \overleftrightarrow{\partial}\psi^c = \bar{\psi}\overleftrightarrow{\partial}\psi. \tag{1.136}$$

From the first condition, we get that

$$\left(\psi_c^\dagger\right)_\alpha\left(\gamma^0\right)_{\alpha\beta}(\psi_c)_\beta = \psi_\gamma\left(\mathcal{C}^\dagger\right)_{\gamma\alpha}\left(\gamma^0\right)_{\alpha\beta}(\mathcal{C})_{\beta\sigma}\psi_\sigma^\dagger = -\psi_\sigma^\dagger\left(\mathcal{C}^\dagger\gamma^0\mathcal{C}\right)_{\gamma\sigma}\psi_\gamma$$

$$= \psi_\sigma^\dagger\left(\gamma^0\right)_{\sigma\gamma}\psi_\gamma = \psi_\sigma^\dagger\left(\gamma^0\right)^T_{\gamma\sigma}\psi_\gamma$$

from which we can extract

$$\mathcal{C}^\dagger \gamma^0 \mathcal{C} = -\gamma^0. \tag{1.137}$$

From the second condition we get

$$\left(\psi_c^\dagger\right)_\alpha \left(\gamma^0 \gamma^\mu\right)_{\alpha\beta} (\partial_\mu \psi_c)_\beta = \psi_\sigma \left(\mathcal{C}^\dagger\right)_{\sigma\alpha} \left(\gamma^0 \gamma^\mu\right)_{\alpha\beta} (\mathcal{C})_{\beta\gamma} \left(\partial_\mu \psi^\dagger\right)_\gamma$$

$$= \psi_\gamma^\dagger \left(\gamma^0 \gamma^\mu\right)_{\gamma\sigma} (\partial_\mu \psi)_\sigma. \tag{1.138}$$

By comparison, we can say

$$\mathcal{C}^\dagger \left(\gamma^0 \gamma^\mu\right) \mathcal{C} = \left(\gamma^0 \gamma^\mu\right)^T = (\gamma^\mu)^T \gamma^0 \tag{1.139}$$

For $\mu = 0$ it is easy to show from equation 1.139 that the operator $\mathcal{C}$ is Hermitian. Adding the unitary quantity $\gamma^0 \gamma^0$, from equation 1.139 we get

$$\mathcal{C}\left(\gamma^0 \gamma^\mu \gamma^0 \gamma^0\right)\mathcal{C} = \mathcal{C}\gamma^{\mu\dagger}\gamma^0 \mathcal{C} = (\gamma^\mu)^T \gamma^0 \tag{1.140}$$

Now we multiply both the sides by γ^0 and we exploit the anticommutation between $\mathcal{C}$ and γ^0 since the equation 1.137 is true, so we get

$$\mathcal{C}\gamma^{\mu\dagger}\gamma^0 \mathcal{C}\gamma^0 = (\gamma^\mu)^T$$

$$-\mathcal{C}\gamma^{\mu\dagger}\mathcal{C} = (\gamma^\mu)^T$$

$$\mathcal{C}\gamma^\mu \mathcal{C} = -\gamma^{\mu*} \tag{1.141}$$

The only thing to do now is to determine the operator. We know that γ^0, γ^1, γ^3 are real and symmetric (like also γ_5) whereas γ^2 is imaginary. Since $\mathcal{C}$ anticommutes with γ^0, γ^1, γ^3 and commutes with γ^2, imposing the condition $\mathcal{C}^2 = 1$ we can define the operator up to a sign

$$\mathcal{C} = i\gamma^2. \tag{1.142}$$

With this definition of charge conjugation we get that a scalar and a pseudovector are unchanged under charge conjugation, vectors and tensors change sign. Therefore we have

$$\begin{aligned}
\mathcal{CP}\, W_\mu^+ \,\mathcal{CP}^{-1} &= -e^{i\xi_W}\eta^\nu{}_\mu W_\nu^- \\
\mathcal{CP}\, W_\mu^- \,\mathcal{CP}^{-1} &= -e^{i\xi_W}\eta^\nu{}_\mu W_\nu^+ \\
\mathcal{CP}\, Z^\mu \,\mathcal{CP}^{-1} &= -\eta_Z \eta^\mu{}_\nu Z^\nu \\
\mathcal{CP}\, h \,\mathcal{CP}^{-1} &= \eta_h h \\
\mathcal{CP}\, u^i \,\mathcal{CP}^{-1} &= e^{i\phi_{u^i}}\gamma^0 \mathcal{C}\bar{u}^{iT} \\
\mathcal{CP}\, d^i \,\mathcal{CP}^{-1} &= e^{i\phi_{d^i}}\gamma^0 \mathcal{C}\bar{d}^{iT}
\end{aligned} \tag{1.143}$$

The question is now: is it possible to choose the phases $\xi_W, \eta_Z, \eta_h, \phi_{u^i}, \phi_{d^i}$ in such a way that the weak Lagrangian is CP invariant? Let's go directly to the culprit, the W boson interactions with quarks. What we have is the following

$$\mathcal{CP}\left[\frac{g}{\sqrt{2}}W_\mu^+ \bar{u}_L^i \gamma^\mu d_L^j V_{ij} + V_{ij}^* \bar{d}_L^j \gamma^\mu u_L^i W_\mu^-\right]\mathcal{CP}^{-1}$$

$$= \frac{g}{\sqrt{2}}V_{ij}\left(W_\mu^- e^{-i\xi_W}\right)e^{i(\phi_d^j - \phi_u^i)}\left(-\bar{d}_L^j \gamma^\mu u_L^i\right) + \frac{g}{\sqrt{2}}V_{ij}^*(W_\mu^+ e^{i\xi_W})e^{i(\phi_u^i - \phi_d^j)}\left(-\bar{u}_L^i \gamma^\mu d_L^j\right). \tag{1.144}$$

The condition for invariance is given by

$$V_{ij}^* e^{-i(\xi_W + \phi_d^j - \phi_u^i)/2} = V_{ij} e^{i(\xi_W + \phi_d^j - \phi_u^i)/2} \tag{1.145}$$

which can only be true if we can choose the phases such that the product between the phase and the CKM matrix elements is real. But we know that the CKM matrix has a complex phase that cannot be reabsorbed in any way and that is present in every choice of basis. This means that the equality eq. (1.145) cannot hold and therefore we have CP violation.

1.6.4   The Jarlskog Invariant

Now that we're familiar with the existence of the CP-violating phase, we would like to be able to quantify it in a meaningful way that is manifestly basis-independent. What we need is some kind of invariant that identifies CP violation. Such an object exists and it is called the Jarlskog invariant, J [63, 81, 98, 97, 150]. It is defined by

$$\text{Im}\left[V_{ij}V_{kl}V_{i\ell}^*V_{kj}^*\right] = J \sum_{mn} \epsilon_{ikm}\epsilon_{j\ell n},$$

where there is no implicit sum on the left-hand side. In terms of the Wolfenstein parametrization, this corresponds to

$$J = c_{12}c_{23}c_{13}^2 s_{12}s_{23}s_{13}\sin\delta \approx \lambda^6 A^2 \eta$$

This parametrization-independent quantity measures the amount of CP violation in our model. The most remarkable observation is that it depends on every physical mixing angle. Thus if any of the mixing angles are zero, there would be no CP violation. In fact, we can see that the amount of CP violation in the Standard Model is small, but it is not small because the CP phase δ is small. Quite on the contrary, it is small because of the mixing angles. We can see this in the Wolfenstein parametrization where the Jarlskog invariant comes along with six powers of λ. The experimental value of J is [152]

$$J = (3.0^{+0.15}_{-0.09}) \times 10^{-5}. \tag{1.146}$$

Chapter 2

Quantum Chromodynamics and Strong Interaction

The strong interaction is the missing piece of the Standard Model which is described by the $SU(3)$ symmetry group. Of the three fundamental forces that the SM can explain, the strong force is by far the most complicated. This force governs the behaviour of quarks and how they bind together to form composite particles which we call *hadrons*. Not only that, but on a larger scale, it also governs how the nuclei of different atoms bind together and their stability. At these two different scales, the particles that mediate the interactions are different: on the smaller, hadronic, scale the force mediator is called *gluon*, while at the larger scale the carriers are light mesons such as the pion. Quantum chromodynamics is the Quantum Field Theory that describes the interactions of *colored* particles. Color is the quantum number of the $SU(3)$ symmetry group in the SM.

What makes the strong force so difficult to work with and to do actual calculations, it its highly non-perturbative structure at low enough energy scales. Perturbation theory is an essential bit of mathematics that enables us to carry out specific computations and without it, unless the model is exactly solvable[1], we cannot go any further. But then, how come that we in fact do calculations which depend on strong dynamics? We use a tool called *lattice QCD*[2]. This approach was introduced by Wilson [146] and is an approximation scheme in which the continuum gauge theory is replaced by a discrete statistical mechanical system on a four-dimensional Euclidean lattice. The basic idea of lattice QCD is to employ a specific ultraviolet regulator, i.e. the lattice, on which we can do computations exactly. Of course, such a tool comes with its benefits and with its drawbacks. One such drawback is that by discretizing space-time, we lose one of the foundations of QFT which is Lorentz invariance. Moreover, a lattice calculation requires some very intensive computations which, in turn, requires a very powerful computer. Although we are going to use heavily the ideas of lattice QCD and lattice regularization, we won't go into much details on how such lattice computations are done, what is important is that even in

---

[1]Sadly we know far too well that most of the actual physical models are not exactly solvable by analytical methods.

[2]This is not the only tool. There are also other theories like the $1/N_c$ [135] expansion or Chiral Perturbation Theory (ChPT).

the non-perturbative regime, physicist know how to do calculations.

The fundamental property of QCD, which causes all the problems we write up until now, is *asymptotic freedom*. What this means is that, at high enough energy, QCD can be treated perturbatively: the theory becomes asymptotically free $g_s(\Lambda) \overset{\Lambda \to \infty}{\longrightarrow} 0$, where Λ is some energy scale. That's right, the coupling depends on the energy at which the process takes place. This is a general feature of any QFT and comes from the process of reabsorbing infinities in a process called *renormalization*. We will see how this process will come into play in this chapter.

2.1 The QCD Lagrangian

The QCD Lagrangian is constructed by taking the kinetic term of the relevant gauge field and the kinetic term for the fermions. This leaves us with a Lagrangian of the form

$$\mathcal{L}_{\text{QCD}} = -\frac{1}{4} G^{\text{a}}_{\mu\nu} G^{\text{a}\mu\nu} + \bar{\psi}^{\text{a}}_q \Big(i \slashed{D}^{\text{ab}} - m \delta^{\text{ab}} \Big) \psi^{\text{b}}_q, \tag{2.1}$$

in which the field G^{a}_μ are the gluons and the fields ψ_q are the quarks. But reality, as always, is more complicated than this. What we glossed over up until now is that gauge freedom completely breaks down our possibility to do calculations. This is due to the fact that when studying QFTs one makes use of an object called *generating functional $Z[J]$*. The generating functional is a functional[3] which is used to find, in any order in perturbation theory, the value of some Feynman diagram: it "generates" at any order, the relevant perturbative terms and is in this bit of mathematics that the problem lies. Take a general gauge field A^a_μ associated with some gauge group G. Let $S[A]$ be the action[4] functional, then the generating functional is defined in Minkowski space as

$$Z[J^\mu_a] = \int \mathcal{D}A \, \exp \left[iS[A] - i \int \mathrm{d}^4 x \, A^a_\mu(x) J^\mu_a(x) \right], \tag{2.2}$$

where J^μ_a are $\dim G$ external currents. Then, green functions can be found by functionally deriving $Z[J]$ and setting the external current to zero. For example, the two-point function (propagator) of the gauge field, is found by

$$G^{ab}_{\mu\nu}(x) = \langle 0 | A^a_\mu(x) A^b_\nu(0) | 0 \rangle = \frac{1}{Z[0]} \frac{\delta}{\delta J^\mu_a} \frac{\delta}{\delta J^\nu_b} Z[J] \Big|_{J=0}. \tag{2.3}$$

If we have some additional fields which interact with the gauge field, just like our initial QCD Lagrangian, equation like eq. (2.3), gives the complete two-point function which incorporates all the possible corrections to the free propagator. But what is the integration measure in the definition of the generating functional of equation eq. (2.2)? Broadly speaking it means that we need to integrate over all possible field configurations. But here's the catch: gauge freedom makes any configuration part of an infinite equivalence class of configurations where the physics is unchanged and we need to integrate over all of them. It is not difficult to see that even naively,

---

[3]Incredible!

[4]The action is defined as the integral over spacetime of the Lagrangian density.

this makes the integration measure divergent. To solve this problem we need to fix the gauge in such a way that the physical result is independent of such a fix but such that makes the integration well defined. The procedure to fix the gauge in a non-Abelian theory was found by Fadeev and Popov[5] [66]. Without going into much more details, what they discovered is that by fixing the gauge there appeared some new fictitious particles which we call *Ghosts*. Ghosts are in no way physical particles, they cannot be measured, they are not real, but they are only a result of the mathematical process of fixing the gauge. This particles appear in the Lagrangian as a bosonic term but they are described by Grassman variables and so obey Fermi-Dirac statistic.

There are a whole plethora of possible gauges: covariant gauges, axial gauges, nonlinear gauges, and so on. In the simplest case of the covariant gauge-fixing $\partial^\mu G^a_\mu = 0$, the full QCD, gauge-fixed, Lagrangian in all of its glory is given by
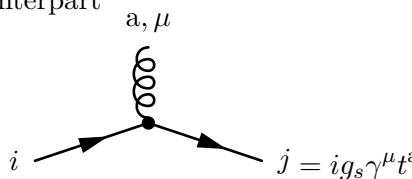
$$\mathcal{L}_{\text{QCD}} = -\frac{1}{4} G^a_{\mu\nu} G^{a\mu\nu} - \frac{1}{2\alpha}\left(\partial^\mu G^a_\mu\right)^2 + (\partial_\mu \chi_a)^* D^{ab}_\mu \chi_b + \bar{\psi}_q (i\slashed{D} - m)\psi_q, \quad (2.4)$$

where α is the gauge parameter, χ_i are the Ghost fields and $D^{ab}_\mu = \delta^{ab}\partial_\mu - g_s f^{abc} A^c_\mu$ is the covariant derivative in the adjoint representation of $SU(3)$.
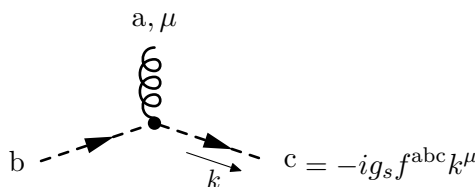
2.2 Perturbative QCD

We are now ready to start the analysis of QCD in the perturbative regime. To employ perturbation theory, we need to choose an energy scale such that quarks and gluons become the asymptotic states of the theory instead of the hadrons.

Given the Lagrangian eq. (2.4) we can extrapolate the various interaction vertices. The non-Abelian nature of the $SU(3)$ symmetry group adds some interesting interactions such as three- and four-gluon vertices which in a simpler theory like QED are not present. We now give a short list of the Feynman rules for the vertices and their mathematical counterpart
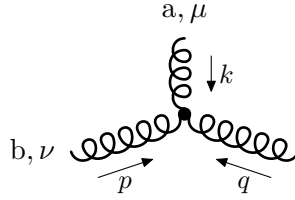
$$= ig_s \gamma^\mu t^a \qquad (2.5)$$
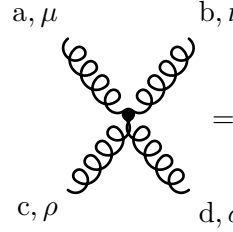
$$= -ig_s f^{abc} k^\mu \qquad (2.6)$$

---

[5]There is still a problem with this approach since fixing an orbit in the guage configuration space can result in ambiguities, the so-called *Gribov ambiguity* [82]
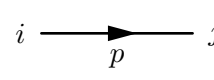
$$c, \rho = g f^{\mathrm{abc}} [g^{\mu\nu}(k-p)^\rho + g^{\nu\rho}(p-q)^\mu + g^{\rho\mu}(q-k)^\nu] \quad (2.7)$$
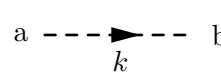
$$= \begin{aligned} -ig^2 \Big[& f^{\mathrm{abe}} f^{\mathrm{cde}} (g^{\mu\rho} g^{\nu\sigma} - g^{\mu\sigma} g^{\nu\rho}) \\ + & f^{\mathrm{ace}} f^{\mathrm{dbe}} (g^{\nu\mu} g^{\rho\sigma} - g^{\mu\sigma} g^{\nu\rho}) \\ + & f^{\mathrm{ade}} f^{\mathrm{bce}} (g^{\mu\nu} g^{\rho\sigma} - g^{\mu\rho} g^{\nu\sigma}) \Big] \end{aligned} \quad (2.8)$$

For the later chapters, we also need the free propagators of both the quarks and the gluon derived from the associated free Lagrangian and come out to be

$$i \xrightarrow{\quad p \quad} j \quad = \frac{-i}{\not{p} - m} \delta_{ij} = \frac{i(\not{p} - m)}{p^2 - m^2} \delta_{ij} \quad (2.9)$$

$$a \dashrightarrow{\quad k \quad} b \quad = \frac{i \delta^{\mathrm{ab}}}{k^2} \quad (2.10)$$

$$a, \mu \,\,\,\text{———}\,\,\, b, \nu = \frac{i \delta^{\mathrm{ab}}}{k^2} \left(-g_{\mu\nu} + (1-\alpha) \frac{k^\mu k^\nu}{k^2 + i\epsilon} \right), \quad (2.11)$$

where α is the covariant gauge-fixing constant appearing in the Lagrangian eq. (2.4).

2.3 Renormalization of QCD

A general feature of most QFTs is the presence of divergences in the perturbative series when evaluating loop diagrams. Since we know, experimentally, that the results should be finite we need a way to systematically eliminate the unphysical divergences. This is done by means of renormalization [56]. In order to deal with divergences that appear at the quantum[6] corrections to Green functions, the theory has to be regularized to have an explicit parametrization of the singularities and subsequently renormalized to render the Green functions finite. There are many ways of regularizing Green functions, but what we will employ is Dimensional

---

[6]I will use quantum and loop corrections interchangeably.

Regularization (DR)[7] [16, 26, 48, 137] by analytically continuing the spacetime dimensions to $d = 4 - 2\epsilon$; the physical limit is taken by letting $\epsilon \to 0$.

There are also many ways upon which we can subtract the singularities. For our interest, we will mostly employ the modified Minimal Subtraction, or $\overline{\text{MS}}$ for short. To eliminate the divergences we firstly need to renormalize the fields and parameters in the Lagrangian eq. (2.4) defining several renormalization constants

$$
\begin{aligned}
G^{\text{a}}_{B\mu} &= Z_3^{1/2} G^{\text{a}}_\mu & \psi_{qB} &= Z_q \psi_q & \chi^{\text{a}}_B &= \tilde{Z}_3^{1/2} \chi^{\text{a}} \\
g_B &= Z_g g \mu^\epsilon & \alpha_B &= Z_3 \alpha & m_B &= Z_m m
\end{aligned}
\tag{2.12}
$$

in which the index B denotes the bare quantities. Note that a scale μ has been added to the coupling constant g to make it dimensionless in $D = 4 - 2\epsilon$ spacetime dimensions.

In the next sections, we are going to evaluate the 1-loop renormalization of QCD within the given framework. In general, the Green functions are going to depend on the gauge-fixing parameter α, but the physical results are gauge-independent. Therefore we are going to use the Feynman gauge $\alpha = 1$ for the following calculations.

2.3.1   Vacuum Polarization

The first loop corrections that we are going to evaluate are the ones to the gluon propagator. At one loop there are four corrections, plus the counterterm which depends on the renormalization constants and absorbs the divergences.
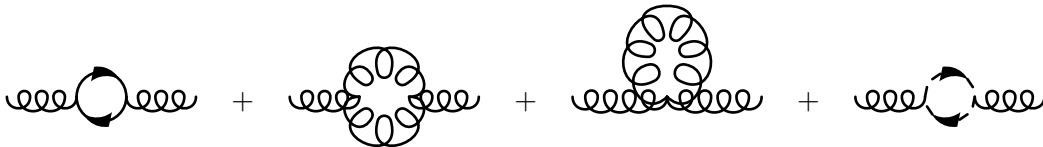
 We consider now a general $SU(n_f)$ Yang-Mills theory with n_f flavours. Let us start from the fermion bubble contribution: after the sum over the n_f flavours

---
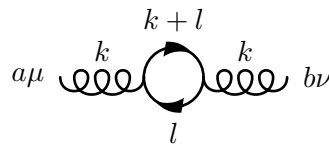
[7]In dimensional regularization there is some liberty when defining γ_5. In our particular case we will use Naive Dimensional Regularization (NDR) where the γ_5 is such that the usual anticommutation rules hold $\{\gamma^\mu, \gamma^\nu\} = 2g^{\mu\nu}$ and $\{\gamma^\mu, \gamma_5\} = 0$. Another useful definition is given by the 't Hooft-Veltmann scheme [137]

$$
\begin{aligned}
&= -n_f \int \frac{\mathrm{d}^d\ell}{(2\pi)^d} \operatorname{Tr} \left[\left(-ig\mu^\epsilon t_{ij}^a \right) \gamma^\mu \frac{i}{\ell + \slashed{k}} \left(-ig\mu^\epsilon t_{ji}^b \right) \gamma^\nu \frac{i}{\slashed{\ell}} \right] \\
&= -g^2\mu^{2\epsilon} n_f T_{\mathrm{F}} \delta^{\mathrm{ab}} \operatorname{Tr} \left\{ \gamma^\mu \gamma^\alpha \gamma^\nu \gamma^\beta \right\} \int \frac{\mathrm{d}^d\ell}{(2\pi)^d} \frac{(\ell+k)^\alpha \ell^\beta}{\ell^2 (\ell+k)^2} \\
&= -g^2\mu^{2\epsilon} n_f T_{\mathrm{F}} \delta^{\mathrm{ab}} 4 \left[g^{\mu\alpha} g^{\nu\beta} - g^{\mu\nu} g^{\alpha\beta} + g^{\mu\beta} g^{\nu\alpha} \right] \left[\mathcal{B}^{\alpha\beta}(k) + k^\alpha \mathcal{B}^\beta(k) \right] \\
&= -g^2\mu^{2\epsilon} n_f T_{\mathrm{F}} \delta^{\mathrm{ab}} 4 \left[g^{\mu\alpha} g^{\nu\beta} - g^{\mu\nu} g^{\alpha\beta} + g^{\mu\beta} g^{\nu\alpha} \right] \left[\frac{dB_0(k)}{4(d-1)} k^\alpha k^\beta - \frac{k^2 B_0(k)}{4(d-1)} g^{\alpha\beta} - \frac{B_0(k)}{2} k^\alpha k^\beta \right] \\
&= g^2\mu^{2\epsilon} n_f T_{\mathrm{F}} \delta^{\mathrm{ab}} \frac{B_0(k)}{(d-1)} \left[g^{\mu\alpha} g^{\nu\beta} - g^{\mu\nu} g^{\alpha\beta} + g^{\mu\beta} g^{\nu\alpha} \right] \left[k^2 g^{\alpha\beta} + (d-2) k^\alpha k^\beta \right] \\
&= g^2\mu^{2\epsilon} n_f T_{\mathrm{F}} \delta^{\mathrm{ab}} \frac{B_0(k)}{(d-1)} 2(d-2) \left(k^\mu k^\nu - k^2 g^{\mu\nu} \right),
\end{aligned}
\tag{2.13}
$$

where $B_0(k)$ is the master massless loop integral given in appendix A.2 and T_{F} is the Dinkin label of the fundamental rep of $SU(n_f)$[8]. We also used the PV decomposition explained in appendix A.3. If we now choose $d = 4 - 2\epsilon$ and expand the scalar loop integral $B_0(k)$ around its pole in $\epsilon = 0$ we find

$$
\begin{aligned}
&= g^2 n_f T_{\mathrm{F}} \delta^{\mathrm{ab}} \frac{2(2-2\epsilon)}{(3-2\epsilon)} \frac{i}{16\pi^2} \frac{\Gamma^2(1-\epsilon)}{\Gamma(2-2\epsilon)} \left[\frac{1}{\epsilon} - \log\left(-\frac{p^2}{4\pi\mu^2 e^{-\gamma_E}} \right) \right] \left(k^\mu k^\nu - k^2 g^{\mu\nu} \right) \\
&= i \frac{g^2}{16\pi^2} n_f T_{\mathrm{F}} \delta^{\mathrm{ab}} 2(2-2\epsilon) \left(\frac{1}{3} + \frac{2}{9}\epsilon \right) \left[\frac{1}{\epsilon} - \log\left(-\frac{p^2}{4\pi\mu^2 e^{-\gamma_E}} \right) \right] \left(k^\mu k^\nu - k^2 g^{\mu\nu} \right) \\
&= i \frac{g^2}{16\pi^2} n_f T_{\mathrm{F}} \delta^{\mathrm{ab}} \left(\frac{4}{3} - \frac{4}{9}\epsilon \right) \left[\frac{1}{\epsilon} - \log\left(-\frac{p^2}{4\pi\mu^2 e^{-\gamma_E}} \right) \right] \left(k^\mu k^\nu - k^2 g^{\mu\nu} \right) \\
&= i \frac{g^2}{16\pi^2} n_f T_{\mathrm{F}} \delta^{\mathrm{ab}} \left[\frac{4}{3} \frac{1}{\epsilon} - \frac{4}{9} + \frac{4}{3} \log \frac{4\pi\mu^2 e^{-\gamma_E}}{-p^2} \right] + \mathcal{O}(\epsilon).
\end{aligned}
\tag{2.14}
$$

Since we are doing renormalization, we are only interested in the divergent part, which is

$$
i \frac{\alpha_s}{4\pi} \left(-\frac{4}{3} n_f T_{\mathrm{F}} \frac{1}{\epsilon} \right) (k^2 g^{\mu\nu} - k^\mu k^\nu) + \mathcal{O}(\epsilon^0).
\tag{2.15}
$$

In the $\overline{\mathrm{MS}}$ scheme, besides the divergent part, the factors of $\log 4\pi - \gamma_E$ get also reabsorbed into the renormalization constant.

The second relevant diagram is the gluon bubble correction:

---
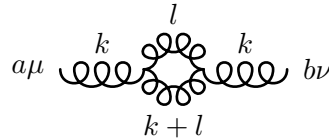
[8] As a convention $T_{\mathrm{F}} = 1/2$.

$$= \frac{1}{2} \int \frac{\mathrm{d}^d \ell}{(2\pi)^d} \left(-g\mu^\epsilon f^{acd} \left[g^{\mu\rho}(k-\ell)^\sigma + g^{\rho\sigma}(2\ell+k)^\mu + g^{\sigma\mu}(-2k-\ell)^\rho \right] \right) \times$$

$$\times \left(-g\mu^\epsilon f^{d'c'b} \left[g^{\sigma'\rho'}(k+2\ell)^\nu + g^{\rho'\nu}(-\ell+k)^{\sigma'} + g^{\nu\sigma'}(-2k-\ell)^{\rho'} \right] \right) \times$$

$$\times \frac{-ig_{\sigma\sigma'}\delta^{dd'}}{(k+\ell)^2} \frac{-ig_{\rho\rho'}\delta^{cc'}}{\ell^2},$$

(2.16)

where the prime indices are related to the internal gluon propaghators. The $1/2$ factor comes from the symmetry factor of the Feynman graph. Then, one has

$$= \frac{1}{2} g^2 \mu^{2\epsilon} C_\mathrm{A} \delta^{\mathrm{ab}} \int \frac{\mathrm{d}^d \ell}{(2\pi)^d} \left[g^{\mu\rho}(k-\ell)^\sigma + g^{\rho\sigma}(2\ell+k)^\mu + g^{\sigma\mu}(-2k-\ell)^\rho \right] \times$$

$$\times \left[g_{\sigma\rho}(k+2\ell)^\nu + g_\rho^\nu(-\ell+k)_\sigma + g_\sigma^\nu(-2k-\ell)_\rho \right] \frac{1}{\ell^2(\ell+k)^2}$$

$$= g^2 \mu^{2\epsilon} \frac{C_\mathrm{A}}{2} \delta^{\mathrm{ab}} \int \frac{\mathrm{d}^d \ell}{(2\pi)^d} \left[(d-6)k^\mu k^\nu + 5k^2 g^{\mu\nu} + (2d-3)k^\mu \ell^\nu + \right.$$

$$\left. + (2d-3)k^\nu \ell^\mu + (4d-6)\ell^\mu \ell^\nu + 2g^{\mu\nu}k_\alpha \ell^\alpha + 2g^{\mu\nu}\ell^2 \right] \frac{1}{\ell^2(\ell+k)^2}$$

$$= g^2 \mu^{2\epsilon} \frac{C_\mathrm{A}}{2} \delta^{\mathrm{ab}} \left[B_0(k) \left((d-6)k^\mu k^\nu + 5k^2 g^{\mu\nu} \right) + (2d-3)k^\mu \mathcal{B}^\nu(k) + \right.$$

$$\left. + (2d-3)k^\nu \mathcal{B}^\mu(k) + (4d-6)\mathcal{B}^{\mu\nu}(k) + 2g^{\mu\nu}k_\alpha \mathcal{B}^\alpha(k) + 2g^{\mu\nu}A_0 \right]$$

$$= g^2 \mu^{2\epsilon} \frac{C_\mathrm{A}}{2} \delta^{\mathrm{ab}} B_0(k) \left[(d-6)k^\mu k^\nu + 5k^2 g^{\mu\nu} - (2d-3)k^\mu k^\nu - k^2 g^{\mu\nu} + \right.$$

$$\left. + \frac{4d-6}{4(d-1)} \left(dk^\mu k^\nu - k^2 g^{\mu\nu} \right) \right]$$

$$= g^2 \mu^{2\epsilon} \frac{C_\mathrm{A}}{2} \delta^{\mathrm{ab}} B_0(k) \left[-\frac{7d-6}{2(d-1)} k^\mu k^\nu + \frac{6d-5}{2(d-1)} k^2 g^{\mu\nu} \right]$$

$$= g^2 \mu^{2\epsilon} C_\mathrm{A} \delta^{\mathrm{ab}} \frac{B_0(k)}{4(d-1)} \left[(6-7d)k^\mu k^\nu + (6d-5)k^2 g^{\mu\nu} \right],$$

(2.17)

where A_0 is the massless vacuum bubble integral given in appendix A.2 and C_A is the Casimir for the adjoint representation[9]. Proceeding exactly as before by substituting $d = 4 - 2\epsilon$ and expanding around the pole $\epsilon = 0$ and taking only the divergent contribution, we find

$$i \frac{\alpha_s}{4\pi} C_A \delta^{\mathrm{ab}} \frac{1}{\epsilon} \left[\frac{19}{12} k^2 g^{\mu\nu} - \frac{11}{16} k^\mu k^\nu \right] + \mathcal{O}(\epsilon^0).$$

(2.18)

---

[9]For $SU(n_f)$ we have $C_\mathrm{A} = (n_f^2 - 1)/n_f$.

The gluon tadpole graph is the simplest one since it is just proportional to

$$\propto \int \frac{\mathrm{d}^d\ell}{(2\pi)^d} \frac{1}{\ell^2} = A_0 = 0 \tag{2.19}$$

 since there is no scale involved.

The last contribution is from the ghost loop where we find

$$= -\int \frac{\mathrm{d}^d\ell}{(2\pi)^d} g\mu^\epsilon f^{acd} (\ell + k)^\mu g\mu^\epsilon f^{bdc} \ell^\nu \frac{i}{\ell^2} \frac{i}{(\ell + k)^2}$$

$$= -g^2\mu^{2\epsilon} C_A \delta^{ab} \int \frac{\mathrm{d}^d\ell}{(2\pi)^d} \frac{\ell^\mu \ell^\nu + k^\mu \ell^\nu}{\ell^2 (\ell + k)^2}$$

$$= -g^2\mu^{2\epsilon} C_A \delta^{ab} \left[\mathcal{B}^{\mu\nu}(k) + k^\mu \mathcal{B}^\nu(k) \right]$$

$$= -g^2\mu^{2\epsilon} C_A \delta^{ab} B_0(k) \left[\frac{dk^\mu k^\nu}{4(d-1)} - \frac{k^2 g^{\mu\nu}}{4(d-1)} - \frac{k^\mu k^\nu}{2} \right]$$

$$= g^2\mu^{2\epsilon} C_A \delta^{ab} \frac{B_0(k)}{4(d-1)} \left[k^2 g^{\mu\nu} + (d-2)k^\mu k^\nu \right]$$

Same, but different, we take $d = 4 - 2\epsilon$ and expand around $\epsilon = 0$. Taking only the divergent part, we get

$$i \frac{\alpha_s}{4\pi} C_A \delta^{ab} \frac{1}{\epsilon} \left[\frac{1}{12} k^2 g^{\mu\nu} + \frac{1}{6} k^\mu k^\nu \right] + \mathcal{O}(\epsilon^0). \tag{2.20}$$
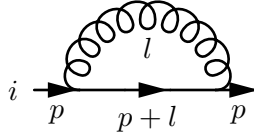
We can now define the renormalization constant Z_3 at 1-loop by summing the three divergent contributions to the gluon propagator in eqs. (2.15), (2.18) and (2.20)

$$Z_3 = 1 + \frac{\alpha_s}{4\pi} \frac{1}{\epsilon} \left(\frac{5}{3} C_A - \frac{4}{3} n_f T_F \right). \tag{2.21}$$

2.3.2 Quark Self-Energy

The next part in the renormalization of QCD is finding the 1-loop corrections to the quark propagator. In this case we have only one contribution from the quark loop since ghosts couple only to gluons and so they only enter in higher-order corrections

to the quark propagator. So we need to evaluate the following Feynman graph

$$i \xrightarrow[p]{} \xrightarrow[p+l]{} \xrightarrow[p]{} j = \int \frac{\mathrm{d}^d \ell}{(2\pi)^d} (-ig\mu^\epsilon t^{\mathrm{a}}_{jk} \gamma^\mu) \frac{i}{\ell - \slashed{p}} (-ig\mu^\epsilon t^{\mathrm{a}}_{ki} \gamma_\mu) \frac{-i}{\ell^2}$$

$$= -g^2 \mu^{2\epsilon} t^{\mathrm{a}}_{jk} t^{\mathrm{a}}_{ki} \int \frac{\mathrm{d}^d \ell}{(2\pi)^d} \gamma^\mu \frac{\ell + \slashed{p}}{(\ell + p)^2} \gamma_\mu \frac{1}{\ell^2}$$

$$= (d-2) g^2 \mu^{2\epsilon} t^{\mathrm{a}}_{jk} t^{\mathrm{a}}_{ki} \int \frac{\mathrm{d}^d \ell}{(2\pi)^d} \frac{\ell + \slashed{p}}{(\ell + p)^2} \frac{1}{\ell^2}, \tag{2.22}$$

where the identity $\gamma^\mu \gamma^\alpha \gamma_\mu = (2-d)\gamma^\alpha$ has been used. Using the properties of the $SU(n_f)$ generators and the integrals given in appendix A.2 we find

$$= (d-2) g^2 \mu^{2\epsilon} \delta_{ij} C_{\mathrm{F}} \gamma_\alpha \int \frac{\mathrm{d}^d \ell}{(2\pi)^d} \frac{\ell^\alpha + p^\alpha}{(\ell + p)^2} \frac{1}{\ell^2}$$

$$= (d-2) g^2 \mu^{2\epsilon} \delta_{ij} C_{\mathrm{F}} \gamma_\alpha [\mathcal{B}^\alpha(p) + p^\mu B_0(p)] \tag{2.23}$$

$$= g^2 \mu^{2\epsilon} \delta_{ij} C_{\mathrm{F}} \slashed{p} \left(\frac{d-2}{2} \right) B_0(p),$$

where we have assumed that the quark momenta is $p^2 \neq 0$ otherwise the integral would be zero in dimensional regularization.

As before, we can now expand around the pole in $\epsilon = 0$

$$= i \frac{g^2}{16\pi^2} C_{\mathrm{F}} \delta_{ij} \slashed{p} (1-\epsilon) \left[\frac{1}{\epsilon} + \log \frac{4\pi\mu^2 e^{-\gamma}}{-p^2} + \mathcal{O}(\epsilon) \right]$$

$$= i \frac{g^2}{16\pi^2} C_{\mathrm{F}} \delta_{ij} \slashed{p} \left[\frac{1}{\epsilon} - 1 + \log \frac{4\pi\mu^2 e^{-\gamma}}{-p^2} \right] + \mathcal{O}(\epsilon) \tag{2.24}$$

$$\simeq i \frac{\alpha_s}{4\pi} \frac{1}{\epsilon} C_{\mathrm{F}} \delta_{ij} \slashed{p} + \mathcal{O}(\epsilon^0).$$

Summing the virtual correction to the bare propagator, we find that the renormalization constant involved is given by

$$Z_2 = 1 - \frac{\alpha_s}{4\pi} \frac{1}{\epsilon} C_{\mathrm{F}}. \tag{2.25}$$

2.3.3 Quark-Gluon Vertex Correction

The 1-loop corrections to the *qqg* vertex are two. The first one is given by the following Feynman diagram
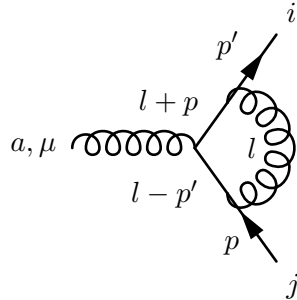
$$
\begin{aligned}
&= \int \frac{\mathrm{d}^d\ell}{(2\pi)^d}(-ig\mu^\epsilon t^{\mathrm{b}}_{jk}\gamma^\nu)\frac{i(\slashed{\ell}-\slashed{p}')}{(\ell-p')^2}(-ig\mu^\epsilon t^{\mathrm{a}}_{kl}\gamma^\mu)\frac{i(\slashed{\ell}+\slashed{p})}{(\ell+p)^2}(-ig\mu^\epsilon t^{\mathrm{b}}_{li}\gamma_\nu)\frac{-i}{\ell^2} \\
&= -\left(C_{\mathrm{F}}-\frac{C_{\mathrm{A}}}{2}\right)t^{\mathrm{a}}_{ji}g^3\mu^{3\epsilon}\int\frac{\mathrm{d}^d\ell}{(2\pi)^d}\frac{\gamma^\nu(\slashed{\ell}-\slashed{p}')\gamma^\mu(\slashed{\ell}+\slashed{p})\gamma_\nu}{\ell^2(\ell-p')^2(\ell+p)^2},
\end{aligned}
\tag{2.26}
$$

where the color factors come from the $SU(n_f)$ algebra[10]. To perform this integral, since we are only interested in the UV behaviour, we make the simplification $p = p' = 0$ with a caveat that we'll see later. In this limit, we have

$$
-g^3\mu^{3\epsilon}t^{\mathrm{a}}_{ji}\left(C_{\mathrm{F}}-\frac{C_{\mathrm{A}}}{2}\right)\int\frac{\mathrm{d}^d\ell}{(2\pi)^d}\frac{\gamma^\nu\slashed{\ell}\gamma^\mu\slashed{\ell}\gamma_\nu}{(\ell^2)^3}.
\tag{2.27}
$$

Inside the integral, the following equality is valid

$$
\ell_\alpha\ell_\beta = \frac{g_{\alpha\beta}}{d}\ell^2
\tag{2.28}
$$

which gives us

$$
-g^3\mu^{3\epsilon}t^{\mathrm{a}}_{ji}\left(C_{\mathrm{F}}-\frac{C_{\mathrm{A}}}{2}\right)\int\frac{\mathrm{d}^d\ell}{(2\pi)^d}\frac{1}{d}\frac{\gamma^\nu\gamma^\alpha\gamma^\mu\gamma_\alpha\gamma_\nu}{(\ell^2)^2}.
\tag{2.29}
$$

Using the Clifford algebra in d-dimensions

$$
\gamma^\nu\gamma^\alpha\gamma^\mu\gamma_\alpha\gamma_\nu = (2-d)\gamma^\nu\gamma^\mu\gamma_\nu = (d-2)^2\gamma^\mu.
\tag{2.30}
$$

Therefore

$$
-g^3\mu^{3\epsilon}\left(C_{\mathrm{F}}-\frac{C_{\mathrm{A}}}{2}\right)\frac{(d-2)^2}{d}\gamma^\mu\int\frac{\mathrm{d}^d\ell}{(2\pi)^d}\frac{1}{(\ell^2)^2}.
\tag{2.31}
$$

The last integral may seem to be zero, but this is only because we have taken out the relevant scales. Therefore we need to introduce a scale back in a sort of Pauli-Villard regularization

$$
\int\frac{\mathrm{d}^d\ell}{(2\pi)^d}\frac{1}{(\ell^2)^2} \to \int\frac{\mathrm{d}^d\ell}{(2\pi)^d}\frac{1}{(\ell^2-m^2)^2} = \frac{i}{(4\pi)^{d/2}}\frac{\Gamma\left(2-\frac{d}{2}\right)}{\Gamma(2)}(m^2)^{\frac{d}{2}-2}.
\tag{2.32}
$$

Now we can put $d = 4 - 2\epsilon$ and expand around the pole $\epsilon = 0$, taking only the divergent part

$$
-igt^{\mathrm{a}}_{ji}\gamma^\mu\frac{\alpha_s}{4\pi}\frac{1}{\epsilon}\left(X_{\mathrm{F}}-\frac{C_{\mathrm{A}}}{2}\right).
\tag{2.33}
$$

The second diagram which contributes to the correction is given by

---
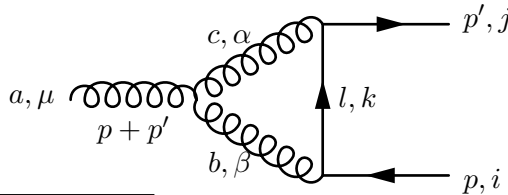
[10]In practice $t^{\mathrm{a}}t^{\mathrm{b}}t^{\mathrm{a}} = (C_{\mathrm{F}}-C_{\mathrm{A}}/2)t^{\mathrm{b}}$.

$$
= \int \frac{\mathrm{d}^d\ell}{(2\pi)^d} (-g\mu^\epsilon f^{\mathrm{abc}}) \left[g^{\mu\beta}(-2p-p'+\ell)^\alpha + g^{\beta\alpha}(-2\ell+p-p')^\mu \right.
$$
$$
\left. + g^{\alpha\mu}(\ell+2p'+p)^\alpha) \right] \frac{-i}{(\ell-p)^2} \frac{-i}{(\ell+p')^2} (-ig\mu^\epsilon \gamma_\alpha t^{\mathrm{c}}_{jk}) \frac{i\slashed{\ell}}{\ell^2} (-ig\mu^\epsilon \gamma_\beta t^{\mathrm{b}}_{ki}). \tag{2.34}
$$

Using the color algebra equality $if^{\mathrm{abc}}t^{\mathrm{c}}t^{\mathrm{b}} = C_{\mathrm{A}}/2t^{\mathrm{a}}$ and by, again, neglecting the momenta p and p', we get

$$
- g^3 \mu^{3\epsilon} \frac{C_{\mathrm{A}}}{2} t^{\mathrm{a}}_{ji} \int \frac{\mathrm{d}^d\ell}{(2\pi)^d} \frac{\left(g^{\mu\beta}\ell^\alpha - 2g^{\beta\alpha}\ell^\mu + g^{\alpha\mu}\ell^\beta \right)\gamma_\alpha\gamma_\rho\gamma_\beta\ell^\rho}{(\ell^2)^3}. \tag{2.35}
$$

With the additional Clifford algebra equality $\gamma_\mu\gamma^\mu = d$, we find that the integral becomes

$$
\int \frac{\mathrm{d}^d\ell}{(2\pi)^d} \frac{\gamma^\mu + 2\frac{(d-2)}{d}\gamma^\mu + \gamma^\mu}{(\ell^2)^2} = 4\frac{d-1}{d}\gamma^\mu \int \frac{\mathrm{d}^d\ell}{(2\pi)^d} \frac{1}{(\ell^2)^2}. \tag{2.36}
$$

The integral is the same as before, so we can proceed exactly in the same manner, obtaining

$$
- ig t^{\mathrm{a}}_{ji} \gamma^\mu \frac{\alpha_s}{4\pi} \frac{1}{\epsilon} \frac{3}{2} C_{\mathrm{A}}. \tag{2.37}
$$

By summing the tree-level amplitude with the 1-loop corrections we find the renormalization constant Z_1 via

$$
Z_1^{-1} = 1 + \frac{\alpha_s}{4\pi} \frac{1}{\epsilon} (C_{\mathrm{A}} + C_{\mathrm{F}}). \tag{2.38}
$$

Let us now concentrate for a moment on the renormalized Lagrangian, and in particular on the strong coupling constant. The bare vertex reads

$$
g_B \bar{\psi}_{qB} \slashed{G}_B \psi_{qB}, \tag{2.39}
$$

where in d-dimensions, the bare coupling constant is dimensionful. If we now replace the bare fields and coupling constant with the renormalized one by virtue of eq. (2.12) we get

$$
g\mu^\epsilon Z_g Z_2 Z_3^{1/2} \bar{\psi}_q \slashed{G} \psi_q. \tag{2.40}
$$

But, from the evaluation of the loop corrections to the vertex, we know that the renormalization constant is Z_1^{-1}. Hence, since what we can actually measure can only be the vertex, we require that the divergent factors obtained by rescaling the fields must be exactly canceled by the multiplicative factor Z_1^{-1}. In this way, whenever we extract physical quantities, they will be finite. This corresponds to choosing

$$
Z_1 = Z_g Z_2 Z_3^{1/2} \implies Z_g = \frac{Z_1}{Z_2 Z_3^{1/2}}. \tag{2.41}
$$

Using the results we found in eqs. (2.21), (2.25) and (2.38) we find

$$
Z_g = 1 - \frac{\alpha_s}{4\pi} \frac{1}{\epsilon} \left(\frac{11}{6} C_{\mathrm{A}} - \frac{4}{6} n_f T_{\mathrm{F}} \right). \tag{2.42}
$$

Note that this result is gauge-independent.

2.4   Renormalization Group Equations

A general feature of renormalization is that it adds an explicit scale dependence μ on physical quantities. But it is important to note that the initial, bare, quantities did not depend on an energy scale. Thus, we have to require that the bare quantities do not depend on μ. By doing so we get the so-called *renormalization group equations* (RGE). These equations govern the dependence on the scale of relevant physical quantities like the coupling constants.

By imposing that the bare coupling constant does not depend on the renormalization scale and searching for a solution to the RGE, a peculiar thing happens: the physical parameters will depend on the energy scale. In particular, we are interested in the scale dependence of the coupling constant. We will see that this scale dependence will be such that two behaviours can arise: when the energy is high then the coupling constant is small or when the energy scale is small, then the coupling constant is small. We call theories with such behaviours *asymptotically free* in the UV for the former or in the IR for the latter. Let us be rigorous now.

Take an observable $\mathcal{O}$ calculated in the $\overline{\text{MS}}$ scheme. We have

$$\mathcal{O} = \mathcal{O}_{\overline{\text{MS}}}\Big(\alpha(\mu), m(\mu), \log\frac{s}{\mu^2}, \cdots\Big), \tag{2.43}$$

where $\sqrt{s}$ is the center-of-mass energy. Here $\alpha \propto g^2$ is the coupling constant and m is the physical mass of the theory. The appearance of logarithms is a general feature of regularization as clearly underlined by the previous calculations of loop corrections.

It is important to note that the physical observable $\mathcal{O}$ is μ independent assuming one works to all orders in perturbation theory. The logarithms can be large whenever $s \gg \mu$, these will be discussed on more general grounds in the following chapters. The μ independence of the observable $\mathcal{O}$ can be expressed in the following form

$$\mu\frac{\mathrm{d}}{\mathrm{d}\mu}\mathcal{O} = \mu\frac{\mathrm{d}\alpha(\mu)}{\mathrm{d}\mu}\frac{\partial\mathcal{O}}{\partial\alpha(\mu)} + \mu\frac{\mathrm{d}m(\mu)}{\mathrm{d}\mu}\frac{\partial\mathcal{O}}{\partial m(\mu)} + \frac{\partial\mathcal{O}}{\partial\mu} = 0. \tag{2.44}$$

These equations are known as Renormalization Group Equations! In this case, we assumed that the observable $\mathcal{O}$ only depends on two quantities: the coupling constant and the mass, but a more general theory can also depend on some other parameters, but the generalization is trivial.

We define then two very important functions

$$\begin{aligned}\mu\frac{\mathrm{d}\alpha(\mu)}{\mathrm{d}\mu} &\equiv \frac{\mathrm{d}\alpha(\mu)}{\mathrm{d}\log\mu} = \beta(\alpha(\mu)) \\ \mu\frac{\mathrm{d}m(\mu)}{\mathrm{d}\mu} &\equiv \frac{\mathrm{d}m(\mu)}{\mathrm{d}\log\mu} = \gamma_m(\alpha(\mu))m(\mu)\end{aligned} \tag{2.45}$$

which we call *beta function* and *mass anomalous dimension* respectively. With these definitions, eq. (2.44) becomes

$$\beta(\alpha)\frac{\partial\mathcal{O}}{\partial\alpha} + \gamma_m(\alpha)m\frac{\partial\mathcal{O}}{\partial m} + \frac{\partial\mathcal{O}}{\partial\mu} = 0. \tag{2.46}$$

2.4.1 The QCD Beta Function

Now, given the general definitions and the 1-loop result for Z_g in eq. (2.42), we are ready to find out if QCD is UV-free or IR-free. Given that

$$g_B = \mu^\epsilon Z_g(\mu) g(\mu) \implies \alpha_{sB} = \mu^{2\epsilon} Z_g^2(\mu) \alpha_s(\mu) \equiv \mu^{2\epsilon} Z_\alpha(\mu) \alpha_s(\mu), \qquad (2.47)$$

where

$$Z_\alpha(\mu) = 1 - \frac{\alpha_s(\mu)}{4\pi\epsilon} \beta_0, \qquad \beta_0 = \left(\frac{11}{3} C_A - \frac{4}{3} n_f T_F \right). \qquad (2.48)$$

From the fact that the bare parameters are scale-independent, we get the RGE for the running coupling

$$\frac{\mathrm{d}\alpha_{Bs}}{\mathrm{d}\log\mu} = 0 = \mu^{2\epsilon} Z_\alpha(\mu) \alpha_s(\mu) \left[2\epsilon + Z_\alpha^{-1} \frac{\mathrm{d}Z_\alpha}{\mathrm{d}\log\mu} + \frac{1}{\alpha_s} \frac{\mathrm{d}\alpha_s}{\mathrm{d}\log\mu} \right], \qquad (2.49)$$

which implies

$$\frac{\mathrm{d}\alpha_s}{\mathrm{d}\log\mu} = \alpha_s \left[-2\epsilon - Z_\alpha^{-1} \frac{\mathrm{d}Z_\alpha}{\mathrm{d}\log\mu} \right] \equiv \beta(\alpha_s(\mu), \epsilon). \qquad (2.50)$$

This more general β function is defined for a finite ϵ where in the limit $\epsilon \to 0$ we get the usual β function.

Consider now the fact that the renormalization constants in this scheme, only contain dependence on $1/\epsilon^n$ factors and thus the dependence on the scale μ is only through the running coupling $\alpha_s(\mu)$. Thus we can recast eq. (2.50) in the more convenient form

$$\beta(\alpha_s, \epsilon) = \alpha_s \left[-2\epsilon - \beta(\alpha_s, \epsilon) \frac{\mathrm{d}Z_\alpha}{\mathrm{d}\alpha_s} \right]. \qquad (2.51)$$

To solve this equation we expand

$$\begin{aligned} \beta(\alpha_s, \epsilon) &= \beta(\alpha_s) + \sum_{k=1}^\infty \epsilon^k \beta^{(k)}(\alpha_s), \\ Z_\alpha &= 1 + \sum_{k=1}^\infty \frac{1}{\epsilon^k} Z_\alpha^{(k)}(\alpha_s). \end{aligned} \qquad (2.52)$$

The solution to the equation is therefore

$$\beta(\alpha_s) = 2\alpha_s^2 \frac{\mathrm{d}Z_\alpha^{(1)}(\alpha_s)}{\mathrm{d}\alpha_s}, \qquad (2.53)$$

which yields

$$\beta(\alpha_s, \epsilon) = -2\epsilon\alpha_s + \beta(\alpha_s) = -2\epsilon\alpha_s + 2\alpha_s^2 \frac{\mathrm{d}Z_\alpha^{(1)}}{\mathrm{d}\alpha_s}. \qquad (2.54)$$

A similar relation holds for the mass anomalous dimension

$$\gamma_m(\alpha_s) = 2\alpha_s \frac{\mathrm{d}Z_m^{(1)}(\alpha_s)}{\mathrm{d}\alpha_s}. \qquad (2.55)$$

These equations are really important. They state that to all orders in perturbation theory, the β-function and the anomalous dimension can be extracted from the

coefficients of the single $1/\epsilon$ pole in the renormalization constants.

In our 1-loop calculation, we find that

$$\frac{\mathrm{d}Z_\alpha^{(1)}}{\mathrm{d}\alpha_s} = -\frac{\mathrm{d}}{\mathrm{d}\alpha_s}\frac{\alpha_s}{4\pi}\beta_0 = \frac{\beta_0}{4\pi}, \tag{2.56}$$

therefore

$$\beta_0(\alpha_s) = -2\alpha_s\left(\beta_0\frac{\alpha_s}{4\pi}\right). \tag{2.57}$$

To this date, the β-function of QCD has been calculated up to 5-loop [19, 91, 112].

2.4.2 Leading-order Solution to the RGE
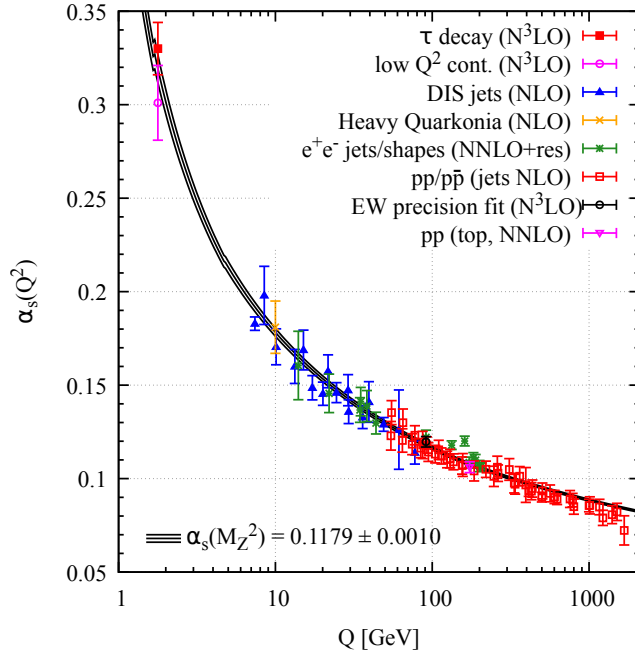
Figure 2.1. Running coupling with experimental data. The best fit value for the $\overline{\text{MS}}$ strong coupling constant is $\alpha_s(m_Z) = 0.1179 \pm 0.0010$. Image from Ref. [152].

Given the 1-loop solution for the β-function eq. (2.57), we can find the running of the strong coupling constant by means of

$$\frac{\mathrm{d}\alpha_s(\mu)}{\mathrm{d}\log\mu} = -2\beta_0\frac{\alpha_s^2(\mu)}{4\pi}. \tag{2.58}$$

This can be solved by simple separation of variables

$$-\int_{\alpha_s(\Lambda)}^{\alpha_s(\mu)}\frac{\mathrm{d}\alpha_s}{\alpha_s^2} = \frac{1}{\alpha_s(\mu)} - \frac{1}{\alpha_s(\Lambda)} = \frac{\beta_0}{4\pi}\log\frac{\mu^2}{\Lambda^2}, \tag{2.59}$$

where $\alpha_s(\Lambda)$ is the strong coupling constant measured at some energy scale Λ. Often one chooses $\Lambda = m_Z \approx 91.188$ GeV at which $\alpha_s(m_Z) = 0.1179 \pm 0.0010$ [152]. By rearranging the above equation, we find the famous expression

$$\alpha_s(\mu) = \frac{\alpha_s(\Lambda)}{1 + \frac{\alpha_s(\Lambda)}{4\pi}\beta_0 \log\frac{\mu^2}{\Lambda^2}}, \qquad \beta_0 = \frac{11}{3}C_{\mathrm{A}} - \frac{4}{3}n_f T_{\mathrm{F}}. \tag{2.60}$$

Here n_f is the effective number of active flavours below the scale μ. Now it is possible to see the fundamental behaviour of the strong coupling constant: being $\beta_0 > 0$, since $n_f < 17$, when we increase the energy scale μ, $\alpha_s(\mu)$ becomes smaller. This phenomenon is referred to as *asymptotic freedom* [83, 123].

At this point, it is important to fix an energy scale with respect to which we define the UV and IR phases. We can rearrange eq. (2.60) in a suitable way as

$$\alpha_s(\mu) = \left[\beta_0 \log\left(\frac{\mu^2}{\Lambda_{\mathrm{QCD}}^2}\right)\right]^{-1}, \tag{2.61}$$

that defines a new constant called Λ_{QCD}[11]. In reality, Λ_{QCD} is not completely defined at LO. One has to evaluate at least the NLO solution to the RGE for α_s which requires the calculation of the 2-loop corrections. Without going into the specific calculations, we give here the second order contribution to the beta function which is needed for the NLO solution of the RGE for α_s

$$\beta_1 = \frac{34}{3}C_{\mathrm{A}}^2 - \frac{20}{3}C_{\mathrm{A}}T_{\mathrm{F}}n_f - 4C_{\mathrm{F}}T_{\mathrm{F}}n_f. \tag{2.62}$$

The solution to the RGE for α_s is therefore

$$\alpha_s(\mu) = \frac{4\pi}{\beta_0 \log\frac{\mu^2}{\Lambda^2}}\left[1 - \frac{\beta_1}{\beta_0^2}\frac{\log\log\frac{\mu^2}{\Lambda^2}}{\log\frac{\mu^2}{\Lambda^2}}\right]. \tag{2.63}$$

If we include higher-order corrections and measure the value of α_s at some energy scale like $\alpha_s(m_Z)$, one finds that $\Lambda_{\mathrm{QCD}} \approx 250$ MeV. At energies below Λ_{QCD}, the theory becomes strongly coupled and therefore ordinary perturbation theory breaks up and we need to use non-perturbative techniques to find meaningful results like lattice QCD. In some regimes, there are other theories like Chiral Perturbation Theory (ChPT) [121] and $1/N$ expansion [136] that contains the main features of QCD but are not an exact solution like lattice QCD.

Note that in the $\overline{\mathrm{MS}}$ scheme, the slope of the curve changes whenever we cross a quark mass threshold. This is because β_0 depends on the number of active flavour below the scale μ so, if we go from $\mu \approx m_b$ to $\mu \approx m_c$, the active flavours go from $n_f = 5$ to $n_f = 4$ thus changing β_0.

---

[11]Note that if we started with a mass-less theory we would have gotten the same result. Hence a completely arbitrary energy scale has appeared even although the theory was scaleless to begin with. This phenomenon is known as dimensional transmutation.

Chapter 3

Effective Field Theories: an Introduction

The study of effective field theories (EFT) [114] arises from a necessity. In principle, one could evaluate the relevant quantities for some weak processes on the lattice. However, the presence of many different energy scales for any given process makes this approach impractical. What one can do for renormalizable theories is to separate the different contributions coming from the different energy scales and evaluate the high-energy part perturbatively while the low-energy contributions can be evaluated on the lattice. This separation is made possible by EFTs. One such process where EFTs are essential is for the study of non-leptonic decays of light mesons such as pions and kaons.

The fundamental idea behind effective field theories (EFT) started in the opposite manner as we are used to today. We can think of the Fermi theory of Weak interactions as really the first effective theory in the history of the SM. In reality, Fermi developed his theory of Weak interactions [67] in the 1930s, well before we knew that a more general theory was present, the now called SM. The Fermi theory was at the time such a speculative theory that even a prestigious peer-reviewed journal like Nature rejected Fermi's paper. We now know that his theory is in fact a *low energy* equivalent of the SM weak interactions!

In this chapter, we are going to introduce the idea behind EFTs with the pedagogical example of the Fermi theory. Then we're going to make a more rigorous definition through the use of the Operator Product Expansion (OPE) which will divide the problem into two main chunks: the Wilson coefficients which encode all the short distance physics and the effective operators matrix elements which deal with the low energy part of the theory. Moreover, we're going to see that QCD corrections give large-log contributions to the amplitude and how we can deal with these large-logs using the RGEs.

3.1 A Historical Example: the Fermi Theory of Weak Interactions

A first historical example that we need to give to set up the background, which we will later develop in more detail, is the Fermi theory of Weak interactions. This

theory was developed by Fermi in the 30s to explain the phenomena of beta decay. He did this by postulating that the decay process can be described by adding to the free Hamiltonians of the particles in the beta process an interaction term containing the wave functions of the four free particles

$$H_F = H_n^0 + H_p^0 + H_e^0 + H_\nu^0 + \sum_i C_i \int d^3x \left(\bar{u}_p \hat{O}_i u_n \right) \left(\bar{u}_e \hat{O}_i u_\nu \right). \qquad (3.1)$$

Here u_p, u_n, u_e, u_ν denote the wave functions of the four particles.
We now concentrate solely the interaction term which is given by the Hamiltonian density

$$\mathcal{H}_F = \sum_i C_i \left(\bar{u}_p \hat{O}_i u_n \right) \left(\bar{u}_e \hat{O}_i u_\nu \right). \qquad (3.2)$$

A question arises: what are the operators $\hat{O}_i$? The answer was found in the deep experimental evidence in the years following the proposed theory.
Firstly, the Hamiltonian needs to be a Lorentz scalar, which implies that the operators need to be one of the fermionic bilinear covariants

$$1 \qquad \gamma^\mu \qquad \sigma^{\mu\nu} = \frac{i}{2}[\gamma^\mu, \gamma^\nu] \qquad \gamma^\mu \gamma_5 \qquad \gamma_5. \qquad (3.3)$$

In principle, one does not know which combination of bilinears enters the Hamiltonian. In the beginning, Gell-Mann and Feynman thought that, like electromagnetism, the interactions should be vectorial in nature. Moreover, from experimental evidence, it was found that only a single helicity appears: electrons and neutrinos are always left-handed while positrons and anti-neutrino are always right-handed. This is a consequence of parity violation in Weak decays. Therefore, the part of the Hamiltonian containing electrons and neutrino spinors should only contain the part of the wave function with negative helicity. This is found by using the chiral projectors like the ones in equations eq. (1.48). Through this process, it was found that only the $V - A$ combination gives a meaningful contribution

$$\hat{O}_{V-A} = \frac{1}{2}(\gamma^\mu - \gamma^\mu \gamma_5). \qquad (3.4)$$

For neutrinos the chiral form of the operators is exact. For the electron, being massive, they are good if the electron momentum is *high enough*[1]. According to these considerations, we must replace the spinors by their components with negative chirality. Lorentz invariance requires that even the nucleonic part of the Fermi Hamiltonian has to be $V - A$ type. Extensive experimental analysis has led to the conclusion that the correct form for the nucleonic part is given by

$$\bar{u}_p \gamma^\mu (g_V + g_A \gamma_5) u_n = g_V \bar{u}_p \left(1 - \frac{g_A}{g_V} \gamma_5 \right) u_n \qquad (3.5)$$

with

$$g_A/g_V = -1.255 \pm 0.006 \qquad (3.6)$$

---

[1]This implies that the statement that electrons have only positive helicity is only approximately correct.

This takes into a fact that protons and neutrons are composite particles and that the axial symmetry is broken.

The complete expression for the Hamiltonian interaction term is therefore given by

$$\mathcal{H}_F = -\frac{G_F}{\sqrt{2}} g_V \left[\bar{p}\, \gamma^\mu \left(1 - \frac{g_A}{g_V} \gamma_5 \right) n \right] [\bar{e}\, \gamma_\mu (1 - \gamma_5) \nu_e]. \tag{3.7}$$

This result can be exploited to find effective Hamiltonians for all kinds of processes like for the muon decay, in which the Hamiltonian takes the form

$$\mathcal{H}_F = -\frac{G_F}{\sqrt{2}} \bar{\nu}_\mu \gamma^\mu (1 - \gamma_5) \mu \bar{e}^- \gamma_\mu (1 - \gamma_5) \nu_e. \tag{3.8}$$

The only problem is now that the theory is clearly non-renormalizable since it is made up of dimension six operators. But fear not, we can circumvent this problem by means of the renormalization group improved perturbation theory which we will explain later.

Here comes the fundamental step: since we know that the SM explains so well weak processes but also does the Fermi theory, the two need to be linked in some way. We will see now that the Fermi theory is a *low energy limit* of the SM.

3.2 Effective Hamiltonians for Weak Decays

We can start by looking at a simpler case of the leptonic decay of a pion $\pi \to \ell \nu_\ell$, we will see that such a process comes with a much simpler QCD structure due to the presence of quarks only in the initial state.

In the 't Hooft-Feynman gauge[2], at tree level, this process is governed by two diagrams
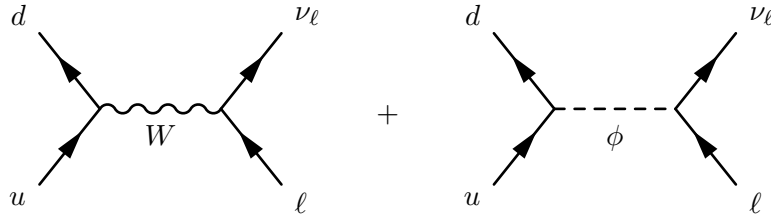
The 't Hooft-Feynman is more useful when dealing with loop diagrams since the W propagator does not have the $p^\mu p^\nu$ term like in eq. (1.120) which would give a complicated ultraviolet behaviour. Moreover, this gauge makes the process of expanding the amplitude more straightforward. The problem is now that we have to deal with Goldstone boson exchange. But since the coupling of the latter is proportional to the light fermion masses, we can ignore them for the following. The amplitude of the W diagram is therefore

$$i\mathcal{A} = \left(\frac{ig_2}{2\sqrt{2}} \right)^2 V_{ud}^* \bar{u}_{\nu_\ell} \gamma^\mu (1 - \gamma_5) v_\ell \frac{ig_{\mu\nu}}{s - M_W^2 + i\epsilon} \bar{v}_d \gamma^\nu (1 - \gamma_5) u_u. \tag{3.9}$$

---

[2]Which is a particular R_ξ gauge with $\xi = 1$.

Given that the typical energy of the process is $s \sim \mathcal{O}(m_\pi) \ll M_W^2$, we can perform an expansion of the W propagator in powers of s, leading to

$$i\mathcal{A} = -i\frac{V_{ud}^* g_2^2}{8M_W^2}\bar{u}_{\nu_\ell}\gamma^\mu(1-\gamma_5)v_\ell\bar{v}_d\gamma_\mu(1-\gamma_5)u_u\sum_{k=0}^{\infty}\left(\frac{s}{M_W^2}\right)^k$$

$$\simeq -i\frac{G_F}{\sqrt{2}}V_{ud}^*\bar{u}_{\nu_\ell}\gamma^\mu(1-\gamma_5)v_\ell\bar{v}_d\gamma_\mu(1-\gamma_5)u_u + \mathcal{O}\left(\frac{s}{M_W^2}\right), \qquad (3.10)$$

where we introduced the Fermi constant as

$$\frac{G_F}{\sqrt{2}} = \frac{g_2^2}{8M_W^2}. \qquad (3.11)$$

As we can see eq. (3.10) is exactly of the same form as eq. (3.8). This is a first simple example of *operator product expansion* (OPE)[147]: the dominant term in the decay $\pi \to \ell\nu_\ell$ is given by the matrix element of a six dimensional effective operator

$$Q^{\bar{d}u\bar{\nu}\ell} = \bar{d}\gamma^\mu\frac{(1-\gamma_5)}{2}u\,\bar{\nu}\gamma_\mu\frac{(1-\gamma_5)}{2}\ell \qquad (3.12)$$

while subsequent orders $k > 0$ correspond to the matrix elements of higher dimensional operators containing $2k$ derivatives.

From a Feynman diagram point of view, the process of expanding the W propagator, thus making its effects local, amounts to contracting the W propagator to a point
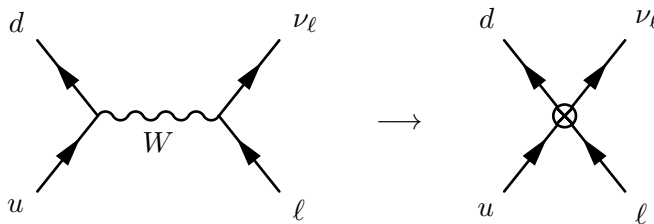
Keeping only dimension six operators in this OPE we obtain that the amplitude is given by

$$\mathcal{A} = \langle\mathcal{H}_{\text{eft}}\rangle + \mathcal{O}\left(\frac{s}{M_W^2}\right) \qquad \mathcal{H}_{\text{eft}} = \frac{4G_F}{\sqrt{2}}V_{ud}^*Q^{\bar{d}u\bar{\nu}\ell}, \qquad (3.13)$$

where $\mathcal{H}_{\text{eft}}$ is the effective Hamiltonian governing the $\pi \to \ell\nu_\ell$ transition. The process of equating the full amplitude with the one given by the effective Hamiltonian is called *matching*.

The effects of the exchange of the heavy W boson are encoded in the expansion coefficients, which are known as *Wilson coefficients*.

In general, let us consider the ampliture $\mathcal{A}$ of a given process. Thanks to the OPE we can put this in the form

$$\mathcal{A} = \langle\mathcal{H}_{\text{eft}}\rangle = \sum_i C_i(\mu, M_W)\langle Q_i(\mu)\rangle \qquad (3.14)$$

when the process takes place at an energy scale $\mu \ll M_W$. We say that the W is being integrated out. The expansion C_iQ_i can be seen as an effective theory
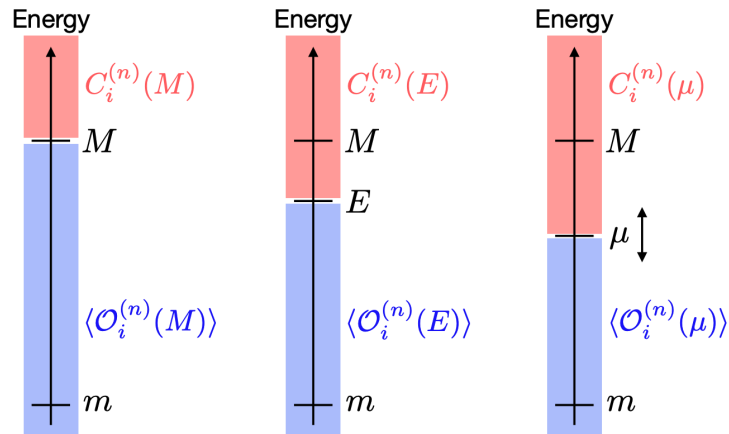
Figure 3.1. Factorization of an observable into short-distance (red) and long-distance (blue) contributions. The panels differ by the choice of the factorization scale. The figure is taken from [116] with the permission of the author.

whose vertices are given by the local operators Q_i and the coupling constants by the expansion coefficients C_i, the Wilson coefficients.

By doing so, we can separate the problem into two main chunks: the Wilson coefficients which contain the short-distance[3] contribution to the amplitude and can therefore be evaluated using ordinary perturbation theory and the effective operator matrix elements which contain the low-energy physics and have to be evaluated by means of lattice QCD or other techniques like the large N [136] expansion or chiral perturbation theory (ChPT) [121].

One may roughly think of this process as splitting up the contributions from virtual particles

$$\int_{-p^2}^{M_W^2} \frac{\mathrm{d}k^2}{k^2} = \int_{\mu^2}^{M_W^2} \frac{\mathrm{d}k^2}{k^2} + \int_{-p^2}^{\mu^2} \frac{\mathrm{d}k^2}{k^2}, \tag{3.15}$$

where the first term is sensitive to UV physics and is found into the Wilson coefficients, while the second is sensitive to IR physics and is absorbed into the operator matrix elements. This can be seen pictorially in fig. (3.1).

We note that on a more formal basis, the procedure of the OPE may be given by considering the generating functional for Green functions in the path integral formalism. Then we "integrate out" the heavy degrees of freedom associated with the high scale M from the generating functional of Green's functions and obtain a non-local action functional, which can be expanded in an infinite tower of local operators $Q_i^{(n)}$ [122].

3.3 QCD Effects

The required QCD corrections to the full theory, in the case of the leptonic decays just mentioned, are the same as the ones in the effective theory since they are just given by external legs corrections and vertex corrections. So under the process of

---

[3]High energy.

matching, those won't influence the Wilson coefficients but are going to be contained in the operator matrix element and so we don't need to take them into account.

3.3.1 Large Logarithms

If we now turn to non-leptonic decays, the situation changes drastically. Consider for example the process $c\bar{s} \to u\bar{d}$. At tree level, after the OPE, we get a dimension six operator which is similar to the one in eq. (3.12)

$$Q_2^{\bar{s}c\bar{d}u} = \bar{s}\gamma^\mu \frac{(1-\gamma_5)}{2}c\bar{u}\gamma_\mu \frac{(1-\gamma_5)}{2}d \equiv \bar{s}_L\gamma^\mu c_L \bar{u}_L \gamma_\mu d_L, \qquad (3.16)$$

where we used the shorthand notation of the chiral spinors. After matching we get that

$$\mathcal{H}_{\text{eff}} = \frac{4G_F}{\sqrt{2}} V_{cs}^* V_{ud} C_2 Q_2^{\bar{s}c\bar{d}u} \qquad C_2 = 1. \qquad (3.17)$$

As for the case of the leptonic decay, the Wilson coefficient is trivial at tree level. When we go to $\mathcal{O}(\alpha_s)$ the situation changes drastically. External legs corrections as well as vertex corrections like the ones following

won't affect the matching since at this order the current are conserved and so they will not generate large-logs. But now, we can have gluon exchange between the initial and the final legs like the following

In the full theory this correction will affect the momentum propagating in the W boson, which will make the overall diagram convergent, but proportional to terms of the form

$$\alpha_s \int \frac{\mathrm{d}^4\ell}{\ell^2[(p-\ell)^2 - M_W^2]} \sim \alpha_s \log\left(\frac{M_W^2}{-p^2}\right) \qquad (3.20)$$

which taken at face value would imply the breakdown of perturbation theory. In fact, when the quark momenta become of the order or Λ_{QCD}, the effective expansion coefficient becomes $\mathcal{O}(1)$. This is the problem of *large logarithms*. Fortunately, the effective theory can save us from this problem.

Let us consider the effective operator for the case at hand $Q_2^{\bar{s}c\bar{u}d}$. The $\mathcal{O}(\alpha_s)$

corrections are given by the following Feynman diagrams
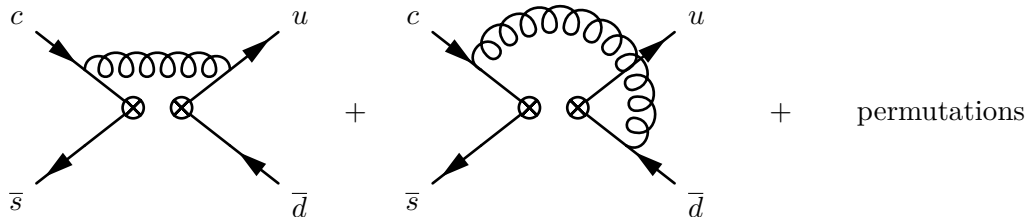
Having removed the W propagator is not a surprise that once we evaluate such diagrams, they come out to be divergent. The effective theory has therefore a much different ultraviolet behaviour with respect to the full SM amplitude. But we know that the EFT is going to be valid up to a cutoff Λ of the order $\mathcal{O}(M_W)$. We can regulate the diagrams by introducing such cutoff, obtaining terms of the form

$$\alpha_s \log\left(\frac{\Lambda^2}{-p^2}\right). \tag{3.21}$$

In reality when dealing with perturbation theory, rather than introducing a specific cutoff, we regulate the theory using dimensional regularization, which introduces a scale μ, and logarithmic terms are going to be of the form $\log(\mu^2/-p^2)$. When we match the amplitudes of diagrams in eq. (3.19) with the ones in section 3.3.1, any infrared logs cancel and we are left with terms of the form

$$\log\left(\frac{M_W^2}{-p^2}\right) - \log\left(\frac{\mu^2}{-p^2}\right) = \log\left(\frac{M_W^2}{\mu^2}\right). \tag{3.22}$$

We have now the liberty of choosing the matching scale in order to get rid of large logs. In this case, setting $\mu \sim M_W$ we get back the ordinary expansion coefficient α_s, without the log. On the other hand, the non-perturbative part of the hadronic matrix elements needs to be evaluated on the lattice which intrinsically introduces a hard energy cutoff tied to the lattice spacing $a \sim 1/\Lambda$. Then the renormalization of the operators is done, mostly, by the RI-SMOM scheme [115] which is a non-perturbative renormalization scheme suitable to evaluate renormalized quantities on the lattice. Moreover, as we will see in more detail in the following chapter, QCD corrections enlarge the operator basis due to the presence of the gluon which can mix the color of the external quarks, and so a different color structure arises. Not only that but even more complex operators are generated which have the required quantum numbers and therefore have to be taken into account.

Up the here, the point of the situation is as follows: we encounter large logs in the full theory which are a consequence of the many energy scales which enter the process. There is no way to get rid of these large logs. Then, we go to the effective theory where the loop diagrams are divergent and large logs appear with a dependence on the renormalization scale. Through matching, we can get rid of large logs, but only in the Wilson coefficients, which can therefore be evaluated, at a scale $\mu \sim M_W$, with ordinary perturbation theory. The operator matrix elements still contain large logs. We see in the next chapter how the Renormalization Group can help us solve this problem.

3.4 Wilsonian Renormalization

The Wilson coefficients now carry an explicit dependence on the renormalization scale μ which has to cancel out with the renormalization scale dependence of the effective operators, since the full amplitude does not depend on μ

$$0 = \frac{\mathrm{d}}{\mathrm{d}\log\mu}\mathcal{A} = \frac{\mathrm{d}C_i(\mu)}{\mathrm{d}\log\mu}\langle Q_i(\mu)\rangle + C_i(\mu)\frac{\mathrm{d}\langle Q_i(\mu)\rangle}{\mathrm{d}\log\mu}. \tag{3.23}$$

Here $Q_i(\mu)$ are the renormalized composite operators defined in dimensional regularization and the $\overline{\mathrm{MS}}$ scheme, while $C_i(\mu)$ are the corresponding renormalized Wilson coefficients.

What we need to find is the dependence on the renormalization scale of the composite operators.

3.4.1 Renormalization of the Effective Operators

At any order, the basis of effective operators $\{Q_i\}_{i=1,\cdots,n}$ can be renormalized in the usual way, as discussed in section 2.4, by allowing however that the operators can mix under renormalization

$$Q_{i,B} = \sum_{j=1}^{n} Z_{ij}(\mu)Q_j(\mu). \tag{3.24}$$

Note that the renormalization constants Z_{ij} contain not only the renormalization factors absorbing the UV divergences of the loop corrections to the operator matrix elements, but even a wave-function renormalization factor $Z_q^{1/2}$ for every field contained in the composite operator.

Note that dimensional regularization rules out the possibility of operator mixing between operators of different dimensions. This is one of the reasons why dimensional regularization is the most convenient renormalization scheme in perturbation theory. Given that the bare operators in eq. (3.24) are independent on the renormalization scale, it follows that

$$\frac{\mathrm{d}Z_{ij}(\mu)}{\mathrm{d}\log\mu}Q_j(\mu) + Z_{ij}(\mu)\frac{\mathrm{d}Q_j(\mu)}{\mathrm{d}\log\mu} = 0 \tag{3.25}$$

which can be rearranged to give

$$\frac{\mathrm{d}Q_i(\mu)}{\mathrm{d}\log\mu} = -Z_{ij}^{-1}(\mu)\frac{\mathrm{d}Z_{jk}(\mu)}{\mathrm{d}\log\mu}Q_k(\mu) \equiv -\gamma_{ik}(\mu)Q_k(\mu), \tag{3.26}$$

where we defined the *anomalous dimension* matrix of the effective operator

$$\boldsymbol{\gamma}(\mu) = \mathbf{Z}^{-1}(\mu)\frac{\mathrm{d}\mathbf{Z}(\mu)}{\mathrm{d}\log\mu} = \frac{\mathrm{d}\log\mathbf{Z}}{\mathrm{d}\log\mu}. \tag{3.27}$$

Therefore, the renormalization scale dependence of the effective operator is governed by the Renormalization Group Equation (RGE) in terms of its anomalous dimension

$$\frac{\mathrm{d}\vec{\mathbf{Q}}(\mu)}{\mathrm{d}\log\mu} = -\boldsymbol{\gamma}\cdot\vec{\mathbf{Q}}(\mu). \tag{3.28}$$

In analogy with the mass anomalous dimension found in eq. (2.45), the anomalous dimension matrix of the effective operators can be obtained from the coefficients of the $1/\epsilon$ pole term in Z

$$\boldsymbol{\gamma} = -2\alpha_s \frac{\partial \mathbf{Z}^{(1)}}{\partial \alpha_s}. \tag{3.29}$$

3.4.2 Getting Rid of the Renormalization Scale

Now that the dependence on the renormalization scale of the effective operators is sorted out, we can get back to eq. (3.23). From that, we find that

$$\frac{\mathrm{d}C_i(\mu)}{\mathrm{d}\log\mu} Q_i(\mu) + C_i(\mu)\frac{\mathrm{d}Q_i(\mu)}{\mathrm{d}\log\mu} = \left[\frac{\mathrm{d}C_i(\mu)}{\mathrm{d}\log\mu}\delta_{ij} - C_i(\mu)\gamma_{ij}(\mu)\right] Q_j(\mu) = 0 \tag{3.30}$$

from which follows

$$\frac{\mathrm{d}\vec{\mathbf{C}}(\mu)}{\mathrm{d}\log\mu} = \boldsymbol{\gamma}^T(\mu)\vec{\mathbf{C}}(\mu). \tag{3.31}$$

This is the differential equation governing the RG evolution of the Wilson Coefficients. In order to solve this equation, we first need to change variable and express the scale dependence of the various quantities via the running QCD coupling $g(\mu)$. Given the definition of the beta function in eq. (2.45)

$$\frac{\mathrm{d}}{\mathrm{d}\log\mu} = \frac{\mathrm{d}g}{\mathrm{d}\log\mu}\frac{\mathrm{d}}{\mathrm{d}g} = \beta(g)\frac{\mathrm{d}}{\mathrm{d}g} \tag{3.32}$$

then

$$\frac{\mathrm{d}\vec{\mathbf{C}}(g(\mu))}{\mathrm{d}g} = \frac{\boldsymbol{\gamma}^T(g)}{\beta(g)} \cdot \vec{\mathbf{C}}(g(\mu)). \tag{3.33}$$

This can be solved by means of an integral evolution matrix U defined as

$$\vec{\mathbf{C}}(\mu) = \mathbf{U}(\mu, m) \cdot \vec{\mathbf{C}}(m) \tag{3.34}$$

which can be found iteratively

$$\mathbf{U}(\mu, m) = 1 + \int_{g(m)}^{g(\mu)} \mathrm{d}g_1 \frac{\boldsymbol{\gamma}^T(g_1)}{\beta(g_1)} + \int_{g(m)}^{g(\mu)} \mathrm{d}g_1 \int_{g(m)}^{g_1} \mathrm{d}g_2 \frac{\boldsymbol{\gamma}^T(g_1)}{\beta(g_1)}\frac{\boldsymbol{\gamma}^T(g_2)}{\beta(g_2)} + \cdots. \tag{3.35}$$

This is exactly the same solution as the Dyson series for the Schrödinger evolution matrix. In fact, eq. (3.33) has the exact same form as Schrödinger's equation, where $\boldsymbol{\gamma}^T/\beta$ takes the place of the Hamiltonian. The series expression can be put in a more compact form by introducing the notion of g-ordering

$$\mathbf{U}(\mu, m) = \mathrm{T}_g \exp\left[\int_{g(m)}^{g(\mu)} \mathrm{d}g' \frac{\boldsymbol{\gamma}^T(g')}{\beta(g')}\right]. \tag{3.36}$$

3.5 RG Improved Perturbation Theory

With the evolution matrix, we can now run down from the scale $\mu_W \sim M_W$ to a low renormalization scale μ_h closer to the physical scale at which the process we are interested in takes place

$$\vec{\mathbf{C}}(\mu_h) = \mathrm{T}_g \exp\left[\int_{g(\mu_h)}^{g(\mu_W)} \mathrm{d}g'\, \frac{\boldsymbol{\gamma}^T(g')}{\beta(g')}\right] \vec{\mathbf{C}}(\mu_W) \tag{3.37}$$

and then compute the relevant matrix elements without encountering large logs since at the scale $\mu_h \sim p_i \sim p_f$ the matrix element

$$\langle f(p_f)|\mathcal{H}_{\mathrm{eff}}|i(p_i)\rangle = C_i(\mu_h)\,\langle f(p_f)|Q_i|i(p_i)\rangle \tag{3.38}$$

is finite. But where have the large logs gone? They have been resummed by means of the renormalization group! Thus, the effective theory allows us to perform the matching using ordinary perturbation theory and then resum the large logs using the RGE. In general, if we expand the Wilson coefficients and the anomalous dimension matrix in powers of α_s

$$\vec{\mathbf{C}}(\mu) = \sum_{k=0}^{n}\left(\frac{\alpha_s}{4\pi}\right)^n \vec{\mathbf{C}}^{(n)}(\mu) \qquad \boldsymbol{\gamma} = \sum_{k=1}^{n}\left(\frac{\alpha_s}{4\pi}\right)^n \boldsymbol{\gamma}^{(0)} \tag{3.39}$$

then we can differentiate the perturbative expansion not on the order at which α_s appears, but on the orders resummed by the RGE.
A *leading order* (LO) calculation resums all terms of the form $\mathcal{O}\big(\alpha_s \log(M_W^2/-p^2)\big)^n$. In the LO case, we have that

$$\mathcal{A}_{\mathrm{LO}} = C_i^{(0)}(\mu_h)\langle Q(\mu_h)_i\rangle^{(0)}, \tag{3.40}$$

where $\langle Q \rangle^{(n)}$ denotes the matrix element computed at n-th order in strong interaction which are needed to do calculations, and

$$\vec{\mathbf{C}}^{(0)}(\mu_h) = \mathbf{U}^{(0)}(\mu_h, \mu_W)\vec{\mathbf{C}}^{(0)}(\mu_W) \qquad \mathbf{U}^{(0)}(\mu_h, \mu_W) = \left(\frac{\alpha_s(\mu_W)}{\alpha_s(\mu_h)}\right)^{\frac{\gamma^{(0)T}}{2\beta_0}}. \tag{3.41}$$

A *(next-to-)^m leading order* (N^{m}LO) calculation resums all terms of the form $\mathcal{O}\big(\alpha_s^{n+m}\log^n(M_W^2/(-p^2))\big)$. We now briefly discuss the general result for the NLO case [30]. At NLO we need to evaluate the full and the effective amplitude at $\mathcal{O}(\alpha_s)$

$$\mathcal{A}_{\mathrm{NLO}} = C^{(0)}(\mu_h)\langle Q(\mu_h)\rangle^{(1)} + \frac{\alpha_s(\mu_h)}{4\pi}C^{(1)}(\mu_h)\langle Q(\mu_h)\rangle^{(0)}, \tag{3.42}$$

where again

$$\vec{\mathbf{C}}^{(1)}(\mu_h) = \mathbf{U}(\mu_h, \mu_W)\vec{\mathbf{C}}^{(1)}(\mu_W). \tag{3.43}$$

To this order, the evolution matrix is given by [39]

$$\mathbf{U}^{(1)}(\mu, m) = \left(\mathbb{1} + \frac{\alpha_s(\mu)}{2\pi}\mathbf{J}\right)\mathbf{U}^{(0)}(\mu, m)\left(\mathbb{1} - \frac{\alpha_s(m)}{2\pi}\mathbf{J}\right), \tag{3.44}$$

where $\mathbf{U}^{(0)}$ is the leading order evolution matrix of eq. (3.41). The matrix $\mathbf{J}$ contains the informations about the next-to-leading order corrections. By means of the expansion of the anomalous dimension matrix in eq. (3.39), we define the $\mathbf{J}$ matrix starting from diagonalizing the tree-level anomalous dimension

$$\boldsymbol{\gamma}_D^{(0)} = \mathbf{V}^{-1}\boldsymbol{\gamma}^{(0)T}\mathbf{V}. \tag{3.45}$$

This transformation makes the LO evolution matrix diagonal as well. Then, if we define the following matrix

$$\mathbf{G} = \mathbf{V}^{-1}\boldsymbol{\gamma}^{(1)T}\mathbf{V} \tag{3.46}$$

and another matrix whose elements are

$$H_{ij} = \delta_{ij}\left(\gamma_D^{(0)}\right)_{ij}\frac{\beta_1}{2\beta_0^2} - \frac{G_{ij}}{2\beta_0 + \left(\gamma_D^{(0)}\right)_{ii} - \left(\gamma_D^{(0)}\right)_{jj}} \tag{3.47}$$

the matrix $\mathbf{J}$ is given by

$$\mathbf{J} = \mathbf{V}\mathbf{H}\mathbf{V}^{-1}. \tag{3.48}$$

There is still an important thing to note. From the basic idea of an EFT, whenever we go below some energy threshold, heavy degrees of freedom have to be integrated out. Therefore, what happens when we evolve the Wilson coefficients from the scale of M_W to the scale of m_b, and then we go even below to the scale of m_c and so on? One after the other, quarks become heavy and have to be integrated out. To account for this we need to include a threshold matrix. Following the same principle as in the case of integrating out the W boson, we require that at the scale of the transition μ_t

$$\vec{\mathbf{C}}_f^T(\mu_t)\langle\vec{\mathbf{Q}}_f(\mu_t)\rangle = \vec{\mathbf{C}}_{f-1}^T(\mu_t)\langle\mathbf{Q}_{f-1}(\mu_t)\rangle, \tag{3.49}$$

where f is the number of active flavours, which changes from f to $f-1$ in the transition.

This behaviour can be encompassed in a new evolution matrix which contains a suitable matching matrix $\mathbf{T}$ [53]

$$\mathbf{U}(\mu, M_W) = \mathbf{U}_4(\mu, m_b)\mathbf{T}\mathbf{U}_5(m_b, M_W), \tag{3.50}$$

where $\vec{\mathbf{U}}_f$ is the evolution matrix with f active flavours and

$$\mathbf{T} = \mathbb{1} + \frac{\alpha_s(m_b)}{4\pi}\delta\mathbf{r}^T. \tag{3.51}$$

Equation (3.51) is valid when only strong corrections are present. We will see later the generalization when electroweak corrections are added.

3.6 Electroweak Corrections

We give now a brief summary of the general results that one gets when adding not only strong corrections but electroweak ones. These corrections enter in Penguin-like operators [139, 140] at leading order. When EM corrections are added, the anomalous dimension matrix at NLO will have the form

$$\gamma = \frac{\alpha_s}{4\pi}\gamma_s^{(0)} + \frac{\alpha_e}{4\pi}\gamma_e^{(0)} + \left(\frac{\alpha_s}{4\pi}\right)^2\gamma_s^{(1)} + \frac{\alpha_e}{4\pi}\frac{\alpha_s}{4\pi}\gamma_{se}^{(1)}, \tag{3.52}$$

where we ignored α_e^2 corrections. Even the evolution matrix will contain corrections of order α_e

$$\mathbf{U}^{(1)}(\mu, m) = \mathbf{M}(\mu)\mathbf{U}^{(0)}(\mu, m)\mathbf{M}'(m), \tag{3.53}$$

where

$$
\begin{aligned}
\mathbf{M}(\mu) &= \left(\mathbb{1} + \frac{\alpha_e}{4\pi}\mathbf{K}\right)\left(\mathbb{1} + \frac{\alpha_s(\mu)}{4\pi}\mathbf{J}\right)\left(\mathbb{1} + \frac{\alpha_e}{\alpha_s(\mu)}\mathbf{P}\right), \\
\mathbf{M}'(m) &= \left(\mathbb{1} - \frac{\alpha_e}{\alpha_s(m)}\mathbf{P}\right)\left(\mathbb{1} - \frac{\alpha_s(m)}{4\pi}\mathbf{J}\right)\left(\mathbb{1} - \frac{\alpha_e}{4\pi}\mathbf{K}\right),
\end{aligned}
\tag{3.54}
$$

where the running of α_e is not considered. The matrices $\mathbf{K}, \mathbf{J}$ and $\mathbf{P}$ are solutions of the equations [52, 53]

$$\mathbf{P} + \left[\mathbf{P}, \frac{\boldsymbol{\gamma}_s^{(0)T}}{2\beta_0}\right] = \frac{\boldsymbol{\gamma}_e^{(0)T}}{2\beta_0}, \tag{3.55}$$

$$\mathbf{J} - \left[\mathbf{J}, \frac{\boldsymbol{\gamma}_s^{(0)T}}{2\beta_0}\right] = \frac{\beta_1}{2\beta_0^2}\boldsymbol{\gamma}_s^{(0)T} - \frac{\boldsymbol{\gamma}_s^{(1)T}}{2\beta_0}, \tag{3.56}$$

$$\left[\mathbf{K}, \boldsymbol{\gamma}_s^{(0)T}\right] = \boldsymbol{\gamma}_e^{(1)T} + \boldsymbol{\gamma}_e^{(0)T}\mathbf{J} + \boldsymbol{\gamma}_s^{(1)T}\mathbf{P} + \left[\boldsymbol{\gamma}_s^{(0)T}, \mathbf{JP}\right] - 2\beta_1\mathbf{P} - \frac{\beta_1}{\beta_0}\mathbf{P}\boldsymbol{\gamma}_s^{(0)T}. \tag{3.57}$$

Besides the more complicated analytical form of the expressions, the theory stays the same. Once we have the evolution matrix, if we cross a quark mass threshold we need the matching matrix, which in the case of QED+QCD corrections is given by

$$\mathbf{T} = \mathbb{1} + \frac{\alpha_s(\mu)}{4\pi}\delta\mathbf{r}^T + \frac{\alpha_e}{4\pi}\delta\mathbf{s}^T, \tag{3.58}$$

where the nature of the two matrices $\delta\mathbf{r}$ and $\delta\mathbf{s}$ is given by the matching condition at the threshold scale.

Contributions from the Z^0 boson must also be added, but the general form of the solutions given up to now stays the same.

Chapter 4

$\Delta F = 1$ & $\Delta F = 2$ Effective Hamiltonians and Kaon Decays

Using the techniques highlighted in the previous chapter of the OPE and the RGE improved perturbation theory, we are now ready to apply them to the more specific case of $\Delta F = 1$ and $\Delta F = 2$ processes. These two effective theories will describe the non leptonic decays of mesons like K, D, B mesons, and in the case of the $\Delta F = 2$ the oscillation of the neutral mesons such as $K^0 - \bar{K}^0$, $B_d - \bar{B}_d$ and so on.

We will mostly concentrate on the ΔS processes since they are the relevant ones to study the direct and indirect CP-violation in the Kaon system, but the discussion can be easily generalized to different mesons. In particular, we will focus on the following

- The $K \to 2\pi$ decays, a $\Delta S = 1$ process, where at the quark level the relevant transition is $\bar{s}u \to \bar{u}d$. This is the process that governs direct CP-violation.

- The $K^0 - \bar{K}^0$ oscillation, a $\Delta S = 2$ process. This is the process that governs indirect CP-violation.

The discussion of the phenomenology of CP-violation in the Kaon system will be given in the subsequent chapter.

4.1 Effective Hamiltonian for $\Delta S = 1$ Processes

As stated in the previous chapter, when we want to analyze low energy processes, due to the appearance of large-logs in the perturbative expansion, we employ the toolkit of effective Hamiltonians.

Consider the process of $K \to 2\pi$. At tree-level the interactions is mediated by a W-boson exchange with a typical energy of the order $k^2 \sim \mathcal{O}(m_K)$. Therefore, the OPE in this case gives

$$\frac{ig_2^2}{4(k^2 - M_W^2)} V_{us}^* V_{ud} [\bar{v}_s \gamma^\mu (1 - \gamma_5) u_u][\bar{u}_u \gamma_\mu (1 - \gamma_5) v_d] = -i\frac{G_F}{\sqrt{2}} V_{us}^* V_{ud} Q_2 + \mathcal{O}\left(\frac{k^2}{M_W^2}\right)$$

$$(4.1)$$

where we find the first effective, current-current, operator

$$Q_2 = \bar{s}_L^i \gamma^\mu u_L^i \bar{u}_L^j \gamma_\mu d_L^j. \tag{4.2}$$

We wrote explicitly how the color indices are summed for reasons that will be obvious in a moment.

After this, we might also need to consider QCD corrections which will enlarge the operator basis. When we do so, we need to evaluate the Feynman diagrams in perturbation theory, both in the full and effective theory as shown, at first order in α_s in fig. (4.1).

One might then think that once these diagrams are taken into account, then there would not be any others. But the reality is that another class of operators needs to be considered, the so-called *penguin operators* [130, 138]. These diagrams play a central role particularly for ϵ'/ϵ and can be mainly divided into three categories: gluonic penguins, electroweak penguins, and magnetic penguins. We will see later in more detail the operators that are generated by such diagrams.

4.1.1 Current-Current Operators

There are two current-current operators. The first one is the operator of eq. (4.2). The fact that is called Q_2 instead of Q_1 is just a convention.

The second current-current operator is generated by the diagrams in fig (4.1), and we will give now the explicit computation. The diagrams we need to consider are just (4.1g) and (4.1h), with their mirror diagrams, since diagram (4.1f), and its mirror, cancel against the renormalization constant of the quark field.

To study the generation of the new operator, we just need to analyze the Dirac structure of the diagram. If we consider all external quark momenta to be zero[1] then the diagram (4.1g) gives in dimensional regularization

$$i\mathcal{A}_g = \frac{4G_F}{\sqrt{2}} V_{us}^* V_{ud} \int \frac{\mathrm{d}^d\ell}{(2\pi)^d} \bar{u}_i^u \Big(ig_s\gamma_\mu t_{ij}^{\mathrm{a}}\Big) \frac{i\slashed{\ell}}{\ell^2} \gamma_\rho P_L v_j^d \bar{v}_k^s \gamma^\rho P_L \frac{i\slashed{\ell}}{\ell^2} \Big(ig_s\gamma_\nu t_{kl}^{\mathrm{b}}\Big) u_l^u \frac{-ig^{\mu\nu}\delta^{\mathrm{ab}}}{\ell^2}, \tag{4.3}$$

where we used the shorthand notation $P_{L/R} = (1 \pm \gamma_5)/2$. Given that $\slashed{\ell}\Gamma\slashed{\ell} = \ell^2/d \gamma^\alpha \Gamma \gamma_\alpha$ since there are no other scales involved, we can take out the Dirac structure

$$-i\frac{4G_F}{\sqrt{2}} \frac{g_s^2}{d} \mu^{4-d} t_{ij}^{\mathrm{a}} t_{kl}^{\mathrm{a}} \Big(\bar{u}_i^u \gamma_\mu \gamma_\alpha \gamma_\rho P_L v_j^d\Big)\Big(\bar{v}_k^s \gamma^\rho P_L \gamma^\alpha \gamma^\mu u_t^u\Big) \int \frac{\mathrm{d}^d\ell}{(2\pi)^d} \frac{1}{\ell^4}. \tag{4.4}$$

We need to manipulate the Dirac structure a bit and to do so we will heavily use the Fierz identities [68, 133] which are just a fancy way of expanding the Dirac algebra on the basis of the matrices $P_L, P_R, \gamma^\nu P_L, \gamma^\nu P_R, \sigma^{\mu\nu}$. In fact, take the following structure

$$P_L v_j^d \bar{v}_k^s \gamma^\rho P_L = P_L v_j^d \bar{v}_k^s P_R \gamma^\rho \implies (P_L v_j^d \bar{v}_k^s P_R)_{\alpha\beta} \tag{4.5}$$

where the equality follows from the Clifford algebra of the γ_5 and we made explicit the Dirac indices. Not considering the γ^ρ, we can project it on the $\gamma^\nu P_R$ element by

---

[1]This will introduce an additional IR divergence which we just ignore since this can be done at the level of accuracy (LO) at which we are working.
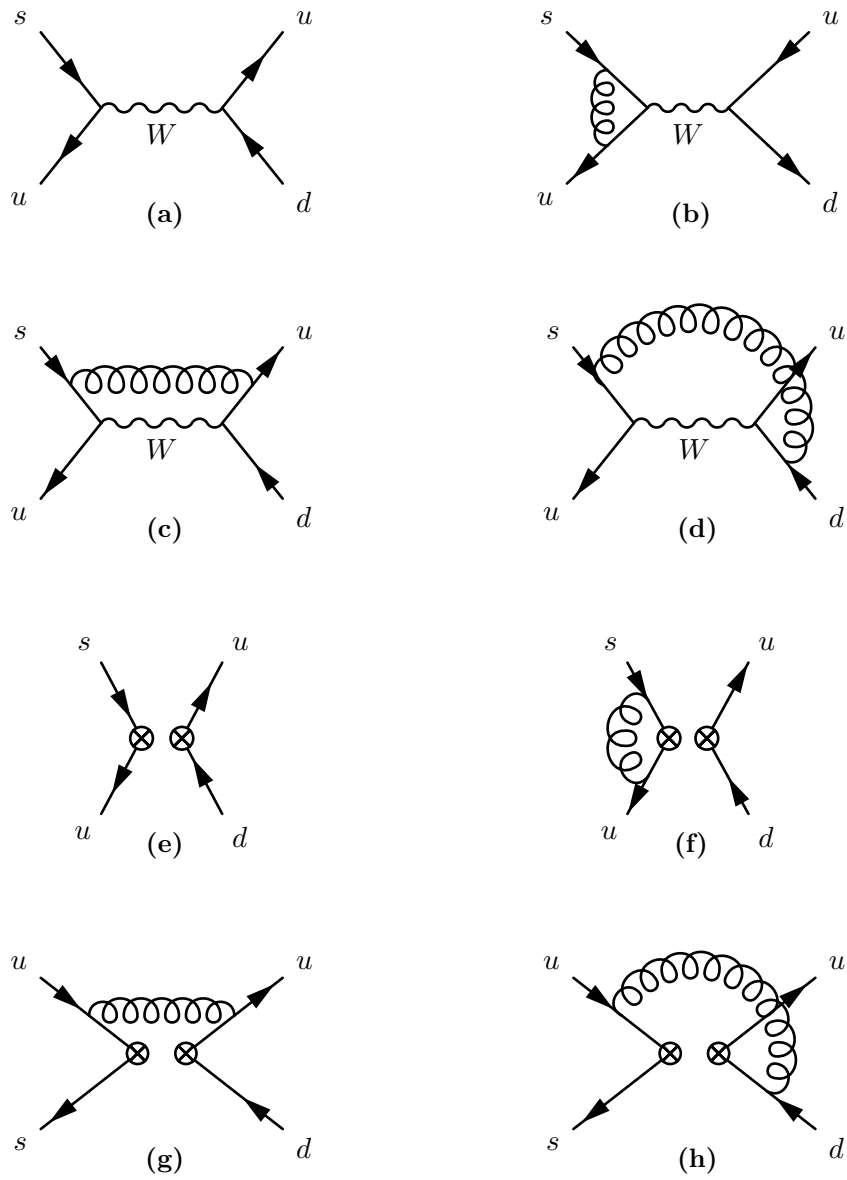
Figure 4.1. Relevant current-current Feynman diagrams for the $s \to \bar{u}u\bar{d}$ process in the full and effective theory up to $\mathcal{O}(\alpha_s)$.

using the trace

$$\frac{1}{2}\operatorname{Tr}\left(\gamma^\nu P_L P_L v_j^d \bar{v}_k^s P_R\right) = \frac{1}{2}\operatorname{Tr}\left(\gamma^\nu P_L v_j^d \bar{v}_k^s P_R\right) = \frac{1}{2}\operatorname{Tr}\left(P_R \gamma^\nu P_L v_k \bar{v}_k^s\right)$$
$$= -\frac{1}{2}\bar{v}_k^s P_R \gamma^\nu P_L v_j^d, \tag{4.6}$$

which simply follows from the usual rules for projectors and the anticommuting spinors. Therefore

$$(P_L v_j \bar{v}_k^s P_R)_{\alpha\beta} = -\frac{1}{2}\bar{v}_k^s \gamma^\nu P_L v_j^d (\gamma_\nu P_R)_{\alpha\beta}. \tag{4.7}$$

If we put this in the spinor structure of eq. (4.4) we obtain

$$\left(\bar{u}_i^u \gamma_\mu \gamma_\alpha \gamma_\rho P_L v_j^d\right)(\bar{v}_k^s \gamma^\rho P_L \gamma^\alpha \gamma^\mu u_t^u)$$
$$= -\frac{1}{2}\bar{v}_k^s \gamma^\beta P_L v_j^d \, \bar{u}_i^u \gamma_\mu \gamma_\alpha \gamma_\rho \gamma^\beta P_R \gamma^\rho \gamma^\alpha \gamma^\mu u_l^u \tag{4.8}$$
$$= -\frac{1}{2}\bar{v}_k^s \gamma^\beta P_L v_j^d \, \bar{u}_i^u \gamma_\mu \gamma_\alpha \gamma_\rho \gamma^\beta \gamma^\rho \gamma^\alpha \gamma^\mu P_L u_l^u$$

where we can now use the usual rules for the d-dimensional gamma matrices

$$\gamma_\mu \gamma_\alpha \underbrace{\gamma_\rho \gamma^\beta \gamma^\rho}\, \gamma^\alpha \gamma^\mu = (2-d)\gamma_\mu \underbrace{\gamma_\alpha \gamma^\beta \gamma^\alpha}\, \gamma^\mu$$
$$= (2-d)^2 \gamma_\alpha \gamma^\beta \gamma^\alpha = (2-d)^3 \gamma^\beta \tag{4.9}$$

to get

$$\left(\bar{u}_i^u \gamma_\mu \gamma_\alpha \gamma_\rho P_L v_j^d\right)(\bar{v}_k^s \gamma^\rho P_L \gamma^\alpha \gamma^\mu u_t^u) = -\frac{(2-d)^3}{2}\bar{v}_k^s \gamma^\beta P_L v_j^d \bar{u}_i^u \gamma_\beta P_L u_l^u$$
$$= -\frac{(2-d)^3}{2}\bar{v}_k^s \gamma^\beta \left(P_L v_j^d \bar{u}_i^u P_R\right)\gamma_\beta u_l^u. \tag{4.10}$$

Since the order of the spinors is inverted with respect to Q_2 we can again use the Fierz trick for the bracketed quantity, obtaining

$$\frac{(2-d)^3}{4}\bar{u}_i^u \gamma_\mu P_L v_j^d \bar{v}_k^s \gamma^\beta \gamma^\mu P_R \gamma_\beta u_l^u = \frac{(2-d)^4}{4}\left(\bar{u}_i^u \gamma_\mu P_L v_j^d\right)(\bar{v}_k^s \gamma^\mu P_L u_l^u) \tag{4.11}$$

henceforth the relevant Dirac structure is back to being

$$\bar{u}_i^u \gamma_\mu P_L v_j^d \bar{v}_k^s \gamma^\mu P_L u_l^u. \tag{4.12}$$

But now comes the important step: the presence of the gluon added an additional $SU(N)$ generator structure that we need to take into account. As we see in eq. (4.4) we have

$$t_{ij}^a t_{kl}^a = \frac{1}{2}\left(\delta_{il}\delta_{jk} - \frac{1}{N}\delta_{ij}\delta_{kl}\right) \tag{4.13}$$

which mixes the color structure of the operator in eq. (4.12) and creates a new operator with the same Dirac structure but mixed color structure

$$t_{ij}^a t_{kl}^a \bar{u}_i^u \gamma_\mu P_L v_j^d \bar{v}_k^s \gamma^\mu P_L u_l^u = \bar{u}_i^u \gamma_\mu P_L v_j^d \bar{v}_j^s \gamma^\mu P_L u_i^u - \frac{1}{N}\bar{u}_i^u \gamma^\mu P_L v_i^d \bar{v}_j^s \gamma_\mu P_L u_j^u$$
$$= \langle Q_1 \rangle - \frac{1}{N}\langle Q_2 \rangle. \tag{4.14}$$

This makes it clear why before we made the color structure of Q_2 evident. The diagram has generated another operator which needs to be considered for the renormalization procedure. Doing a similar calculation for diagram (4.1h) gives the same answer but obviously with a different divergent behaviour due to the loop integral and the different Fierz.

Therefore we have two current-current operators

$$Q_1 = \bar{s}_L^i \gamma^\mu u_L^j \bar{u}_L^j \gamma_\mu d_L^i, \qquad Q_2 = \bar{s}_L^i \gamma^\mu u_L^i \bar{u}_L^j \gamma_\mu d_L^j. \tag{4.15}$$

4.1.2 Wilson Coefficients and Renormalization

Before we did not evaluate the integral of diagram (4.1g) since we only needed to control the Dirac structure to find the new effective operator. If we then want to find the Wilson coefficients and the anomalous dimension matrix for the RGE, we need to evaluate the various loop integrals, find the $1/\epsilon$ poles do to the OPE and then match the full and effective theory for the Wilson coefficients.

This is a tremendous task when one takes into account all possible operators since, as we will see later, there are not only current-current ones. Fortunately, the theory for these calculations has been carried out many times before even at NLO including also electromagnetic corrections [30, 39, 53] in the two different regularization schemes NDR and HV. NNLO calculations are also available [33, 80]. Therefore we give here only a summary of the main results with some simple pedagogical calculations.

Where we left off for diagram (4.1g) was, beside the spinors,

$$-i\frac{4G_F}{\sqrt{2}} V_{us}^* V_{ud} g_s^2 \frac{\mu^{4-d}}{8} \frac{(2-d)^4}{d} \int \frac{\mathrm{d}^d\ell}{(2\pi)^d} \frac{1}{\ell^4}. \tag{4.16}$$

As we know, the integral vanishes in dimensional regularization, but this is only an artifact of the fact that we chose the external quarks to have zero momentum. Therefore, to solve this integral, as we did in eq. (2.32), we introduce a fictious scale and solve the integral with it. After we do so, we set $d = 4 - 2\epsilon$ to get, beside the $4G_F V_{us}^* V_{ud}/\sqrt{2}$ factors,

$$-\frac{i}{8} \left(\frac{4\pi\mu^2}{m^2}\right)^\epsilon \frac{(2\epsilon - 2)^4}{4 - 2\epsilon} \frac{i}{(4\pi)^2} g_s^2 \Gamma(\epsilon), \tag{4.17}$$

which in the limit of $\epsilon \to 0$

$$\left(\frac{4\pi\mu^2}{m^2}\right)^\epsilon = 1 + \epsilon \log\left(\frac{4\pi\mu^2}{m^2}\right) + \mathcal{O}\left(\epsilon^2\right)$$

$$\Gamma(\epsilon) = \frac{1}{\epsilon} + \psi(1) + \frac{\epsilon}{2}\left[\frac{\pi^2}{3} + \psi^2(1) - \psi'(1)\right] + \mathcal{O}\left(\epsilon^2\right) \tag{4.18}$$

$$\frac{(2\epsilon - 2)^4}{4 - 2\epsilon} = 4 - 14\epsilon + \mathcal{O}\left(\epsilon^2\right),$$

eq. (4.17) becomes[2]

$$\frac{\alpha_s}{4\pi}\left[\frac{1}{2\epsilon} - 14 + 4\log\left(\frac{4\pi\mu^2 e^{-\gamma}}{m^2}\right)\right.$$
$$\left. + \epsilon\left[(-14 - 4\gamma)\log\left(\frac{4\pi\mu^2}{m^2}\right) + \frac{2\pi^2}{3} - 2\gamma^2 - 2\psi'(1)\right]\right] + \mathcal{O}\left(\epsilon^2\right). \tag{4.19}$$

Retrieving only the $1/\epsilon$ pole we get that the divergent part of the diagram (4.1g) is

$$i\mathcal{A}_g = \frac{4G_F}{\sqrt{2}}V_{us}^*V_{ud}\frac{\alpha_s}{4\pi}\frac{1}{2\epsilon}\left(Q_1 - \frac{1}{3}Q_2\right), \tag{4.20}$$

where we set $N = 3$.

We can do a similar calculation for diagram (4.1h) that reads

$$i\mathcal{A}_h = \frac{4G_F}{\sqrt{2}}V_{us}^*V_{ud}\int\frac{\mathrm{d}^d\ell}{(2\pi)^d}\bar{u}_i^u\gamma_\mu P_L\frac{i\slashed{\ell}}{\ell^2}\left(ig_s t_{ij}^{\mathrm{a}}\gamma_\beta\right)v_j^d\bar{v}_k^s\gamma^\mu P_L\frac{i\slashed{\ell}}{\ell^2}\left(ig_s t_{kl}^{\mathrm{b}}\gamma_\alpha\right)u_t^u\frac{-ig^{\alpha\beta}\delta^{\mathrm{ab}}}{\ell^2}. \tag{4.21}$$

Under the usual simplifications, we get

$$-i\frac{4G_F}{\sqrt{2}}V_{us}^*V_{ud}\frac{g_s^2}{d}\mu^{4-d}t_{ij}^{\mathrm{a}}t_{kl}^{\mathrm{a}}\left(\bar{u}_i^u\gamma_\mu P_L\gamma_\rho\gamma_\beta v_j^d\right)\left(\bar{v}_k^s\gamma^\mu P_L\gamma^\rho\gamma^\beta u_t^u\right)\int\frac{\mathrm{d}^d\ell}{(2\pi)^d}. \tag{4.22}$$

Proceeding on with the Dirac structure simplification, which is a bit more involved in this case when dealing with d-dimensional Clifford algebra, we get

$$\bar{u}_i^u\gamma_\mu\gamma_\rho\gamma_\beta\left(P_L v_j^d\bar{v}_k^s P_R\right)\gamma^\mu\gamma^\rho\gamma^\beta u_t^u$$
$$= -\frac{1}{2}\bar{v}_k^s\gamma^\alpha P_L v_j^d\bar{u}_i^u\underbrace{\gamma_\mu\gamma_\rho\gamma_\beta\gamma_\alpha\gamma^\mu}\gamma^\rho\gamma^\beta P_L u_t^u \tag{4.23}$$
$$= \bar{v}_k^s\gamma^\alpha P_L v_j^d\bar{u}_i^u\gamma_\alpha\gamma_\beta\gamma_\rho\gamma^\rho\gamma^\beta P_L u_t^u + \frac{(d-4)}{2}\bar{v}_k^s\gamma^\alpha P_L v_j^d\bar{u}_i^u\gamma_\rho\gamma_\beta\gamma_\alpha\gamma^\rho\gamma^\beta P_L u_t^u.$$

The first bit becomes

$$\bar{v}_k^s\gamma^\alpha P_L v_j^d\bar{u}_i^u\gamma_\alpha\underbrace{\gamma_\beta\gamma_\rho\gamma^\rho\gamma^\beta}P_L u_t^u$$
$$= d^2\bar{v}_k^s\gamma^\alpha\left(P_L v_j^d\bar{u}_i^u P_R\right)\gamma_\alpha u_t^u = -\frac{d^2}{2}\bar{u}_i^u\gamma^\mu P_L v_j^d\bar{v}_k^s\gamma^\alpha\gamma_\mu P_R\gamma_\alpha u_t^u \tag{4.24}$$
$$= -\frac{d^2(2-d)}{2}\left(\bar{u}_i^u\gamma^\mu P_L v_j^d\right)(\bar{v}_k^s\gamma_\mu P_L u_t^u),$$

while the second bit

$$\frac{(d-4)}{2}\bar{v}_k^s\gamma^\alpha P_L v_j^d\bar{u}_i^u\underbrace{\gamma_\rho\gamma_\beta\gamma_\alpha\gamma^\rho}\gamma^\beta P_L u_t^u$$
$$= \frac{(d-4)^2}{2}\bar{v}_k^s\gamma^\alpha P_L v_j^d\bar{u}_i^u\gamma_\beta\gamma_\alpha\gamma^\beta P_L u_t^u + 2(d-4)\bar{v}_k^s\gamma^\alpha P_L v_j^d\bar{u}_i^u\gamma_\alpha P_L u_t^u \tag{4.25}$$
$$= -\left[\frac{(d-4)^2(2-d)^2}{4} - (d-4)(2-d)\right]\left(\bar{u}_i^u\gamma_\mu P_L v_j^d\right)(\bar{v}_k^s\gamma^\mu P_L u_t^u).$$

---

[2]The scale m^2 is not physical. When taking the limit $m^2 \to 0$ to get beck to the original result, we find another divergence which is the IR divergence noted before due to the zero quark momenta.

Therefore the whole expression becomes

$$- \left[\frac{d^2(2-d)}{2} + \frac{(d-4)^2(2-d)^2}{4} - (d-4)(2-d) \right] \left(\bar{u}_i^u \gamma_\mu P_L v_j^d \right) \left(\bar{v}_k^s \gamma^\mu P_L u_t^u \right). \quad (4.26)$$

When taking into account the $1/d$ factor from the amplitude in eq. (4.22) and substituting $d = 4 - 2\epsilon$, we obtain

$$\frac{-4(\epsilon-1)^2(\epsilon^2 + \epsilon - 4)}{4 - 2\epsilon} = 16 - 36\epsilon + \mathcal{O}\left(\epsilon^2\right). \quad (4.27)$$

Taking only the $1/\epsilon$ pole in eq. (4.22) together with the previous expansion, we find

$$\frac{4G_F}{\sqrt{2}} V_{us}^* V_{ud} \frac{\alpha_s}{4\pi} (-2) \frac{1}{\epsilon} \left(Q_1 - \frac{1}{N} Q_2 \right). \quad (4.28)$$

Summing the contribution from diagrams (4.1g) and (4.1h) with their mirrors, we get the final amplitude

$$i\mathcal{A} = \frac{4G_F}{\sqrt{2}} V_{us}^* V_{ud} \frac{\alpha_s}{4\pi} \frac{-3}{\epsilon} \left(Q_1 - \frac{1}{N} \right) Q_2. \quad (4.29)$$

In order to compute the two-by-two anomalous dimension matrix, we need to compute the one-loop renormalization of the operator Q_1 inserting it in diagrams (4.1g) and (4.1h) and their mirrors. The only difference between this and the ones evaluated before for Q_1 is the color structure given by the $SU(N)$ generators being

$$t_{il}^a t_{kj}^a = \frac{1}{2} \left(\delta_{ij} \delta_{kl} - \frac{1}{N} \delta_{il} \delta_{kj} \right). \quad (4.30)$$

It is clear that this does not generate other operators, therefore if we consider only current-current operators, the discussion ends here. With this, we renormalize the operators as prescribed in eq. (3.24) to obtain, in the $\overline{\text{MS}}$ scheme,

$$\mathbf{Z} = \mathbb{1} + \frac{\alpha_s}{4\pi} \mathbf{Z}_1 = \mathbb{1} + \frac{\alpha_s}{4\pi} \frac{1}{\epsilon} \begin{pmatrix} 3/N & -3 \\ -3 & 3/N \end{pmatrix}, \quad (4.31)$$

which gives the following anomalous dimension matrix, from its definition in eq. (3.27)

$$\boldsymbol{\gamma}^{(0)} = \begin{pmatrix} -6/N & 6 \\ 6 & -6/N \end{pmatrix}. \quad (4.32)$$

In this simple case, the evolution matrix can be found by diagonalizing the anomalous dimension, defining

$$Q_\pm = \frac{Q_1 \pm Q_2}{2}, \quad C_\pm = C_1 \pm C_2, \quad \gamma_\pm^{(0)} = \pm 6 \frac{N \mp 1}{N}, \quad (4.33)$$

therefore

$$U_0^\pm = \left(\frac{\alpha_s(\mu_W)}{\alpha_s(\mu_h)} \right)^{\gamma_\pm^{(0)}/2\beta_0}, \quad (4.34)$$

where $C_{1/2}$ are the Wilson coefficients which, at LO, are just $C_1 = 0$ and $C_2 = 1$. Note that, as we discussed before, β_0 depends on the number of active flavours which means that if we want to evaluate the Wilson coefficients at a scale $\mu_h \sim 2$ GeV we need to take into account the bottom quark threshold at a scale $\mu_b \sim m_b$

$$C_{\pm}(2 \text{ GeV}) = \left(\frac{\alpha_s(\mu_b)}{\alpha_s(2 \text{ GeV})} \right)^{\gamma_{\pm}^{(0)}/2\beta_0(4)} \left(\frac{\alpha_s(\mu_W)}{\alpha_s(2 \text{ GeV})} \right)^{\gamma_{\pm}^{(0)}/2\beta_0}. \tag{4.35}$$

At NLO the situation becomes more complicated. The anomalous dimension matrix needs to be evaluated at $\mathcal{O}(\alpha_s^2)$ and the Wilson coefficients start at

$$C_{\pm}(\mu_W) = 1 \pm \frac{\alpha_s(\mu_W)}{4\pi} 11 \frac{N \mp 1}{2N} \tag{4.36}$$

in the NDR scheme. A complete discussion can be found in [30, 53].

4.1.3 QCD Penguin Operators

Up until now, we found that the effective Hamiltonian for the $\Delta S = 1$ processes, like the decay $K \to 2\pi$, is built up by two operators

$$\mathcal{H}_{\text{eff}}^{\bar{s} \to \bar{d}} = \frac{4G_F}{\sqrt{2}} V_{us}^* V_{ud}[C_1 Q_1 + C_2 Q_2]. \tag{4.37}$$

But looking at the quark content of the operators, it is clear that when evaluating their renormalization, additional diagrams arise from the contraction of the u and $\bar{u}$ fields in $Q_{1,2}$ by attaching a gluon, as seen in fig (4.2).
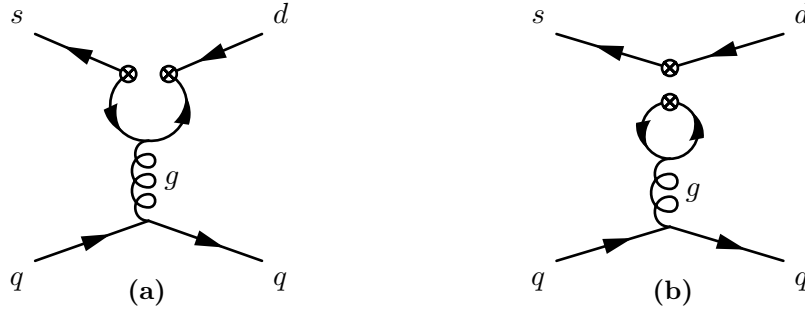
Figure 4.2. Effective QCD Penguins for the $\bar{s} \to \bar{d}$ transition.

The form of these operators can be easily found by considering that they are FCNC and therefore must be of the form $\bar{s}_i \Gamma^\mu t_{ij}^a d_j$ which cannot be generated at tree-level by the SM Lagrangian. If we take the momenta of the quark to be q, then the possible form of these operators must be

$$\bar{s}_i \Gamma^\mu t_{ij}^a d_j = A(q^2) \bar{s}_i \gamma^\mu t_{ij}^a d_j + B(q^2) \bar{s}_i q^\mu t_{ij}^a d_j + C(q^2) \bar{s}_i \sigma^{\mu\nu} q_\nu t_{ij}^a d_j. \tag{4.38}$$

Given that gauge invariance assures us that $q_\mu \bar{s}_i \Gamma^\mu t_{ij}^a d_j = 0$, we have that

$$A(q^2) \bar{s}_i \slashed{q} t_{ij}^a d_j + C(q^2) \bar{s}_i q^2 t_{ij}^a d_j = 0 \tag{4.39}$$

by choosing, without loss of generality, $A(q^2) = q^2$ and $B(q^2) = -\slashed{q}$, we have

$$\bar{s}_i \Gamma^\mu t^{\mathrm{a}}_{ij} d_j = \bar{s}_i \left(q^2 \gamma^\mu - \slashed{q} q^\mu \right) t^{\mathrm{a}}_{ij} d_j + C(q^2) \bar{s}_i \sigma^{\mu\nu} q_\nu t^{\mathrm{a}}_{ij} d_j. \tag{4.40}$$

The second operator connects spinors with different helicity and therefore must be proportional to the quark mass, so for massless quarks cannot be generated.

By using the equations of motion, we see that the first structure corresponds to the matrix elements of the operator $\bar{s}_i \gamma^\mu t^{\mathrm{a}}_{ij} d_j D^\nu G^{\mathrm{a}}_{\mu\nu}$, in fact

$$D^\nu G^{\mathrm{a}}_{\mu\nu} = g_s \sum_f \bar{q}^i_f \gamma_\mu t^{\mathrm{a}}_{ij} q^j_f \tag{4.41}$$

where f is any active quark flavour, gives

$$\bar{s}_i \gamma_\mu t^{\mathrm{a}}_{ij} d_j \sum_f \bar{q}^k_f \gamma^\mu t^{\mathrm{a}}_{kl} q^l_f. \tag{4.42}$$

Consider diagram (4.2a) with the insertion of the operator of eq. (4.40), roughly speaking

$$\bar{q}_f \gamma^\mu t^{\mathrm{a}} q_f \frac{1}{q^2} \bar{s} (q^2 \gamma_\mu - q_\mu \slashed{q}) t^{\mathrm{a}} d \tag{4.43}$$

since the quarks q_f carry momentum q, due to the equation of motion $q_\mu q_f = 0$, therefore there remain just

$$\bar{q}_f \gamma^\mu t^{\mathrm{a}} q_f \frac{1}{q^2} \bar{s} q^2 \gamma_\mu t^{\mathrm{a}} d, \tag{4.44}$$

where the q^2 cancels with the pole of the propagator, leaving just the matrix element of the local operator in eq. (4.42)

$$\bar{s} \gamma^\mu t^{\mathrm{a}} d \bar{q}_f \gamma_\mu t^{\mathrm{a}} q. \tag{4.45}$$

These diagrams are log-divergent which means that they need to be renormalized forcing us to enlarge the operator basis again. When inserting operators $Q_{1/2}$ in the effective vertex of the gluonic penguin a total of four more operators is generated

$$\begin{aligned}
Q_3 &= \bar{s}^i_L \gamma^\mu d^i_L \sum_f \bar{q}^j_{fL} \gamma_\mu q^j_{fL}, \\
Q_4 &= \bar{s}^i_L \gamma^\mu d^j_L \sum_f \bar{q}^j_{fL} \gamma_\mu q^i_{fL}, \\
Q_5 &= \bar{s}^i_L \gamma^\mu d^i_L \sum_f \bar{q}^j_{fR} \gamma_\mu q^j_{fR}, \\
Q_6 &= \bar{s}^i_L \gamma^\mu d^j_L \sum_f \bar{q}^j_{fR} \gamma_\mu q^i_{fR}.
\end{aligned} \tag{4.46}$$

As a matter of fact, we give a little computation to see how these operators are generated by considering the diagram (4.2a) with the insertion of operator Q_2 in

the effective vertex. Again we consider the external quark momenta to be zero and the momentum flowing in the gluon to be q.

$$
\begin{aligned}
i\mathcal{A} &= \int \frac{\mathrm{d}^d\ell}{(2\pi)^d} \bar{v}_i^d \gamma^\mu P_L \frac{i(\slashed{\ell} - \slashed{q})}{(\ell - q)^2} \Big(ig_s t_{ij}^{\mathrm{a}} \gamma^\alpha \Big) \frac{i\slashed{\ell}}{\ell^2} \gamma_\mu P_L v_j^s \bar{u}_k^q \Big(ig_s t_{kl}^{\mathrm{b}} \gamma^\beta \Big) u_l^q \frac{-ig_{\alpha\beta}\delta^{\mathrm{ab}}}{q^2} \\
&= -i\mu^{4-d} \frac{g_s^2}{q^2} \Big(\bar{v}_i^d \gamma^\mu P_L \gamma^\rho t_{ij}^{\mathrm{a}} \gamma^\alpha \gamma^\sigma \gamma_\mu P_L v_j^s \Big) \big(\bar{u}_k^q \gamma_\alpha t_{kl}^{\mathrm{a}} u_l^q \big) I_{\rho\sigma},
\end{aligned}
\tag{4.47}
$$

where the integral, without going into much details, is just

$$
I_{\rho\sigma} = -\frac{i}{16\pi^2} \left(\frac{g_{\rho\sigma}}{2} q^2 + q_\rho q_\sigma \right) \frac{1}{6\epsilon} + \mathcal{O}\big(\epsilon^0\big).
\tag{4.48}
$$

Putting this into the amplitude, we find, besides constant factors[3]

$$
\begin{aligned}
&\big(\bar{v}_i^d \gamma^\mu P_L \gamma^\rho t_{ij}^{\mathrm{a}} \gamma^\alpha \gamma^\sigma \gamma_\mu P_L v_j^s \big) \big(\bar{u}_k^q \gamma_\alpha t_{kl}^{\mathrm{a}} u_l^q \big) \left(\frac{g_{\rho\sigma}}{2} + q_\rho q_\sigma \right) \frac{1}{q^2} \\
&= \frac{1}{2} \bar{v}_i^d t_{ij}^{\mathrm{a}} \gamma^\mu P_L \left(\gamma^\rho \gamma^\alpha \gamma_\rho + 2\frac{\slashed{q}\gamma^\alpha \slashed{q}}{q^2} \right) \gamma_\mu P_L v_j^s \bar{u}_k^q \gamma_\alpha t_{kl}^{\mathrm{a}} u_l^q.
\end{aligned}
\tag{4.49}
$$

Given that $\gamma^\rho \gamma^\alpha \gamma_\rho = -2\gamma^\alpha$ and that $\gamma^\alpha \slashed{q} = \left\{ \gamma^\alpha, \slashed{q} \right\} - \slashed{q}\gamma^\alpha = 2q^\alpha - \slashed{q}\gamma^\alpha$, the parenthesis becomes

$$
\left(\gamma^\rho \gamma^\alpha \gamma_\rho + 2\frac{\slashed{q}\gamma^\alpha \slashed{q}}{q^2} \right) = -4(\gamma^\alpha - \frac{\slashed{q}q^\alpha}{q^2})
\tag{4.50}
$$

and therefore the Dirac structure is

$$
q^2 \bar{v}_i^d t_{ij}^{\mathrm{a}} \gamma^\mu P_L \big(q^2 \gamma^\alpha - q^\alpha \slashed{q} \big) \gamma_\mu P_L v_j^s \bar{u}_k^q \gamma_\alpha t_{kl}^{\mathrm{a}} u_l^q.
\tag{4.51}
$$

which gives back the FCNC vertex we conjectured earlier.

It is clear now that in the quark loop of the penguin diagram there can also run the charm quark, but not the top quark since it has been integrated out by the OPE. In the full theory even the top quark is present, but not in the low energy one. This means that we should add to the effective Hamiltonian for the $\bar{s} \to \bar{d}$ transition even the current-current operators with the charm quark, leading to

$$
\mathcal{H}_{\mathrm{eff}}^{\bar{s} \to \bar{d}} = \frac{4G_F}{\sqrt{2}} \left[V_{us}^* V_{ud} \big(C_1 Q_1^{\bar{s}u\bar{u}d} + C_2 Q_2^{\bar{s}u\bar{u}d} \big) + V_{cs}^* V_{cd} \big(C_1 Q_1^{\bar{s}c\bar{c}d} + C_2 Q_2^{\bar{s}c\bar{c}d} \big) \right].
\tag{4.52}
$$

When these operators are inserted into the penguin diagrams, they will give exactly the same divergent part since it does not depend on the mass of the quarks. Therefore the penguin diagram is going to be generated with a coefficient

$$
V_{us}^* V_{ud} + V_{cs}^* V_{cd} = -V_{ts}^* V_{td}
\tag{4.53}
$$

---

[3]For simplicity we go back to $d = 4$ since we just want to understand the Dirac structure.

due to the unitarity relation of the CKM matrix. All in all, the full effective Hamiltonian including current-current operators and QCD penguins becomes

$$
\mathcal{H}_{\text{eff}}^{\bar{s}\to\bar{d}} = \frac{4G_F}{\sqrt{2}} \left\{ V_{us}^* V_{ud} \left[C_1\left(Q_1^{\bar{s}u\bar{u}d} - Q_1^{\bar{s}c\bar{c}d}\right) + C_2\left(Q_2^{\bar{s}u\bar{u}d} - Q_2^{\bar{s}c\bar{c}d}\right) \right] \right.
$$
$$
\left. - V_{ts}^* V_{td} \left[Q_1^{\bar{s}c\bar{c}d} + C_2 Q_2^{\bar{s}c\bar{c}d} + \sum_{i=1}^{6} C_i Q_i^{\bar{s}d} \right] \right\},
\tag{4.54}
$$

where again the CKM unitarity has been used to eliminate the factor $V_{cs}^* V_{cd}$.

4.1.4 Wilson Coefficients and Renormalization

Since we have now a total of six operators, the RGE is governed by a 6×6 anomalous dimension matrix which has to be evaluated by inserting all the current-current as well as QCD penguin operators in diagrams (4.1e) to (4.1h) and in the penguin diagrams (4.2a) and (4.2b).

To perform the matching for the Wilson coefficients, one needs also to evaluate the full theory equivalent of the penguin diagram in fig. (4.3) where now even the top quark can run in the loop.
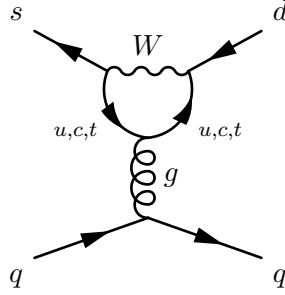
Figure 4.3. QCD penguin in the full theory.

At LO the anomalous dimension matrix $\boldsymbol{\gamma}^{(0)}$ has the explicit form [13, 70, 76, 84, 138]

$$
\boldsymbol{\gamma}^{(0)} = \begin{pmatrix}
\frac{-6}{N} & 6 & 0 & 0 & 0 & 0 \\
6 & \frac{-6}{N} & \frac{-2}{3N} & \frac{2}{3} & \frac{-2}{3N} & \frac{2}{3} \\
0 & 0 & \frac{-22}{3N} & \frac{22}{3} & \frac{-4}{3N} & \frac{4}{3} \\
0 & 0 & 6 - \frac{2f}{3N} & \frac{-6}{N} + \frac{2f}{3} & \frac{-2f}{3N} & \frac{2f}{3} \\
0 & 0 & 0 & 0 & \frac{6}{N} & -6 \\
0 & 0 & \frac{-2f}{3N} & \frac{2f}{3} & \frac{-2f}{3N} & \frac{-6(-1+N^2)}{N} + \frac{2f}{3}
\end{pmatrix},
\tag{4.55}
$$

while at NLO the second order expansion coefficient of the anomalous dimension

matrix reads [39, 53]

$$
\gamma^{(1)}\Big|_{N=3} =
$$

$$
\begin{pmatrix}
-\frac{21}{2} - \frac{2f}{9} & \frac{7}{2} + \frac{2f}{3} & \frac{79}{9} & -\frac{7}{3} & -\frac{65}{9} & -\frac{7}{3} \\
\frac{7}{2} + \frac{2f}{3} & -\frac{21}{2} - \frac{2f}{9} & -\frac{202}{243} & \frac{1354}{81} & -\frac{1192}{243} & \frac{904}{81} \\
0 & 0 & -\frac{5911}{486} + \frac{71f}{9} & \frac{5983}{162} + \frac{f}{3} & -\frac{2384}{243} - \frac{71f}{9} & \frac{1808}{81} - \frac{f}{3} \\
0 & 0 & \frac{379}{18} + \frac{56f}{243} & -\frac{91}{6} + \frac{808f}{81} & -\frac{130}{9} - \frac{502f}{243} & -\frac{14}{3} + \frac{646f}{81} \\
0 & 0 & \frac{-61f}{9} & \frac{-11f}{3} & \frac{71}{3} + \frac{61f}{9} & -99 + \frac{11f}{3} \\
0 & 0 & \frac{-682f}{243} & \frac{106f}{81} & -\frac{225}{2} + \frac{1676f}{243} & -\frac{1343}{6} + \frac{1348f}{81}
\end{pmatrix},
$$

$$\tag{4.56}$$

where f is the number of active quark flavours at the scale μ. Both matrices are given in the NDR scheme; the HV scheme results can be found in the sources just cited.

The fact that the top quark can run in the penguin loop in the full theory is fundamental since when performing the matching, one finds that the top quark contribution generates a non-trivial contribution to the $C_{3-6}(\mu_W)$ Wilson coefficients, while the contributions from u and c quarks cancels up to a constant and corrections of order p^2/M_W^2 [39, 96]. After matching, one finds the following Wilson coefficients at NLO

$$
\begin{aligned}
C_1\left(M_{\rm W}\right) &= \frac{11}{2} \frac{\alpha_{\rm s}\left(M_{\rm W}\right)}{4\pi}, \\
C_2\left(M_{\rm W}\right) &= 1 - \frac{11}{6} \frac{\alpha_{\rm s}\left(M_{\rm W}\right)}{4\pi}, \\
C_3\left(M_{\rm W}\right) &= -\frac{\alpha_{\rm s}\left(M_{\rm W}\right)}{24\pi} \widetilde{E}_0\left(x_t\right), \\
C_4\left(M_{\rm W}\right) &= \frac{\alpha_{\rm s}\left(M_{\rm W}\right)}{8\pi} \widetilde{E}_0\left(x_t\right) \\
C_5\left(M_{\rm W}\right) &= -\frac{\alpha_{\rm s}\left(M_{\rm W}\right)}{24\pi} \widetilde{E}_0\left(x_t\right), \\
C_6\left(M_{\rm W}\right) &= \frac{\alpha_{\rm s}\left(M_{\rm W}\right)}{8\pi} \widetilde{E}_0\left(x_t\right),
\end{aligned}
$$

$$\tag{4.57}$$

where

$$
\begin{aligned}
E_0(x) &= -\frac{2}{3}\log x + \frac{x(18 - 11x - x^2)}{12(1-x)^3} + \frac{x^2(15 - 16x + 4x^2)}{6(1-x)^4}\log x, \\
\tilde{E}_0(x) &= E_0(x) - \frac{2}{3}
\end{aligned}
$$

$$\tag{4.58}$$

with $x_t = m_t^2/M_W^2$. It is easy to see that coefficients C_{3-6} are directly related to the top quark as stated before.

4.1.5 Electroweak Penguin Operators
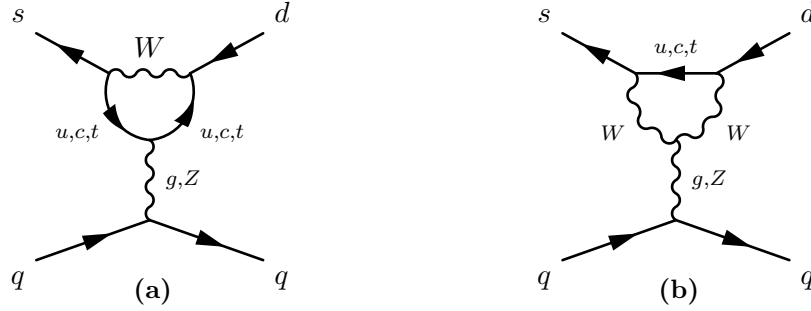
Figure 4.4. Electroweak penguin diagrams for the $\bar{s} \to \bar{d}$ process.

One may now ask the question of what would happen if the gluons in the QCD penguin diagrams of figs. (4.2) and (4.3) were to be replaced by a photon exchange. Then, electromagnetic corrections will also get log-enhanced making them comparable with the NLO-QCD corrections $\alpha \log(\mu_W^2/\mu_h^2) \sim \alpha_s$. These contributions do not need to be resummed but should be included when working with NLO-QCD [38, 53]. The relevant diagrams that we need to consider when dealing with EW contributions are given in fig. (4.4a).

When introducing also EW contributions, the operator basis needs to be enlarged again. While FCNC of diagram (4.4a) is equivalent to the gluonic one, the equation of motion introduces an explicit charge dependence giving rise to the operator structures

$$
\begin{aligned}
Q_7 &= \frac{3}{2}\bar{s}_L^i \gamma^\mu d_L^i \sum_f e_q \bar{q}_{fL}^j \gamma_\mu q_{fL}^j, \\
Q_8 &= \frac{3}{2}\bar{s}_L^i \gamma^\mu d_L^j \sum_f e_q \bar{q}_{fL}^j \gamma_\mu q_{fL}^i, \\
Q_9 &= \frac{3}{2}\bar{s}_L^i \gamma^\mu d_L^i \sum_f e_q \bar{q}_{fR}^j \gamma_\mu q_{fR}^j, \\
Q_{10} &= \frac{3}{2}\bar{s}_L^i \gamma^\mu d_L^j \sum_f e_q \bar{q}_{fR}^j \gamma_\mu q_{fR}^i.
\end{aligned}
\tag{4.59}
$$

When performing the matching for the new EW-penguin operators, as in the case for the gluonic one, one gets a contribution also from the top quark running in the loop. But in this case, this is not the only contribution. One must also consider the diagram where a Z^0 boson is exchanged and the box diagrams (4.6) where two W bosons are exchanged so that one can obtain a gauge-invariant result.

4.1.6 Wilson Coefficients and Renormalization

The RGE is now governed by a 10×10 anomalous dimension matrix, whose LO form is given by

$$
\gamma_s^{(0)} =
$$

$$
\begin{pmatrix}
-\frac{6}{N_c} & 6 & -\frac{2}{3N_c} & \frac{2}{3} & -\frac{2}{3N_c} & \frac{2}{3} & 0 & 0 & 0 & 0 \\
6 & -\frac{6}{N_c} & 0 & 0 & 0 & 0 & 0 & 0 & 0 & 0 \\
0 & 0 & -\frac{22}{3N_c} & \frac{22}{3} & -\frac{4}{3N_c} & \frac{4}{3} & 0 & 0 & 0 & 0 \\
0 & 0 & 6 - \frac{2n_f}{3N_c} & -\frac{6}{N_c} + \frac{2n_f}{3} & -\frac{2n_f}{3N_c} & \frac{2n_f}{3} & 0 & 0 & 0 & 0 \\
0 & 0 & 0 & 0 & \frac{6}{N_c} & -6 & 0 & 0 & 0 & 0 \\
0 & 0 & -\frac{2n_f}{3N_c} & \frac{2n_f}{3} & -\frac{2n_f}{3N_c} & 6\frac{1-N_c^2}{N_c} + \frac{2n_f}{3} & 0 & 0 & 0 & 0 \\
0 & 0 & 0 & 0 & 0 & 0 & \frac{6}{N_c} & -6 & 0 & 0 \\
0 & 0 & \frac{-2(n_u-n_d/2)}{3N_c} & \frac{2(n_u-n_d/2)}{3} & \frac{-2(n_u-n_d/2)}{3N_c} & \frac{2(n_u-n_d/2)}{3} & 0 & 6\frac{1-N_c^2}{N_c} & 0 & 0 \\
0 & 0 & \frac{2}{3N_c} & -\frac{2}{3} & \frac{2}{3N_c} & -\frac{2}{3} & 0 & 0 & -\frac{6}{N_c} & 6 \\
0 & 0 & \frac{-2(n_u-n_d/2)}{3N_c} & \frac{2(n_u-n_d/2)}{3} & \frac{-2(n_u-n_d/2)}{3N_c} & \frac{2(n_u-n_d/2)}{3} & 0 & 0 & 6 & -\frac{6}{N_c}
\end{pmatrix},
$$

$$\tag{4.60}$$

where n_d is the number of active down-like quarks and n_u the one of up-like quarks. Moreover $n_f = n_u + n_d$. The NLO anomalous dimension will have contributions from $\mathcal{O}(\alpha_s^2)$ corrections, but also $\mathcal{O}(\alpha)$ and $\mathcal{O}(\alpha_s\alpha)$, like in eq. (3.52). The specific form of the other coefficients can be found in [38, 53].

The NLO Wilson coefficients at the high scale are found by the matching procedure to be

$$
\begin{aligned}
C_1(M_W) &= \frac{11}{2}\frac{\alpha_s(M_W)}{4\pi} \\
C_2(M_W) &= 1 - \frac{11}{6}\frac{\alpha_s(M_W)}{4\pi} - \frac{35}{18}\frac{\alpha}{4\pi}, \\
C_3(M_W) &= -\frac{\alpha_s(M_W)}{24\pi}\widetilde{E}_0(x_t) + \frac{\alpha}{6\pi}\frac{1}{\sin^2\theta_W}\left[2B_0(x_t) + C_0(x_t)\right] \\
C_4(M_W) &= \frac{\alpha_s(M_W)}{8\pi}\widetilde{E}_0(x_t), \\
C_5(M_W) &= -\frac{\alpha_s(M_W)}{24\pi}\widetilde{E}_0(x_t), \\
C_6(M_W) &= \frac{\alpha_s(M_W)}{8\pi}\widetilde{E}_0(x_t), \\
C_7(M_W) &= \frac{\alpha}{6\pi}\left[4C_0(x_t) + \widetilde{D}_0(x_t)\right], \\
C_8(M_W) &= 0, \\
C_9(M_W) &= \frac{\alpha}{6\pi}\left[4C_0(x_t) + \widetilde{D}_0(x_t) + \frac{1}{\sin^2\theta_W}\left(10B_0(x_t) - 4C_0(x_t)\right)\right] \\
C_{10}(M_W) &= 0,
\end{aligned}
$$

$$\tag{4.61}$$

where

$$B_0(x) = \frac{1}{4}\left[\frac{x}{1-x} + \frac{x\ln x}{(x-1)^2}\right]$$

$$C_0(x) = \frac{x}{8}\left[\frac{x-6}{x-1} + \frac{3x+2}{(x-1)^2}\ln x\right]$$

$$D_0(x) = -\frac{4}{9}\ln x + \frac{-19x^3 + 25x^2}{36(x-1)^3} + \frac{x^2\left(5x^2 - 2x - 6\right)}{18(x-1)^4}\ln x \tag{4.62}$$

$$\widetilde{D}_0(x_t) = D_0(x_t) - \frac{4}{9}.$$

4.1.7 Magnetic Penguin Operators
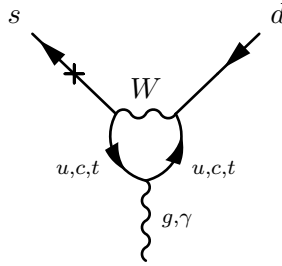
Figure 4.5. Magnetic penguin operators.

In principle, two additional operators contribute to the $\Delta S = 1$ transitions. These are known as *chromomagnetic* and *electromagnetic* penguin operators and have the following form

$$Q_{11} = \frac{g_s}{16\pi^2}m_s\bar{s}_i\sigma^{\mu\nu}t_{ij}^{\mathrm{a}}G_{\mu\nu}^{\mathrm{a}}(1-\gamma_5)d_j, \qquad Q_{12} = \frac{ee_d}{16\pi^2}m_s\bar{s}\sigma^{\mu\nu}F_{\mu\nu}(1-\gamma_5)d. \tag{4.63}$$

However their contribution for the $K \to 2\pi$ transitions are chiral suppressed two times: one from the strange mass term and one from the operator matrix element [24, 57], therefore we will not consider them from now on. Even in the RBC lattice analysis, [2] this operator was excluded.

4.1.8 A Note on the Operator Basis

What we found until now is that the $|\Delta S| = 1$ transitions can be described by an effective Hamiltonian containing ten operators

- **Current-Current Operators**:

$$Q_1 = (\bar{s}_i\gamma^\mu P_L u_j)(\bar{u}_j\gamma_\mu P_L d_i) \qquad Q_2 = (\bar{s}\gamma^\mu P_L u)(\bar{u}\gamma_\mu P_L d) \tag{4.64}$$

- **QCD-Penguins Operators**

$$Q_3 = (\bar{s}\gamma^\mu P_L d)\sum_q(\bar{q}\gamma_\mu P_L q) \qquad Q_4 = (\bar{s}_i\gamma^\mu P_L d_j)\sum_q(\bar{q}_j\gamma_\mu P_L q_i)$$

$$Q_5 = (\bar{s}\gamma^\mu P_L d)\sum_q(\bar{q}\gamma_\mu P_R q) \qquad Q_6 = (\bar{s}_i\gamma^\mu d_j)\sum_q(\bar{q}_j\gamma_\mu P_R q_i) \tag{4.65}$$

- **Electrowark-Penguins Operators**

$$Q_7 = \frac{3}{2}(\bar{s}\gamma^\mu P_L d)\sum_q e_q(\bar{q}\gamma_\mu P_R q) \qquad Q_8 = \frac{3}{2}(\bar{s}_i\gamma^\mu P_L d_j)\sum_q e_q(\bar{q}_j\gamma_\mu P_R q_i)$$

$$Q_9 = \frac{3}{2}(\bar{s}\gamma^\mu P_L d)\sum_q e_q(\bar{q}\gamma_\mu P_L q) \qquad Q_{10} = \frac{3}{2}(\bar{s}_i\gamma^\mu d_j)\sum_q e_q(\bar{q}_j\gamma_\mu P_L q_i)$$

$$(4.66)$$

where $P_{L/R} = (1 \mp \gamma_5)/2$ are the chiral projectors and e_q is the quark charge in units of e.

These operators are useful in the lattice calculations but when it comes to renormalization, another basis is better suited for the task: the so-called *chiral basis*. This comes in handy since in the usual 10-operator basis, the operators are not linearly independent. In fact, by Fierz transforming operators Q_1, Q_2 and Q_3

$$\begin{aligned}
\tilde{Q}_1 &= (\bar{s}\gamma^\mu P_L d)(\bar{u}\gamma_\mu P_L u), \\
\tilde{Q}_2 &= (\bar{s}_i\gamma^\mu P_L d_j)(\bar{u}_j\gamma_\mu P_L u_i), \\
\tilde{Q}_3 &= \sum_q (\bar{s}_i\gamma^\mu P_L q_j)(\bar{q}_j\gamma_\mu P_L d_i),
\end{aligned} \qquad (4.67)$$

we can eliminate operators Q_4, Q_9 and Q_{10} in such a way

$$\begin{aligned}
Q_4 &= \tilde{Q}_2 + \tilde{Q}_3 - Q_1, \\
Q_9 &= \frac{3}{2}\tilde{Q}_1 - \frac{1}{2}Q_3, \\
Q_{10} &= \frac{1}{2}(Q_1 - \tilde{Q}_3) + \tilde{Q}_2.
\end{aligned} \qquad (4.68)$$

The remaining seven operators can then be recombined according to irreducible representations (irrep) of the chiral flavour-symmetry group $SU(3)_L \otimes SU(3)_R$. All the details of the decomposition can be found in the literature [109]. The chiral operator basis, which we will indicate with a primed, is thus given by

$$\begin{aligned}
(27,1) \quad & Q_1' = 3\tilde{Q}_1 + 2Q_2 - Q_3, \\
(8,1) \quad & Q_2' = \frac{1}{5}(2\tilde{Q}_1 - 2Q_2 + Q_3), \\
(8,1) \quad & Q_3' = \frac{1}{5}(-3\tilde{Q}_1 + 3Q_2 + Q_3), \\
(8,1) \quad & Q_{5,6}' = Q_{5,6}, \\
(8,8) \quad & Q_{7,8}' = Q_{7,8}
\end{aligned} \qquad (4.69)$$

where (L,R) denotes the respective irrep of $SU(3)_L \otimes SU(3)_R$.

The conversion from the 7-operators chiral basis and the usual 10-operator basis is simply given by

$$Q_i = \sum_i T_{ij} Q_j' \qquad (4.70)$$
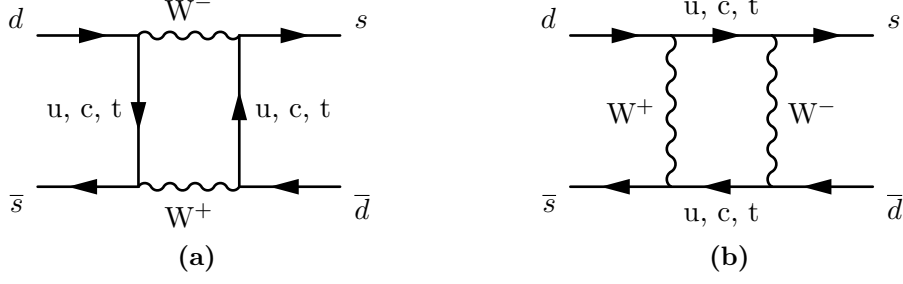
Figure 4.6. Box diagrams contributing to the $\Delta S = 2$ transitions.

where $1 \leq i \leq 10$ and $j \in \{1, 2, 3, 5, 6, 7, 8\}$ and the matrix T is given by

$$
T = \begin{pmatrix}
1/5 & 1 & 0 & 0 & 0 & 0 & 0 \\
1/5 & 0 & 1 & 0 & 0 & 0 & 0 \\
0 & 3 & 2 & 0 & 0 & 0 & 0 \\
0 & 2 & 3 & 0 & 0 & 0 & 0 \\
0 & 0 & 0 & 1 & 0 & 0 & 0 \\
0 & 0 & 0 & 0 & 1 & 0 & 0 \\
0 & 0 & 0 & 0 & 0 & 1 & 0 \\
0 & 0 & 0 & 0 & 0 & 0 & 1 \\
3/10 & 0 & -1 & 0 & 0 & 0 & 0 \\
3/10 & -1 & 0 & 0 & 0 & 0 & 0
\end{pmatrix}
\tag{4.71}
$$

4.2 Effective Hamiltonian for $\Delta S = 2$ Processes

Now we would like to do similar computations for $\Delta F = 2$ processes like the oscillations $K^0 \to \bar{K}^0$, which specifically are a $\Delta S = 2$ process since the underlying quark transition is given by $\bar{s}d \to \bar{d}s$.

Such FCNC process cannot arise at tree-level in the SM so we must consider one-loop contributions that, not considering the Goldstone boson exchange for now, are just the ones in fig. (4.6). Let us give now the computation for diagram (4.6a). Considering the external quark momenta to be zero, the amplitude can be easily found to be

$$
\begin{aligned}
i\mathcal{A}_a &= \int \frac{\mathrm{d}^d\ell}{(2\pi)^d} \bar{u}^s \left(\frac{ig_2}{\sqrt{2}}\right) \gamma^\mu P_L V^*_{u_j s} \frac{i(\ell - m_j)}{\ell^2 - m_j^2} \left(\frac{ig_2}{\sqrt{2}}\right) \gamma^\nu P_L V_{u_j d} v^d \\
&\qquad \bar{v}^s \left(\frac{ig_2}{\sqrt{2}}\right) \gamma_\nu P_L V^*_{u_i s} \frac{i(\ell - m_i)}{\ell^2 - m_i^2} \gamma_\mu P_L V_{u_i d} u^d \left(\frac{-i}{\ell^2 - M_W^2}\right)^2 \\
&= i\frac{g_2^4}{4} V^*_{u_i s} V_{u_i d} V^*_{u_j s} V_{u_j d} \int \frac{\mathrm{d}^4\ell}{(2\pi)^4 (\ell^2 - M_W^2)^2} \\
&\qquad \bar{u}^s \gamma^\mu P_L \frac{\ell - m_j}{\ell^2 - m_j^2} \gamma^\nu P_L v^d \bar{v}^s \gamma_\nu P_L \frac{\ell - m_i}{\ell^2 - m_i^2} \gamma_\mu P_L u^d,
\end{aligned}
\tag{4.72}
$$

where m_i is the mass of the up-like quark u_i between the initial quarks and m_j the mass of the up-like quark u_j between the final quarks. The terms proportional to the mass in eq. (4.72) vanish because of the chiral projectors

$$
m_j \bar{u}^s \gamma_\mu P_L \gamma_\nu P_L v^d = m_j \bar{u}^s \gamma_\mu \gamma_\nu \underbrace{P_R P_L}_{} v^d = 0,
\tag{4.73}
$$

therefore the amplitude simplifies to

$$i\frac{g_2^4}{4}V_{u_is}^*V_{u_id}V_{u_js}^*V_{u_jd}\left(\bar{u}^s\gamma^\mu P_L\gamma^\alpha\gamma^\nu P_Lv^d\right)\left(\bar{v}^s\gamma_\nu P_L\gamma^\beta\gamma_\mu P_Lu^d\right)I_{\alpha\beta}^{ij}, \tag{4.74}$$

where

$$I_{\alpha\beta}^{ij} = \int \frac{\mathrm{d}^4\ell}{(2\pi)^4} \frac{\ell_\alpha\ell_\beta}{(\ell^2-m_i^2)(\ell^2-m_j^2)^2(\ell^2-M_W^2)^2}. \tag{4.75}$$

Let us consider for now the tensor integral $I_{\alpha\beta}^{ij}$. We can simplify its structure by means of partial fractioning as follows

$$\frac{1}{(\ell^2-m_i^2)(\ell^2-m_j)^2} = \frac{A}{\ell^2-m_i^2} + \frac{B}{\ell^2-m_j^2}$$
$$= \frac{(A+B)\ell^2-(Am_j^2+Bm_i^2)}{(\ell^2-m_i^2)(\ell^2-m_j^2)}, \tag{4.76}$$

which simply implies that

$$A = -B, \qquad A = \frac{1}{m_i^2-m_j^2} \tag{4.77}$$

therefore

$$\frac{1}{(\ell^2-m_i^2)(\ell^2-m_j^2)} = \frac{1}{m_i^2-m_j^2}\left(\frac{1}{\ell^2-m_i^2}-\frac{1}{\ell^2-m_j^2}\right). \tag{4.78}$$

From this, we obtain that

$$I_{\alpha\beta}^{ij} = \frac{I_{\alpha\beta}^i - I_{\alpha\beta}^j}{m_i^2-m_j^2}, \tag{4.79}$$

where

$$\begin{aligned}
I_{\alpha\beta}^i &= \int \frac{\mathrm{d}^4\ell}{(2\pi)^4}\frac{\ell_\alpha\ell_\beta}{(\ell^2-m-i^2)(\ell^2-M_W^2)^2} \\
&= \frac{g_{\alpha\beta}}{4}\int\frac{\mathrm{d}^4\ell}{(2\pi)^4}\frac{(\ell^2-m_i^2)+m_i^2}{(\ell^2-M_W^2)^2(\ell^2-m_i^2)} \\
&= \frac{g_{\alpha\beta}}{4}\left[m_i^2\int\frac{\mathrm{d}^4\ell}{(2\pi)^4}\left(\frac{1}{(\ell^2-M_W^2)^2(\ell^2-m_i^2)}+\frac{1}{(\ell^2-M_W^2)^2}\right)\right].
\end{aligned} \tag{4.80}$$

The second term which does not depend on the quark mass cancels in the difference in eq. (4.79), therefore we can neglect it. While the first term becomes

$$\begin{aligned}
\int\frac{\mathrm{d}^4\ell}{(2\pi)^d}\frac{1}{(\ell^2-M_W^2)^2(\ell^2-m_i^2)} &= 2\int_0^1\mathrm{d}x\int\frac{\mathrm{d}^4\ell}{(2\pi)^d}\frac{x}{\left[(\ell^2-M_W^2)x+(\ell^2-m_i^2)(1-x)\right]^3} \\
&= 2\int_0^1\mathrm{d}x\int\frac{\mathrm{d}^4\ell}{(2\pi)^4}\frac{x}{[\ell^2-(xM_W^2+(1-x)m_i^2)]^3}.
\end{aligned} \tag{4.81}$$

The integral in the loop momentum is convergent

$$\int\frac{\mathrm{d}^4\ell}{(2\pi)^4}\frac{x}{[\ell^2-(xM_W^2+(1-x)m_i^2)]^3} = -\frac{i}{16\pi^2}\frac{1}{2}\frac{1}{xM_W^2+(1-x)m_i^2} \tag{4.82}$$

as can be easily seen by analytically continuing to d-dimensions and then taking the limit $d \to 4$. Hence the integral of eq. (4.81) becomes

$$
\begin{aligned}
&= -\frac{i}{16\pi^2} \int_0^1 \mathrm{d}x \, \frac{x}{xM_W^2 + (1-x)m_i^2} \\
&= -\frac{i}{16\pi^2 M_W^2} \int_0^1 \frac{x}{x + x_i(1-x)} \\
&= -\frac{i}{16\pi^2 M_W^2} \int_0^1 \mathrm{d}x \, \frac{x}{x_i + x(1-x_i)} \\
&= -\frac{i}{16\pi^2 M_W^2} \int_0^1 \frac{\mathrm{d}x}{(1-x_i)} \, \frac{(1-x_i)x + x_i - x_i}{x_i + x(1-x_i)} \\
&= -\frac{i}{16\pi^2 M_W^2} \left(\frac{-x_i}{1-x_i} \int_0^1 \mathrm{d}x \, \frac{1}{(1-x_i)x + x_i} + \frac{1}{1-x_i} \right) \\
&= -\frac{i}{16\pi^2 M_W^2} \left(\frac{1}{1-x_i} + \frac{x_i \log x_i}{(1-x_i)^2} \right),
\end{aligned}
\tag{4.83}
$$

where $x_i = m_i^2/M_W^2$. Thus, up to terms that do not depend on m_i we get

$$
\begin{aligned}
I_{\alpha\beta}^i &= -\frac{g_{\alpha\beta}}{4} \frac{i}{16\pi^2} \frac{m_i^2}{M_W^2} \left(\frac{1}{1-x_i} + \frac{x_i \log x_i}{(1-x_i)^2} \right) \\
&= -\frac{g_{\alpha\beta}}{4} \frac{i}{16\pi^2} J(x_i),
\end{aligned}
\tag{4.84}
$$

where

$$
J(x_i) = \frac{x_i}{1-x_i} + \frac{x_i^2 \log x_i}{(1-x_i)^2}.
\tag{4.85}
$$

Therefore

$$
I_{\alpha\beta}^{ij} = -\frac{g_{\alpha\beta}}{4M_W^2} \frac{i}{16\pi^2} A(x_i, x_j),
\tag{4.86}
$$

where

$$
A(x_i, x_j) = \frac{J(x_i) - J(x_j)}{x_i - x_j}.
\tag{4.87}
$$

This is our first, actually computed, Inami-Lim function [96] which encodes the loop information of the diagram.

We now turn our attention to the Dirac structure of eq. (4.74)

$$
\bar{u}^d \gamma^\mu P_L \gamma^\alpha \gamma^\nu P_L v^d \bar{v}^s \gamma_\nu P_L \gamma^\beta \gamma_\mu P_L u^d.
\tag{4.88}
$$

By using the usual projector rules and Clifford algebra, together with the $g_{\alpha\beta}$ from the integral, we can highlight the usual structure

$$
\bar{u}^s \gamma^\mu \gamma^\alpha \gamma^\nu \left(P_L v^d \bar{v}^s P_R \right) \gamma_\nu \gamma_\alpha \gamma_\mu u^d
\tag{4.89}
$$

and by using the Fierz identities

$$
(P_L v^d \bar{v}^s P_R)_{\alpha\beta} = -\frac{1}{2} \bar{v}^s \gamma^\rho P_L v^d (\gamma_\rho P_R)_{\alpha\beta}
\tag{4.90}
$$

we obtain

$$-\frac{1}{2}\bar{v}^s\gamma^\rho P_L v^d \bar{u}^s \gamma^\mu \gamma^\alpha \gamma^\nu \gamma_\rho P_R \gamma_\nu \gamma_\alpha \gamma_\mu u^d, \tag{4.91}$$

then by jumping the P_R over the gamma matrices

$$-\frac{1}{2}\bar{v}^s\gamma^\rho P_L v^d \bar{u}^s \gamma^\mu \gamma^\alpha \gamma^\nu \gamma_\rho \gamma_\nu \gamma_\alpha \gamma_\mu P_L u^d = 4\bar{v}^s\gamma^\rho P_L v^d \bar{u}^s \gamma_\rho P_L u^d, \tag{4.92}$$

where we used the usual relation $\gamma^\alpha \gamma^\mu \gamma_\alpha = -2\gamma^\mu$ four times.

Putting everything together we obtain the amplitude for the diagram (4.6a) as

$$
\begin{aligned}
i\mathcal{A}_a &= -\frac{i}{16\pi^2}\frac{4g_2^4}{16M_W^2}\sum_{i,j=u,c,t} V_{is}^* V_{id} V_{js}^* V_{jd} A(x_i, x_j)\bar{v}^s \gamma^\mu P_L v^d \bar{u}^s \gamma_\mu P_L u^d \\
&= -\frac{iG_F^2 M_W^2}{2\pi^2}\sum_{i,j=u,c,t}\lambda_{sd}^i \lambda_{sd}^j A(x_i, x_j)\bar{v}^s \gamma^\mu P_L v^d \bar{u}^s \gamma_\mu P_L u^d,
\end{aligned}
\tag{4.93}
$$

where $\lambda_{sd}^i = V_{is}^* V_{id}$.

The computation of diagram (4.6b) goes along the same lines ad for diagram (4.6a), where we just need to exchange an incoming $\bar{s}$ to an outgoing s and vice-versa. If we put the spinors in the amplitude

$$
\begin{aligned}
i\mathcal{A}_a &= -\frac{iG_F^2 M_W^2}{2\pi^2}\sum_{i,j=u,c,t}\lambda_{sd}^i \lambda_{sd}^j A(x_i, x_j)\bar{v}_s \gamma^\mu P_L v_d \bar{u}_s \gamma_\mu P_L u_d \\
i\mathcal{A}_b &= \frac{iG_F^2 M_W^2}{2\pi^2}\sum_{i,j=u,c,t}\lambda_{sd}^i \lambda_{sd}^j A(x_i, x_j)\bar{u}_s \gamma^\mu P_L u_d \bar{v}_s \gamma_\mu P_L v_d.
\end{aligned}
\tag{4.94}
$$

Both these amplitudes can be written as the matrix elements of the same local operator, which lets us write the effective $\Delta S = 2$ Hamiltonian as

$$\mathcal{H}_{\text{eff}}^{\Delta S=2} = C\bar{s}\gamma^\mu P_L d \bar{s}\gamma_\mu P_L d \tag{4.95}$$

where C is a Wilson coefficient. This effective Hamiltonian generates the following amplitude

$$-iC\left\langle \bar{d}s\left|\bar{s}\gamma^\mu P_L d\bar{s}\gamma_\mu P_L d\right|\bar{s}d\right\rangle = -2iC(\bar{u}_s \gamma^\mu P_L v_d \bar{v}_s \gamma_\mu P_L u_d - \bar{u}_s \gamma^\mu P_L u_d \bar{v}_s \gamma_\mu P_L v_d). \tag{4.96}$$

By matching with the full amplitude, we get that

$$C^{a+b} = \frac{G_F^2 M_W^2}{4\pi^2}\sum_{i,j=u,c,t}\lambda_{sd}^i \lambda_{sd}^j A(x_i, x_j). \tag{4.97}$$

There remains to evaluate also the box diagrams with the Goldstone boson exchange. We do not delve into the details of the calculation but, once evaluated, the same matching procedure as before can be done, obtaining three more Wilson coefficients, two coming from a single Goldstone exchange and one from the double Goldstone exchange, which are given by

$$
\begin{aligned}
C_2 = C_3 &= -\frac{G_F^2 M_W^2}{4\pi^2}\sum_{i,j=u,c,t}\lambda_{sd}^i \lambda_{sd}^j A'(x_i, x_j) x_i x_j \\
C_4 &= \frac{G_F^2 M_W^2}{8\pi^2}\sum_{i,j=u,c,t}\lambda_{sd}^i \lambda_{sd}^j A(x_i, x_j) x_i x_j,
\end{aligned}
\tag{4.98}
$$

where

$$A'(x_i, x_j) = \frac{J'(x_i) - J'(x_j)}{x_i - x_j}, \qquad J'(x) = \frac{1}{1-x} + \frac{x \log x}{(1-x)^2}. \tag{4.99}$$

In the end, by putting everything together, we get

$$C = \frac{G_F^2 M_W^2}{4\pi^2} \sum_{i,j=u,c,t} \lambda_{sd}^i \lambda_{sd}^j \bar{A}(x_i, x_j), \tag{4.100}$$

where

$$\bar{A}(x_i, x_j) = A(x_i, x_j) - x_i x_j A'(x_i, x_j) + \frac{1}{4} x_i x_j A(x_i, x_j). \tag{4.101}$$

By using the CKM unitarity, we can finally write down the full $\Delta S = 2$ effective Hamiltonian as

$$\mathcal{H}_{\text{eff}}^{\Delta S=2} = \frac{G_F^2 M_W^2}{4\pi^2} \Big[(\lambda_{sd}^t)^2 S_0(x_t) + (\lambda_{sd}^c)^2 S_0(x_c) + 2\lambda_{sd}^t \lambda_{sd}^c S_0(x_c, x_t) \Big] \bar{s}\gamma^\mu P_L d\bar{s}\gamma_\mu P_L d, \tag{4.102}$$

where

$$\begin{aligned} S_0(x) &= \bar{A}(x, x) + \bar{A}(x_u, x_u) - 2\bar{A}(x_u, x), \\ S_0(x, y) &= \bar{A}(x, y) + \bar{A}(x_u, x_u) - \bar{A}(x_u, x) - \bar{A}(x_u, y). \end{aligned} \tag{4.103}$$

All the calculations we have done so far are in the limit of zero external quark momenta. This is a good limit if there is no explicit dependence on the quark momenta. This turns out to be a good approximation but with some additional details that we will not discuss here [46, 133].

What we might want now to do, is to include LO QCD corrections in the same fashion as done for the $\Delta S = 1$ effective Hamiltonian. What changes is that the inclusion of loop corrections, does not add a new operator with a different color structure to the basis since, by means of Fierz identities, we can go back to the original color structure.

This leads to the following anomalous dimension

$$\gamma^{(0)} = 6\frac{N-1}{N}. \tag{4.104}$$

A complete treatment of the NLO QCD corrections is beyond the scope of this thesis but can be found in the literature [31, 88, 89, 90]. These corrections are usually parametrized by three factors η_1, η_2 and η_3. The effective Hamiltonian is usually written in the following form

$$\begin{aligned} \mathcal{H}_{\text{eff}}^{\Delta S=2} = \frac{G_F^2 M_W^2}{4\pi^2} \Big[&(\lambda_{sd}^t)^2 \eta_2 S_0(x_t) + (\lambda_{sd}^c)^2 \eta_1 S_0(x_c) \\ &+ 2\lambda_{sd}^t \lambda_{sd}^c \eta_3 S_0(x_c, x_t) \Big] \bar{s}\gamma^\mu P_L d\bar{s}\gamma_\mu P_L d, \end{aligned} \tag{4.105}$$

where $\eta_i = 1 + \mathcal{O}(\alpha_s)$.

Chapter 5

Phenomenology of CP-violation

CP-violation is a key feature of the SM and it is encoded into the matrix elements of the CKM matrix, as we discussed. Our current knowledge on the origin of CP violation is rather limited, both at the experimental and theoretical levels. This feature is of fundamental importance for many physical phenomena starting from allowed particle decays to one possible explanation of the matter-antimatter asymmetry in our universe. CP-violation has been observed in the neutral kaon system[1] which is the one we will focus on for the following chapter.

In this system, CP-violation can be tied to two observables called ϵ and ϵ'. The second observable is often referred to as the ration ϵ'/ϵ. These two observables measure the amount of CP-violation in the oscillations and decay respectively. We call ϵ the parameter of *indirect* CP-violation, while we refer to ϵ'/ϵ as the parameter of *direct* CP-violation.

In this chapter, we are going to discuss these two observables, their analytical form, and the experimental and theoretical subtleties they carry. To do so, we first need to introduce the neutral Kaon system, its isospin quantum numbers, which will help us construct the relevant theoretical quantities associated with the two CP parameters. A comprehensive review of the topics to be discussed can be found in [29, 59, 113].

5.1 The Neutral Kaon System
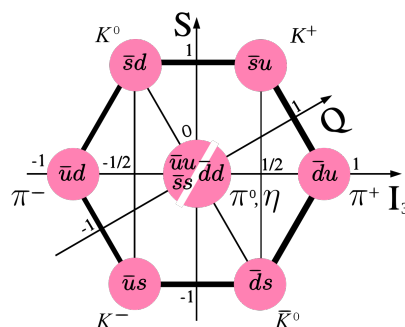
Figure 5.1. Pseudoscalar meson octet. Credits: Wikipedia - "Quark Model"

---

[1]Not only in the K mesons but also in B and D mesons.

The neutral kaons K^0 and $\bar{K}^0$ are two of the eight members of the pseudoscalar meson octet, which also include charged kaons $K^{\pm}$, the pions $\pi^{\pm}$ and π^0, and the η. These particles can be organised in the Cartan plane based on their strangeness S and isospin I_z quantum numbers, as we can see in figure (5.1). This structure is a result of the $SU(3)$ flavour symmetry.

The kaons are strange particles, the strangeness of K^0 and K^+ being $+1$, while the one for $\bar{K}^0$ and K^- being -1 for convention.

Considering the Isospin quantum number, which is the relevant quantum number to consider for evaluating matrix elements of Hamiltonians containing quarks, we have that

$$
\begin{aligned}
\left|K^0\right\rangle &\sim \left|\frac{1}{2}, -\frac{1}{2}\right\rangle & \left|K^+\right\rangle &\sim \left|\frac{1}{2}, \frac{1}{2}\right\rangle \\
\left|K^-\right\rangle &\sim \left|\frac{1}{2}, -\frac{1}{2}\right\rangle & \left|\bar{K}^0\right\rangle &\sim \left|\frac{1}{2}, \frac{1}{2}\right\rangle.
\end{aligned}
\tag{5.1}
$$

This classification will be useful later in conjunction with the $SU(3)$ structure of the $\Delta S = 1, 2$ Hamiltonians and the Wigner-Eckart theorem.

The reasoning we are going to give in the following is not specific only to the neutral kaons. Besides the kaons, there are three neutral mesons that differ from their antiparticles because of their flavour content and they are: D^0, B_d, and B_s mesons. They will decay, but moreover, they have the peculiarity of mixing with their relative antimeson, just like the K^0 and $\bar{K}^0$.

5.2   Kaon Mixing

If only electromagnetic and strong interactions existed, the K^0 and $\bar{K}^0$ would be stable and form particle-antiparticle pairs with the same mass m_0. Because of weak interactions, the two kaons decay. Moreover, neither electric charge conservation nor any other conservation law respected by weak interactions can prevent K^0 and $\bar{K}^0$ from having both real and virtual transitions to common states $|n\rangle$. As a consequence, K^0 and $\bar{K}^0$ can oscillate between themselves before decaying, which entails a difference of mass and width between the two eigenstates [72].

A general state $|\psi\rangle$ which describes a neutral kaon, will be a linear combination of the two strong and electromagnetic eigenstates $|K\rangle$ and $\left|\bar{K}^0\right\rangle$, that have definite strangeness.

By introducing the vector of the components of $|\psi\rangle$, $\psi^T = (\psi_1 \quad \psi_2)$, such that $|\psi\rangle = \psi_1 \left|K^0\right\rangle + \psi_2 \left|\bar{K}^0\right\rangle$, when we switch on the weak interactions, the time evolution of the state, in the particle rest frame, is governed by Schrödinger's equation

$$
i\frac{\partial \psi(t)}{\partial t} = H_W \psi(t) = \left(M - \frac{i}{2}\Gamma\right)\psi(t),
\tag{5.2}
$$

where the Hamiltonian is, in general, not Hermitian since we are restricting the total Hilbert space to that of only the Kaons. This is because kaons can decay to other particles and so the Hilbert space will contain even all possible decay products. This simplification is known as the Wigner-Weisskopf approximation [144] which is rather accurate because of the smallness of weak interactions.

The matrices M and Γ in eq. (5.2) are Hermitian and are given, in second-order perturbation theory [125], by the sum over intermediate states

$$
\begin{aligned}
M_{ij} &= m_0 \delta_{ij} + \langle i|H_W|j\rangle + \text{PV} \sum_n \frac{\langle i|H_W|n\rangle \langle n|H_W|j\rangle}{m_0 - E_n}, \\
\Gamma_{ij} &= 2\pi \sum_n \delta(m_0 - E_n) \langle i|H_W|n\rangle \langle n|H_W|j\rangle,
\end{aligned}
\tag{5.3}
$$

where $PV(f)$ is the principal value of f. The intermediate states $|n\rangle$ which contribute to M_{ij} are virtual states, while the ones contributing to Γ_{ij} are real states to which the two kaons can decay to. The matrix Γ_{ij} encodes the possibility for the particles to decay.

We can now impose different conditions on the elements of M and Γ by imposing either CP-invariance or CPT-invariance, the second being a necessary requisite for any Lorentz invariant QFT [129, 110]. In quantum mechanics, all kets may be rephased at will without any consequence on the measured quantities

$$
\left|K^0\right\rangle \to e^{i\alpha} \left|K^0\right\rangle \qquad \left|\bar{K}^0\right\rangle \to e^{i\bar{\alpha}} \left|\bar{K}^0\right\rangle.
\tag{5.4}
$$

The diagonal matrix elements of the weak Hamiltonian H_W are invariant under this rephasing, in fact

$$
\begin{pmatrix} H_{11} & H_{12} \\ H_{21} & H_{22} \end{pmatrix} \to \begin{pmatrix} H_{11} & e^{i(\bar{\alpha}-\alpha)}H_{12} \\ e^{i(\alpha-\bar{\alpha})}H_{21} & H_{22} \end{pmatrix},
\tag{5.5}
$$

where

$$
H_W = \begin{pmatrix} H_{11} & H_{12} \\ H_{21} & H_{22} \end{pmatrix} = \begin{pmatrix} \langle K^0|H_W|K^0\rangle & \langle K^0|H_W|\bar{K}^0\rangle \\ \langle \bar{K}^0|H_W|\bar{K}^0\rangle & \langle \bar{K}^0|H_W|K^0\rangle \end{pmatrix}.
\tag{5.6}
$$

As a consequence of this rephasing invariance, of the eight real numbers of H_W, only seven have physical significance.

The discrete CP transformation interchanges K^0 with $\bar{K}^0$ and vice-versa. By choosing $CP^2 = 1$ we get [108, 107]

$$
\mathcal{CP}\left|K^0\right\rangle = e^{i\xi}\left|\bar{K}^0\right\rangle \qquad \mathcal{CP}\left|\bar{K}^0\right\rangle = e^{-i\xi}\left|K^0\right\rangle.
\tag{5.7}
$$

In the same manner under CPT transformation we have

$$
\mathcal{CPT}\left|K^0\right\rangle = e^{i\nu}\left|\bar{K}^0\right\rangle \qquad \mathcal{CPT}\left|\bar{K}^0\right\rangle = e^{i\nu}\left|K^0\right\rangle.
\tag{5.8}
$$

since the CPT operator is anti-unitary. What does the invariance under these discrete transformations say about H_W? The effects can be easily computed from the matrix elements and the definitions in eqs. (5.7) and (5.8) and we summarize them in table (5.1).

Table 5.1. Effects under discrete symmetries

Symmetry	Diagonal Elements	Off-Diagonal Elements
CP	$M_{11} = M_{22}, \Gamma_{11} = \Gamma_{22}$	$M_{21} = \exp(2i\xi)M_{12}, \Gamma_{21} = \exp(2i\xi)\Gamma_{12}$
CPT	$M_{11} = M_{22}, \Gamma_{11} = \Gamma_{22}$	-

CP conservation gives us information about the off-diagonal matrix elements, and the result can be parametrized in a more convenient way as

$$H_{12} = e^{2i\xi} H_{21} \implies |H_{12}| = |H_{21}| \implies \text{Im}(M_{12}^* \Gamma_{12}) = 0, \tag{5.9}$$

or equivalently

$$\text{Im}\left(\frac{\Gamma_{12}}{M_{12}}\right) = 0. \tag{5.10}$$

The two eigenstates of the Hamiltonian H_W, being non-Hermitian, are going to be, in general, complex and we may rewrite them as

$$\lambda_{1,2} = m_{1,2} - \frac{i}{2}\Gamma_{1,2}, \tag{5.11}$$

where $m_{1,2}$ are the masses of the two eigenstates $K_{1,2}$ while $\Gamma_{1,2}$ are their decay widths. If we define

$$\Delta m = m_1 - m_2 \qquad \Delta\Gamma = \Gamma_1 - \Gamma_2 \tag{5.12}$$

we may ask ourselves what are the signs of these two quantities. Generally speaking, we could have two cases: one where $\Delta m > 0$ and so K_1 is heavier than K_2 or $\Delta\Gamma > 0$ where the lifetime of K_2 is greater than the one of K_1. In the case of the neutral kaons, we distinguish the two eigenstates based on their lifetime, and so we label them by L for the *Long lived* kaon K_L and S for the *Short lived* kaon K_S. Experimentally one finds [152]

$$\begin{aligned}
\tau_L &= \frac{1}{\Gamma_L} = (5.116 \pm 0.021) \times 10^{-8} \text{ s}, \\
\tau_S &= \frac{1}{\Gamma_S} = (8.954 \pm 0.009) \times 10^{-11} \text{ s},
\end{aligned} \tag{5.13}$$

while

$$\Delta m = (3.491 \pm 0.009) \times 10^{-12} \text{ MeV}. \tag{5.14}$$

Usually one also defines the quantities

$$\begin{aligned}
m &= \frac{m_L + m_S}{2}, & \Gamma &= \frac{\Gamma_S + \Gamma_L}{2}, \\
x &= \frac{\Delta m}{\Gamma}, & y &= \frac{\Delta\Gamma}{2\Gamma},
\end{aligned} \tag{5.15}$$

where x and y are dimensionless parameters. In the case of the neutral kaons system $\Delta\Gamma = \Gamma_L - \Gamma_S \approx -\Gamma_S$ and $\Gamma \approx \Gamma_S/2$. Moreover $x \approx -y \approx 1$. The average of the mass of the neutral kaons is [152]

$$m_K = 497.611 \pm 0.012 \text{ MeV}. \tag{5.16}$$

Let us rewrite the eigenstates $K_{L,S}$ as follows

$$|K_{L,S}\rangle = p\left|K^0\right\rangle \pm q\left|\bar{K}^0\right\rangle, \qquad \text{with } |p|^2 + |q|^2 = 1, \tag{5.17}$$

or equivalently

$$\left|K^0\right\rangle = \frac{1}{2p}(|K_L\rangle + |K_S\rangle),$$
$$\left|\bar{K}^0\right\rangle = \frac{1}{2q}(|K_L\rangle - |K_S\rangle).$$

(5.18)

Then, under this parametrization, we have that

$$H_{11}p \pm H_{21}q = \lambda_{L,S}p \implies H_{11} \pm \frac{p}{q}H_{12} = H_{11} \pm \sqrt{H_{12}H_{21}}$$

(5.19)

where we used the diagonalization of the Hamiltonian in eq. (5.6) that gives $\lambda_{L/S} = H_{11} \pm \sqrt{H_{12}H_{21}}$. Then eq. (5.19) gives

$$\frac{q}{p} = \sqrt{\frac{H_{21}}{H_{12}}} = \frac{\Delta m - \frac{i}{2}\Delta\Gamma}{2M_{12} - i\Gamma_{12}}.$$

(5.20)

Now we can easily see that CP conservation, using eq. (5.10), implies

$$\frac{q}{p} = e^{i\xi} \implies \left|\frac{q}{p}\right| = 1.$$

(5.21)

Thus, we denote the condition of *CP violation in mixing* or *indirect CP-violation*, as

$$\left|\frac{q}{p}\right| \neq 1.$$

(5.22)

In the limit where CP is an exact symmetry, the two CP eigenstates are given, under a suitable choice of the phases in eq. (5.4), by the following linear combinations

$$|K_1\rangle = \frac{1}{\sqrt{2}}\left(\left|K^0\right\rangle + \left|\bar{K}^0\right\rangle\right), \qquad |K_2\rangle = \frac{1}{\sqrt{2}}\left(\left|K^0\right\rangle - \left|\bar{K}^0\right\rangle\right),$$

(5.23)

where $|K_1\rangle$ is the CP-even (or CP-positive) eigenstate, while $|K_2\rangle$ is CP-odd (or CP-negative).

Finally, CP-violation in mixing can be also expressed in terms of the parameter δ defined as

$$\delta = \frac{|H_{12}| - |H_{21}|}{|H_{12}| + |H_{21}|} = \langle K_L|K_S\rangle = |p|^2 - |q|^2 = \frac{1 - |q/p|^2}{1 + |q/p|^2}.$$

(5.24)

Equivalently

$$|p|^2 = \frac{1 + \delta}{2}, \qquad |q|^2 = \frac{1 - \delta}{2}.$$

(5.25)

Notice that the transformation in eq. (5.17) is unitary only if $|p|^2 - |q|^2 = \delta = 0$, so only if CP is conserved. Therefore, if CP is violated, one must be careful with the definition of the bra states $\langle K_{L,S}|$ using the so-called *reciprocal basis*. We are not going into the details but many references are available [65, 124, 132, 148].

5.3 Kaon Decay

Before going into the various definitions of the observables that we can associate to CP violation in both mixing and decay, we must deal with the other CP-violating physics in the kaon system: nonleptonic decays, in particular $K \to 2\pi$ decays.

We can start by analyzing the isospin decomposition of the various matrix elements that can be constructed then make use of the Wigner-Eckart theorem to find the non-zero ones based on the isospin form of the weak $|\Delta S| = 1$ Hamiltonian. Both kaons and pions are spinless particles, therefore when a neutral kaon decays to two pions, the final state must come with zero angular momentum. Moreover, pions are bosons and so their total wavefunction must be symmetric. With all of this, the angular momentum part is symmetric and therefore their isospin state must be even. This means that the total isospin I must be either $I = 0, 2$. This is true since pions form an isospin triplet and so their tensor product must have total isospin either $0, 1$ or 2.
With this in mind, let us start from the definition

$$\left\langle \pi^+ \right| = \langle 1, 1| , \qquad \left\langle \pi^0 \right| = \langle 1, 0| , \qquad \left\langle \pi^- \right| = \langle 1, -1| . \tag{5.26}$$

The relevant two pions final states that we can construct are

$$
\begin{aligned}
\langle 2, 1| &= \frac{1}{\sqrt{2}} \left(\left\langle \pi^+ \pi^0 \right| + \left\langle \pi^0 \pi^+ \right| \right), \\
\langle 2, 0| &= \frac{1}{\sqrt{6}} \left(\left\langle \pi^+ \pi^- \right| + \left\langle \pi^- \pi^+ \right| + 2 \left\langle \pi^0 \pi^0 \right| \right), \\
\langle 0, 0| &= \frac{1}{\sqrt{3}} \left(\left\langle \pi^+ \pi^- \right| + \left\langle \pi^- \pi^+ \right| - \left\langle \pi^0 \pi^0 \right| \right),
\end{aligned}
\tag{5.27}
$$

where we used the Clebsh-Gordan decomposition [145]. On the other hand, kaons form two distinct isospin doublets which are given in eq. (5.1). What we need to evaluate are matrix elements of the form

$$_{\text{out}}\langle 2\pi, I | \mathcal{H}_{\text{eff}}^{|\Delta S|=1} |K\rangle_{\text{in}} . \tag{5.28}$$

If we take, for example, the decay $K^+ \to \pi^0 \pi^0$ we see that

$$\left\langle \pi^+ \pi^0 \middle| \mathcal{H}_{\text{eff}}^{|\Delta S|=1} \middle| K^+ \right\rangle \sim \left\langle 2, 1 \middle| \mathcal{H}_{\text{eff}}^{|\Delta S|=1} \middle| \frac{1}{2}, \frac{1}{2} \right\rangle \neq 0 \iff \mathcal{H}_{\text{eff}}^{|\Delta S|=1} \sim \left| \frac{3}{2}, \frac{1}{2} \right\rangle \tag{5.29}$$

by virtue of the Wigner-Eckart theorem, so that not all the operators for the $|\Delta S| = 1$ Hamiltonian contribute to the matrix element. The Hamiltonian contains also $I = 1/2$ components. Therefore, the action of the effective Hamiltonian on the

initial kaon states can be parametrized as follows[2]

$$\mathcal{H}_{\text{eff}} \left| K^0 \right\rangle = \left(\mathcal{H}_{3/2,1/2} + \mathcal{H}_{1/2,1/2} \right) \left| \frac{1}{2}, -\frac{1}{2} \right\rangle,$$
$$= \frac{1}{\sqrt{2}} A_{3/2} \left| 2, 0 \right\rangle + \frac{1}{\sqrt{2}} A_{3/2} \left| 1, 0 \right\rangle + \frac{1}{\sqrt{2}} A_{1/2} \left| 1, 0 \right\rangle + \frac{1}{\sqrt{2}} A_{1/2} \left| 0, 0 \right\rangle$$
$$\mathcal{H}_{\text{eff}} \left| K^+ \right\rangle = \left(\mathcal{H}_{3/2,1/2} + \mathcal{H}_{1/2,1/2} \right) \left| \frac{1}{2}, \frac{1}{2} \right\rangle$$
$$= \sqrt{\frac{3}{4}} A_{3/2} \left| 2, 1 \right\rangle - \frac{1}{2} A_{3/2} \left| 1, 1 \right\rangle + A_{1/2} \left| 1, 1 \right\rangle$$

(5.30)

again by virtue of the Clebsh-Gordan decomposition. Using what we found in eq. (5.30) and the definitions in eq. (5.27), we see that

$$A(K^+ \to \pi^+ \pi^0) = \frac{\sqrt{3}}{2\sqrt{2}} A_{3/2},$$
$$A(K^0 \to \pi^+ \pi^-) = \frac{1}{2\sqrt{3}} \left(A_{3/2} + A_{1/2} \right),$$
$$A(K^0 \to \pi^0 \pi^0) = \frac{1}{\sqrt{6}} \left(\sqrt{2} A_{3/2} - A_{1/2} \right).$$

(5.31)

Here we neglected the effects of isospin breaking which come from the difference in the mass of the up and down quarks and from EM interactions [49]. These effects will be considered later on. Most of the times, it is convenient to define the amplitudes as $A_{0,2} = 1/\sqrt{6} A_{1/2,3/2}$. In both A_0 and A_2 there are two main phases: a strong phase which comes from the scattering of the final states and are CP-invariant, and a weak phase which is not CP-invariant. Under the elastic threshold, there are only two strong phases. Let us consider the $2\pi \to 2\pi$ scattering solely under the influence of the strong interaction. Denoting S_{strong} the strong isospin conserving S-matrix, we define

$$_{\text{out}}\langle 2\pi, I | 2\pi, I \rangle_{\text{out}} = \langle 2\pi, I | S_{\text{strong}} | 2\pi, I \rangle.$$

(5.32)

Assuming that we are below elastic threshold, given the unitarity of the S-matrix

$$S_{\text{strong}}^\dagger S_{\text{strong}} = 1 \implies S_{\text{strong}} = e^{2i\delta_I}.$$

(5.33)

Under these conditions, Watson's theorem [69, 141] assures us that the weak phase is just half of the strong phase of eq. (5.33) describing the strong interaction of the final state.

Then we can explicitly extract a CP-invariant phase $\delta_{0,2}$ from each isospin amplitude, so that $A_{0,2} \to A_{0,2}^*$ under CP. With this definition one finds

$$A(K^0 \to \pi^+ \pi^-) = A_0 e^{i\delta_0} + \frac{A_2}{\sqrt{2}} e^{i\delta_2},$$
$$A(K^0 \to \pi^0 \pi^0) = -A_0 e^{i\delta_0} + \sqrt{2} A_2 e^{i\delta_2},$$
$$A(K^+ \to \pi^+ \pi^0) = \frac{3}{2} A_2 e^{i\delta_2}.$$

(5.34)

---

[2]The same goes for the other kaon doublet.

When considering neutral kaons decaying to some final state f, we can find the condition of CP-invariance in decay from the decay amplitudes. In fact, by considering how CP acts on the initial kaons, in eq. (5.7), and how it acts on the final states

$$\mathcal{CP}\left|f\right\rangle = e^{i\xi_f}\left|\bar{f}\right\rangle, \qquad \mathcal{CP}\left|\bar{f}\right\rangle = e^{-i\xi_f}\left|f\right\rangle \tag{5.35}$$

we are led to the condition of CP-invariance for the decay amplitudes

$$\bar{A}_{\bar{f}} = e^{i(\xi_f - \xi)}A_f, \qquad A_{\bar{f}} = e^{i(\xi_f + \xi)}\bar{A}_f, \tag{5.36}$$

where $A_f = \left\langle f|\mathcal{H}|K^0\right\rangle$ with the other straightforward definitions. We can recast the condition in a more suitable form as

$$|A_f| = \left|\bar{A}_{\bar{f}}\right|, \qquad \left|A_{\bar{f}}\right| = \left|\bar{A}_f\right|. \tag{5.37}$$

These conditions are what one would expect if CP was a symmetry: the probability of the decay $K^0 \to f$ should be the same as the one for the decay $\bar{K}^0 \to \bar{f}$. Analogous conditions hold for the decay of charged kaons. When the conditions of eq. (5.37) are not met, we speak of *CP-violation in decays* or *direct CP-violation.*

5.3.1 The $\Delta I = 1/2$ Rule

The most important experimental feature of kaon decays is that there is a striking dominance of the $\Delta I = 1/2$ amplitude, which contributes to A_0, over the $\Delta I = 3/2$ amplitude, which contributes only to A_2. What is found experimentally is that

$$\frac{\Gamma(K^0 \to \pi^+\pi^-)}{\Gamma(K^+ \to \pi^+\pi^0)} \simeq 400, \tag{5.38}$$

which gives us that

$$\frac{|A_0|^2 + |A_2|^2}{|A_2|^2} \simeq 400 \implies A_0 \gg A_2. \tag{5.39}$$

This phenomenon is known as the $\Delta I = 1/2$ *rule* [15, 72, 73], or *octet enhancement* [13]. The latter is due to the fact that in A_2 enters a **27** of $SU(3)$, while in A_0 and **8**.
This rule can be cast in a more convenient form as

$$\frac{\operatorname{Re}A_2}{\operatorname{Re}A_0} \simeq \frac{1}{22}. \tag{5.40}$$

One of the most difficult problems in the study of these weak decays is in fact the theoretical prediction of this ratio. From what we knew before the lattice results from the RBC-UKQCD collaboration [2], part of the reason for the enhancement is due to the RG evolution of the dominant Wilson coefficients. This accounts for a factor of two. Another contribution comes from QCD penguin operators being purely $\Delta I = 1/2$ [138]. Still, this does not account for the full 22 times enhancement. The effect must largely come from the hadronic matrix elements which are much harder to evaluate due to their nonperturbative nature.

Is here that the RBC results [2, 18] come into play. What they found not only gave the expected enhancement on the A_2/A_0 amplitude, but underlined a large deviation from the naïve factorizations based on the Vacuum Insertion Approximation (VIA) in the matrix elements of the current-current operators. In fact using VIA, one finds that the two Wick contractions of the operator

$$Q^{(27,1)} = 3\tilde{Q}_1 + 2Q_2 - Q_3, \tag{5.41}$$

where $\tilde{Q}_1$ is the Fierz transform of Q_1

$$\tilde{Q}_1 = (\bar{s}d)_{\text{V}-\text{A}}(\bar{u}u)_{\text{V}-\text{A}}, \tag{5.42}$$

come with the same sign plus a factor of 3 due to color contractions. In reality, the two Wick contractions have the opposite sign, effectively cancelling each other (see fig. 11 of [18]).

Quoting the result from the article [2], the RBC collaboration found that

$$\frac{\text{Re}\,A_0}{\text{Re}\,A_2} = 19.9(2.3)(4.4), \tag{5.43}$$

where the first error is statistical while the latter is systematic.

5.4   CP Observables

We are now ready to construct the two fundamental observables connected to CP violation in the kaon system.

Conventionally it is useful to define, for an arbitrary decay channel f, the parameters

$$\eta_f = |\eta_f|e^{i\phi_f} = \frac{\langle f|\mathcal{H}_{\text{eff}}^{|\Delta S|=1}|K_L\rangle}{\langle f|\mathcal{H}_{\text{eff}}^{|\Delta S|=1}|K_S\rangle}r, \tag{5.44}$$

where the factor r is there for rephasing invariance [100, 105]. We shall assume $r = 1$ from now on. It is also convenient to define the four decay amplitudes by normalizing them by the largest one

$$\begin{aligned}
\omega &= \frac{\langle 2\pi(2)|\mathcal{H}_{\text{eff}}^{|\Delta S|=1}|K_S\rangle}{\langle 2\pi(0)|\mathcal{H}_{\text{eff}}^{|\Delta S|=1}|K_S\rangle}, \\
\epsilon &= \frac{\langle 2\pi(0)|\mathcal{H}_{\text{eff}}^{|\Delta S|=1}|K_L\rangle}{\langle 2\pi(0)|\mathcal{H}_{\text{eff}}^{|\Delta S|=1}|K_S\rangle}, \\
\epsilon_2 &= \frac{\langle 2\pi(2)|\mathcal{H}_{\text{eff}}^{|\Delta S|=1}|K_L\rangle}{\langle 2\pi(0)|\mathcal{H}_{\text{eff}}^{|\Delta S|=1}|K_S\rangle},
\end{aligned} \tag{5.45}$$

where $\langle 2\pi(I)| \equiv \langle 2\pi, I|$. Notice that the parameters ϵ and ϵ_2 violate CP, while the parameters ω and ϵ_2 violate the $\Delta I = 1/2$ rule. Instead of ϵ_2 we define another parameter which violates both CP and the $\Delta I = 1/2$ rule

$$\begin{aligned}
\epsilon' &= \frac{\epsilon_2 - \epsilon\omega}{\sqrt{2}} \\
&= \frac{\langle 2\pi(2)|\mathcal{H}_{\text{eff}}^{|\Delta S|=1}|K_L\rangle\,\langle 2\pi(0)|\mathcal{H}_{\text{eff}}^{|\Delta S|=1}|K_S\rangle - \langle 2\pi(0)|\mathcal{H}_{\text{eff}}^{|\Delta S|=1}|K_L\rangle\,\langle 2\pi(2)|\mathcal{H}_{\text{eff}}^{|\Delta S|=1}|K_S\rangle}{\sqrt{2}\,\langle 2\pi(2)|\mathcal{H}_{\text{eff}}^{|\Delta S|=1}|K_L\rangle\,\langle 2\pi(0)|\mathcal{H}_{\text{eff}}^{|\Delta S|=1}|K_S\rangle^2}.
\end{aligned} \tag{5.46}$$

If $\epsilon' \neq 0$ we have the condition for direct CP-violation, i.e. CP-violation in the decay amplitudes.

Following eqs. (5.44) to (5.46) we find that

$$
\begin{aligned}
\eta_{+-} &= \epsilon + \frac{\epsilon'}{1 + \omega/\sqrt{2}} \approx \epsilon + \epsilon', \\
\eta_{00} &= \epsilon - \frac{2\epsilon'}{1 - \sqrt{2}\omega} \approx \epsilon - 2\epsilon',
\end{aligned}
\tag{5.47}
$$

where we used the fact that $|\omega| \ll 1$ due to the $\Delta I = 1/2$ rule. These constitute the definition of the two observables ϵ and ϵ' in terms of measurable quantities. It is useful to cast them in a more "experimentalist" form

$$
\epsilon = \frac{2\eta_{+-} + \eta_{00}}{3}, \qquad \epsilon' = \frac{\eta_{+-} - \eta_{00}}{3}.
\tag{5.48}
$$

5.4.1 Kaon Mixing and ϵ_K

We have seen that if CP is a symmetry, the mass eigenstates $\left|K_{L/S}\right\rangle$ would become CP eigenstates of the form in eq. (5.23). In this limit

$$
|K_L\rangle \to |K_1\rangle, \qquad |K_S\rangle \to |K_2\rangle,
\tag{5.49}
$$

and so the K_S would decay only into CP-even final states, like the $\pi\pi$ state, whereas K_L would decay only to CP-odd eigenstates like $\pi\pi\pi$. This also explains why the two particles have such a different lifetime: the 3π state has a considerably smaller phase space than the 2π states, the decay width of the former is much bigger than the latter making its lifetime smaller.

It is convenient to expand the $K_{L/S}$ state on the basis of the CP-eigenstates as follows

$$
\begin{aligned}
|K_L\rangle &= \frac{1}{\sqrt{1 + |\bar{\epsilon}|^2}}(|K_2\rangle + \bar{\epsilon}\,|K_1\rangle), \\
|K_S\rangle &= \frac{1}{\sqrt{1 + |\bar{\epsilon}|^2}}(|K_1\rangle + \bar{\epsilon}\,|K_2\rangle),
\end{aligned}
\tag{5.50}
$$

where, in the convention of eq. (5.17)

$$
\frac{q}{p} = \frac{1 + \bar{\epsilon}}{1 - \bar{\epsilon}}.
\tag{5.51}
$$

By the definition of ϵ in eq. (5.45), with eqs. (5.34) and (5.50), given that $\bar{\epsilon} \ll 1$[3] and neglecting terms of order $(\operatorname{Im} A_0/\operatorname{Re} A_0)^2$, we get that

$$
\begin{aligned}
\epsilon &= \frac{(1 + \bar{\epsilon})A_0^* - (1 - \bar{\epsilon})A_0}{(1 + \bar{\epsilon})A_0^* + (1 - \bar{\epsilon})A_0} = \frac{(A_0 - A_0^*) + \bar{\epsilon}(A_0 + A_0^*)}{(A_0 + A_0^*) + \bar{\epsilon}(A_0 - A_0^*)} \\
&= \frac{i\operatorname{Im} A_0 + \bar{\epsilon}\operatorname{Re} A_0}{\operatorname{Re} A_0 + i\bar{\epsilon}\operatorname{Im} A_0} = \frac{\bar{\epsilon} + i\operatorname{Im} A_0/\operatorname{Re} A_0}{1 + i\bar{\epsilon}\operatorname{Im} A_0/\operatorname{Re} A_0} \\
&\simeq \left(\bar{\epsilon} + i\frac{\operatorname{Im} A_0}{\operatorname{Re} A_0}\right)\left(1 - i\bar{\epsilon}\frac{\operatorname{Im} A_0}{\operatorname{Re} A_0}\right) \simeq \bar{\epsilon} + i\frac{\operatorname{Im} A_0}{\operatorname{Re} A_0}.
\end{aligned}
\tag{5.52}
$$

---

[3]CP violation in SM is small.

The $\bar{\epsilon}$ coefficient is tied to the diagonalization of the matrix of eq. (5.6), thus, by means of eq. (5.51), we have

$$\bar{\epsilon} = \frac{p-q}{p+q} \simeq \frac{i}{2} \frac{\operatorname{Im} M_{12} - i \operatorname{Im} \Gamma_{12}/2}{\operatorname{Re} M_{12} - i \operatorname{Re} \Gamma_{12}/2} \simeq \frac{1}{2} \frac{M_{12} - M_{21} - i/2(\Gamma_{12} - \Gamma_{21})}{\Delta m + i/2\Delta\Gamma}. \tag{5.53}$$

Experimentally, one finds that for the kaon system $\Delta m/\Delta\Gamma \approx -1$. Thus we can simplify the above expression as

$$\bar{\epsilon} \simeq \frac{1+i}{2} \frac{\operatorname{Im} M_{12}}{2\operatorname{Re} M_{12}} - \frac{1-i}{2} \frac{\operatorname{Im} \Gamma_{12}}{2\operatorname{Re} \Gamma_{12}}. \tag{5.54}$$

In addition, from the definition of eq. (5.3) and the fact that the decay $K^0 \to 2\pi$ is dominated by the $I = 0$ transition due to the $\Delta I = 1/2$ rule, we have

$$\Gamma_{12} = 2\pi \sum_n \delta(m - k - E_n) \left\langle K^0 \middle| H_W \middle| n \right\rangle \left\langle n \middle| H_W \middle| \bar{K}^0 \right\rangle \simeq (A_0^*)^2, \tag{5.55}$$

therefore

$$\operatorname{Im} \Gamma_{12} = -2 \operatorname{Re} A_0 \operatorname{Im} A_0, \qquad \operatorname{Re} \Gamma_{12} = \operatorname{Re}^2 A_0 - \operatorname{Im}^2 A_0. \tag{5.56}$$

Using this in eqs. (5.52) and (5.54), with the usual expansion, we find

$$\begin{aligned}
\epsilon &\simeq \frac{1+i}{2} \frac{\operatorname{Im} M_{12}}{2\operatorname{Re} M_{12}} + \frac{1-i}{2} \frac{\operatorname{Re} A_0 \operatorname{Im} A_0}{\operatorname{Re}^2 A_0 - \operatorname{Im}^2 A_0} + i \frac{\operatorname{Im} A_0}{\operatorname{Re} A_0} \\
&= \frac{1+i}{2} \frac{\operatorname{Im} M_{12}}{2\operatorname{Re} M_{12}} + \frac{1-i}{2} \frac{\operatorname{Im} A_0}{\operatorname{Re} A_0} \frac{1}{\left(1 - \frac{\operatorname{Im}^2 A_0}{\operatorname{Re}^2 A_0}\right)} + i \frac{\operatorname{Im} A_0}{\operatorname{Re} A_0} \\
&\simeq \frac{1+i}{2} \left(\frac{\operatorname{Im} M_{12}}{2\operatorname{Re} M_{12}} + \frac{\operatorname{Im} A_0}{\operatorname{Re} A_0} \right) = \frac{e^{i\frac{\pi}{4}}}{\sqrt{2}} \left(\frac{\operatorname{Im} M_{12}}{2\operatorname{Re} M_{12}} + \frac{\operatorname{Im} A_0}{\operatorname{Re} A_0} \right).
\end{aligned} \tag{5.57}$$

To first approximation

$$\epsilon \simeq -\frac{e^{i\frac{\pi}{4}}}{\sqrt{2}} \left(\frac{\operatorname{Im} M_{12}}{\Delta m_k} \right) \tag{5.58}$$

since $-2 \operatorname{Re} M_{12} \simeq \Delta m_k$.

We are now ready to connect the general theory for the observable with the relevant effective Hamiltonian that lets us make theoretical predictions on the value of such observable. In order to calculate M_{12} it is necessary to use the $|\Delta S| = 2$ effective Hamiltonian which fortunately we found in the previous chapter and is given in eq. (4.105). Since

$$\operatorname{Im} M_{12} = \frac{1}{2m_K} \operatorname{Im} \left(\left\langle \bar{K}^0 \middle| \mathcal{H}_{\text{eff}}^{\Delta S = 2} \middle| K^0 \right\rangle \right), \tag{5.59}$$

it can be easily seen that

$$\begin{aligned}
|\epsilon| = \frac{G_F^2 M_W^2}{4\sqrt{2}\pi^2 m_k \Delta m_k} A^2 \lambda^6 \sigma \sin\delta \left\langle \bar{K}^0 \middle| \bar{s}\gamma^\mu P_L d \bar{s}\gamma_\mu P_L d \middle| K^0 \right\rangle \\
\times \left[\eta_3 S_0(x_c, x_t) - \eta_1 S_0(x_c) + A^2 \lambda^4 (1 - \sigma \cos\delta) \eta_2 S_0(x_t) \right],
\end{aligned} \tag{5.60}$$

where A, λ are the Wolfenstein CKM parameters introduced in eq. (1.103), while σ and δ are defined as $\sigma e^{i\delta} = \rho + i\eta$. Notice that both the NLO-QCD parameters η_i and the hadronic matrix element depend on the renormalization scale μ but their product is scale independent.

The most problematic factor to evaluate is the hadronic matrix element. This can be parametrized at LO in the following way [55, 54]

$$\left\langle \bar{K}^0 \middle| (\bar{s}_L \gamma^\mu d_L)^2 \middle| K^0 \right\rangle = \frac{8}{3} f_K^2 m_k^2 B_K \alpha_s(\mu)^{6/25}, \tag{5.61}$$

where f_K is the Kaon decay constant and B_K is a *bag parameter* which is μ-independent and encodes all the hadronic contributions.

5.4.2 Kaon Decays and ϵ'/ϵ

This is the parameter we are most interested in. Starting from the definitions in eqs. (5.34) and (5.46), we can easily show that

$$
\begin{aligned}
\epsilon' &= \frac{e^{i(\delta_2 - \delta_0)}}{\sqrt{2}} \left[\frac{((1+\bar{\epsilon})A_2 - (1-\bar{\epsilon})A_2^*)((1+\bar{\epsilon})A_0^* + (1-\bar{\epsilon})A_0)}{((1+\bar{\epsilon})A_0^* + (1-\bar{\epsilon})A_0)^2} \right. \\
&\quad \left. - \frac{((1+\bar{\epsilon})A_0 - (1-\bar{\epsilon})A_0^*)((1+\bar{\epsilon})A_2^* + (1-\bar{\epsilon})A_2)}{((1+\bar{\epsilon})A_0^* + (1-\bar{\epsilon})A_0)^2} \right] \\
&= \frac{e^{i(\delta_2 - \delta_0)}}{\sqrt{2}} \left[\frac{(i\,\mathrm{Im}\,A_2 + \bar{\epsilon}\,\mathrm{Re}\,A_2)(\mathrm{Re}\,A_0 + i\bar{\epsilon}\,\mathrm{Im}\,A_0)}{(\mathrm{Re}\,A_0 + i\bar{\epsilon}\,\mathrm{Im}\,A_0)^2} \right. \\
&\quad \left. - \frac{(i\,\mathrm{Im}\,A_0 + \bar{\epsilon}\,\mathrm{Re}\,A_0)(\mathrm{Re}\,A_2 + i\bar{\epsilon}\,\mathrm{Im}\,A_2)}{(\mathrm{Re}\,A_0 + i\bar{\epsilon}\,\mathrm{Im}\,A_0)^2} \right].
\end{aligned}
\tag{5.62}
$$

Neglecting terms of order $\bar{\epsilon}^2$, the numerator becomes

$$
\begin{aligned}
& i\,\mathrm{Im}\,A_2\,\mathrm{Re}\,A_0 + i\bar{\epsilon}\,\mathrm{Im}\,A_2\,\mathrm{Im}\,A_0 + \bar{\epsilon}\,\mathrm{Re}\,A_2\,\mathrm{Re}\,A_0 \\
& - i\,\mathrm{Im}\,A_0\,\mathrm{Re}\,A_2 - \bar{\epsilon}\,\mathrm{Re}\,A_0\,\mathrm{Re}\,A_2 - i\bar{\epsilon}\,\mathrm{Im}\,A_0\,\mathrm{Im}\,A_2 \\
& = i(\mathrm{Im}\,A_2\,\mathrm{Re}\,A_0 - \mathrm{Im}\,A_0\,\mathrm{Re}\,A_2).
\end{aligned}
\tag{5.63}
$$

By explicitly taking our a $\mathrm{Re}\,A_0$ and introducing the parameter ω from eq. (5.45), which is $\omega = \mathrm{Re}\,A_2 / \mathrm{Re}\,A_0$, then eq. (5.62) becomes

$$
\begin{aligned}
\epsilon' &= \frac{i e^{i(\delta_2 - \delta_0)}}{\sqrt{2}} \frac{\mathrm{Re}\,A_0(\mathrm{Im}\,A_2 - \omega\,\mathrm{Im}\,A_0)}{\mathrm{Re}^2 A_0 + 2i\bar{\epsilon}\,\mathrm{Re}\,A_0\,\mathrm{Im}\,A_0} \\
&= \frac{i e^{i(\delta_2 - \delta_0)}}{\sqrt{2}} \frac{\omega}{\mathrm{Re}\,A_0} \frac{\omega^{-1}\,\mathrm{Im}\,A_2 - \mathrm{Im}\,A_0}{1 + 2i(\bar{\epsilon}\,\mathrm{Im}\,A_0 / \mathrm{Re}\,A_0)}.
\end{aligned}
\tag{5.64}
$$

Since $\mathrm{Im}\,A_0 \ll \mathrm{Re}\,A_0$ then we can expand the denominator in orders of the parameter in brackets, obtaining the desired result

$$\epsilon' \simeq \frac{i\omega e^{i(\delta_2 - \delta_0)}}{\sqrt{2}} \left[\frac{\mathrm{Im}\,A_2}{\mathrm{Re}\,A_2} - \frac{\mathrm{Im}\,A_0}{\mathrm{Re}\,A_0} \right]. \tag{5.65}$$

Most of the time, ϵ' is normalized to ϵ

$$\frac{\epsilon'}{\epsilon} = \frac{i\omega e^{i(\delta_2 - \delta_0)}}{\sqrt{2}\epsilon}\left[\frac{\operatorname{Im} A_2}{\operatorname{Re} A_2} - \frac{\operatorname{Im} A_0}{\operatorname{Re} A_0}\right]. \tag{5.66}$$

Note that this new quantity, being the ratio of two CP-violating parameters, is not itself CP-violating.

The experimental world average of ϵ'/ϵ from NA48 [23] and KTeV [5, 11] collaborations reads

$$\left(\frac{\epsilon'}{\epsilon}\right)_{\text{exp}} = (16.6 \pm 2.3) \times 10^{-4}. \tag{5.67}$$

The theoretical analysis of ϵ'/ϵ has been subject to different refinements over the years. To obtain a non-zero value for ϵ', one must compute the loop level corrections. These corrections, as well as the operators that they generate in the effective theory, have been discussed before. It is important to note that the gluonic penguins play a central role in the generation of a non-vanishing ϵ' [76, 131, 138]. Moreover, electroweak penguins, due to their increasing contribution with the top quark mass m_t, become important for a sufficiently heavy top [35, 62, 111]. Not only that, but electroweak penguins tend to counteract the effect of the gluonic penguins, making the value of ϵ' smaller with an increasing top mass. These strong cancellations are what make the computation of ϵ'/ϵ so difficult. Moreover, because of the uncertainties in the determination of the hadronic matrix elements, an accurate prediction of ϵ'/ϵ, which was in line with the experimental value, was not possible.

This was before the RBC collaboration made enormous progress in the precise determination of both A_0 [2] and A_2 [18], where special attention was given to decreasing the uncertainties on the hadronic matrix elements as much as possible. For a comprehensive review on the history of ϵ'/ϵ and its recent development, one can read ref. [32].

Now we have an analytical formula per ϵ'/ϵ that depends on the two amplitudes A_0 and A_2 which we can compute using the $\Delta S = 1$ effective Hamiltonian [30]

$$A_I e^{i\delta_I} = \frac{G_F}{\sqrt{2}} V_{us}^* V_{ud} \sum_{i=1}^{10} [z_i(\mu) + \tau y_i(\mu)] \left\langle 2\pi, I \middle| Q_i(\mu) \middle| K^0 \right\rangle \tag{5.68}$$

where $\tau = -V_{ts}^* V_{td}/V_{us}^* V_{ud}$. Here z_i and y_i are a suitable redefinition of the Wilson coefficients computed in the $\overline{\text{MS}}$ scheme as a function of the scale μ. The hadronic matrix elements of the 10 operators we found in the previous chapter, also depend on the scale μ in such a way that the product of it with the Wilson coefficients is scale independent. These operator matrix elements are what made difficult the task of predicting the value of ϵ'/ϵ over the years. Some basic estimates have been done using the VIA approximation but it should be stressed that this method has no QCD basis and gives even the wrong sign for the $1/N$ corrections to the hadronic matrix elements [20, 21, 22, 34] which was even numerically confirmed by the RBC collaboration [2].

Nonetheless, it is instructive to see how this approximation works and the results it leads to. Usually, the hadronic matrix elements are given in terms of the B-parameters
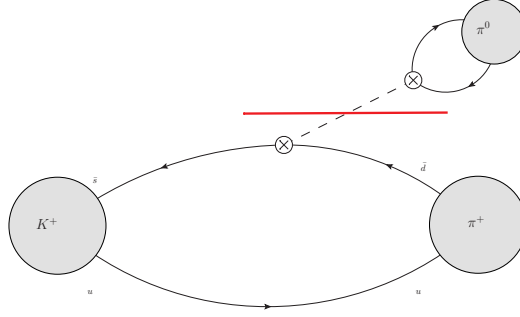
Figure 5.2. Wick contraction (disconnected) diagram for the $K^+ \to \pi^+\pi^0$ transition with effective operator insertion. The Vacuum Insertion Approximation is done by cutting along the red line.

(B for bag as before)

$$\langle 2\pi, I = 0|Q_i(\mu)|K\rangle = B_i^{(1/2)}(\mu)\,\langle 2\pi, I = 0|Q_i|K\rangle_{\text{VIA}}$$
$$\langle 2\pi, I = 2|Q_i(\mu)|K\rangle = B_i^{(3/2)}(\mu)\,\langle 2\pi, I = 2|Q_i|K\rangle_{\text{VIA}}$$

(5.69)

where the subscript VIA stands for the matrix elements in the Vacuum Insertion Approximation. If we take, as an example, the matrix element of the Q_2 type current-current operator

$$\left\langle \pi^+\pi^0 \middle| \bar{s}_L\gamma_\mu u_L \bar{u}_L\gamma^\mu d_L \middle| K^+ \right\rangle \simeq \left\langle \pi^0 \middle| \bar{s}_L\gamma^\mu u_L \middle| K^+ \right\rangle \left\langle \pi^+ \middle| \bar{u}_L\gamma_\mu d_L \middle| 0 \right\rangle \quad (5.70)$$

which, given that both the K^+ and the pions are pseudoscalars, can be simplified, following the cut on the disconnected diagram in fig. (5.2), to

$$\left\langle \pi^0 \middle| \bar{s}_L\gamma^\mu u_L \middle| K^+ \right\rangle \left\langle \pi^+ \middle| \bar{u}\gamma_\mu\gamma_5 d_L \middle| 0 \right\rangle$$
$$= \left[f_+(q^2)(\pi_{\pi^0} + p_{K^+})^\mu + f_0(q^2)(\pi_{\pi^0} - p_{K^+})^\mu \right] i f_\pi p_{\pi^+}^\mu,$$

(5.71)

where $q^2 = m_{\pi^+}^2$. Given that

$$p_{\pi^+}^\mu + p_{K^+}^\mu = p_{\pi^0}^\mu \implies \pi_{\pi^+} \cdot p_{\pi^+} = \frac{1}{2}\left(m_{\pi^+}^2 + m_{\pi^0}^2 - m_{K^+}^2\right) \quad (5.72)$$

and similarly

$$p_{\pi^+} \cdot p_{K^+} = \frac{1}{2}\left(m_{K^+}^2 + m_{\pi^+}^2 - m_{\pi^0}^2\right), \quad (5.73)$$

then the matrix element becomes

$$= i f_\pi \left[\frac{1}{2}\left(f_+(m_{\pi^+}^2) + f_0(m_{\pi^+}^2)\right)\left(m_{\pi^+}^2 + m_{\pi^0}^2 - m_{K^+}^2\right) \right.$$
$$\left. + \frac{1}{2}\left(f_+(m_{\pi^+}^2) - f_0(m_{\pi^+}^2)\right)\left(m_{K^+}^2 + m_{\pi^+}^2 - m_{\pi^0}^2\right) \right]$$

(5.74)

$$= i f_\pi \left[f_0(m_{\pi^+}^2)\left(m_{\pi^0}^2 - m_{K^+}^2\right) + f_+(m_{\pi^+}^2)m_{\pi^+}^2 \right].$$

And this is the VIA approximation for one of the two Wick contractions of the Q_2 hadronic matrix element. The other Wick contraction can be Fierzed back to the

one just found but with a factor $1/N$.

For $\mu < m_c$ one finds that the various matrix elements are given in VIA by [38]

$$\langle Q_1 \rangle_0 = -\frac{1}{9} X B_1^{(1/2)}, \tag{5.75}$$

$$\langle Q_2 \rangle_0 = \frac{5}{9} X B_2^{(1/2)}, \tag{5.76}$$

$$\langle Q_3 \rangle_0 = \frac{1}{3} X B_3^{(1/2)}, \tag{5.77}$$

$$\langle Q_4 \rangle_0 = \langle Q_3 \rangle_0 + \langle Q_2 \rangle_0 - \langle Q_1 \rangle_0, \tag{5.78}$$

$$\langle Q_5 \rangle_0 = \frac{1}{3} B_5^{(1/2)} \left\langle \overline{Q_6} \right\rangle_0, \tag{5.79}$$

$$\langle Q_6 \rangle_0 = -4\sqrt{\frac{3}{2}} \left[\frac{m_K^2}{m_s(\mu) + m_d(\mu)} \right]^2 \frac{F_\pi}{\kappa} B_6^{(1/2)} \tag{5.80}$$

$$\langle Q_7 \rangle_0 = -\left[\frac{1}{6} \left\langle \overline{Q_6} \right\rangle_0 (\kappa + 1) - \frac{X}{2} \right] B_7^{(1/2)} \tag{5.81}$$

$$\langle Q_8 \rangle_0 = -\left[\frac{1}{2} \left\langle \overline{Q_6} \right\rangle_0 (\kappa + 1) - \frac{X}{6} \right] B_8^{(1/2)} \tag{5.82}$$

$$\langle Q_9 \rangle_0 = \frac{3}{2} \langle Q_1 \rangle_0 - \frac{1}{2} \langle Q_3 \rangle_0, \tag{5.83}$$

$$\langle Q_{10} \rangle_0 = \langle Q_2 \rangle_0 + \frac{1}{2} \langle Q_1 \rangle_0 - \frac{1}{2} \langle Q_3 \rangle_0, \tag{5.84}$$

$$\langle Q_1 \rangle_2 = \langle Q_2 \rangle_2 = \frac{4\sqrt{2}}{9} X B_1^{(3/2)} \tag{5.85}$$

$$\langle Q_i \rangle_2 = 0, \quad i = 3, \ldots, 6 \tag{5.86}$$

$$\langle Q_7 \rangle_2 = -\left[\frac{\kappa}{6\sqrt{2}} \left\langle \overline{Q_6} \right\rangle_0 + \frac{X}{\sqrt{2}} \right] B_7^{(3/2)} \tag{5.87}$$

$$\langle Q_8 \rangle_2 = -\left[\frac{\kappa}{2\sqrt{2}} \left\langle \overline{Q_6} \right\rangle_0 + \frac{\sqrt{2}}{6} X \right] B_8^{(3/2)} \tag{5.88}$$

$$\langle Q_9 \rangle_2 = \langle Q_{10} \rangle_2 = \frac{3}{2} \langle Q_1 \rangle_2, \tag{5.89}$$

where

$$\kappa = \frac{F_\pi}{F_K - F_\pi}, \tag{5.90}$$

$$X = \sqrt{\frac{3}{2}} F_\pi \left(m_K^2 - m_\pi^2 \right), \tag{5.91}$$

and

$$\left\langle \overline{Q_6} \right\rangle_0 = \frac{\langle Q_6 \rangle_0}{B_6^{(1/2)}}. \tag{5.92}$$

As stated in eq. (5.34), electromagnetic contributions break isospin symmetry which generates two different A_2 amplitudes. The difference in mass between the up and down quark induces a mixing between the π^0 and the two isospin-singlet η and η'. As a consequence, the transition $K^0 \to \pi^0 \pi^0$ can also occur through the

intermediate state $\pi^0\eta$ or $\pi^0\eta'$. Due to the $\Delta I = 1/2$ rule we know that $A_0 \gg A_2$; since isospin breaking corrections are perturbative we can neglect isospin breaking effects in A_0. Therefore, the effect of isospin breaking can be reduced to corrections to $\operatorname{Im} A_2$ which are proportional to $\operatorname{Im} A_0$ [62]. One can define [35, 62]

$$\operatorname{Im} A_2 = \operatorname{Im} A_2' + \Omega_{IB}\omega \operatorname{Im} A_0, \qquad (5.93)$$

where A_2' is the $\Delta I = 3/2$ transition without isospin breaking effects. The Ω_{IB} term can be estimated using ChPT [50].

Thus, the analytical formula for ϵ'/ϵ in eq. (5.66) can be updated to include isospin-breaking effects

$$\epsilon' = \frac{ie^{i(\delta_2-\delta_0)}\omega}{\sqrt{2}}\frac{1}{\operatorname{Re} A_0}\Big[\omega^{-1}\operatorname{Im} A_2' - (1 - \Omega_{IB})\operatorname{Im} A_0\Big]. \qquad (5.94)$$

Chapter 6

UTfit Analysis

As seen in section 1.4.8, the Unitarity Triangle encodes all the important features of the flavour structure of the Standard Model. It is then of fundamental importance that the elements of the CKM matrix be measured with as much precision as possible. There are of course loads of observables we can look at to find the value of the CKM matrix elements, but one compelling way of inferring their value is by using all the possible measurements and theoretical predictions to constrain the $(\bar{\rho}, \bar{\eta})$ vertex. This kind of statistical analysis is central since it enables us not only to find the best possible prediction for the CKM matrix elements but even to constrain nonperturbative parameters, New Physics (NP) models and the energy scales at which the NP becomes relevant. This is due to the fact that we need to fit two parameters but the space of possible measurements and theoretical predictions is much bigger than two. This overconstrains the system enabling us to use the fitted values of the CKM parameters to find the posterior distribution of other interesting quantities.

Of course, one can take two possible statistical routes to find the posterior distribution of any given parameter or observables: one is the frequentist approach, which is followed by the CKMfitter group [47], and the other is the Bayesian approach [28] which is the one used by the UTfit collaboration and the one we will focus on. Both methods are valid in their own way and having two different approaches gives us the opportunity to check for consistency between the two results.

In this chapter, we are going to briefly discuss the basic idea behind this kind of analysis and how the Bayesian framework works. Then we give the specific setup to analyze and include in the updated UT analysis the direct CP-violation observable ϵ'/ϵ. For the second task, we are going to implement the code using the `HEPfit` library [60].

6.1 Statistical Methods

Imagine having a set of measured quantities, for example $\Delta m_d / \Delta m_s$, $|\epsilon_K|$, $\Gamma(b \to u)/\Gamma(b \to c)$ and so on. All these constraints, we label them as c_j, are related in some fashion to the CKM-triangle parameters $\bar{\rho}, \bar{\eta}$. The theoretical formulas which relate the CKM parameters and the constraints contains also other various parameters, we call it ancillary parameters, $\mathbf{x} = \{x_1, x_2, \cdots, x_N\}$. Some examples of these relations

can be found in section 6.3. What we have is some kind of equation of the form

$$c_j = c_j(\bar{\rho}, \bar{\eta}, \mathbf{x}). \tag{6.1}$$

In theory, the exact knowledge of c_j and $\mathbf{x}$, would imply the exact knowledge of both $\bar{\rho}, \bar{\eta}$ as long as the constraints are at least two. Each of the constraints c_j traces a curve in the $(\bar{\rho}, \bar{\eta})$ plane, whose intersection would give the vertex of the UT. In the realistic case, we do not know precisely the values of the constraints c_j and neither do for the model parameters $\mathbf{x}$. Moreover, we would like to give different probabilities to those values which we "know" must be in some region. For example, in the case of ϵ'/ϵ we are more likely to accept a value of zero than a value of a hundred. This means that instead of curves in the plane, we will have regions that depend on the distribution of the set $\{c_j, \mathbf{x}\}$ and our confidence on the values of $\bar{\rho}$ and $\bar{\eta}$ clusters in a region of the plane. This can be formalised using the Bayesian approach [58].

If we consider the distribution of the various parameters $\bar{\rho}, \bar{\eta}, c_j$ and $\mathbf{x}$ given the measured values of the constraints $\hat{c}_j$, we can make use of Bayes theorem so that

$$f(\bar{\rho}, \bar{\eta}, c_j, \mathbf{x}|\hat{c}_j) \propto f(\hat{c}_j|c_j, \bar{\rho}, \bar{\eta}, \mathbf{x}) \cdot f(c_j, \bar{\rho}, \bar{\eta}, \mathbf{x}), \tag{6.2}$$

where $f(\cdot)$ is the probability distribution and $f(\cdot|\cdot)$ is the conditional probability distribution.

If we assume the independence of the different quantities and the fact that $\hat{c}_j$ depends on $(\bar{\rho}, \bar{\eta}, \mathbf{x})$ only via c_j, then by making use of simple probability rules we get

$$f(\bar{\rho}, \bar{\eta}, c_j, \mathbf{x}|\hat{c}_j) \propto f(\hat{c}_j|c_j) \cdot f(c_j|\bar{\rho}, \bar{\eta}, \mathbf{x}) \cdot f(\mathbf{x}, \bar{\rho}, \bar{\eta}). \tag{6.3}$$

It is safe to assume that the distribution of the constraints given $\bar{\rho}, \bar{\eta}$ and $\mathbf{x}$ is simply given by

$$f(c_j|\bar{\rho}, \bar{\eta}, \mathbf{x}) \propto \delta(c_j - c_j(\bar{\rho}, \bar{\eta}, \mathbf{x})), \tag{6.4}$$

then

$$f(\bar{\rho}, \bar{\eta}, c_j, \mathbf{x}|\hat{c}_j) \propto f(\hat{c}_j|c_j) \cdot \delta(c_j - c_j(\bar{\rho}, \bar{\eta}, \mathbf{x})) \cdot f(\mathbf{x}) \cdot f_o(\bar{\rho}, \bar{\eta}). \tag{6.5}$$

In eq. (6.5) enters the first important new quantity, $f_o(\bar{\rho}, \bar{\eta})$ which is the *prior distribution* of the two parameters. This distribution is chosen to be flat most of the time since we do not have any reason to consider some values as more probable than others. The specific choice of the prior distribution is the most debated subject when dealing with the Bayesian approach, even if the choice of a flat prior is sensible.

At the end, to find the distribution of the CKM parameters $f(\bar{\rho}, \bar{\eta})$, is just a matter of integrating eq. (6.5) over c_j and $\mathbf{x}$.

This is the basic concept behind Bayesian inference. The extension of these concepts to the case of several constraints is straightforward

$$f(\bar{\rho}, \bar{\eta}, \mathbf{x}|\hat{c}_1, \hat{c}_2, \cdots, \hat{c}_M) \propto \prod_{j=1}^{M} f_j(\hat{c}_j|\bar{\rho}, \bar{\eta}) \times \prod_{i=1}^{N} f_i(x_i) \cdot f_o(\bar{\rho}, \bar{\eta}), \tag{6.6}$$

where the explicit dependence on the c_j has been excluded by integration. If we then integrate over $\mathbf{x}$, we get the interesting relation

$$f(\bar{\rho}, \bar{\eta}|\hat{\mathbf{c}}) \propto \mathcal{L}(\hat{\mathbf{c}}|\bar{\rho}, \bar{\eta}, \mathbf{x}) \cdot f_o(\bar{\rho}, \bar{\eta}), \tag{6.7}$$

where $\hat{\mathbf{c}}$ stands for the set of measured constraints, and

$$\mathcal{L}(\hat{\mathbf{c}}|\bar{\rho},\bar{\eta},\mathbf{x}) \propto \int \prod_{j=1}^{M} f_j(c_j|\bar{\rho},\bar{\eta},\mathbf{x}) \prod_{i=1}^{N} f_i(x_i) \tag{6.8}$$

is the *likelihood function.*

We can see now that, even if a priori all the values of $\bar{\rho}$ and $\bar{\eta}$ are considered equally likely, a posteriori the probability clusters around the point which maximises the likelihood. In conclusion, the final probability distribution obtaining starting from a flat prior of $\bar{\rho}$ and $\bar{\eta}$ is

$$f(\bar{\rho},\bar{\eta}) \propto \int \prod_{j=1}^{M} f_j(\hat{c}_j|\bar{\rho},\bar{\eta},\mathbf{x}) \prod_{i=1}^{N} f_i(x_i)\,\mathrm{d}x_i\,. \tag{6.9}$$

The normalization of this distribution is trivial.

In general, the posterior distribution specified in eq. (6.9), cannot be computed easily. The integration has to be done using Monte Carlo sampling algorithms that can, in most cases, lead to unacceptable computing time because of the intrinsic inefficacy of sampling the parameter space. In the case of the `HEPfit` library, this problem is overcome by means of Markov Chain Monte Carlo (MCMC) methods using a Metropolis-Hastings algorithm for the sampling [44] a summary of which is given in Appendix B.

6.2 Preliminary Setup

As a first step, we need to build up the code for the determination of ϵ'/ϵ starting from the hadronic matrix elements given by the RBC collaboration which come with their own errors and correlation matrix. Since in the relevant formula for ϵ'/ϵ, given in equation eq. (5.66), there appears both the $\Delta I = 1/2$ and the $\Delta I = 3/2$ amplitudes, we will take the first contributions from the recent paper [2] and implement them directly in the code the determination for the A_0 amplitude while for the latter we will directly use the values of the amplitudes found in the companion paper [25] since no correlation matrix for the hadronic matrix elements is given in that case. I will now outline the two main strategies for the determination of ϵ'/ϵ

The pure lattice strategy: in this case we will start from the unrenormalized infinite-volume lattice matrix elements in the chiral basis and then implement in the code the renormalization to the non-perturbative scheme [115] SMOM($\not{q},\not{q}$), the perturbative matching to $\overline{\text{MS}}$ and the conversion to the 10-operator basis. To check if the result is consistent, we will also cut out a step, starting from the SMOM($\not{q},\not{q}$) renormalized matrix elements in the chiral basis and implement only the perturbative matching and the conversion to the 10-operator basis. Then, in both cases, the lattice values of both A_0 and A_2 are used in the evaluation ϵ'/ϵ.

Mixed lattice-experimental strategy: in this case we will use the experimental value of $\text{Re}\,A_0$ as input to the lattice value of $\text{Im}\,A_0$ in order to decrease

the error [37, 102]. The specific procedure is discussed in the RBC article [2] and we will give a brief overview later. Then for the evaluation of ϵ'/ϵ the improved lattice value of $\text{Im} A_0$, the standard lattice value of $\text{Im} A_2$ and the experimental values of $\text{Re} A_0$ and $\text{Re} A_2$ are used.

When the basic code is implemented, we can make a Monte Carlo simulations by varying all the relevant parameters which, besides the hadronic matrix elements, are: the values of the $\text{SMOM}(\slashed{q}, \slashed{q})$ renormalization matrix elements, where used, the CKM matrix elements which enter in the formula for ϵ'/ϵ, the Fermi constant G_F, the strong phases δ_0 and δ_2, the ϵ parameter, the experimental values of $\text{Re} A_0$ and $\text{Re} A_2$, the lattice value of $\text{Re} A_2$ and $\text{Im} A_2$. All these parameters, together with their central values and errors are given in table (6.1).

It is important to note that when the full UT-analysis is in place, the coefficients related to the CKM matrix are going to be extrapolated by the various input parameters and are going to be varied accordingly. Therefore the CKM coefficients are in tab. (6.1) are temporary, used for the preliminary results to reconstruct the RBC value of ϵ'/ϵ.

For the moment, we did not implement the evaluation of the Wilson coefficients directly in the code. This is indeed needed for the Monte Carlo to calculate the error associated to the truncation of the perturbative series. The Wilson coefficients of table (6.2) were therefore taken directly from the RBC article and the error on the final result was added as a systematic error taking the significant figure given by the RBC collaboration [2]. This is for now a good approximation, but we are currently working on adding the code to the `HEPfit` package.

We are now going to give more details on the two approaches mentioned before.

In the `HEPfit` framework, all the parameters which enter in the Monte Carlo simulations, are given to the code by a configuration file. In this file, we list the various parameters with their central values as well as their error which we can give as both a standard error associated to normal prior distribution for the values of the parameter, or as the error associated to a flat prior distribution. In our case, the priors are all chosen to be gaussian.

6.2.1 The Pure Lattice Strategy & General Remarks

When we started from the unrenormalized infinite-volume lattice matrix elements, even the $\text{SMOM}(\slashed{q}, \slashed{q})$ matrix elements have to be given by the configuration file since they come with their own error being evaluated on the lattice.

The values of the matrix elements are given in table (6.3), while the ones for the $\text{SMOM}(\slashed{q}, \slashed{q})$ renormalization matrix $Z_{ij}^{\text{SMOM}(\slashed{q},\slashed{q})\leftarrow\text{lat}}$ are given in table (6.4).

Table 6.1. Standard Model and other experimental inputs required to determine A_0 and $\text{Re}(\epsilon'/\epsilon)$. These values are obtained from thew PDG Review of Particle Physics [152], apart from those of $\text{Re}\,A_0$, $\text{Re}\,A_2$ and their ratio ω, that were taken from [18]. The parameter τ is given by the CKM ratio $\tau = -V_{ts}^* V_{td}/V_{us}^* V_{ud}$. The quantities marked with (†) are the ones which error enters in the statistical error while the ones marked with (∗) enter as systematic errors. The second block of parameters enter in the Wilson coefficients.

Quantity	Value	
G_F	$1.16638 \times 10^{-5}\,\text{GeV}^{-2}$	
λ	0.2255	
A	0.82	
$\bar{\rho}$	0.132	
$\bar{\eta}$	0.351	
ϕ_ε	$0.7596\,\text{rad}$	(†)
τ	$0.001558(65) - 0.000663(33)\text{i}$	(∗)
$|\varepsilon|$	$0.002228(11)$	(†)
ω	$0.04454(12)$	(†)
δ_0	$32.3(2.1)^\circ$	(†)
δ_2	$-11.6(2.8)^\circ$	(†)
$\text{Re}\,(A_0)_{\text{expt}}$	$3.3201(18) \times 10^{-7}\,\text{GeV}$	(†)
$\text{Re}\,(A_2)_{\text{expt}}$	$1.479(4) \times 10^{-8}\,\text{GeV}$	(†)
$\text{Re}(A_2)_{\text{lat}}$	$1.50(15) \times 10^{-8}$	(†)
$\text{Im}(A_2)_{\text{lat}}$	$-8.34(1.03) \times 10^{-13}$	(†)
$m_c\,(m_c)$	$1.27(2)\,\text{GeV}$	(∗)
$m_b\,(m_b)$	$4.18(3)\,\text{GeV}$	(∗)
$m_W\,(m_W)$	$80.379(12)\,\text{GeV}$	(∗)
$m_Z\,(m_Z)$	$91.1876(21)\,\text{GeV}$	(∗)
$m_t\,(m_t)$	$160.0(4.8)\,\text{GeV}$	(∗)
$\alpha_s^{N_f=5}\,(m_Z)$	0.1181	(∗)
α	$1/127.955(10)$	(∗)
$\sin^2(\theta_W)$	$0.23122(3)$	(∗)

Table 6.2. MSbar Wilson coefficients at $\mu = 4.006$ GeV computed via NLO QCD+EW perturbation theory.

i	y_i	z_i
1	0	-0.199111
2	0	1.08976
3	0.0190166	-0.00525073
4	-0.0560629	0.0244698
5	0.0132642	-0.00607434
6	-0.0562033	0.0174607
7	-0.000271245	0.000134906
8	0.000521236	-0.000119628
9	-0.00946862	5.60698×10^{-5}
10	0.00186152	9.34113×10^{-5}

Table 6.3. Bare lattice matrix elements in the 7-operator basis given by the minimization procedure discussed in the article. These are quoted in physical units and contain the Lellouch-Lüscher finite-volume correction.

i	$Q_i'\left(\text{GeV}^3\right)$
1	$0.143(93)$
2	$-0.147(24)$
3	$0.233(23)$
4	$-$
5	$-0.723(91)$
6	$-2.211(144)$
7	$1.876(52)$
8	$5.679(107)$
9	$-$
10	$-$

Table 6.4. Renormalization matrices for SMOM($\not{q}, \not{q}$) scheme at $\mu = 4.006$ GeV.

0.42011(43)	0	0	0	0	0	0
0	0.422(38)	-0.207(36)	-0.005(13)	0.0084(77)	0	0
0	-0.094(24)	0.570(24)	-0.0120(83)	0.0059(47)	0	0
0	-0.14(14)	-0.15(12)	0.424(44)	0.013(26)	0	0
0	-0.030(63)	-0.073(66)	-0.106(23)	0.620(15)	0	0
0	0	0	0	0	0.47715(49)	-0.02113(24)
0	0	0	0	0	-0.05960(55)	0.6030(14)

Of fundamental importance for our analysis is the correlation between the operators. Instead of correlations, the authors give the covariance between them, but the two are related by the simple formula

$$\Sigma_{ij} = \sigma_i \sigma_j \rho_{ij}, \qquad (6.10)$$

where Σ_{ij} is the covariance matrix, σ_i is the error associated to the operator Q_i and ρ_{ij} is the correlation matrix. Both correlation and covariance matrices between the unrenormalized infinite-volume lattice matrix elements in the chiral basis are given in table (6.5).

Table 6.5. The 7×7 covariance (upper) and correlation (lower) matrices between the un-renormalized, infinite-volume matrix elements in the chiral basis.

0.008592	0.0001823	-0.0003235	0.0006934	-0.001432	0.002596	0.003095
0.0001823	0.0005819	-0.0001568	0.0008119	0.0007138	6.741×10^{-5}	-0.0005478
-0.0003235	-0.0001568	0.0005280	0.0004485	0.001028	-0.0001371	0.0003523
0.0006934	0.0008119	0.0004485	0.008201	0.004850	-0.0004420	-0.001480
-0.001432	0.0007138	0.001028	0.004850	0.02069	-0.001612	-0.005933
0.002596	6.741×10^{-5}	-0.0001371	-0.0004420	-0.001612	0.002693	0.004010
0.003095	-0.0005478	0.0003523	-0.001480	-0.005933	0.004010	0.01145

1.	0.0816756	-0.151239	0.0819331	-0.10693	0.536807	0.311024
0.0816756	1.	-0.284058	0.371749	0.206539	0.0540144	-0.213318
-0.151239	-0.284058	1.	0.214286	0.310386	-0.114632	0.143153
0.0819331	0.371749	0.214286	1.	0.370116	-0.0934066	-0.151998
-0.10693	0.206539	0.310386	0.370116	1.	-0.215278	-0.38506
0.536807	0.0540144	-0.114632	-0.0934066	-0.215278	1.	0.720705
0.311024	-0.213318	0.143153	-0.151998	-0.38506	0.720705	1.

To check the final result, rather than starting from the unrenormalized matrix elements, for which the renormalization matrix enters in the Monte Carlo, we started from the SMOM($\not{q}, \not{q}$) renormalized matrix elements whose values are given in table (6.6).

Table 6.6. Physical, infinite-volume matrix elements in the SMOM($\not{q}, \not{q}$) scheme at $\mu = 4.007$ GeV in the chiral basis.

i	SMOM($\not{q}, \not{q}$) $\left(\text{GeV}^3\right)$
1	0.060(39)
2	$-0.125(19)$
3	0.142(17)
4	$-$
5	$-0.351(62)$
6	$-1.306(90)$
7	0.775(23)
8	3.312(63)
9	$-$
10	$-$

While their covariance, as well as correlation, matrices are given in table (6.7).

Table 6.7. The 7×7 covariance (upper) and correlation(lower) matrices between the renormalized, infinite-volume matrix elements in the SMOM$(\not{q},\not{q})$ scheme in the chiral basis.

0.001516	5.385×10^{-5}	-9.167×10^{-5}	0.0001252	-0.0003965	0.0004930	0.0007192
5.385×10^{-5}	0.0003563	-4.099×10^{-5}	0.0007596	0.0002981	2.914×10^{-5}	-0.0002118
-9.167×10^{-5}	-4.099×10^{-5}	0.0002808	0.0003784	0.0004679	-4.656×10^{-5}	0.0001516
0.0001252	0.0007596	0.0003784	0.003904	0.001679	-8.000×10^{-5}	-0.0004013
-0.0003965	0.0002981	0.0004679	0.001679	0.008188	-0.0003817	-0.002110
0.0004930	2.914×10^{-5}	-4.656×10^{-5}	-8.000×10^{-5}	-0.0003817	0.0005395	0.0009460
0.0007192	-0.0002118	0.0001516	-0.0004013	-0.002110	0.0009460	0.003937

1.	0.0726721	-0.138265	0.0517783	-0.112963	0.54961	0.292715
0.0726721	1.	-0.126904	0.644822	0.174327	0.0666819	-0.176942
-0.138265	-0.126904	1.	0.359013	0.305817	-0.119079	0.14155
0.0517783	0.644822	0.359013	1.	0.300896	-0.056101	-0.102739
-0.112963	0.174327	0.305817	0.300896	1.	-0.184396	-0.372134
0.54961	0.0666819	-0.119079	-0.056101	-0.184396	1.	0.652864
0.292715	-0.176942	0.14155	-0.102739	-0.372134	0.652864	1.

The following step is then, in both cases, to match the non-perturbative matrix elements to a perturbative scheme. In this case, since the Wilson coefficients are given in the $\overline{\text{MS}}$ scheme, we need to match to this. The perturbative matching is known up to first order in α_s [109]. We give here the result for the matching from SMOM$(\not{q},\not{q})$ given in the article where

$$Z_{ij}^{\overline{\text{MS}}\leftarrow\text{SMOM}(\not{q},\not{q})} = \mathbb{1} + \frac{\alpha_s(\mu)}{4\pi}\left(\Delta r_{ij}^{\overline{\text{MS}}\leftarrow\text{RI}} \Big/ \frac{\alpha_s(\mu)}{4\pi}\right) \tag{6.11}$$

(i,j)	$\Delta r_{ij}^{\overline{\text{MS}}\leftarrow\text{RI}} \Big/ \frac{\alpha_s(\mu)}{4\pi}$
$(1,1)$	$\xi\left(\frac{C_0}{N_c} - C_0 - \frac{4\log(2)}{N_c} + 4\log(2)\right) - \frac{12\log(2)}{N_c} + 12\log(2) + \frac{9}{N_c} - 9$
$(2,2)$	$\xi\left(\frac{4C_0 N_c}{5} + \frac{C_0}{N_c} - \frac{6C_0}{5} - \frac{4\log(2)}{N_c} - \frac{4N_c}{5} + \frac{6}{5}\right) - \frac{12\log(2)}{N_c} + \frac{8N_c}{5} + \frac{9}{N_c} - \frac{12}{5}$
$(2,3)$	$\xi\left(\frac{6C_0 N_c}{5} - \frac{9C_0}{5} + 4\log(2) - \frac{6N_c}{5} + \frac{4}{5}\right) + 12\log(2) + \frac{12N_c}{5} - \frac{53}{5}$
$(3,2)$	$\xi\left(-\frac{6C_0 N_c}{5} + \frac{4C_0}{5} + 4\log(2) + \frac{6N_c}{5} - \frac{9}{5}\right) + 12\log(2) - \frac{12N_c}{5} + \frac{2}{3N_c} - \frac{263}{45}$
$(3,3)$	$\xi\left(-\frac{9C_0 N_c}{5} + \frac{C_0}{N_c} + \frac{6C_0}{5} - \frac{4\log(2)}{N_c} + \frac{9N_c}{5} - \frac{6}{5}\right) - \frac{12\log(2)}{N_c} - \frac{18N_c}{5} + \frac{85}{9N_c} + \frac{26}{15}$
$(3,5)$	$\frac{2}{9N_c}$
$(3,6)$	$-\frac{2}{9}$
$(5,5)$	$\xi\left(\frac{C_0}{2N_c} - \frac{2\log(2)}{N_c} - \frac{1}{2N_c}\right) + \frac{3C_0}{2N_c} - \frac{2\log(2)}{N_c} - \frac{2}{N_c}$
$(5,6)$	$\xi\left(-\frac{C_0}{2} + 2\log(2) + \frac{1}{2}\right) - \frac{3C_0}{2} + 2\log(2) + 2$
$(6,2)$	$\frac{5}{N_c} - \frac{10}{3}$
$(6,3)$	$\frac{10}{3N_c} - 5$
$(6,5)$	$\left(2\log(2) - \frac{1}{2}\right)\xi + 2\log(2) + \frac{5}{3N_c} - 2$
$(6,6)$	$\xi\left(-\frac{C_0 N_c}{2} + \frac{C_0}{2N_c} - \frac{2\log(2)}{N_c} + N_c - \frac{1}{2N_c}\right) - \frac{3C_0 N_c}{2} + \frac{3C_0}{2N_c} - \frac{2\log(2)}{N_c} + 4N_c - \frac{2}{N_c} - \frac{5}{3}$
$(7,7)$	$\xi\left(\frac{C_0}{2N_c} - \frac{2\log(2)}{N_c} - \frac{1}{2N_c}\right) + \frac{3C_0}{2N_c} - \frac{2\log(2)}{N_c} - \frac{2}{N_c}$
$(7,8)$	$\xi\left(-\frac{C_0}{2} + 2\log(2) + \frac{1}{2}\right) - \frac{3C_0}{2} + 2\log(2) + 2$
$(8,7)$	$\left(2\log(2) - \frac{1}{2}\right)\xi + 2\log(2) - 2$
$(8,8)$	$\xi\left(-\frac{C_0 N_c}{2} + \frac{C_0}{2N_c} - \frac{2\log(2)}{N_c} + N_c - \frac{1}{2N_c}\right) - \frac{3C_0 N_c}{2} + \frac{3C_0}{2N_c} - \frac{2\log(2)}{N_c} + 4N_c - \frac{2}{N_c}$

where ξ is the gauge fixing parameter[1], $C_0 \approx 2.34391$ is a constant whose definition can be found in reference and N_c is the number of colors. The value of α_s at the relevant scale $\mu = 4.006$ GeV is

$$\alpha_s(\mu = 4.006 \text{ GeV}) = 0.21499825. \tag{6.12}$$

Once we have the $\overline{\text{MS}}$ renormalized, infinite-volume, matrix elements in the chiral basis, we need to go to the usual 10-operator basis. To do this we employ the transformation of eq. (4.70).

Sadly, we could not start directly from the $\overline{\text{MS}}$ 10-operator matrix elements since the covariance matrix given in the article had a negative determinant. This is probably due to the precision to which the matrix is given. We reached out to the authors of the article, which gave us a covariance matrix with more digits, for which I am very grateful, but still, the issue remained. In the end, we implemented the code starting from either the lattice matrix elements with their associated covariance matrix or the SMOM renormalized matrix elements with their covariance matrix.

Now we had all the ingredients to evaluate the A_0 amplitude and consequently ϵ'/ϵ. We leave the results to the following chapter.

6.2.2 Mixed Lattice-Experimental Strategy

For this approach, only the unrenormalized, infinite-volume, lattice matrix elements are used. This is because of the specific procedure which is discussed in the paper and we are going to summarize now.

The general idea is to use the experimental value of $\text{Re}\,A_0$ to "eliminate" one of the lattice matrix elements in order to decrease the error. The operator which is eliminated is chosen based on how much the final error decreases. What the authors found is that the most significant gain in statistical error is achieved by replacing the matrix elements M_3.

The final formula then becomes

$$\text{Im}\,A_0 = \frac{G_F}{\sqrt{2}} V_{us}^* V_{ud} \sum_{\substack{k=1 \\ k\neq 3}}^{7} \text{Im}(w_k^{\overline{\text{MS}}\leftarrow\text{lat}}) M_k'^{\text{lat}}$$

$$+ \frac{\text{Im}(w_3^{\overline{\text{MS}}\leftarrow\text{lat}})}{\text{Re}(w_3^{\overline{\text{MS}}\leftarrow\text{lat}})} \left[\text{Re}\,A_0 - \frac{G_F}{\sqrt{2}} V_{us}^* V_{ud} \sum_{\substack{k=1 \\ k\neq 3}}^{7} \text{Re}(w_k^{\overline{\text{MS}}\leftarrow\text{lat}}) M_k'^{\text{lat}} \right], \tag{6.13}$$

where

$$\text{Re}\left(w_k^{\overline{\text{MS}}\leftarrow\text{lat}} \right) = \sum_{i=1}^{10} \sum_{j=1}^{7} \left(z_i^{\overline{\text{MS}}} + \text{Re}(\tau) y_i^{\overline{\text{MS}}} \right) T_{ij} Z_{jk}^{\overline{\text{MS}}\leftarrow\text{lat}}$$

$$\text{Im}\left(w_k^{\overline{\text{MS}}\leftarrow\text{lat}} \right) = \sum_{i=1}^{10} \sum_{j=1}^{7} \left(\text{Im}(\tau) y_i^{\overline{\text{MS}}} \right) T_{ij} Z_{jk}^{\overline{\text{MS}}\leftarrow\text{lat}} \tag{6.14}$$

---

[1] We will set this to $\xi = 1$ which is the Landau gauge used in the RBC article.

are the "Lattice Wilson Coefficients" and $Z^{\overline{\text{MS}} \leftarrow \text{lat}}$ is the product of the SMOM renormalization matrix and the $\overline{\text{MS}}$ matching matrix. $M_k'^{\text{lat}}$ are the lattice matrix elements in the chiral basis.

This value of Im A_0 is then used to find $\text{Re}(\epsilon'/\epsilon)$ where now $\text{Re}\,A_0$ and $\text{Re}\,A_2$ are taken from experiments and Im A_2 is still the lattice result.

6.2.3 Including Isospin-Breaking Contributions

All the discussions carried so far are based on the hypothesis that isospin is a perfectly valid quantum number. Unfortunately, this is not the case. There are many sources of isospin symmetry breaking, the main one being the difference in mass between the two first family quarks induced by electromagnetic interactions: the up and the down quarks. Being their masses different, we cannot consider them as part of the same $SU(2)$ doublet. This mass difference is very tiny but, while for most quantities the corrections including isospin breaking are very small, for ϵ' this behaviour does not hold.

As we can see from the master formula for ϵ'/ϵ eq. (5.66), the two amplitudes for the $I = 0$ and $I = 2$ case enter with the same weight. However, we know from the $\Delta I = 1/2$ rule, eq. (5.40), that the amplitude of A_2 is much greater than A_0, thus even a small correction to A_0 can introduce a 20 times bigger correction to A_2 and potentially a similar order of magnitude correction to ϵ'.

The effects of isospin breaking have been thoroughly studied before by means of chiral perturbation theory [35, 49, 50, 51], and even very recently including the effects of the η^0 to the chiral Lagrangian [7, 36]. As we have seen in the previous chapter, the contribution is parametrized by a quantity $\hat{\Omega}_{IB}$ which includes the appropriate correction due to the electroweak penguin. Following the master formula of [49], which is just a rearrangement of eq. (5.94),

$$\frac{\epsilon'}{\epsilon} = \frac{i\omega_+ e^{i(\delta_2 - \delta_0)}}{\sqrt{2}\epsilon} \left[\frac{\text{Im}\left(A_2^{\text{emp}}\right)}{\text{Re}\left(A_2^{(0)}\right)} - (1 - \hat{\Omega}_{IB}) \frac{\text{Im}\left(A_0^{(0)}\right)}{\text{Re}\left(A_0^{(0)}\right)} \right], \qquad (6.15)$$

they find $\hat{\Omega}_{IB} = (17.0^{+9.1}_{-9.0}) \times 10^{-2}$. This parameter can be simply introduced in our evaluation of ϵ'/ϵ by taking $\text{Re}\left(A_{0,2}^{(0)}\right)$ ad the experimental ones, while $\text{Im}\left(A_2^{\text{emp}}\right)$ and $\text{Im}\left(A_0^{(0)}\right)$ are given by the lattice results. The quantity $\omega_+ = \text{Re}(A_2^+)/\text{Re}(A_0)$ coming from the charged kaon decay is given, again, experimentally.

6.3 Standard UT Analysis

Virtually any process involving weak interactions is connected in some way to the CKM matrix. Its matrix elements are therefore fundamental parameters and should be measured as precisely as possible.

One way of finding these matrix elements is by combining all experimental, as well as theoretical, observables and fit them together under a chosen statistical framework. This is the idea behind the standard Unitarity Triangle analysis. In particular, the UTfit collaboration, uses a Bayesian framework to infer the region of highest

probability for the various CKM parameters.

Let us give some basic examples of observables and how they relate to the UT

- The ratio of the semileptonic decay rates of charmed and charmless b-hadrons allows to measure the ratio

$$\left|\frac{V_{ub}}{V_{cb}}\right| = \frac{\lambda}{1 - \lambda^2/2}\sqrt{\bar{\rho}^2 + \bar{\eta}^2}, \tag{6.16}$$

where the RHS has been experimentally measured and is tied to the Wolfenstein parameters $\bar{\rho}, \bar{\eta}$.

- The mass difference between the light and heavy mass eigenstates of the $B_d^0 - \bar{B}_d^0$ system

$$\Delta m_d = \frac{G_F^2}{6\pi^2} M_W^2 \eta_c S(x_t) A^2 \lambda^6 \left[(1-\bar{\rho})^2 + \bar{\eta}^2\right] m_{B_d} f_{B_d}^2 \hat{B}_{B_d}, \tag{6.17}$$

where $S(x)$ is the relevant Inami-Lim function [96], $x_t = m_t^2/m_w^2$ and m_t is the top quark mass in the $\overline{\text{MS}}$ scheme at the top quark mass. The other factors, beside the CKM ones, encode nonperturbative quantities. This is most of the time used as a ratio with Δm_s.

- The indirect CP-violation parameter in the kaon system, as of eq. (5.60),

$$|\epsilon_K| = C_\epsilon A^2 \lambda^6 \bar{\eta} \left[-\eta_1 S_0(x_c) + \eta_2 S_0(x_t)\left(A^2 \lambda^4 (1-\bar{\rho})\right) + \eta_3 S_0(x_c, x_t)\right] \hat{B}_K, \tag{6.18}$$

where again $S_0(x), S_0(x_i, x_j)$ are the appropriate Inami-Lim functions [30, 40, 96].

and many more. If we knew these observables with infinite precision, they would trace curves in the $(\bar{\rho}, \bar{\eta})$ plane whose intersection would give us the precise value of $\bar{\rho}, \bar{\eta}$. Of course, this is not the case and every measurement, as well as lattice quantity, comes with its own error. In this case, we would not find curves but regions whose intersection would give us the highest probability region for both $\bar{\rho}$ and $\bar{\eta}$.

Since the observables we have at hand are much more than the two parameters we are trying to extract, the system is clearly over-constrained. This means that we can not only find the CKM parameters but even infer the value of other quantities like other observables, like Δm_s, or nonperturbative parameters like $f_{B_d}^2 \hat{B}_{B_d}$.

Moreover, one can check for SM consistency since if we find an observable whose curve in the $(\bar{\rho}, \bar{\eta})$ plane does not intersect with the others in the right spot, then we clearly have a case where Beyond the SM contributions are relevant and need to be taken into account.

In the case of this thesis, what we are going to do is to first implement the UT analysis into `HEPfit` and then find how much the inclusion of ϵ'/ϵ changes the result on the various CKM related parameters.

A complete list of the observables and parameters used in our analysis can be found in Appendix C, where all the relevant configuration files used in the analysis are given. The name of the various parameters and observables can be easily understood.

6.4   BSM Analysis

A similar analysis can be carried out to infer the bounds of relevant BSM contributions to a given observable. In this thesis, we are not going to delve into the BSM analysis but in the near future, we certainly will. Particularly in the case of ϵ'/ϵ since it is thought that BSM contributions to this observable are really important and help us get a theoretical value that is consistent with the experimental one [8, 9, 10].

What one can do is, not only to bound the value of effective operator hadronic matrix elements which are hard to evaluate, but even bound the Wilson coefficients together with the scale at which the NP contribution associated to such operators becomes relevant [28].

The BSM analysis will be the subject of a future study.

Chapter 7

Results

In this chapter, we give a summary of the various results obtained in this thesis work. We start from the preliminary analysis on $\mathrm{Re}(\epsilon'/\epsilon)$ as discussed in the previous chapter, with some comments on the comparison between our results and the RBC ones. Then we are going to discuss the UT fit results with and without the inclusion of ϵ'/ϵ and see how much the result changes between the two. We do not expect an appreciable difference between the two results and this is in fact what we will find.

7.1 Preliminary Results

Here we give the results for the posterior distributions of $\mathrm{Re}(\epsilon'/\epsilon)$ found by Monte Carlo simulations for the two strategies outlined in the previous chapter. We will start with the plots and then make some comments and checks with the results found by the RBC collaboration. Of course, we need to remember that the RBC collaboration used a jackknife technique on all lattice quantities when evaluating their central values and errors.

7.1.1 Pure Lattice Approach

As we can see from figures (7.1) and (7.2), the central values are consistent with each other

$$\mathrm{Re}(\epsilon'/\epsilon)_{\mathrm{lat}} = 0.00305 \pm 0.00127 \qquad \mathrm{Re}(\epsilon'/\epsilon)_{\mathrm{SMOM}} = 0.00309 \pm 0.00114. \quad (7.1)$$

But these results are somewhat different from the smaller value found by the RBC collaboration. In their case, they find

$$\mathrm{Re}(\epsilon'/\epsilon)_{\mathrm{lat}}^{\mathrm{RBC}} = 0.00293 \pm 0.00104. \quad (7.2)$$

This difference can be probably caused by the different analysis methods used by us vs the one used by the RBC collaboration. In the latter, the authors used a bootstrap method to find the central value and the error [45], while we followed a Monte Carlo procedure.

In any case, this result will not be added to the analysis since the relevant result is the one that includes the experimental values of $\mathrm{Re}\, A_{0/2}$ together with isospin breaking corrections.
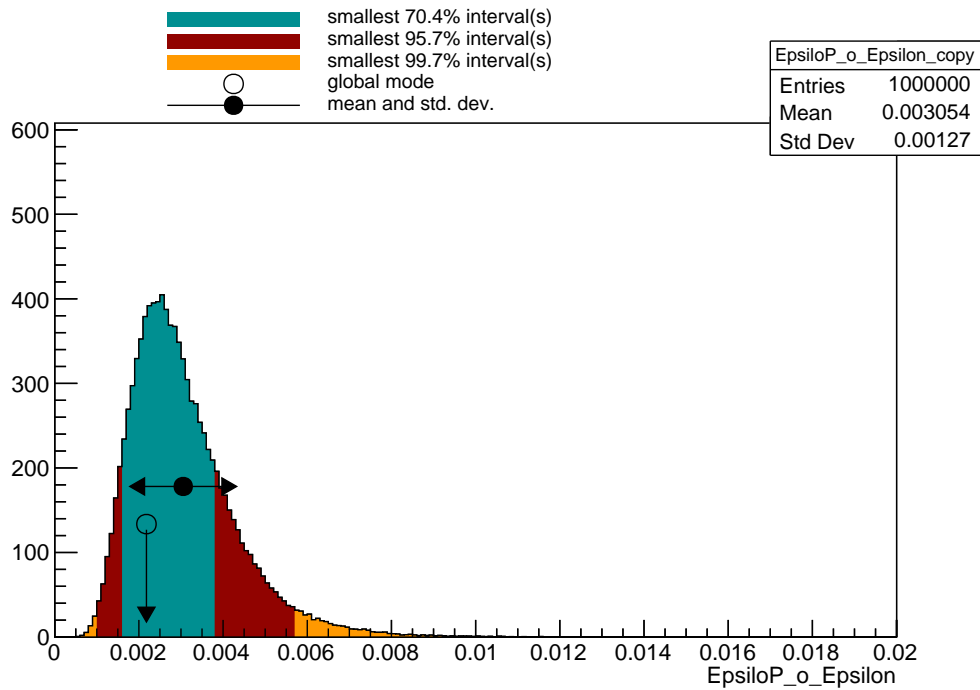
Figure 7.1. Posterior distribution for $\mathrm{Re}(\epsilon'/\epsilon)$ from Monte Carlo simulation starting from unrenormalized, infinite-volume, lattice matrix elements.
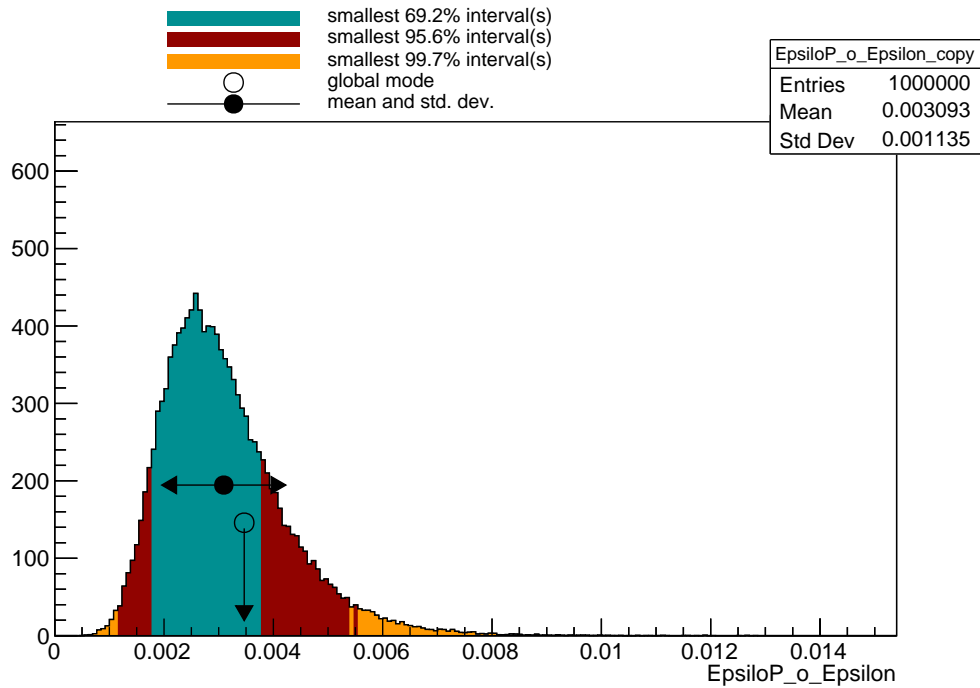
Figure 7.2. Posterior distribution for $\mathrm{Re}(\epsilon'/\epsilon)$ from Monte Carlo simulation starting from SMOM renormalized, infinite-volume, lattice matrix elements.

7.1.2   Mixed Lattice-Experimental Approach
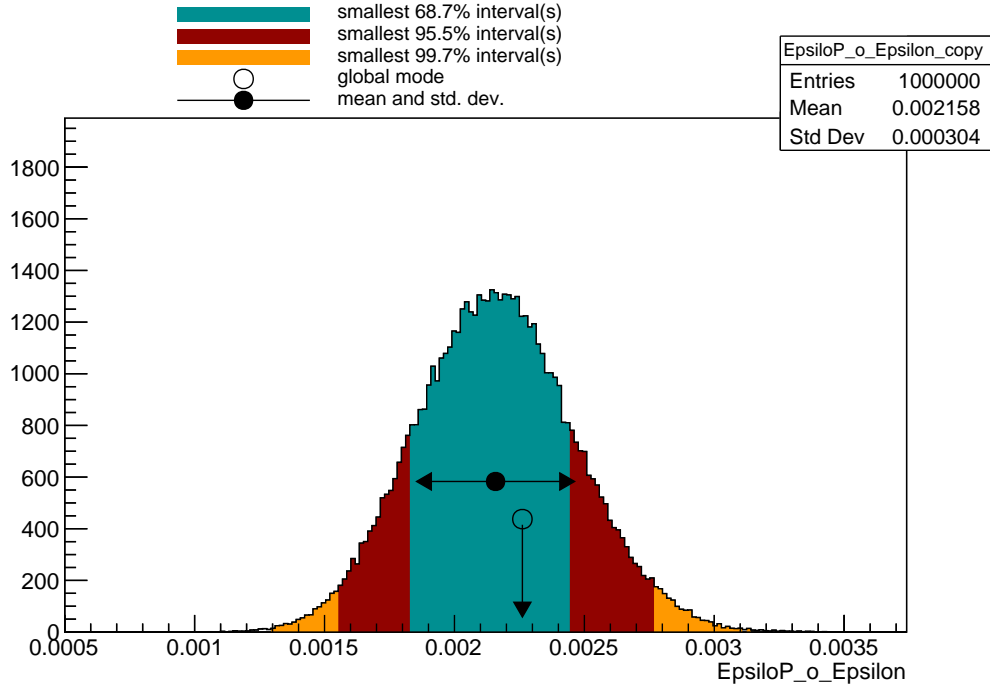
Figure 7.3. Posterior distribution for $\mathrm{Re}(\epsilon'/\epsilon)$ from Monte Carlo simulation using the experimental value of $\mathrm{Re}\,A_{0,2}$.

With this approach, we find that

$$\mathrm{Re}(\epsilon'/\epsilon)_{\mathrm{mix}} = 0.00216 \pm 0.00030 \tag{7.3}$$

which is quite in line with the result found by the RBC collaboration

$$\mathrm{Re}(\epsilon'/\epsilon)_{\mathrm{mix}}^{\mathrm{RBC}} = 0.00217 \pm 0.00026. \tag{7.4}$$

This particular result is what we are going to use in the following UT analysis. What remains now, before introducing this result in the UTfit, is a careful treatment of the systematic, which contains not only the errors associated to the lattice calculations but also, most importantly, the ones coming from the scale dependence of the Wilson coefficients. This is important since currently, the variation of the Wilson coefficients is not implemented yet in the code, but is not so crucial for a simple UT analysis. Fortunately, the authors of the RBC paper had us covered since they give all the relevant contributions to the systematic errors both in the $I = 1/2$ and in the $I = 3/2$ cases. The relevant figure they find is that the systematic errors amount to 20.7% on $\mathrm{Im}(A_0)$. We can brute force this figure in the code by simply adding a parameter SysImA0 $= (0.00 \pm 0.207)$ to the configuration file, and changing the final contribution from $\mathrm{Im}(A_0)$ in the code for ϵ'/ϵ to $(1 + \mathrm{SysImA0})\,\mathrm{Im}\,A_0$. This gives in fact the expected systematic error which, from the RBC result, should be

$$\mathrm{Re}(\epsilon'/\epsilon)_{\mathrm{mix}}^{\mathrm{RBC}} = 0.00216 \pm 0.00062_{\mathrm{sys}} \tag{7.5}$$
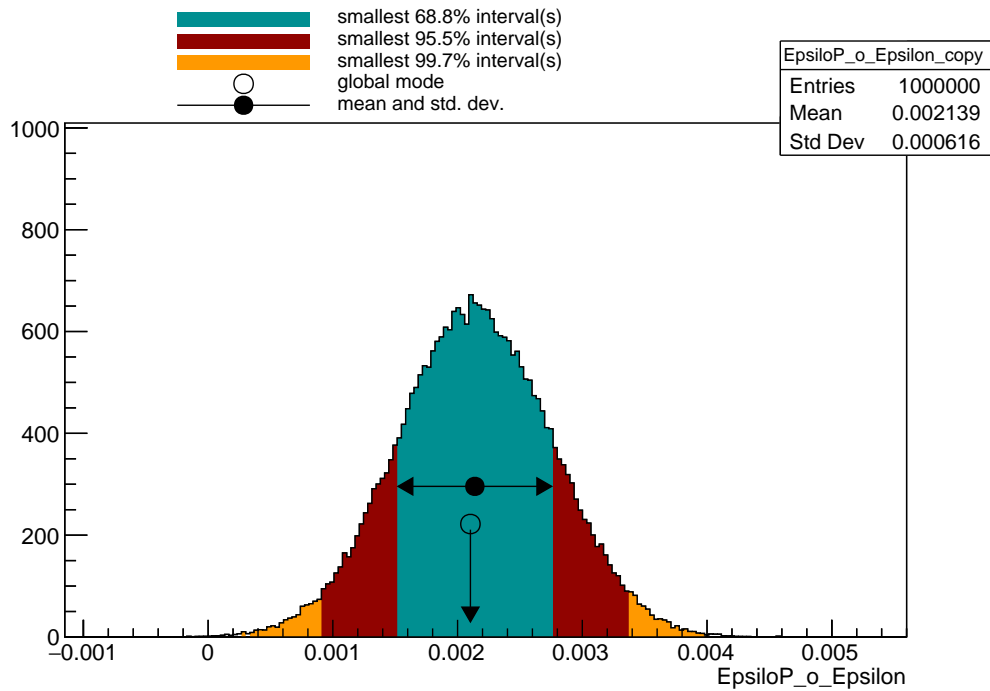
Figure 7.4. Posterior distribution for $\mathrm{Re}(\epsilon'/\epsilon)$ from Monte Carlo simulation using the experimental value of $\mathrm{Re}\,A_{0,2}$; only systematic errors.

while we get, as seen in figure (7.4), a value of

$$\mathrm{Re}(\epsilon'/\epsilon)_{\mathrm{mix}} = 0.00214 \pm 0.00062_{\mathrm{sys}}. \tag{7.6}$$

7.2 Final Result Including IB

Once a careful treatment of the systematic errors is in place, we can introduce the isospin breaking correction. Due to the fact that the $\hat{\Omega}_{IB}$ parameter has asymmetric errors, we first symmetrize it to $\hat{\Omega}_{IB} = (17.05 \pm 9.05) \times 10^{-2}$. This drastically lowers the value of $\mathrm{Re}(\epsilon'/\epsilon)$ making it more in line with the experimental result, whilst having an appreciable error. The final posterior distribution for the mix result including isospin breaking and systematic errors is found in figure (7.5).
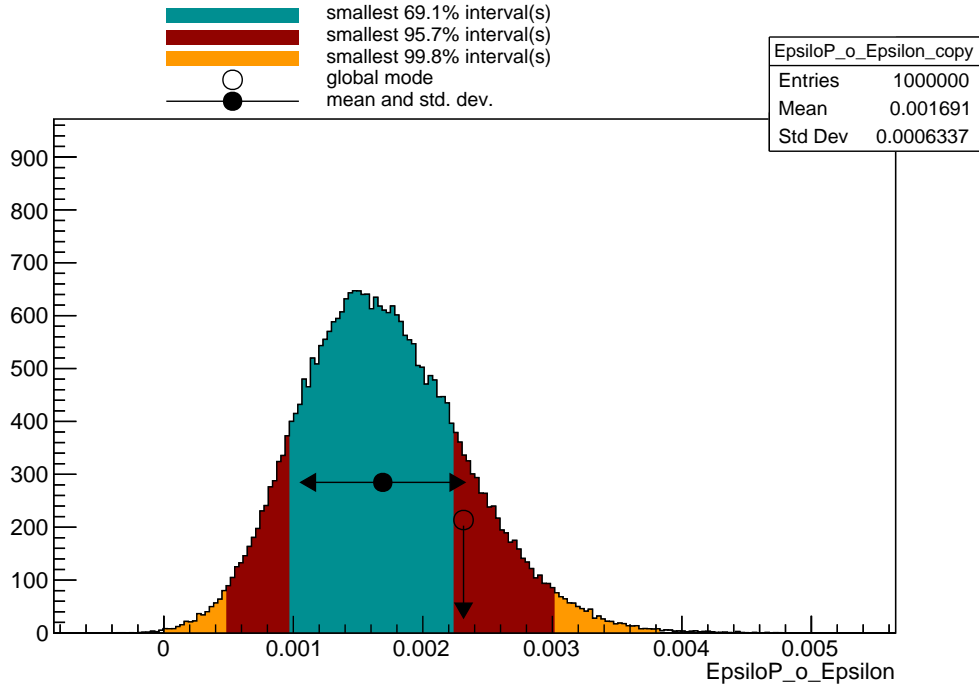
Figure 7.5. Posterior distribution for $\mathrm{Re}(\epsilon'/\epsilon)$ from Monte Carlo simulation in the mixed case, including systematic errors and isospin breaking contribution.

The final result comes out to be

$$\mathrm{Re}(\epsilon'/\epsilon) = 0.00169 \pm 0.00063. \tag{7.7}$$

If we do consider, like the authors of [2], the error associated with not considering isospin breaking as the difference between the results with and without the correction, the final result comes out to be

$$\mathrm{Re}(\epsilon'/\epsilon) = 0.00216 \pm 0.00030_{\mathrm{stat}} \pm 0.00062_{\mathrm{sys}} \pm 0.00047_{\mathrm{IB}}, \tag{7.8}$$

to be compared with the result in [2]

$$\mathrm{Re}(\epsilon'/\epsilon)^{\mathrm{RBC}} = 0.00217 \pm 0.00026_{\mathrm{stat}} \pm 0.00062_{\mathrm{sys}} \pm 0.00050_{\mathrm{IB}}. \tag{7.9}$$

7.3   Standard UT analysis

Now that we have the code for ϵ'/ϵ that gives the expected result, eq. (7.7), we can insert it into the analysis of the Unitarity Triangle together with all the other interesting observables at our disposal.

Before doing so, we need to first compute the value of $\bar{\rho}, \bar{\eta}$ without including ϵ'/ϵ so to check how much this new observable influences the result. The obtained result can be found in fig. (7.6), where we can see that the obtained best fit value for the $\bar{\rho}, \bar{\eta}$ CKM parameters is given by

$$\bar{\rho} = 0.1695 \pm 0.0146, \qquad \bar{\eta} = 0.3667 \pm 0.0176. \tag{7.10}$$
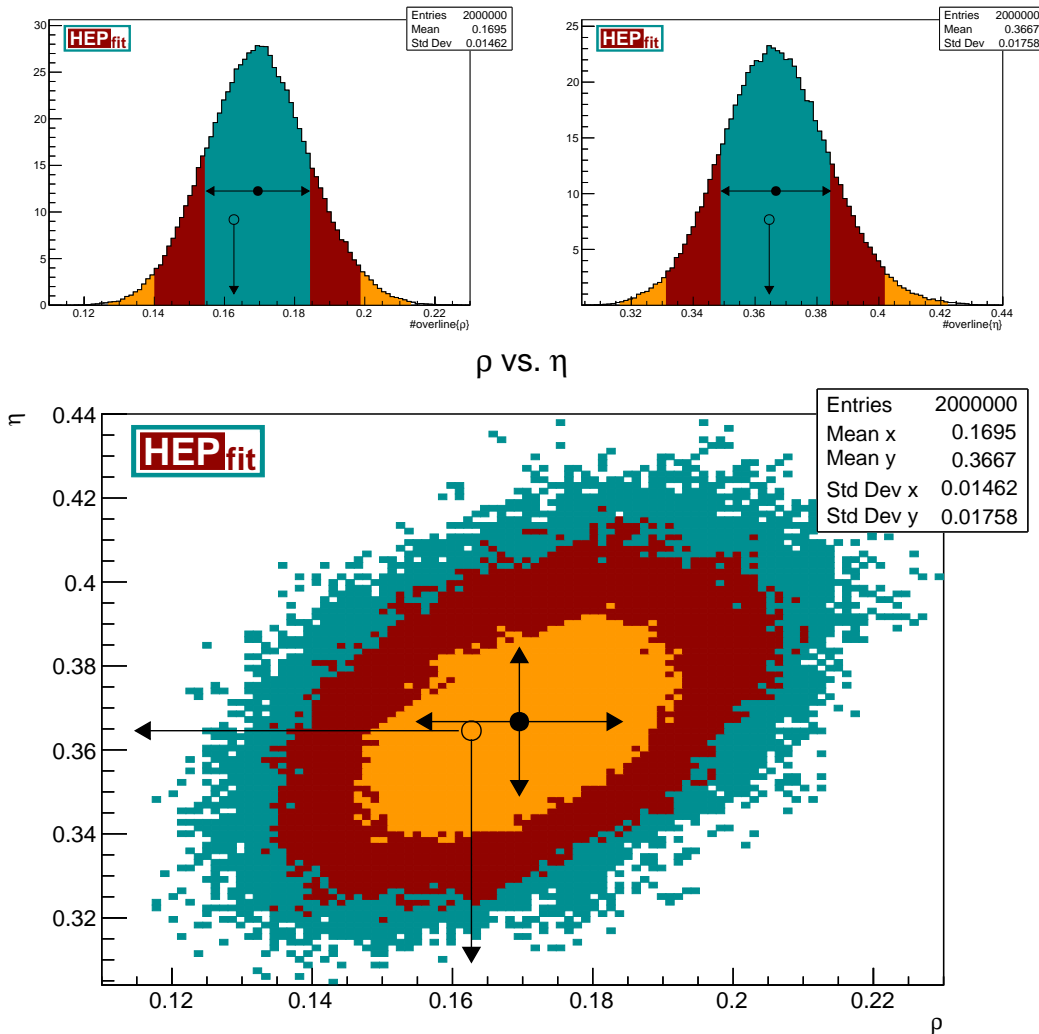
Figure 7.6. Posterior distribution of the $\bar{\rho}$ (upper left) and $\bar{\eta}$ (upper right) parameters. Joint distribution in the $(\bar{\rho}, \bar{\eta})$ plane (lower). The colored regions represent the 69% (blue), 95% (red) and 99% (orange) confidence intervals. The best fit value represents the CKM UT vertex in the $(\bar{\rho}, \bar{\eta})$ plane. This result *does not* contain ϵ'/ϵ.

Another interesting CKM parameter that we can find by this analysis is the Jarlskog invariant J_{CP} which we defined in section 1.6.4. As we explained in that section, J_{CP} is a rephasing invariant parameter of the CKM matrix which measures the amount of CP-violation in the Standard Model. In that section, we gave the value of J_{CP} as given by [152]. What we find is that

$$J_{CP} = (3.19 \pm 0.12) \times 10^{-5} \tag{7.11}$$

as can be seen in figure (7.7).
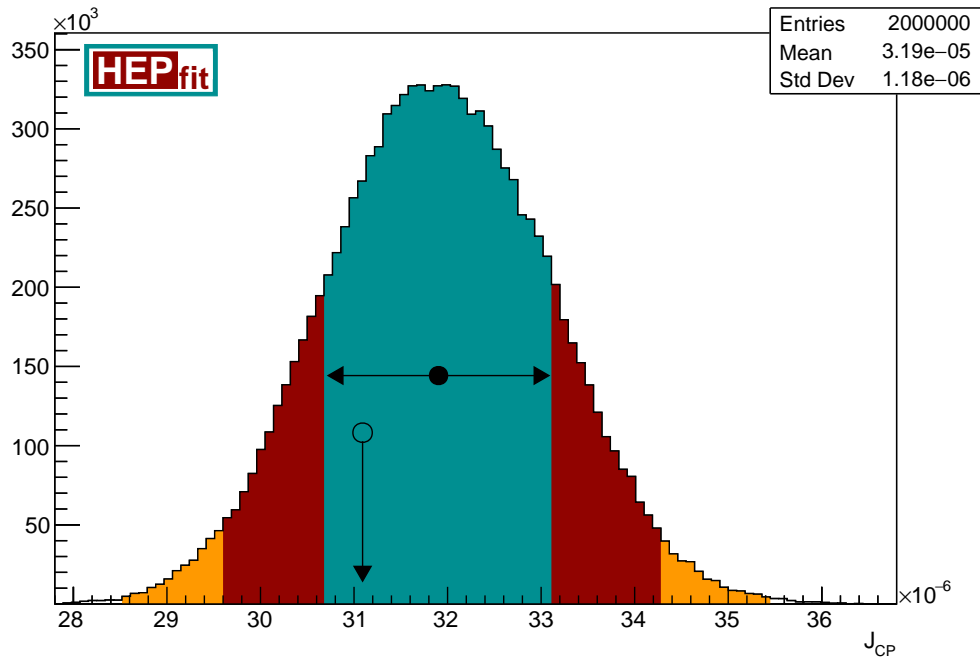
Figure 7.7. Posterior distribution for the Jarlskog invariant in the SM without the inclusion of ϵ'/ϵ.

A full list of the results found by this first UT analysis is given in tables (7.1) and (7.2).

Then we can add ϵ'/ϵ to the UT analysis and see how much the result changes. We do not expect a noticeable difference between the two results. The obtained result can be found in fig. (7.8), where we can see that the obtained best fit value for the $\bar{\rho}, \bar{\eta}$ CKM parameters is given by

$$\bar{\rho} = 0.1702 \pm 0.0150, \qquad \bar{\eta} = 0.3677 \pm 0.0185. \tag{7.12}$$

Table 7.1. Standard Model fit results with and without the inclusion of ϵ'/ϵ.

| Parameter	SM fit with ϵ'/ϵ	SM fit without ϵ'/ϵ
$\bar{\rho}$	0.1702 ± 0.0150	0.1695 ± 0.0146
$\bar{\eta}$	0.3677 ± 0.0185	0.3667 ± 0.0175
ρ	0.1743 ± 0.0154	0.174 ± 0.015
η	0.3774 ± 0.0189	0.376 ± 0.018
A	0.8104 ± 0.0117	0.811 ± 0.0113
λ	0.2258 ± 0.0003	0.2258 ± 0.0003
$\sin\theta_{12}$	0.2258 ± 0.0003	0.2258 ± 0.0003
$\sin\theta_{23}$	0.04132 ± 0.00058	0.04132 ± 0.00056
$\sin\theta_{13}$	0.003878 ± 0.000169	0.003867 ± 0.000163
δ [rad]	1.138 ± 0.030	1.139 ± 0.029
α [°]	90.95 ± 1.95	91.000 ± 1.891
β [°]	23.9 ± 1.3	23.83 ± 1.24
γ [°]	65.18 ± 1.69	65.21 ± 1.67
$2\beta + \gamma$ [°]	113 ± 3	112.9 ± 2.7
β_s [°]	-0.0391 ± 0.0019	-0.039 ± 0.002
$\sin(2\beta)$	0.7401 ± 0.0303	0.7385 ± 0.0290
$\cos(2\beta)$	0.6719 ± 0.0335	0.6738 ± 0.0319
$J_{CP} \times 10^5$	3.198 ± 0.122	3.19 ± 0.12
f_{B_s}	0.2299 ± 0.0012	0.2299 ± 0.0012
f_{B_s}/f_{B_d}	1.208 ± 0.005	1.208 ± 0.005
B_{B_s}	0.8653 ± 0.0245	0.865 ± 0.024
B_{B_s}/B_{B_d}	1.029 ± 0.028	1.029 ± 0.028
B_K	0.5546 ± 0.0120	0.5544 ± 0.0115
$|\epsilon_K| \times 10^3$	2.227 ± 0.0011	2.227 ± 0.011
$\epsilon'/\epsilon \times 10^3$	1.696 ± 0.657	-
R_b	0.4053 ± 0.0210	0.4042 ± 0.0196
R_t	0.9079 ± 0.0121	0.9081 ± 0.0118
R_{ts}	1.0090 ± 0.0008	1.0090 ± 0.0008
$S_{J/\psi K}$	0.7395 ± 0.0303	0.7376 ± 0.0290
$\mathrm{BR}(B \to \tau\nu) \times 10^5$	9.643 ± 0.860	9.585 ± 0.822
$\mathrm{BR}(B_d \to \mu\mu) \times 10^{11}$	9.113 ± 0.679	9.097 ± 0.678
$\mathrm{BR}(B_s \to \mu\mu) \times 10^9$	3.1 ± 0.2	3.095 ± 0.214
$\mathrm{BR}(\bar{B}_s \to \mu\mu) \times 10^9$	3.311 ± 0.228	3.307 ± 0.229
Δm_s [ps^{-1}]	17.77 ± 0.01	17.77 ± 0.01
Δm_d [ps^{-1}]	0.5065 ± 0.0019	0.5065 ± 0.0019

Table 7.2. Moduli of the CKM matrix elements from the UT fit with and without the inclusion of ϵ'/ϵ.

Parameter	SM fit with ϵ'/ϵ	SM fit without ϵ'/ϵ
$|V_{ud}|$	0.97420 ± 0.00008	0.97420 ± 0.00008
$|V_{us}|$	0.2258 ± 0.0003	0.2258 ± 0.0003
$|V_{ub}|$	0.003878 ± 0.000169	0.003867 ± 0.000163
$|V_{cd}|$	0.2257 ± 0.0003	0.2257 ± 0.0003
$|V_{cs}|$	0.97330 ± 0.00008	0.97330 ± 0.00008
$|V_{cb}|$	0.04132 ± 0.00058	0.04132 ± 0.00056
$|V_{td}|$	0.008472 ± 0.000152	0.008474 ± 0.000148
$|V_{ts}|$	0.04063 ± 0.00057	0.04063 ± 0.00054
$|V_{tb}|$	0.99910 ± 0.00002	0.99910 ± 0.00002
$|V_{td}/V_{ts}|$	0.2086 ± 0.0030	0.2086 ± 0.0028
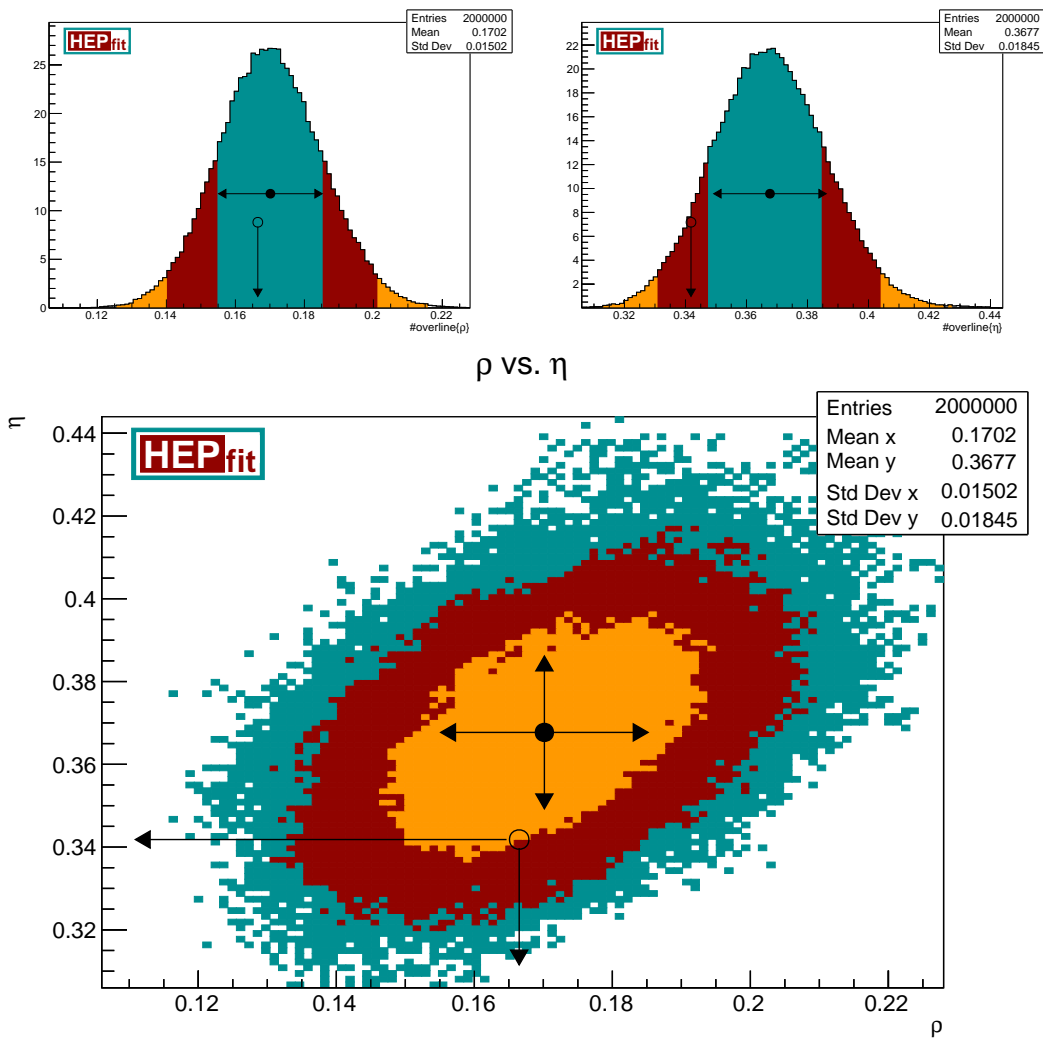
Figure 7.8. Posterior distribution of the $\bar{\rho}$ (upper left) and $\bar{\eta}$ (upper right) parameters. Joint distribution in the $(\bar{\rho}, \bar{\eta})$ plane (lower). The colored regions represent the 69% (blue), 95% (red) and 99% (orange) confidence intervals. The best fit value represents the CKM UT vertex in the $(\bar{\rho}, \bar{\eta})$ plane. This result *does* contain ϵ'/ϵ.

Table 7.3. Highest probability regions (HPR) for $\bar{\rho}$ and $\bar{\eta}$ in the two analyses with and without ϵ'/ϵ.

HPR		Without ϵ'/ϵ	With ϵ'/ϵ
68%	$\bar{\rho}$	$(0.154, 0.184)$	$(0.155, 0.185)$
	$\bar{\eta}$	$(0.349, 0.384)$	$(0.347, 0.385)$
95%	$\bar{\rho}$	$(0.14, 0.199)$	$(0.14, 0.201)$
	$\bar{\eta}$	$(0.331, 0.402)$	$(0.331, 0.404)$
99%	$\bar{\rho}$	$(0.127, 0.213)$	$(0.126, 0.216)$
	$\bar{\eta}$	$(0.316, 0.422)$	$(0.313, 0.425)$
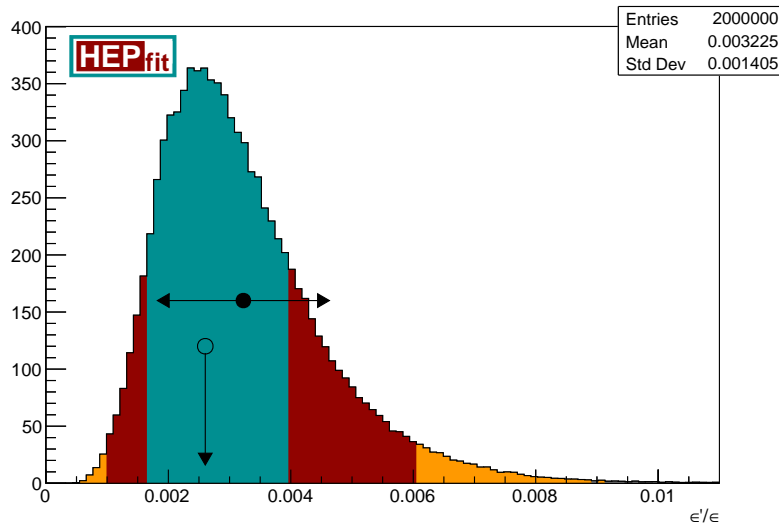
Figure 7.9. Posterior distribution for ϵ'/ϵ from the UT analysis using the pure lattice result.

What we see is an increase in both $\bar{\rho}$ and $\bar{\eta}$, but the difference can be probably traced to statistical fluctuations in the Monte Carlo, more than a relevant impact of the inclusion of ϵ'/ϵ. The two results are, in fact, in the same range when considering the associated errors. If we consider the two results in the 69%, 96% and 99% probability regions, as given in table (7.3), we can easily see that the two results agree pretty well.

For completeness, we also ran the analysis using the pure-lattice strategy described in section 6.2.1, and we found that

$$\bar{\rho} = 0.1697 \pm 0.0149 \qquad \bar{\eta} = 0.3672 \pm 0.0178 \tag{7.13}$$

as can be seen in figure (7.10). The resulting value for ϵ'/ϵ is

$$\text{Re}(\epsilon'/\epsilon) = 0.003225 \pm 0.001405 \tag{7.14}$$

as can be seen from the Monte Carlo in figure (7.9). This is to be compared with the similar value found before in eq. (7.1).
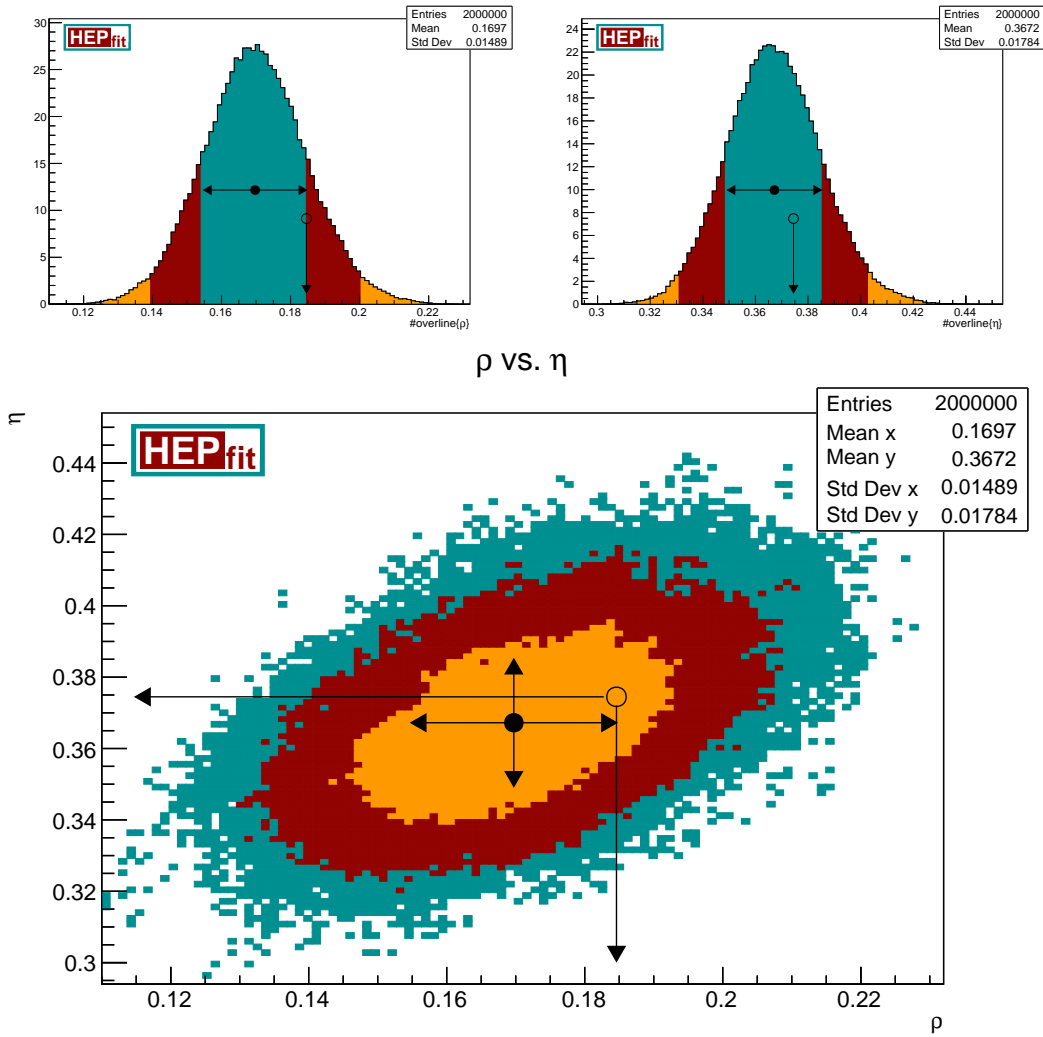
Figure 7.10. Posterior distribution of the $\bar{\rho}$ (upper left) and $\bar{\eta}$ (upper right) parameters. Joint distribution in the $(\bar{\rho}, \bar{\eta})$ plane (lower). The colored regions represent the 69% (blue), 95% (red) and 99% (orange) confidence intervals. The best fit value represents the CKM UT vertex in the $(\bar{\rho}, \bar{\eta})$ plane. This result *does* contain ϵ'/ϵ evaluated with the pure lattice strategy.

Chapter 8

Conclusions and Prospects

In this thesis, an updated analysis of the Unitarity Triangle within the Standard Model has been presented. Besides the usual observables and parameters, we included the new and improved result on ϵ'/ϵ which was finally calculated in lattice QCD with acceptable results by the RBC collaboration [2, 18].

What we found is that the updated analysis, not surprisingly, gave us results that were in line with the previous ones which did not contain the new observable. In particular, what we found was that, without ϵ'/ϵ, the two relevant CKM Wolfenstein parameters were

$$\bar{\rho} = 0.1695 \pm 0.0146, \qquad \bar{\eta} = 0.3667 \pm 0.0176, \tag{8.1}$$

while by including ϵ'/ϵ gave

$$\bar{\rho} = 0.1702 \pm 0.0150, \qquad \bar{\eta} = 0.3677 \pm 0.0185, \tag{8.2}$$

thus we did not find any appreciable difference.

This was to be expected since even if some New Physics effects are at play in the small value of ϵ'/ϵ, these effects would be really small and would not influence very much the Standard Model value, thus the result would be very much consistent with it.

The final result for ϵ'/ϵ from the full UT fit, including isospin breaking corrections, in the mixed strategy which includes information from the experimental value of $\mathrm{Re}\,A_0$, comes out to be

$$\mathrm{Re}(\epsilon'/\epsilon) = (16.96 \pm 6.57) \times 10^{-4}. \tag{8.3}$$

In the future, we will implement the code for the evaluation of the Wilson Coefficients which is fundamental to get a more accurate result. Moreover, we are going to work on a possible BSM analysis of ϵ'/ϵ since we hope that this observable can give interesting insights on the scales and contributions of NP effects.

Appendix A

Mathematical Tools

We give here a brief mathematical appendix on the relevant methods and integrals which can commonly be found in field theories when evaluating loop diagrams.

A.1   Feynman Parametrization

The Feynman parametrization is a very useful tool that is employed almost every time one has to isolate divergences from loop integrals.
The simplest Feynman parametrization is the following

$$\frac{1}{AB} = \int_0^1 dx \, \frac{1}{[A + (B - A)x]^2} = \int dx \, dy \, \delta(x + y - 1) \frac{1}{[xA + yB]^2} \qquad (A.1)$$

which can be easily proven. The powers in the denominator can be raised by simple derivation

$$\frac{1}{AB^n} = \frac{(-1)^{n-1}}{(n-1)!} \frac{\partial^{n-1}}{\partial B^{n-1}} \frac{1}{AB} = \int_0^1 dx \, dy \, \delta(x + y - 1) \frac{ny^{n-1}}{[xA + yB]^{n+1}}. \qquad (A.2)$$

More terms in the denominator can be added by simple iteration of eq. (A.1)

$$\frac{1}{ABC} = \frac{1}{AB} \frac{1}{C} = 2 \int_0^1 dx \, dy \, dz \, \delta(x + y + z - 1) \frac{1}{[xA + yB + zC]^3}. \qquad (A.3)$$

From this, one can get the most general formula which gives

$$\prod_{k=1}^n \frac{1}{A_k^{c_k}} = \frac{\Gamma(\sum_k c_k)}{\prod_k \Gamma(c_k)} \int_0^1 \prod_{k=1}^n x_k^{c_k-1} \, dx_k \, \delta\left(\sum_{k=1}^n x_k - 1\right) \frac{1}{[\sum_{k=1}^n x_k A_k]^{\sum_k c_k}}, \qquad (A.4)$$

where $\Gamma(z)$ is the Euler gamma function.

A.2   Scalar One-Loop Integrals

Here we give a list of interesting integrals which come up in this thesis. The general scalar one loop integral with n external massive legs, with masses m_i, carrying

momentum p_i is of the form

$$I = \int \frac{\mathrm{d}^d\ell}{(2\pi)^d} \frac{1}{[(\ell+p_1)^2 - m_1^2 + i\epsilon][(\ell+p_{12})^2 - m_2^2 + i\epsilon]\cdots[(\ell+p_{12\cdots n})^2 - m_n^2 + i\epsilon]}, \tag{A.5}$$

where we employed dimensional regularization, ℓ is the loop momenta and $p_{12\cdots n} = \sum_{k=1}^n p_k$.

Using the Feynman parametrization eq. (A.4) we can write

$$I = \Gamma(n) \int_0^1 \prod_{k=1}^n \mathrm{d}x_k \int \frac{\mathrm{d}^d\ell}{(2\pi)^d} \frac{\delta(\sum_{k=1}^n x_k - 1)}{[\sum_{k=1}^n x_k A_k]^n}, \tag{A.6}$$

where

$$\begin{aligned}
\sum_{k=1}^n x_k A_k &= \sum_{k=1}^n x_k \Big[(\ell+p_{12\cdots k})^2 - m_k^2 + i\epsilon\Big] \\
&= \ell^2 + 2\ell \cdot \left(\sum_{k=1}^n x_k p_{12\cdots k}\right) + \sum_{k=1}^n x_k \left(p_{12\cdots k}^2 - m_k^2 + i\epsilon\right) \\
&= \ell^2 + 2\ell \cdot P + K^2 + i\epsilon.
\end{aligned} \tag{A.7}$$

Therefore, by substitution in the integral and translating the loop momentum integration $\ell \to \ell + P$, one gets

$$I = \Gamma(n) \int_0^1 \prod_{k=1}^n \mathrm{d}x_k\, \delta\left(\sum_{k=1}^n x_k - 1\right) \int \frac{\mathrm{d}^d\ell}{(2\pi)^d} \frac{1}{(\ell^2 - m^2 + i\epsilon)^n}, \tag{A.8}$$

where $m^2 = K^2 - P^2$. The integral over the loop momentum can be performed by Wick rotating the temporal ℓ^0 coordinate and then using polar coordinates in Euclidean space. Therefore the integral I becomes

$$\begin{aligned}
I &= i\Gamma(n) \int_0^1 \prod_{k=1}^n \mathrm{d}x_k\, \delta\left(\sum_{k=1}^n x_k - 1\right) \int \frac{\mathrm{d}\ell_0^E\, \mathrm{d}^{d-1}\ell}{(2\pi)^d} \frac{1}{\left(-(\ell_0^E)^2 - |\ell|^2 - m^2\right)^n} \\
&= \frac{(-1)^n i\Gamma(n)}{(2\pi)^d} \int_0^1 \prod_{k=1}^n \mathrm{d}x_k\, \delta\left(\sum_{k=1}^n x_k - 1\right) \int \mathrm{d}^d\Omega\, \mathrm{d}\ell_E \frac{\ell_E^{d-1}}{(\ell_E^2 + m^2)^n} \\
&= \frac{(-1)^n i\Gamma(n)\Omega_d}{2(2\pi)^d} B\left(\frac{d}{2}, n - \frac{d}{2}\right) \int_0^1 \prod_{k=1}^n \mathrm{d}x_k\, \delta\left(\sum_{k=1}^n x_k - 1\right)(m^2)^{\frac{d}{2}-n}, \tag{A.9}
\end{aligned}$$

where in the last step we changed variables $x = \frac{1}{1+\ell_E^2/m^2}$ and used the definition of the Beta function

$$B(a,b) = \int_0^1 \mathrm{d}x\, x^{a-1}(1-x)^{b-1}. \tag{A.10}$$

Ending with a few manipulations on m^2

$$m^2 = P^2 - K^2 = \left(\sum_{i=1}^{n} x_k p_{1\dots i}\right)^2 - \sum_{i=1}^{n} x_k (p_{1\dots i}^2 - m_i^2 + i\epsilon)$$

$$= \sum_{i=1}^{n} \alpha_i^2 p_{1\dots i}^2 + 2\sum_{i>j}^{n} \alpha_i \alpha_j p_{1\dots i} p_{1\dots j} - \sum_{i=1}^{n} \alpha_i p_{1\dots i}^2 + \sum_{i=1}^{n} \alpha_i m_i^2 - i\epsilon$$

$$= -\sum_{i=1}^{n} \alpha_i \sum_{j\neq i} \alpha_j p_{1\dots i}^2 + 2\sum_{i>j}^{n} \alpha_i \alpha_j p_{1\dots i} p_{1\dots j} + \sum_{i=1}^{n} \alpha_i m_i^2 - i\epsilon$$

$$= -\sum_{i>j}^{n} \alpha_i \alpha_j p_{1\dots i}^2 - \sum_{i>j}^{n} \alpha_i \alpha_j p_{1\dots i} p_{1\dots j} \qquad \text{(A.11)}$$

$$\quad - \sum_{j>i}^{n} \alpha_i \alpha_j p_{1\dots i}^2 - \sum_{j>i}^{n} \alpha_j \alpha_i p_{1\dots j} p_{1\dots i} + \sum_{i=1}^{n} \alpha_i m_i^2 - i\epsilon$$

$$= -\sum_{i>j}^{n} \alpha_i \alpha_j p_{1\dots i} p_{j+1\dots i} + \sum_{j>i}^{n} \alpha_i \alpha_j p_{1\dots i} p_{i+1\dots j} + \sum_{i=1}^{n} \alpha_i m_i^2 - i\epsilon$$

$$= -\sum_{i>j}^{n} \alpha_i \alpha_j p_{j+1\dots i}^2 + \sum_{i=1}^{n} \alpha_i m_i^2 - i\epsilon = \Delta.$$

In summary

$$I = (-1)^n \frac{i}{(4\pi)^{d/2}} \Gamma\left(n - \frac{d}{2}\right) \int_0^1 \prod_{k=1}^{n} \mathrm{d}x_k \, \delta\left(\sum_{k=1}^{n} x_k - 1\right) \frac{1}{\Delta^{n-d/2}} \qquad \text{(A.12)}$$

A.2.1   One-point Green Function

The integral for the one point Green function, which appears in tadpole diagrams, is given by

$$A_0(m^2) = \int \frac{\mathrm{d}^d \ell}{(2\pi)^d} \frac{1}{\ell^2 - m^2 + i\epsilon} = \frac{-i\Gamma\left(\frac{2-d}{2}\right)}{(4\pi)^{d/2}} \int_0^1 \mathrm{d}x \, \delta(x-1)(xm^2 - i\epsilon)^{\frac{d-2}{2}}$$

$$= \frac{i\Gamma\left(\frac{2-d}{2}\right)}{(4\pi)^{d/2}} (m^2 - i\epsilon)^{\frac{2-d}{2}}.$$

$$\text{(A.13)}$$

When the mass of the particle propagating in the loop is zero we get that $A_0 = 0$ which is what we expect since there are no dimensionful variables that carry the dimension of A_0 after integrating.

When $m \neq 0$, defining as usual $d = 4 - 2\epsilon$, the integral diverges as $1/\epsilon$ as $\epsilon \to 0$, in fact

$$A_0(m^2) = \frac{i}{16\pi^2} \frac{(4\pi)^\epsilon \Gamma(1+\epsilon)}{\epsilon(1-\epsilon)} (m^2)^{1-\epsilon}. \qquad \text{(A.14)}$$

A.2.2   Two-point Massless Green Function

The two point function is more interesting in our case, in particular when the particles in the loop are considered massless. If the particles in the loop are massless $m_1 = m_2 = 0$, the external particles need to carry a non zero momentum $p^2 \neq 0$ otherwise the whole integral would be zero just like A_0. The integral is given by

$$
\begin{aligned}
B_0(p^2) &= \int \frac{\mathrm{d}^d \ell}{(2\pi)^d} \frac{1}{[\ell^2 + i\epsilon][(\ell + p)^2 + i\eta]} \\
&= \frac{i\Gamma\left(\frac{4-d}{2}\right)}{(4\pi)^{d/2}} \int_0^1 \mathrm{d}x\, \mathrm{d}y\, \delta(x + y - 1) \frac{1}{(-xyp^2 - i\eta)^{\frac{4-d}{2}}} \\
&= \frac{i\Gamma\left(\frac{4-d}{2}\right)}{(4\pi)^{d/2}} \int_0^1 \mathrm{d}x \left(x(1-x)(-p^2 - i\eta) \right)^{-\frac{4-d}{2}} \\
&= \frac{i\Gamma\left(\frac{4-d}{2}\right)}{(4\pi)^{d/2}} (-p^2 - i\eta)^{\frac{4-d}{2}} \frac{\Gamma^2\left(\frac{d-2}{2}\right)}{\Gamma(d-2)}.
\end{aligned}
\tag{A.15}
$$

Choosing $d = 4 - 2\epsilon$ we have

$$
B_0(p^2) = \frac{i}{16\pi^2} \frac{(4\pi)^\epsilon \Gamma(\epsilon)\Gamma^2(1-\epsilon)}{\Gamma(2-2\epsilon)} (-p^2 - i\eta)^{-\epsilon}.
\tag{A.16}
$$

In the limit $\epsilon \to 0$, the multiplicative factors are finite and amount to a one, while we have to deal with the p^2 term

$$
(-p^2 - i\eta)^{-\epsilon} = 1 - \epsilon \log\left(-p^2 - i\eta\right) + \mathcal{O}(\epsilon^2).
\tag{A.17}
$$

When $p^2 < 0$ the logarithm is perfectly defined while if $p^2 > 0$, then $-p^2 - i\eta$ is a complex negative number with a small imaginary part, so that is below the branch cut for the definition of the logarithm. In this case

$$
(-p^2 - i\eta)^{-\epsilon} = 1 - \epsilon \left[\log\left(p^2\right) - i\pi\right] + \mathcal{O}(\epsilon^2).
\tag{A.18}
$$

In general

$$
B_0(p^2) = \frac{i}{16\pi^2} \frac{\Gamma^2(1-\epsilon)}{\Gamma(2-2\epsilon)} \left[\frac{1}{\epsilon} - \gamma_E - \log\left(-\frac{p^2}{4\pi}\right) + \mathcal{O}(\epsilon^2)\right],
\tag{A.19}
$$

where the factor $(4\pi)^\epsilon$ has been absorbed into the factor $(-p^2)^{-\epsilon}$ and the $\Gamma(\epsilon)$ has been expanded

$$
\Gamma(\epsilon) = \frac{1}{\epsilon} + \psi(1) + \frac{\epsilon}{2} \left[\frac{\pi^2}{6} + \psi^2(1) - \psi'(1)\right] + \mathcal{O}(\epsilon^2),
\tag{A.20}
$$

where $\psi(1) = -\gamma_E$ is the digamma function evaluated in one and $\psi'(1) = \pi^2/6$ is its derivative.

A.3   Passarino-Veltman Tensor Integral Decomposition

Up to now, we have only dealt with scalar integrals. For tensor integrals, we can use the Passarino-Veltmann [118] decomposition with which, in many cases, we can go back to a scalar integral times some tensor quantity that depends on the specific form and properties of the integrand. We will give now some useful examples that we will use throughout the thesis.

A.3.1   Vector Two-Point Function

Let us first compute the simplest tensor integral

$$\mathcal{B}^{\mu}(p) = \int \frac{\mathrm{d}^d \ell}{(2\pi)^d} \frac{\ell^{\mu}}{\ell^2 (\ell + p)^2}, \tag{A.21}$$

where $p^2 \neq 0$ and we employ dimensional regularization. We can easily see that the only relevant 4-vector on which the integral can depend is p^{μ}, therefore we can write

$$\mathcal{B}^{\mu}(p) = B_{11} p^{\mu}. \tag{A.22}$$

In order to find the coefficient, we can just project onto p^{μ} and get back to a scalar integral

$$p_{\mu} \mathcal{B}^{\mu}(p) = B_{11} p^2 = \int \frac{\mathrm{d}^d \ell}{(2\pi)^d} \frac{p \cdot \ell}{\ell^2 (\ell + p)^2}. \tag{A.23}$$

Since $(\ell + p)^2 = p^2 + \ell^2 + 2p \cdot \ell$ we have that

$$p \cdot \ell = \frac{1}{2} \Big[(\ell + p)^2 - \ell^2 - p^2 \Big]. \tag{A.24}$$

Using this in the integral we have

$$p^2 B_{11} = \frac{1}{2} \int \frac{\mathrm{d}^d \ell}{(2\pi)^d} \left[\frac{1}{\ell^2} - \frac{1}{(\ell + p)^2} - \frac{p^2}{\ell^2 (\ell + p)^2} \right], \tag{A.25}$$

but this are just scalar one-loop integrals of the form of eq. (A.15), therefore

$$p^2 B_{11} = -\frac{p^2}{2} B_0(p^2) \implies B_{11} = -\frac{B_0(p^2)}{2}. \tag{A.26}$$

This gives us the final result

$$\mathcal{B}^{\mu}(p^2) = -\frac{B_0(p^2)}{2} p^{\mu}. \tag{A.27}$$

This computation gives the basic idea behind the Passarino-Veltmann decomposition: if we have a general p-tensor integral, we list all the possible p-tensors upon which the integral can depend. Then we project on such tensors by simply contracting the integral with them and one obtains a set of linear equations that can be solved to find the coefficients.

A.3.2 2-Tensor Two-Point Funcion

We would like to compute now the 2-tensor two point function, which is a tensor integral of the form

$$\mathcal{B}^{\mu\nu}(p) = \int \frac{\mathrm{d}^d\ell}{(2\pi)^d} \frac{\ell^\mu \ell^\nu}{\ell^2(\ell+p)^2}. \tag{A.28}$$

The only 2-tensors we can construct are $p^\mu p^\nu$ and $g^{\mu\nu}$, therefore

$$\mathcal{B}^{\mu\nu}(p) = B_{21}p^\mu p^\nu + B_{22}g^{\mu\nu}. \tag{A.29}$$

By projecting onto the two tensors

$$p_\mu \mathcal{B}^{\mu\nu}(p) = p^\nu\left(p^2 B_{21} + B_{22}\right) = \frac{1}{2}\int \frac{\mathrm{d}^d\ell}{(2\pi)^d} \frac{\ell^\nu}{\ell^2(\ell+p)^2}\left[(\ell+p)^2 - \ell^2 - p^2\right], \tag{A.30}$$

$$g_{\mu\nu}\mathcal{B}^{\mu\nu}(p) = p^2 B_{21} + dB_{22} = \int \frac{\mathrm{d}^d\ell}{(2\pi)^d} \frac{\ell^2}{\ell^2(\ell+p)^2} = 0. \tag{A.31}$$

From eq. (A.31) one obtains that

$$B_{22} = -\frac{p^2}{d} B_{21}, \tag{A.32}$$

while from eq. (A.30)

$$p^\nu\left(p^2 - \frac{p^2}{d}\right)B_{21} = -p^\nu \frac{p^2 B_{11}}{2}, \tag{A.33}$$

which gives

$$B_{21} = \frac{d}{d-1}\frac{B_{11}}{2} = \frac{d}{d-1}\frac{B_0(p^2)}{4} \tag{A.34}$$

and consequently

$$B_{21} = -\frac{p^2}{d-1}\frac{B_0(p^2)}{4}. \tag{A.35}$$

Therefore

$$\mathcal{B}^{\mu\nu}(p) = \frac{1}{d-1}\left[\frac{d}{4}B_0(p^2)p^\mu p^\nu - \frac{p^2}{4}B_0(p^2)g^{\mu\nu}\right]. \tag{A.36}$$

Appendix B

Markov Chain Monte Carlo and Metropolis-Hastings Algorithm

In general, the posterior distribution of eq. (6.9) cannot be computed easily, especially when there are many model parameters. Using a naive Monte Carlo sampling algorithm can lead to enormous computing times because of their inherent inefficiency in sampling the parameter space. Then, the Markov Chain Monte Carlo (MCMC) technique can help us overcome this problem and make the application of Bayes theorem feasible. On the surface, a MCMC technique is nothing but a way of sampling the parameter space using Markov Chains.

In `HEPfit`, the implementation of the MCMC is done using a Metropolis-Hastings algorithm to sample the parameter space from the posterior. The basic steps, starting from a probability density $f(\mathbf{x})$, are as follows

- Start at a random point in the parameter space $\mathbf{x}$.

- Generate a proposal point $\mathbf{y}$ according to a symmetric probability distribution $g(\mathbf{x}, \mathbf{y})$.

- Compare the value of the function f at the proposal point $\mathbf{y}$ with the value at the point $\mathbf{x}$. The proposal point is accepted if $f(\mathbf{y}) \geq f(\mathbf{x})$. Otherwise, a random number r is generated from a uniform distribution in $[0, 1]$ and accept the proposal if $f(\mathbf{y})/f(\mathbf{x}) > r$. If neither conditions are satisfied, the proposal point is rejected.

- Start from point 1.

In our case, the probability density $f(\mathbf{y})$ is the unnormalized posterior of eq. (6.9). the MCMC implementation in the `HEPfit` code consists in two main parts. The first is the pre-run where the chains start from arbitrary random points in the parameter space and reach a steady state after a certain number of iterations. After the pre-run is made, the samples of the parameter space are collected in the main run to get the marginalized distributions of all the parameters and the corresponding posterior distributions of the observable and of any other derived quantity that may have been defined.

Appendix C

Configuration Files for the UT Analysis

In this section, we give the various configuration files used in the UT analysis. For the relevant commands that are passed to `HEPfit` for the analysis, one can read the `HEPfit` documentation [60].

Elements with the hash # are being commented out and do not enter in the final analysis.

C.1 Standard Model input Parameters

─────────────────────── StandardModel.conf ───────────────────────

```
StandardModel
#####################################################################
# Mandatory configuration files
#-------------------------------------------------------------------
IncludeFile Flavour.conf
IncludeFile UTfit.conf
#
#####################################################################
# Optional configuration files
#-------------------------------------------------------------------
# IncludeFile GeneralSUSY.conf
# IncludeFile THDM.conf
#
#####################################################################
# Model Parameters
#                name       ave        errg       errf
#-------------------------------------------------------------------
### Parameters in StandardModel
ModelParameter  GF         1.1663787e-5 0.         0.
# alpha=1/137.035999074
ModelParameter  ale    7.2973525698e-3 0.         0.
ModelParameter  AlsMz      0.11792    0.00094    0.
ModelParameter  dAle5Mz    0.02766    0.00010    0.
ModelParameter  Mz         91.1875    0.0021     0.
ModelParameter       Mw_inp        80.354      0.007          0.
ModelParameter  delMw      0.         0.         0.
```

```
ModelParameter  delSin2th_l 0.          0.          0.
ModelParameter  delSin2th_q 0.          0.          0.
ModelParameter  delSin2th_b 0.          0.          0.
ModelParameter  delGammaZ   0.          0.          0.
ModelParameter  delsigma0H  0.          0.          0.
ModelParameter  delR0l      0.          0.          0.
ModelParameter  delR0c      0.          0.          0.
ModelParameter  delR0b      0.          0.          0.
# mtpole
ModelParameter  mtop        172.58      0.45        0.
ModelParameter  mHl         125.09      0.          0.
#
# light quark masses at 2 GeV
ModelParameter  mup         0.00250     0.00017     0.
ModelParameter  mdown       0.00488     0.00020     0.
ModelParameter  mstrange    0.09291     0.00068     0.
# mcmc
ModelParameter  mcharm      1.289       0.007       0.
# mbmb
ModelParameter  mbottom     4.191       0.014       0.
ModelParameter  muc         1.3         0.          0.
ModelParameter  mub         4.177          0.          0.
ModelParameter  mut         163.74         0.          0.
#ModelParameter  mut         170.           0.          0.
#
ModelParameter  mneutrino_1 0.          0.          0.
ModelParameter  mneutrino_2 0.          0.          0.
ModelParameter  mneutrino_3 0.          0.          0.
ModelParameter  s12_pmns    0.          0.          0.
ModelParameter  s13_pmns    0.          0.          0.
ModelParameter  s23_pmns    0.          0.          0.
ModelParameter  delta_pmns  0.          0.          0.
ModelParameter  alpha21_pmns 0.            0.            0.
ModelParameter  alpha31_pmns 0.            0.            0.
ModelParameter  melectron   5.109989e-4 0.          0.
ModelParameter  mmu         0.10565837  0.          0.
ModelParameter  mtau        1.77682     0.          0.
#
################################################################
#Observable MtMSbar MtMSbar MtMSbar 1. -1. noMCMC noweight
#Observable Mw Mw Mw 0. 0. noMCMC noweight
```

C.2 Flavour Parameters

In the Flavour.conf file are contained the relevant model parameters for ϵ'/ϵ like the values of the hadronic matrix elements of the effective operators and, where given, the correlation matrix between them. Not only this, but the non-perturbative renormalization matrix elements, called *Zqq*, are given in this file.

————————————————— `Flavour.conf` —————————————————

```
################################################################
# Model Parameters
```

```
#              name      ave       errg      errf
#-----------------------------------------------------------
ModelParameter  tKl       5.116e4   2.1e2     0.
ModelParameter  lambdaB      0.350     0.           0.150
ModelParameter  SM_M12D   0.        0.        0.
ModelParameter  tD        0.4101       0.0015    0.
ModelParameter  MD        1.865     0.        0.
ModelParameter       BD1         0.765       0.025          0.0
ModelParameter       BD2         0.65        0.02         0.0
ModelParameter       BD3         0.99        0.05         0.0
ModelParameter       BD4         0.98        0.06         0.0
ModelParameter       BD5         1.05        0.09         0.0
#ModelParameter      BD1         0.77        0.05          0.0
#ModelParameter      BD2         0.64        0.04          0.0
#ModelParameter      BD3         0.97        0.08          0.0
#ModelParameter      BD4         0.95        0.07          0.0
#ModelParameter      BD5         1.05        0.11          0.0
ModelParameter       FD          0.2092      0.0033    0.0
ModelParameter  BDscale   3.        0.        0.
ModelParameter  BDscheme  0.        0.        0.
####################################################################

ModelParameter  BK_RBC1/2scale    4.006        0.          0.
ModelParameter  BK_RBC1/2scheme   0            0           0
CorrelatedGaussianParameters  BFactorsRBC 7
ModelParameter  BK_RBC1/21        0.143        0.093       0.
ModelParameter  BK_RBC1/22       -0.147        0.024       0.
ModelParameter  BK_RBC1/23        0.233        0.023       0.
ModelParameter  BK_RBC1/24       -0.723        0.091       0.
ModelParameter  BK_RBC1/25       -2.211        0.144       0.
ModelParameter  BK_RBC1/26        1.876        0.052       0.
ModelParameter  BK_RBC1/27        5.679        0.107       0.
1.         0.0816756 -0.151239  0.0819331  -0.10693  0.536807  0.311024
0.0816756  1.               -0.284058  0.371749  0.206539        0.0540144 -0.213318
-0.151239 -0.284058  1.              0.214286   0.310386        -0.114632   0.143153
0.0819331  0.371749  0.214286   1.              0.370116        -0.0934066 -0.151998
-0.10693         0.206539  0.310386  0.370116   1.              -0.215278  -0.38506
0.536807         0.0540144 -0.114632 -0.0934066  -0.215278 1.              0.720705
0.311024         -0.213318  0.143153 -0.151998  -0.38506        0.720705  1.

ModelParameter  BK_RBC3/2scale    3.           0.          0.
ModelParameter  BK_RBC3/2scheme   0.           0.          0.
ModelParameter  BK_RBC3/21        0.0292       0.0008      0.
ModelParameter  BK_RBC3/22        0.579        0.013       0.
ModelParameter  BK_RBC3/23        2.56         0.07        0.

ModelParameter  ImA2_RBC         -8.34e-13    1.03e-13    0.
ModelParameter  ReA2_RBC          1.50e-08    0.15e-08    0.
ModelParameter  ReTau             0.001558    0.000065    0.
ModelParameter  ImTau            -0.000663    0.000033    0.

ModelParameter  ReA0_Kd   3.3201e-07  0.0018e-07  0. #Modificato
ModelParameter  ReA2_Kd   1.479e-08   0.004e-08   0  #Modificato
ModelParameter  omega     0.04454     0.00012     0. #Aggiunto
ModelParameter  delta_0   32.3        2.1         0. #Aggiunto
ModelParameter  delta_2   -11.6       2.8         0. #Aggiunto
ModelParameter  EpsK      0.002228    0.000011    0.
```

```
ModelParameter SysImA0    0.   0.207  0.
ModelParameter SysReA0    0.   0.198  0.

ModelParameter OmegaIB    0.1705  0.0905  0.

ModelParameter Zqq00      0.42011     0.00043     0.
ModelParameter Zqq11      0.422       0.038       0.
ModelParameter Zqq12     -0.207       0.036       0.
ModelParameter Zqq13     -0.005       0.013       0.
ModelParameter Zqq14      0.0084      0.0077      0.
ModelParameter Zqq21     -0.094       0.024       0.
ModelParameter Zqq22      0.570       0.024       0.
ModelParameter Zqq23     -0.0120      0.0083      0.
ModelParameter Zqq24      0.0059      0.0047      0.
ModelParameter Zqq31     -0.14        0.14        0.
ModelParameter Zqq32     -0.15        0.12        0.
ModelParameter Zqq33      0.424       0.044       0.
ModelParameter Zqq34      0.013       0.026       0.
ModelParameter Zqq41     -0.030       0.063       0.
ModelParameter Zqq42     -0.073       0.066       0.
ModelParameter Zqq43     -0.106       0.023       0.
ModelParameter Zqq44      0.620       0.015       0.
ModelParameter Zqq55      0.47715     0.00049     0.
ModelParameter Zqq56     -0.02113     0.00024     0.
ModelParameter Zqq65     -0.05960     0.00055     0.
ModelParameter Zqq66      0.6030      0.0014      0.
```

C.3   UT Parameters and Observables

─────────── UTfit.conf ───────────

```
ModelFlag FlagCsi false
ModelFlag Wolfenstein false
##########################################################################
# Model Parameters
#                name      ave       errg       errf
#------------------------------------------------------------------
### Parameters for Flavour Mandatory for all models
#   scheme for bag parameters [NDR=0, HV=1, LRI=2]
#ModelParameter  lambda    0.2       0.         0.1
#ModelParameter  A         0.8       0.         0.3
#ModelParameter  rhob      0.0       0.         1.0
#ModelParameter  etab      0.0       0.         1.0
ModelParameter  V_us      0.2249     0.0004     0.
ModelParameter  V_cb      0.0411     0.0010     0.0
ModelParameter  V_ub      0.00389    0.00021    0.
ModelParameter  gamma     1.154      0.061      0.
#ModelParameter  V_us      0.225787     0.0004      0.
#ModelParameter  V_cb      0.0408948    0.00         0.01
#ModelParameter  V_ub      0.0035987    0.00013     0.
#ModelParameter  gamma     1.22173    0.07         0.
ModelParameter  MBd       5.2796     0.         0.
ModelParameter  tBd       1.519      0.004      0.
ModelParameter  MBs       5.3668     0.         0.
ModelParameter  tBs       1.516      0.006      0.
# exp number in the meanwhile
```

```
ModelParameter  DGs_Gs      0.128        0.009       0.
ModelParameter  MBp         5.2793       0.          0.
ModelParameter  tBp         1.638        0.004       0.
ModelParameter  MK0         0.49761      0.          0.
ModelParameter  MKp         0.49368      0.          0.
ModelParameter  MKstar      0.89581      0.          0.
ModelParameter  MKstarP     0.89166      0.          0.
ModelParameter  tKstar      1.           0.          0.
ModelParameter  Mphi        1.019461     0.          0.
ModelParameter  tphi        1.           0.          0.
ModelParameter  FK          0.1561       0.          0.
ModelParameter  FBs         0.2301       0.0012      0.
ModelParameter  FKstar      0.225        0.          0.
ModelParameter  FKstarp     0.185        0.          0.
ModelParameter  Fphi        0.2          0.          0.
ModelParameter  Fphip       0.215        0.          0.
ModelParameter  alpha2phi   0.           0.          0.
ModelParameter  FBsoFBd     1.208        0.005       0.
ModelParameter  BBsoBBd     1.032        0.038       0.
ModelParameter  BBs1        0.888        0.04        0.
ModelParameter  BBs2        0.75         0.03        0.
ModelParameter  BBs3        0.97         0.1         0.
ModelParameter  BBs4        0.98         0.08        0.
ModelParameter  BBs5        1.66         0.13        0.
#ModelParameter  BBs2       0.77         0.06        0.
#ModelParameter  BBs3       1.           0.17        0.
#ModelParameter  BBs4       1.03         0.12        0.
#ModelParameter  BBs5       1.7          0.18        0.
ModelParameter  BBd2        0.73         0.03        0.
ModelParameter  BBd3        0.93         0.11        0.
ModelParameter  BBd4        0.99         0.08        0.
ModelParameter  BBd5        1.58         0.18        0.
#ModelParameter  BBd2       0.74         0.06        0.
#ModelParameter  BBd3       0.98         0.2         0.
#ModelParameter  BBd4       1.05         0.13        0.
#ModelParameter  BBd5       1.67         0.26        0.
ModelParameter  BBsscale    4.177        0.          0.
ModelParameter  BBdscale    4.177        0.          0.
# Scheme [NDR=0, HV=1, LRI=2];
ModelParameter  BBsscheme   0.           0.          0.
ModelParameter  BBdscheme   0.           0.          0.
ModelParameter  muw         80.          0.          60.
#ModelParameter  muw        100.         0.          60.
ModelParameter  phiEpsK     43.51        0.05        0.
ModelParameter  KbarEpsK    .97          0.02        0.
ModelParameter  DeltaMK     3.483e-15    0.006e-15   0.
ModelParameter  DmkSM       5.5e-15      1.7e-15     0.
ModelParameter  BK1         0.552        0.012       0.
ModelParameter  BK2         0.495        0.016       0.
ModelParameter  BK3         0.774        0.026       0.
ModelParameter  BK4         0.904        0.053        0.
ModelParameter  BK5         0.618        0.114        0.
#ModelParameter  BK2        0.49         0.04         0.
#ModelParameter  BK3        0.77         0.06         0.
#ModelParameter  BK4        0.89         0.10         0.
#ModelParameter  BK5        0.65         0.13         0.
ModelParameter  BKscale     2.           0.          0.
ModelParameter  BKscheme    0.           0.          0.
####################################################################
Observable  MtMSbar MtMSbar MtMSbar  1. -1. noMCMC noweight
Observable  Dmd       DmBd    #Deltam_{d}  1. -1.  MCMC weight 0.5065   0.0019    0.
Observable  Dms       DmBs    #Deltam_{s}  1. -1.  MCMC weight 17.765   0.006    0.
Observable  EpsilonK EpsilonK #epsilon_{K} 1. -1.  MCMC weight 0.002228  0.000011   0.
Observable  EpsiloP_o_Epsilon EpsiloP_o_Epsilon #epsilon'/#epsilon 0. 0. noMCMC noweight
#
### Flag 2019 + Hardy & Towner
```

```
Observable  Vus      Vus      V_{us}         1. -1.  noMCMC noweight 0.2249    0.0004    0.
Observable  Vud      Vud      V_{ud}         1. -1.  MCMC weight 0.97370   0.00014   0.
#
### Vcb from exclusive, inclusive, and UTfit combination
Observable  Vcb      Vcb      V_{cb}         1. -1.  noMCMC noweight 0.0409    0.0011    0.
Observable  Vub      Vub      V_{ub}         1. -1.  noMCMC noweight 0.00381   0.00040   0.
#
### alpha from UTfit combinations: pipi, rhopi, and rhorho
Observable  alpha_pipi    alpha_2a #alpha  1. -1.  MCMC file input/pipi_sum21 Input/pipi_input_alpha
Observable  alpha_rhopi   alpha_2a #alpha  1. -1.  MCMC file input/rhopi_win10 Input/alpharhopi
Observable  alpha_rhorho  alpha_2a #alpha  1. -1.  MCMC file input/rhorho_sum21 Input/rhorho_input_alpha
Observable  alpha         alpha    #alpha            1. -1. noMCMC noweight 93.3       5.6        0.
#
### gamma from UTfit combination
#Observable gamma    gamma    #gamma         1. -1.  noMCMC file input/gamma_sum16 Input/gamma_all
#
### S coefficient of JPsiK time-dependent CPA
Observable  SJPsiK   SJPsiK   S_{J/#PsiK} 1. -1.  noMCMC noweight  0.688 0.020 0.
Observable  C2beta   C2beta   Cos2#beta            1. -1.  MCMC file  input/cos2b_sum18 Input/input_cos2b
#
Observable  Phis_JPsiPhi Phis_JPsiPhi #beta_{s}       1. -1. MCMC weight -0.05   0.019  0.
### posterior histograms
Observable  BK1      BK1      B_{K}                 1. -1. noMCMC noweight
Observable  FBsoFBd  FBsoFBd  F_{B_{s}}/F_{B_{d}} 1. -1. noMCMC noweight
Observable  FBs      FBs      F_{B_{s}}             1. -1. noMCMC noweight
Observable  BBsoBBd  BBsoBBd  B_{B_{s}}/B_{B_{d}} 1. -1. noMCMC noweight
Observable  BBs1     BBs1     B_{B_{s}}             1. -1. noMCMC noweight
Observable  btaunu   btaunu   BRB#to#tau#nu   1. -1. noMCMC noweight
Observable  etab     etab              #overline{#eta}   1. -1. noMCMC noweight
Observable  rhob     rhob             #overline{#rho}  1. -1. noMCMC noweight
Observable  gammaAR  CKM_gamma         #gamma         1. -1. noMCMC noweight
Observable  lambda   lambda   #lambda         1. -1. noMCMC noweight
Observable  A        A                 A                1. -1. noMCMC noweight
Observable  beta     CKM_beta          #beta          1. -1. noMCMC noweight
Observable  2betapgamma  CKM_2betapgamma  2#beta+#gamma   1. -1. noMCMC noweight
Observable  s2beta   CKM_s2beta        sin2#beta      1. -1. noMCMC noweight
Observable  c2beta   CKM_c2beta        cos2#beta      1. -1. noMCMC noweight
Observable  sintheta12  CKM_sintheta12   sin#theta_{12}  1. -1. noMCMC noweight
Observable  sintheta13  CKM_sintheta13   sin#theta_{13}  1. -1. noMCMC noweight
Observable  sintheta23  CKM_sintheta23   sin#theta_{23}  1. -1. noMCMC noweight
Observable  ckmdelta  CKM_delta        #delta         1. -1. noMCMC noweight
Observable  J_CP     J_CP     J_{CP}                1. -1. noMCMC noweight
Observable  Rt       Rt       R_{t}                 1. -1. noMCMC noweight
Observable  Rts      Rts      R_{ts}                1. -1. noMCMC noweight
Observable  Rb       Rb       R_{b}                 1. -1. noMCMC noweight
Observable  VtdoVts  VtdoVts  V_{td}/V_{ts}         1. -1. noMCMC noweight
Observable  CKM_rho  CKM_rho  #rho                  1. -1. noMCMC noweight
Observable  CKM_eta  CKM_eta  #eta                  1. -1. noMCMC noweight
### CKM elements absolute values
Observable  Vud      Vud      V_{ud}                1. -1. noMCMC noweight
Observable  Vus      Vus      V_{us}                1. -1. noMCMC noweight
Observable  Vub      Vub      V_{ub}                1. -1. noMCMC noweight
Observable  Vcd      Vcd      V_{cd}                1. -1. noMCMC noweight
Observable  Vcs      Vcs      V_{cs}                1. -1. noMCMC noweight
Observable  Vcb      Vcb      V_{cb}                1. -1. noMCMC noweight
Observable  Vtd      Vtd      V_{td}                1. -1. noMCMC noweight
Observable  Vts      Vts      V_{ts}                1. -1. noMCMC noweight
Observable  Vtb      Vtb      V_{tb}                1. -1. noMCMC noweight
#
### Correlations
Observable2D  alphavsgamma CKM_alpha #alpha   1. -1. noMCMC noweight CKM_gamma #gamma 1. -1.
Observable2D  etavsrho     rhob  #rho    1. -1. noMCMC noweight etab  #eta  1. -1.
############################################################################
# B to mu mu decays
Observable  BR_Bdmumu    BR_Bdmumu    BRB_{d}#rightarrow#mu#mu   1.   -1.      noMCMC    noweight
Observable  BR_Bsmumu    BR_Bsmumu    BRB_{s}#rightarrow#mu#mu   1.   -1.      noMCMC    noweight
```

```
Observable  BRbar_Bsmumu    BRbar_Bsmumu    BRB_{s}#rightarrow#mu#mu   1.    -1.      noMCMC     noweight
######################################################################
### Observables not used
#measurement Bs2llBR = 2.9e-9, 0.7e-9, 0.000
#measurement Bd2llBR = 0.39e-9, 0.15e-9, 0.000

# Observable  BRbar_Bdmumu    BRbar_Bdmumu    BRB_{d}#rightarrow#mu#mu 1. 1.      MCMC     weight 1.05e-10      0
# Observable2D  M12vsphi12    ArgD    #Phi_{12} -180. 180. MCMC file input/ANP_DDmix Input/HNP M12D M_{12}^D 0. 0.03
# Observable  Amumu_Bd    Amumu_Bd    A#mu#mu^{B_{d}}    1.    1.     noMCMC     noweight  1    0    0.
# Observable  Smumu_Bd    Smumu_Bd    S#mu#mu^{B_{d}}    1.    1.     noMCMC     noweight  1    0    0.
# Observable  Amumu_Bs    Amumu_Bs    A#mu#mu^{B_{s}}    1.    1.     noMCMC     noweight  1    0    0.
# Observable  Smumu_Bs    Smumu_Bs    S#mu#mu^{B_{s}}    1.    1.     noMCMC     noweight  1    0    0.
######################################################################
```

Bibliography

[1] ABAZOV, V. M. ET AL. Precision measurement of the ratio B($t \to Wb$)/B($t \to Wq$) and Extraction of V_{tb}. *Phys. Rev. Lett.*, **107** (2011), 121802. `arXiv: 1106.5436`, `doi:10.1103/PhysRevLett.107.121802`.

[2] ABBOTT, R. ET AL. Direct CP violation and the $\Delta I = 1/2$ rule in $K \to \pi\pi$ decay from the standard model. *Phys. Rev. D*, **102** (2020), 054509. `arXiv: 2004.09440`, `doi:10.1103/PhysRevD.102.054509`.

[3] ABLIKIM, M. ET AL. Measurement of the $D_s^+ \to \ell^+\nu_\ell$ branching fractions and the decay constant $f_{D_s^+}$. *Phys. Rev. D*, **94** (2016), 072004. `arXiv:1608.06732`, `doi:10.1103/PhysRevD.94.072004`.

[4] ABLIKIM, M. ET AL. Determination of the pseudoscalar decay constant $f_{D_s^+}$ via $D_s^+ \to \mu^+\nu_\mu$. *Phys. Rev. Lett.*, **122** (2019), 071802. `arXiv:1811.10890`, `doi:10.1103/PhysRevLett.122.071802`.

[5] ABOUZAID, E., ET AL. Precise measurements of directcpviolation,cptsymmetry, and other parameters in the neutral kaon system. *Physical Review D*, **83** (2011). Available from: `http://dx.doi.org/10.1103/PhysRevD.83.092001`, `doi:10.1103/physrevd.83.092001`.

[6] ACOSTA, D. ET AL. Measurement of $B(t \to Wb)/B(t \to Wq)$ at the Collider Detector at Fermilab. *Phys. Rev. Lett.*, **95** (2005), 102002. `arXiv:hep-ex/0505091`, `doi:10.1103/PhysRevLett.95.102002`.

[7] AEBISCHER, J., BOBETH, C., AND BURAS, A. J. ε'/ε in the Standard Model at the Dawn of the 2020s. *Eur. Phys. J. C*, **80** (2020), 705. `arXiv:2005.05978`, `doi:10.1140/epjc/s10052-020-8267-1`.

[8] AEBISCHER, J., BOBETH, C., BURAS, A. J., GÉRARD, J.-M., AND STRAUB, D. M. Master formula for ε'/ε beyond the Standard Model. *Phys. Lett. B*, **792** (2019), 465. `arXiv:1807.02520`, `doi:10.1016/j.physletb.2019.04.016`.

[9] AEBISCHER, J., BOBETH, C., BURAS, A. J., AND KUMAR, J. BSM Master Formula for ε'/ε in the WET Basis at NLO in QCD. (2021). `arXiv:2107.12391`.

[10] AEBISCHER, J., BOBETH, C., BURAS, A. J., AND STRAUB, D. M. Anatomy of ε'/ε beyond the standard model. *Eur. Phys. J. C*, **79** (2019), 219. `arXiv: 1808.00466`, `doi:10.1140/epjc/s10052-019-6715-6`.

[11] ALAVI-HARATI, A. ET AL. Measurements of direct CP violation, CPT symmetry, and other parameters in the neutral kaon system. *Phys. Rev. D*, **67** (2003), 012005. [Erratum: Phys.Rev.D 70, 079904 (2004)]. `arXiv:hep-ex/0208007`, `doi:10.1103/PhysRevD.70.079904`.

[12] ALEXANDER, J. P. ET AL. Measurement of $BD_s^+ \to \ell^+ \nu$ and the Decay Constant $f_{D_s^+}$ From $600/pb^{-1}$ of $e^{\pm}$ Annihilation Data Near 4170 MeV. *Phys. Rev. D*, **79** (2009), 052001. `arXiv:0901.1216`, `doi:10.1103/PhysRevD.79.052001`.

[13] ALTARELLI, G. AND MAIANI, L. Octet Enhancement of Nonleptonic Weak Interactions in Asymptotically Free Gauge Theories. *Phys. Lett. B*, **52** (1974), 351. `doi:10.1016/0370-2693(74)90060-4`.

[14] ANTONELLI, M. ET AL. An Evaluation of $|V_{us}|$ and precise tests of the Standard Model from world data on leptonic and semileptonic kaon decays. *Eur. Phys. J. C*, **69** (2010), 399. `arXiv:1005.2323`, `doi:10.1140/epjc/s10052-010-1406-3`.

[15] ANTONELLI, V., BERTOLINI, S., FABBRICHESI, M., AND LASHIN, E. I. The Delta I = 1/2 selection rule. *Nucl. Phys. B*, **469** (1996), 181. `arXiv:hep-ph/9511341`, `doi:10.1016/0550-3213(96)00145-9`.

[16] ASHMORE, J. F. A Method of Gauge Invariant Regularization. *Lett. Nuovo Cim.*, **4** (1972), 289. `doi:10.1007/BF02824407`.

[17] BAEZ, J. C. AND HUERTA, J. The Algebra of Grand Unified Theories. *Bull. Am. Math. Soc.*, **47** (2010), 483. `arXiv:0904.1556`, `doi:10.1090/S0273-0979-10-01294-2`.

[18] BAI, Z. ET AL. Standard Model Prediction for Direct CP Violation in K→ππ Decay. *Phys. Rev. Lett.*, **115** (2015), 212001. `arXiv:1505.07863`, `doi:10.1103/PhysRevLett.115.212001`.

[19] BAIKOV, P. A., CHETYRKIN, K. G., AND KÜHN, J. H. Five-Loop Running of the QCD coupling constant. *Phys. Rev. Lett.*, **118** (2017), 082002. `arXiv:1606.08659`, `doi:10.1103/PhysRevLett.118.082002`.

[20] BARDEEN, W. A., BURAS, A. J., AND GERARD, J. M. The Delta I = 1/2 Rule in the Large N Limit. *Phys. Lett. B*, **180** (1986), 133. `doi:10.1016/0370-2693(86)90150-4`.

[21] BARDEEN, W. A., BURAS, A. J., AND GERARD, J. M. A Consistent Analysis of the Delta I = 1/2 Rule for K Decays. *Phys. Lett. B*, **192** (1987), 138. `doi:10.1016/0370-2693(87)91156-7`.

[22] BARDEEN, W. A., BURAS, A. J., AND GERARD, J. M. The K —> pi pi Decays in the Large n Limit: Quark Evolution. *Nucl. Phys. B*, **293** (1987), 787. `doi:10.1016/0550-3213(87)90091-5`.

[23] BATLEY, J., ET AL. A precision measurement of direct cp violation in the decay of neutral kaons into two pions. *Physics Letters B*, **544** (2002), 97–112. Available from: `http://dx.doi.org/10.1016/S0370-2693(02)02476-0`, `doi:10.1016/s0370-2693(02)02476-0`.

[24] BERTOLINI, S., EEG, J. O., AND FABBRICHESI, M. Studying epsilon-prime / epsilon in the chiral quark model: gamma(5) scheme independence and NLO hadronic matrix elements. *Nucl. Phys. B*, **449** (1995), 197. `arXiv:hep-ph/9409437`, `doi:10.1016/0550-3213(95)00274-V`.

[25] BLUM, T. ET AL. $K \to \pi\pi \ \Delta I = 3/2$ decay amplitude in the continuum limit. *Phys. Rev. D*, **91** (2015), 074502. `arXiv:1502.00263`, `doi:10.1103/PhysRevD.91.074502`.

[26] BOLLINI, C. G. AND GIAMBIAGI, J. J. Dimensional Renormalization: The Number of Dimensions as a Regularizing Parameter. *Nuovo Cim. B*, **12** (1972), 20. `doi:10.1007/BF02895558`.

[27] BONA, M. ET AL. The 2004 UTfit collaboration report on the status of the unitarity triangle in the standard model. *JHEP*, **07** (2005), 028. `arXiv:hep-ph/0501199`, `doi:10.1088/1126-6708/2005/07/028`.

[28] BONA, M. ET AL. Model-independent constraints on $\Delta F = 2$ operators and the scale of new physics. *JHEP*, **03** (2008), 049. `arXiv:0707.0636`, `doi:10.1088/1126-6708/2008/03/049`.

[29] BRANCO, G. C., LAVOURA, L., AND SILVA, J. P. *CP Violation*, vol. 103. Oxford University Press (1999). International Series of Monographs on Physics.

[30] BUCHALLA, G., BURAS, A. J., AND LAUTENBACHER, M. E. Weak decays beyond leading logarithms. *Rev. Mod. Phys.*, **68** (1996), 1125. `arXiv:hep-ph/9512380`, `doi:10.1103/RevModPhys.68.1125`.

[31] BURAS, A. J. Weak Hamiltonian, CP violation and rare decays. In *Les Houches Summer School in Theoretical Physics, Session 68: Probing the Standard Model of Particle Interactions* (1998). `arXiv:hep-ph/9806471`.

[32] BURAS, A. J. The ϵ'/ϵ-Story: 1976-2021. *Acta Phys. Polon. B*, **52** (2021), 7. `arXiv:2101.00020`, `doi:10.5506/APhysPolB.52.7`.

[33] BURAS, A. J., GAMBINO, P., AND HAISCH, U. A. Electroweak penguin contributions to nonleptonic Delta F = 1 decays at NNLO. *Nucl. Phys. B*, **570** (2000), 117. `arXiv:hep-ph/9911250`, `doi:10.1016/S0550-3213(99)00810-X`.

[34] BURAS, A. J. AND GERARD, J. M. 1/n Expansion for Kaons. *Nucl. Phys. B*, **264** (1986), 371. `doi:10.1016/0550-3213(86)90489-X`.

[35] BURAS, A. J. AND GERARD, J. M. Isospin Breaking Contributions to Epsilon-prime / Epsilon. *Phys. Lett. B*, **192** (1987), 156. `doi:10.1016/0370-2693(87)91159-2`.

[36] Buras, A. J. and Gérard, J.-M. Isospin-breaking in ε'/ε: impact of η_0 at the dawn of the 2020s. *Eur. Phys. J. C*, **80** (2020), 701. `arXiv:2005.08976`, `doi:10.1140/epjc/s10052-020-8299-6`.

[37] Buras, A. J., Gorbahn, M., Jäger, S., and Jamin, M. Improved anatomy of ε'/ε in the Standard Model. *JHEP*, **11** (2015), 202. `arXiv:1507.06345`, `doi:10.1007/JHEP11(2015)202`.

[38] Buras, A. J., Jamin, M., and Lautenbacher, M. E. Two loop anomalous dimension matrix for Delta S = 1 weak nonleptonic decays. 2. O(alpha-alphas). *Nucl. Phys. B*, **400** (1993), 75. `arXiv:hep-ph/9211321`, `doi:10.1016/0550-3213(93)90398-9`.

[39] Buras, A. J., Jamin, M., Lautenbacher, M. E., and Weisz, P. H. Effective Hamiltonians for $\Delta S = 1$ and $\Delta B = 1$ nonleptonic decays beyond the leading logarithmic approximation. *Nucl. Phys. B*, **370** (1992), 69. [Addendum: Nucl.Phys.B 375, 501 (1992)]. `doi:10.1016/0550-3213(92)90345-C`.

[40] Buras, A. J., Jamin, M., and Weisz, P. H. Leading and Next-to-leading QCD Corrections to ϵ Parameter and $B^0 - \bar{B}^0$ Mixing in the Presence of a Heavy Top Quark. *Nucl. Phys. B*, **347** (1990), 491. `doi:10.1016/0550-3213(90)90373-L`.

[41] Buras, A. J., Lautenbacher, M. E., and Ostermaier, G. Waiting for the top quark mass, $K^+ \to \pi^+ \nu \bar{\nu}$, $B^0_{(s)} - \bar{B_{(s)}}^0$ mixing and CP asymmetries in B decays. *Phys. Rev. D*, **50** (1994), 3433. `arXiv:hep-ph/9403384`, `doi:10.1103/PhysRevD.50.3433`.

[42] Cabibbo, N. Unitary Symmetry and Leptonic Decays. *Phys. Rev. Lett.*, **10** (1963), 531. `doi:10.1103/PhysRevLett.10.531`.

[43] Cabibbo, N., Swallow, E. C., and Winston, R. Semileptonic hyperon decays. *Ann. Rev. Nucl. Part. Sci.*, **53** (2003), 39. `arXiv:hep-ph/0307298`, `doi:10.1146/annurev.nucl.53.013103.155258`.

[44] Caldwell, A., Kollár, D., and Kröninger, K. Bat – the bayesian analysis toolkit. *Computer Physics Communications*, **180** (2009), 2197–2209. Available from: `http://dx.doi.org/10.1016/j.cpc.2009.06.026`, `doi:10.1016/j.cpc.2009.06.026`.

[45] Carlstein, E. The Use of Subseries Values for Estimating the Variance of a General Statistic from a Stationary Sequence. *The Annals of Statistics*, **14** (1986), 1171 . Available from: `https://doi.org/10.1214/aos/1176350057`, `doi:10.1214/aos/1176350057`.

[46] Cata, O. and Peris, S. Long distance dimension eight operators in B(K). *JHEP*, **03** (2003), 060. `arXiv:hep-ph/0303162`, `doi:10.1088/1126-6708/2003/03/060`.

[47] Charles, J., Hocker, A., Lacker, H., Laplace, S., Le Diberder, F. R., Malcles, J., Ocariz, J., Pivk, M., and Roos, L. CP violation and the CKM matrix: Assessing the impact of the asymmetric B factories. *Eur. Phys. J. C*, **41** (2005), 1. `arXiv:hep-ph/0406184`, `doi:10.1140/epjc/s2005-02169-1`.

[48] Cicuta, G. M. and Montaldi, E. Analytic renormalization via continuous space dimension. *Lett. Nuovo Cim.*, **4** (1972), 329. `doi:10.1007/BF02756527`.

[49] Cirigliano, V., Ecker, G., Neufeld, H., Pich, A., and Portoles, J. Kaon Decays in the Standard Model. *Rev. Mod. Phys.*, **84** (2012), 399. `arXiv:1107.6001`, `doi:10.1103/RevModPhys.84.399`.

[50] Cirigliano, V., Gisbert, H., Pich, A., and Rodríguez-Sánchez, A. Isospin-violating contributions to ϵ'/ϵ. *JHEP*, **02** (2020), 032. `arXiv:1911.01359`, `doi:10.1007/JHEP02(2020)032`.

[51] Cirigliano, V., Pich, A., Ecker, G., and Neufeld, H. Isospin violation in epsilon-prime. *Phys. Rev. Lett.*, **91** (2003), 162001. `arXiv:hep-ph/0307030`, `doi:10.1103/PhysRevLett.91.162001`.

[52] Ciuchini, M., Franco, E., Martinelli, G., and Reina, L. ϵ'/ϵ at the Next-to-leading order in QCD and QED. *Phys. Lett. B*, **301** (1993), 263. `arXiv:hep-ph/9212203`, `doi:10.1016/0370-2693(93)90699-I`.

[53] Ciuchini, M., Franco, E., Martinelli, G., and Reina, L. The Delta S = 1 effective Hamiltonian including next-to-leading order QCD and QED corrections. *Nucl. Phys. B*, **415** (1994), 403. `arXiv:hep-ph/9304257`, `doi:10.1016/0550-3213(94)90118-X`.

[54] Ciuchini, M., Franco, E., Martinelli, G., and Reina, L. Estimates of ϵ'/ϵ (1995). `arXiv:hep-ph/9503277`.

[55] Ciuchini, M., Franco, E., Martinelli, G., Reina, L., and Silvestrini, L. An Upgraded analysis of epsilon-prime epsilon at the next-to-leading order. *Z. Phys. C*, **68** (1995), 239. `arXiv:hep-ph/9501265`, `doi:10.1007/BF01566672`.

[56] Collins, J. C. *Renormalization: An Introduction to Renormalization, The Renormalization Group, and the Operator Product Expansion*, vol. 26 of *Cambridge Monographs on Mathematical Physics*. Cambridge University Press, Cambridge (1986). ISBN 978-0-521-31177-9, 978-0-511-86739-2. `doi:10.1017/CBO9780511622656`.

[57] Constantinou, M., Costa, M., Frezzotti, R., Lubicz, V., Martinelli, G., Meloni, D., Panagopoulos, H., and Simula, S. $K \to \pi$ matrix elements of the chromomagnetic operator on the lattice. *Phys. Rev. D*, **97** (2018), 074501. `arXiv:1712.09824`, `doi:10.1103/PhysRevD.97.074501`.

[58] D'Agostini, G. *Bayesian reasoning in high-energy physics: principles and applications.* CERN Yellow Reports: Monographs. CERN, Geneva

(1999). Available from: `https://cds.cern.ch/record/395902`, `doi:10.5170/CERN-1999-003`.

[59] D'Ambrosio, G. and Isidori, G. CP violation in kaon decays. *Int. J. Mod. Phys. A*, **13** (1998), 1. `arXiv:hep-ph/9611284`, `doi:10.1142/S0217751X98000020`.

[60] De Blas, J. et al. HEPfit: a code for the combination of indirect and direct constraints on high energy physics models. *Eur. Phys. J. C*, **80** (2020), 456. `arXiv:1910.14012`, `doi:10.1140/epjc/s10052-020-7904-z`.

[61] del Amo Sanchez, P. et al. Measurement of the Absolute Branching Fractions for $D_s^- \to \ell^- \bar{\nu}_\ell$ and Extraction of the Decay Constant f_{D_s}. *Phys. Rev. D*, **82** (2010), 091103. [Erratum: Phys.Rev.D 91, 019901 (2015)]. `arXiv:1008.4080`, `doi:10.1103/PhysRevD.82.091103`.

[62] Donoghue, J. F., Golowich, E., Holstein, B. R., and Trampetic, J. Electromagnetic and Isospin Breaking Effects Decrease ϵ'/ϵ. *Phys. Lett. B*, **179** (1986), 361. [Erratum: Phys.Lett.B 188, 511 (1987)]. `doi:10.1016/0370-2693(86)90493-4`.

[63] Dunietz, I., Greenberg, O. W., and Wu, D.-d. A Priori Definition of Maximal CP Violation. *Phys. Rev. Lett.*, **55** (1985), 2935. `doi:10.1103/PhysRevLett.55.2935`.

[64] Englert, F. and Brout, R. Broken Symmetry and the Mass of Gauge Vector Mesons. *prl*, **13** (1964), 321. `doi:10.1103/PhysRevLett.13.321`.

[65] Enz, C. P. and Lewis, R. R. On the phenomenological description of CP violation for K mesons and its consequences. *Helv. Phys. Acta*, **38** (1965), 860.

[66] Faddeev, L. D. and Popov, V. N. Feynman Diagrams for the Yang-Mills Field. *Phys. Lett. B*, **25** (1967), 29. `doi:10.1016/0370-2693(67)90067-6`.

[67] Fermi, E. An attempt of a theory of beta radiation. 1. *Z. Phys.*, **88** (1934), 161. `doi:10.1007/BF01351864`.

[68] Fierz, M. Zur fermischen theorie des β-zerfalls. *Zeitschrift für Physik*, **104** (1937), 553. Available from: `https://doi.org/10.1007/BF01330070`, `doi:10.1007/BF01330070`.

[69] Franco, E., Mishima, S., and Silvestrini, L. The Standard Model confronts CP violation in $D^0 \to \pi^+\pi^-$ and $D^0 \to K^+K^-$. *JHEP*, **05** (2012), 140. `arXiv:1203.3131`, `doi:10.1007/JHEP05(2012)140`.

[70] Gaillard, M. K. and Lee, B. W. Δ I = 1/2 Rule for Nonleptonic Decays in Asymptotically Free Field Theories. *Phys. Rev. Lett.*, **33** (1974), 108. `doi:10.1103/PhysRevLett.33.108`.

[71] Gell-Mann, M. The interpretation of the new particles as displaced charge multiplets. *Il Nuovo Cimento*, **4** (1956), 848. `doi:10.1007/BF02748000`.

[72] GELL-MANN, M. AND PAIS, A. Behavior of neutral particles under charge conjugation. *Phys. Rev.*, **97** (1955), 1387. `doi:10.1103/PhysRev.97.1387`.

[73] GELL-MANN, M. AND ROSENFELD, A. H. Hyperons and heavy mesons (systematics and decay). *Ann. Rev. Nucl. Part. Sci.*, **7** (1957), 407. `doi:10.1146/annurev.ns.07.120157.002203`.

[74] GEORGI, H. *Lie Algebras In Particle Physics: from Isospin To Unified Theories*. Frontiers in Physics. Avalon Publishing (1999). ISBN 9780813346113.

[75] GILMAN, F. J., KLEINKNECHT, K., AND RENK, B. The Cabibbo-Kobayashi-Maskawa quark-mixing matrix. *Phys. Lett. B*, **592** (2004), 793.

[76] GILMAN, F. J. AND WISE, M. B. Effective Hamiltonian for Delta s = 1 Weak Nonleptonic Decays in the Six Quark Model. *Phys. Rev. D*, **20** (1979), 2392. `doi:10.1103/PhysRevD.20.2392`.

[77] GLASHOW, S. L. The renormalizability of vector meson interactions. *Nucl. Phys.*, **10** (1959), 107. `doi:10.1016/0029-5582(59)90196-8`.

[78] GLASHOW, S. L. Partial Symmetries of Weak Interactions. *Nucl. Phys.*, **22** (1961), 579. `doi:10.1016/0029-5582(61)90469-2`.

[79] GLASHOW, S. L., ILIOPOULOS, J., AND MAIANI, L. Weak Interactions with Lepton-Hadron Symmetry. *Phys. Rev. D*, **2** (1970), 1285. `doi:10.1103/PhysRevD.2.1285`.

[80] GORBAHN, M. AND HAISCH, U. Effective Hamiltonian for non-leptonic $|\Delta F| = 1$ decays at NNLO in QCD. *Nucl. Phys. B*, **713** (2005), 291. `arXiv:hep-ph/0411071`, `doi:10.1016/j.nuclphysb.2005.01.047`.

[81] GREENBERG, O. W. Rephase Invariant Formulation of CP Violation in the Kobayashi-Maskawa Framework. *Phys. Rev. D*, **32** (1985), 1841. `doi:10.1103/PhysRevD.32.1841`.

[82] GRIBOV, V. N. Quantization of Nonabelian Gauge Theories. *Nucl. Phys. B*, **139** (1978), 1. `doi:10.1016/0550-3213(78)90175-X`.

[83] GROSS, D. J. AND WILCZEK, F. Ultraviolet Behavior of Nonabelian Gauge Theories. *Phys. Rev. Lett.*, **30** (1973), 1343. `doi:10.1103/PhysRevLett.30.1343`.

[84] GUBERINA, B. AND PECCEI, R. D. Quantum Chromodynamic Effects and CP Violation in the Kobayashi-Maskawa Model. *Nucl. Phys. B*, **163** (1980), 289. `doi:10.1016/0550-3213(80)90404-6`.

[85] GURALNIK, G. S., HAGEN, C. R., AND KIBBLE, T. W. B. Global Conservation Laws and Massless Particles. *Phys. Rev. Lett.*, **13** (1964), 585. `doi:10.1103/PhysRevLett.13.585`.

[86] GURALNIK, G. S., HAGEN, C. R., AND KIBBLE, T. W. B. Global conservation laws and massless particles. *Phys. Rev. Lett.*, **13** (1964), 585. Available from: `https://link.aps.org/doi/10.1103/PhysRevLett.13.585`, `doi:10.1103/PhysRevLett.13.585`.

[87] HARDY, J. AND TOWNER, I. S. $|V_{ud}|$ from nuclear β decays. *PoS*, **CKM2016** (2016), 028. `doi:10.22323/1.291.0028`.

[88] HERRLICH, S. AND NIERSTE, U. Enhancement of the K(L) - K(S) mass difference by short distance QCD corrections beyond leading logarithms. *Nucl. Phys. B*, **419** (1994), 292. `arXiv:hep-ph/9310311`, `doi:10.1016/0550-3213(94)90044-2`.

[89] HERRLICH, S. AND NIERSTE, U. Indirect CP violation in the neutral kaon system beyond leading logarithms. *Phys. Rev. D*, **52** (1995), 6505. `arXiv:hep-ph/9507262`, `doi:10.1103/PhysRevD.52.6505`.

[90] HERRLICH, S. AND NIERSTE, U. The Complete |delta S| = 2 - Hamiltonian in the next-to-leading order. *Nucl. Phys. B*, **476** (1996), 27. `arXiv:hep-ph/9604330`, `doi:10.1016/0550-3213(96)00324-0`.

[91] HERZOG, F., RUIJL, B., UEDA, T., VERMASEREN, J. A. M., AND VOGT, A. The five-loop beta function of Yang-Mills theory with fermions. *JHEP*, **02** (2017), 090. `arXiv:1701.01404`, `doi:10.1007/JHEP02(2017)090`.

[92] HIGGS, P. W. Broken Symmetries and the Masses of Gauge Bosons. *Phys. Rev. Lett.*, **13** (1964), 508. `doi:10.1103/PhysRevLett.13.508`.

[93] HIGGS, P. W. Broken symmetries and the masses of gauge bosons. *Phys. Rev. Lett.*, **13** (1964), 508. Available from: `https://link.aps.org/doi/10.1103/PhysRevLett.13.508`, `doi:10.1103/PhysRevLett.13.508`.

[94] HIGGS, P. W. Broken symmetries, massless particles and gauge fields. *Phys. Lett.*, **12** (1964), 132. `doi:10.1016/0031-9163(64)91136-9`.

[95] HIGGS, P. W. Spontaneous Symmetry Breakdown without Massless Bosons. *Phys. Rev.*, **145** (1966), 1156. `doi:10.1103/PhysRev.145.1156`.

[96] INAMI, T. AND LIM, C. S. Effects of Superheavy Quarks and Leptons in Low-Energy Weak Processes $K_L \to \mu\bar{\mu}$, $K^+ \to \pi^+\nu\bar{\nu}$ and $K^0 - \bar{K}^0$. *Prog. Theor. Phys.*, **65** (1981), 297. [Erratum: Prog.Theor.Phys. 65, 1772 (1981)]. `doi:10.1143/PTP.65.297`.

[97] JARLSKOG, C. A Basis Independent Formulation of the Connection Between Quark Mass Matrices, CP Violation and Experiment. *Z. Phys. C*, **29** (1985), 491. `doi:10.1007/BF01565198`.

[98] JARLSKOG, C. Commutator of the Quark Mass Matrices in the Standard Electroweak Model and a Measure of Maximal CP Violation. *Phys. Rev. Lett.*, **55** (1985), 1039. `doi:10.1103/PhysRevLett.55.1039`.

[99] KAYIS-TOPAKSU, A. ET AL. Measurement of topological muonic branching ratios of charmed hadrons produced in neutrino-induced charged-current interactions. *Phys. Lett. B*, **626** (2005), 24. `doi:10.1016/j.physletb.2005.08.082`.

[100] KAYSER, B. AND STODOLSKY, L. Cascade mixing, a new kind of particle mixing phenomenon. (1996). `arXiv:hep-ph/9610522`.

[101] KIBBLE, T. W. B. Symmetry breaking in nonAbelian gauge theories. *Phys. Rev.*, **155** (1967), 1554. `doi:10.1103/PhysRev.155.1554`.

[102] KITAHARA, T., NIERSTE, U., AND TREMPER, P. Singularity-free next-to-leading order $\Delta S = 1$ renormalization group evolution and ϵ'_K/ϵ_K in the Standard Model and beyond. *JHEP*, **12** (2016), 078. `arXiv:1607.06727`, `doi:10.1007/JHEP12(2016)078`.

[103] KOBAYASHI, M. AND MASKAWA, T. CP Violation in the Renormalizable Theory of Weak Interaction. *Prog. Theor. Phys.*, **49** (1973), 652. `doi:10.1143/PTP.49.652`.

[104] KOWALEWSKI, R. AND MANNEL, T. Semileptonic b-Hadron Decays, Determination of V_{cb}, V_{ub} (2020). `doi:10.1093/ptep/ptaa104`.

[105] LAVOURA, L. Phenomenology of the Neutral Kaon System in the Presence of CPT Noninvariance. *Annals Phys.*, **207** (1991), 428. `doi:10.1016/0003-4916(91)90065-G`.

[106] LEADER, E. AND PREDAZZI, E. *An Introduction to gauge theories and modern particle physics. Vol. 2: CP violation, QCD and hard processes*, vol. 4. Cambridge University Press (1996). ISBN 978-0-521-49951-4, 978-1-139-24099-4.

[107] LEE, T. *Particle Physics and Introduction to Field Theory: Revised and Updated First Edition.* Contemporary concepts in physics. Taylor & Francis (1981). ISBN 9783718600328. Available from: `https://books.google.it/books?id=CMYdFEntAHUC`.

[108] LEE, T. D. AND WU, C. S. Weak Interactions: Decays of neutral K mesons. *Ann. Rev. Nucl. Part. Sci.*, **16** (1966), 511. `doi:10.1146/annurev.ns.16.120166.002455`.

[109] LEHNER, C. AND STURM, C. Matching factors for Delta S=1 four-quark operators in RI/SMOM schemes. *Phys. Rev. D*, **84** (2011), 014001. `arXiv:1104.4948, doi:10.1103/PhysRevD.84.014001`.

[110] LUDERS, G. On the Equivalence of Invariance under Time Reversal and under Particle-Antiparticle Conjugation for Relativistic Field Theories. *Kong. Dan. Vid. Sel. Mat. Fys. Med.*, **28N5** (1954), 1.

[111] LUSIGNOLI, M. Electromagnetic Corrections to the Effective Hamiltonian for Strangeness Changing Decays and ϵ'/ϵ. *Nucl. Phys. B*, **325** (1989), 33. `doi:10.1016/0550-3213(89)90371-4`.

[112] LUTHE, T., MAIER, A., MARQUARD, P., AND SCHRODER, Y. The five-loop Beta function for a general gauge group and anomalous dimensions beyond Feynman gauge. *JHEP*, **10** (2017), 166. `arXiv:1709.07718, doi:10.1007/JHEP10(2017)166`.

[113] MAIANI, L., PANCHERI, G., AND PAVER, N. (eds.). *The second DAPHNE physics handbook. Vol. 1, 2.* INFN, Frascati, Italy (1995). ISBN 978-88-86409-02-5.

[114] MANOHAR, A. V. Effective field theories. *Lect. Notes Phys.*, **479** (1997), 311. `arXiv:hep-ph/9606222, doi:10.1007/BFb0104294`.

[115] MARTINELLI, G., PITTORI, C., SACHRAJDA, C. T., TESTA, M., AND VLADIKAS, A. A General method for nonperturbative renormalization of lattice operators. *Nucl. Phys. B*, **445** (1995), 81. `arXiv:hep-lat/9411010, doi:10.1016/0550-3213(95)00126-D`.

[116] NEUBERT, M. Renormalization Theory and Effective Field Theories. (2019). `arXiv:1901.06573, doi:10.1093/oso/9780198855743.003.0001`.

[117] NISHIJIMA, K. Charge Independence Theory of V Particles. *Progress of Theoretical Physics*, **13** (1955), 285. `doi:10.1143/PTP.13.285`.

[118] PASSARINO, G. AND VELTMAN, M. J. G. One Loop Corrections for e+ e-Annihilation Into mu+ mu- in the Weinberg Model. *Nucl. Phys. B*, **160** (1979), 151. `doi:10.1016/0550-3213(79)90234-7`.

[119] PECCEI, R. D. The Strong CP problem and axions. *Lect. Notes Phys.*, **741** (2008), 3. `arXiv:hep-ph/0607268, doi:10.1007/978-3-540-73518-2_1`.

[120] PESKIN, M. *Concepts of Elementary Particle Physics.* Oxford Master Series in Condensed Matter Physics Series. Oxford University Press (2019). ISBN 9780198812197.

[121] PICH, A. Chiral perturbation theory. *Rept. Prog. Phys.*, **58** (1995), 563. `arXiv:hep-ph/9502366, doi:10.1088/0034-4885/58/6/001`.

[122] POLCHINSKI, J. Effective field theory and the Fermi surface. In *Theoretical Advanced Study Institute (TASI 92): From Black Holes and Strings to Particles* (1992). `arXiv:hep-th/9210046`.

[123] POLITZER, H. D. Reliable Perturbative Results for Strong Interactions? *Phys. Rev. Lett.*, **30** (1973), 1346. `doi:10.1103/PhysRevLett.30.1346`.

[124] SACHS, R. G. CP Violation in K0 Decays. *Phys. Rev. Lett.*, **13** (1964), 286. `doi:10.1103/PhysRevLett.13.286`.

[125] SAKURAI, J. AND NAPOLITANO, J. *Modern Quantum Mechanics.* Addison-Wesley (2011). ISBN 9780805382914.

[126] SALAM, A. Weak and Electromagnetic Interactions. *Conf. Proc. C*, **680519** (1968), 367. `doi:10.1142/9789812795915_0034`.

[127] SALAM, A. AND WARD, J. C. Weak and electromagnetic interactions. *Il Nuovo Cimento*, **11** (1959), 568. `doi:10.1007/BF02726525`.

[128] SCHWARTZ, M. *Quantum Field Theory and the Standard Model*. Quantum Field Theory and the Standard Model. Cambridge University Press (2014). ISBN 9781107034730.

[129] SCHWINGER, J. The Theory of Quantized Fields. I. *Physical Review*, **82** (1951), 914. `doi:10.1103/PhysRev.82.914`.

[130] SHIFMAN, M. A. Foreword to ITEP lectures in particle physics (1995). `arXiv:hep-ph/9510397`.

[131] SHIFMAN, M. A., VAINSHTEIN, A. I., AND ZAKHAROV, V. I. Nonleptonic Decays of K Mesons and Hyperons. *Sov. Phys. JETP*, **45** (1977), 670.

[132] SILVA, J. P. Phenomenological aspects of CP violation. In *Central European School in Particle Physics* (2004). `arXiv:hep-ph/0410351`.

[133] SILVESTRINI, L. Effective theories for quark flavour physics (2021). `arXiv:1905.00798`.

[134] SREDNICKI, M. *Quantum Field Theory*. Cambridge University Press (2007). ISBN 9781139462761.

[135] 'T HOOFT, G. A Planar Diagram Theory for Strong Interactions. *Nucl. Phys. B*, **72** (1974), 461. `doi:10.1016/0550-3213(74)90154-0`.

[136] 'T HOOFT, G. Large N. In *The Phenomenology of Large N(c) QCD* (2002). `arXiv:hep-th/0204069, doi:10.1142/9789812776914_0001`.

[137] 'T HOOFT, G. AND VELTMAN, M. J. G. Regularization and Renormalization of Gauge Fields. *Nucl. Phys. B*, **44** (1972), 189. `doi:10.1016/0550-3213(72)90279-9`.

[138] VAINSHTEIN, A. I., ZAKHAROV, V. I., AND SHIFMAN, M. A. A Possible mechanism for the Delta T = 1/2 rule in nonleptonic decays of strange particles. *JETP Lett.*, **22** (1975), 55.

[139] VAĬNSHTEĬN, A. I., ZAKHAROV, V. I., AND SHIFMAN, M. A. A possible mechanism for the $\Delta T = 1/2$ rule in nonleptonic decays of strange particles. *Soviet Journal of Experimental and Theoretical Physics Letters*, **22** (1975), 55.

[140] VAĬNSHTEĬN, A. I., ZAKHAROV, V. I., AND SHIFMAN, M. A. A possible mechanism for the $\Delta T = 1/2$ rule in nonleptonic decays of strange particles. *ZhETF Pisma Redaktsiiu*, **22** (1975), 123.

[141] WATSON, K. M. Some general relations between the photoproduction and scattering of pi mesons. *Phys. Rev.*, **95** (1954), 228. `doi:10.1103/PhysRev.95.228`.

[142] WEINBERG, S. A Model of Leptons. *Phys. Rev. Lett.*, **19** (1967), 1264. `doi:10.1103/PhysRevLett.19.1264`.

[143] WEINBERG, S. A Model of Leptons. *prl*, **19** (1967), 1264. `doi:10.1103/PhysRevLett.19.1264`.

[144] WEISSKOPF, V. AND WIGNER, E. P. Calculation of the natural brightness of spectral lines on the basis of Dirac's theory. *Z. Phys.*, **63** (1930), 54. `doi:10.1007/BF01336768`.

[145] WIGNER, E. *Group Theory: And its Application to the Quantum Mechanics of Atomic Spectra*. Pure and applied physics. Elsevier Science (2012). ISBN 9780323152785. Available from: `https://books.google.it/books?id=ENZzI49uZMcC`.

[146] WILSON, K. G. Confinement of Quarks. *Phys. Rev. D*, **10** (1974), 2445. `doi:10.1103/PhysRevD.10.2445`.

[147] WILSON, K. G. AND ZIMMERMANN, W. Operator product expansions and composite field operators in the general framework of quantum field theory. *Commun. Math. Phys.*, **24** (1972), 87. `doi:10.1007/BF01878448`.

[148] WOLFENSTEIN, L. S matrix formulation of k(l) and k(s) decays and unitarity relations. *Phys. Rev.*, **188** (1969), 2536. `doi:10.1103/PhysRev.188.2536`.

[149] WOLFENSTEIN, L. Parametrization of the Kobayashi-Maskawa Matrix. *Phys. Rev. Lett.*, **51** (1983), 1945. `doi:10.1103/PhysRevLett.51.1945`.

[150] WU, D.-D. The Rephasing Invariants and CP. *Phys. Rev. D*, **33** (1986), 860. `doi:10.1103/PhysRevD.33.860`.

[151] ZUPANC, A. ET AL. Measurements of branching fractions of leptonic and hadronic D_s^+ meson decays and extraction of the D_s^+ meson decay constant. *JHEP*, **09** (2013), 139. `arXiv:1307.6240`, `doi:10.1007/JHEP09(2013)139`.

[152] ZYLA, P. A. ET AL. Review of Particle Physics. *PTEP*, **2020** (2020), 083C01. `doi:10.1093/ptep/ptaa104`.